

Dissertation zur Erlangung des Doktorgrades  
der Fakultät für Chemie und Pharmazie  
der Ludwig-Maximilians-Universität München

“Transition Metal Catalyzed  
Selective Oxidations of Sugars and Polyols”

**Matthias Bierenstiel**

aus  
Memmingen

**2005**

### Erklärung

Diese Dissertation wurde im Sinne von § 13 Abs. 3 bzw. 4 der Promotionsordnung vom 29. Januar 1998 (in der Fassung der vierten Änderungssatzung vom 26. November 2004) außerhalb der Fakultät von **Assistant Professor Dr. Marcel Schlaf**, University of Guelph, Guelph, Ontario, Kanada betreut. Die Arbeit wird von **Univ.-Professor Dr. Peter Klüfers** vor der Fakultät vertreten.

### Ehrenwörtliche Versicherung

Diese Dissertation wurde selbständig, ohne unerlaubte Hilfe erarbeitet.

Guelph, Ontario, Kanada, den 17. März 2005

A handwritten signature in black ink, appearing to read 'Matthias Bierenstiel', written in a cursive style.

(Matthias Bierenstiel)

Dissertation eingereicht am 22. März 2005

1. Gutachter Professor Dr. Marcel Schlaf

2. Gutachter Professor Dr. Peter Klüfers

Mündliche Prüfung am 29. April 2005

“Chemistry began by saying it would change baser metals into gold; by not doing so it has done much greater things.”

Ralph Waldo Emerson

## Table of Contents

Table of Contents .....	i
Acknowledgements .....	v
Abstract.....	vi
Zusammenfassung .....	viii
Abbreviations.....	xi
<b>Chapter 1 The Chemistry of Sugars, Transition Metal Catalysis and Research Motivation.....</b>	<b>1</b>
1.1 General Significance and Features of Sugars and Their Oxidation Products.....	1
1.1.1 Definitions and Properties of Sugars .....	1
1.1.2 Equilibria and Mutarotation of Sugars .....	3
1.1.3 Sugar Derivatives and Their Applications .....	4
1.1.4 Oxidation Products of Sugars .....	6
1.1.4.1 Definition, Occurrence and Applications of Sugar Lactones .....	8
1.1.4.2 Synthesis of Sugar Lactones .....	9
1.1.4.3 General Significance and Occurrence of Keto-sugars .....	13
1.1.4.4 Synthesis of Keto-sugars.....	13
1.1.4.5 Synthesis of Usolidulosides .....	14
1.1.4.6 Application of Keto-sugars in Reactions .....	18
1.1.4.7 Aldehydo-Sugars .....	20
1.1.4.8 Other Sugar Oxidation Products.....	20
1.2 Transition Metal Catalyzed Transfer Hydrogenation Reaction as a Strategy for Sugar Transformations .....	20
1.2.1 Hydrogen Transfer Reactions .....	20
1.2.2 Other Metal Catalyzed Oxidation Reactions .....	23
1.2.3 Representative Examples of Metal Sugar Complexes .....	24
1.2.4 Examples of Transition Metal Complex Catalyzed Transformations of Sugars .....	25
1.3 Motivation, Research Objectives and Potential Applications.....	28
1.3.1 Motivation .....	28
1.3.2 Research Objectives.....	29
1.3.3 Potential Applications of Sugar Lactones and Keto-Sugars.....	30
1.4 References.....	31

<b>Chapter 2 Selective Oxidation of Hemiacetals to Lactones</b> .....	36
2.1 Synthesis and Properties of $\delta$ - and $\gamma$ -Sugar Lactones .....	36
2.2 Transition Metal Catalysis .....	38
2.2.1 $\text{RuH}_2(\text{PPh}_3)_4$ and $\text{RhH}(\text{PPh}_3)_4$ in the Synthesis of Sugar Lactones .....	38
2.2.2 Shvo's Catalyst .....	41
2.3 Results and Discussion .....	44
2.3.1 Rationale for the Selection of Catalyst and Reaction Conditions .....	44
2.3.2 Synthesis and Isolation of $\delta$ -Lactones .....	45
2.3.2.1 Variation in Hydrogen Acceptor .....	45
2.3.2.2 Variation of Co-solvent .....	48
2.3.2.3 Oxidation Reactions without Co-solvent .....	50
2.3.2.4 Modification of Catalyst .....	53
2.3.2.5 Optimized Reaction Conditions .....	54
2.3.3 NMR and Conformational Analysis .....	57
2.3.4 $\delta$ to $\gamma$ Lactone Rearrangement .....	62
2.3.4.1 Thermodynamic Considerations .....	62
2.3.4.2 Mechanistic Considerations .....	65
2.4 Conclusions .....	67
2.5 Experimental section .....	68
2.6 References .....	70
<b>Chapter 3 Oxidation of 2° Alcohols in Unprotected Sugars</b> .....	73
3.1 General Overview and Research Strategy .....	73
3.1.1 Chemical Properties of Keto-Sugars .....	73
3.1.2 Catalyst and Reaction Condition Requirements .....	78
3.1.2.1 Reaction Medium .....	78
3.1.2.2 Solubility .....	79
3.1.2.3 Reaction Temperature .....	79
3.1.2.4 Transition Metal Catalyst .....	80
3.1.2.5 Mediator .....	80
3.1.2.6 Reaction Time Scale .....	81
3.1.2.7 Other Factors .....	81
3.1.3 Research Strategy and Model Systems .....	82
3.1.3.1 <i>Vicinal</i> -Diols .....	83
3.1.3.2 Thermodynamic and Kinetic Parameters .....	83
3.1.3.3 Theoretical Calculations of Diol Oxidations .....	87
3.1.3.4 Mono-alcohol Model Systems .....	93
3.1.3.5 Diol Model Systems .....	95
3.1.4 Reaction Monitoring .....	96
3.1.4.1 Monitoring of Model Systems .....	96
3.1.4.2 Monitoring of Sugar Substrate Systems .....	97

3.2 Catalytic Hydrogen Transfer Reactions Investigated .....	98
3.2.1 Shvo's Catalyst .....	98
3.2.1.1 Shvo's System in the Oxidation of Secondary Alcohols .....	98
3.2.1.2 Experimental Section .....	100
3.2.2 Noyori System .....	101
3.2.2.1 Introduction to Metal-Ligand Bifunctional Catalysis and Motivation .....	101
3.2.2.2 Results and Discussion .....	106
3.2.2.3 Conclusions .....	141
3.2.2.4 Experimental Section .....	142
3.3 Investigated Transition Metal Catalyzed Peroxide Oxidations .....	152
3.3.1 Molybdenum/ Tungsten Peroxide Systems .....	153
3.3.1.1 Oxidations with $(\text{NH}_4)_6\text{Mo}_7\text{O}_{24}$ and $\text{Na}_2\text{MoO}_4$ .....	153
3.3.1.2 $\text{MoO}_2(\text{acac})_2$ System .....	155
3.3.1.3 Modification of the Molybdenum Catalyst .....	159
3.3.1.4 Mo and W Oxo-Diperoxo-Pyridine-2-Carboxylate Complexes .....	163
3.3.1.5 Concluding Remarks .....	168
3.3.1.6 Experimental Section .....	169
3.3.2 $\text{NiCl}_2$ Mediated Benzoylperoxide System .....	173
3.3.2.1 Known Applications of $\text{NiBr}_2/\text{Bz}_2\text{O}_2$ in Alcohol Oxidations .....	173
3.3.2.2 Results and Discussion .....	176
3.3.2.3 Conclusion .....	186
3.3.2.4 Experimental Section .....	187
3.4 Investigated Stoichiometric Oxidation Reaction .....	188
3.4.1 Introduction to the $\text{NaBrO}_3/\text{NaHSO}_3$ System .....	188
3.4.2 Results .....	189
3.4.2.1 pH dependence .....	189
3.4.2.2 $\text{NaBrO}_3/\text{NaHSO}_3$ Reagent Stoichiometry .....	191
3.4.2.3 Solvent and Temperature .....	193
3.4.2.4 Substrates .....	193
3.4.2.5 Other Oxidizing Conditions .....	195
3.4.3 Discussion .....	197
3.4.3.1 Equilibria and $\text{HOBr}$ .....	197
3.4.3.2 pH Dependence .....	197
3.4.3.3 Control Experiments .....	198
3.4.3.4 Oxidation Mechanism and Selectivity .....	199
3.4.4 Conclusion .....	201
3.4.5 Experimental Section .....	201
3.5 References .....	203

---

Appendix .....	209
Calculation spread-sheet for $k_1 = k_2 = k_3$ .....	210
$^1\text{H}$ and $^{13}\text{C}$ NMR spectra.....	211
$\delta$ -D-gluconolactone .....	212
$\gamma$ -D-gluconolactone .....	216
$\delta$ -D-mannonolactone .....	220
$\gamma$ -D-mannonolactone .....	224
$\delta$ -D-galactonolactone .....	228
$\gamma$ -D-galactonolactone .....	232
<i>N</i> -( <i>p</i> -toluyl-sulfonyl)-1,2-diamino-1,1,2,2-tetramethylethane ( <b>72</b> ).....	236
( $\eta^6$ -1-isopropyl-4-methyl-benzene) <i>N</i> - <i>p</i> -tosyl- <i>ortho</i> -diaminobenzene ruthenium(II) ( <b>77</b> ). .....	238
( $\eta^6$ -1-isopropyl-4-methyl-benzene)- <i>N</i> -( <i>p</i> -tolyl-sulfonyl)-1,2-diamino- 1,1,2,2-tetramethyl-ethane ruthenium(II) ( <b>78</b> ) .....	240
Table of Figures .....	246
Table of Schemes .....	248
Table of Tables .....	250
Curriculum Vitae.....	252

## Acknowledgements

I thank my supervisor Prof. Marcel Schlaf at the University of Guelph for his guidance through this research project and nurturing my interest in chemistry. I gained invaluable experience in the past years and hope to adopt his style of research in the future. I also thank Prof. Peter Klüfers as my advisory representative at the Ludwig-Maximilians Universität München whose support enabled me to conduct this international research project.

A special thank you goes to the Ernst-Schering Research Foundation, Berlin, Germany, for the financial support with a generous doctoral stipend.

I would like to thank the Prof. Schlaf research group members Dr. Martin Bosch, Dr. Mee-Kyung Chung, Ryan Dykeman, Michelle Thibault and Zie Xie as well my peers from other research laboratories for interesting academic and non-academic discussions. I appreciated the assistance of undergraduate students who conducted the preliminary works on the Noyori systems: Ebbing de Jong and Magda Dymarska. As well, I thank Jennessa Youm (NiBr<sub>2</sub> Benzoylperoxide System), Paul D'Hondt (NaHSO<sub>3</sub>/ NaBrO<sub>3</sub> reagent) and De-ann Rollings (Mo Catalyzed Peroxidations) who conducted an undergraduate research project under my laboratory assistance. I learned a lot about assisting and guiding others in research and wish them the best for their future.

I also would like to thank Valerie Robertson of the NMR centre of the University of Guelph for her help and technical support with NMR experiments and Prof. John Goddard for helpful discussion about computational methods and *in silico* experiments.

Last but not least, I would like to thank my friends and family, especially my wife Melanie Gunson, for their support in my endeavour of conducting this research project.



## Abstract

Oxidation reactions of sugars to their corresponding lactones and the selective oxidation of a secondary alcohol of sugar substrates to keto-sugars using transition metal catalysis were investigated.

Research results demonstrate that Shvo's hydrogen-transfer catalyst,  $[(\eta^4\text{-C}_6\text{H}_4\text{CO})(\text{CO})_2\text{Ru}]_2$ , selectively oxidized unprotected sugars to  $\delta$ -lactones under very mild conditions. This is the first method to synthesize  $\delta$ -D-galactonolactone, the first oxidation product of the 3<sup>rd</sup> most abundant sugar.  $\delta$ -D-Galactonolactone was fully characterized by conformational analysis through NMR experiments and computational methods. We propose that in aprotic, anhydrous solvents the  $\delta \rightarrow \gamma$  lactone rearrangement mechanism proceeds via a bicyclic transition state.

The oxidation of alicyclic *vicinal* diols to  $\alpha$ -hydroxy ketones was investigated as a model system for the selective oxidation of a secondary hydroxyl group in sugar substrates to keto-sugars. The challenge was to develop a method that allows selective oxidation, yet prevents over-oxidation to the dione or dicarboxylic acids products. Based on a mathematical model of consecutive bimolecular reactions, the rate constants for the initial oxidation step  $k_1(\text{diol} \rightarrow \alpha\text{-OH ketone})$  and second oxidation step  $k_2(\alpha\text{-OH ketone} \rightarrow \text{dione})$  must be  $k_1 > 10 k_2$  in order to obtain a synthetically useful method for  $\alpha$ -hydroxy ketone synthesis.

The metal-ligand bifunctional hydrogen transfer reactions of Shvo's catalyst and Noyori's  $\eta^6$ -arene *N*-tosyl-1,2-diaminoethane ruthenium(II) complexes were investigated with alcohol model systems and it was concluded that hydrogen transfer reactions are insufficient in the oxidation of *vicinal* diols due to an unfavourable position of the equilibrium. Under oxidizing conditions, the 16-electron ruthenium complexes of the Noyori systems compete with a  $\beta$ -elimination process and thus new degradation resistant ligands were synthesized. The apparent slower oxidation of Noyori's  $\eta^6$ -arene *N*-tosyl-1,2-diaminoethane ruthenium(II) complexes under oxidizing conditions, i.e. in acetone or cyclohexanone solvent, was investigated through NMR and IR experiments finding no evidence of a kinetic inhibition by the solvent. We

propose that the slower reactions depend on a relatively high energy barrier for the reaction of the 16-electron complex with a hydrogen donor and that a kinetic model must account for two effectively different oxidation and reduction catalysts. In an alcohol/ketone equal-concentration experiment with Noyori-type ruthenium(II) complexes a linear relationship was found between the initial rate of alcohol consumption/production and  $\Delta G^\circ$ .

Reactions involving peroxides as the oxidant were investigated in order to avoid equilibrium processes. The oxidation of alcohol model systems with several Mo and W catalysts and peroxide sources indicated a deactivation of the Mo and W catalysts by formation of water or hydroxide complexes. The product distribution of the oxidation of *trans*-1,2-cyclohexanediol with the  $\text{MoO}_2(\text{acac})_2/\text{Na}_2\text{CO}_3 \times 1.5 \text{ H}_2\text{O}_2$  method was in agreement with the theoretical model, yet only had a  $k_1 = 1.5 k_2$  rate ratio resulting in a maximum  $\alpha$ -hydroxy cyclohexanone content of 45 %.

The  $\text{NiBr}_2$  mediated oxidation of alcohols and benzoylperoxide was investigated. The selective oxidation of *vicinal* diols was unsuccessful with this method. However, the oxidation reaction of mono-alcohol substrates was greatly improved using water in the reaction. The reaction mechanism was investigated and we propose that the actual oxidant in the  $\text{NiBr}_2$  mediated benzoylperoxide method is  $[\text{Br}^+]$ , which is generated by the hydrolysis product of benzoylhypobromite, hypobromic acid ( $\text{HOBr}$ ).

Ishii's stoichiometric  $\text{NaHSO}_3/\text{NaBrO}_3$  reagent selectively oxidized *vicinal* diols to  $\alpha$ -OH ketone without overoxidation. This oxidation reaction was investigated with regards to substrate, concentration and *pH*. The reactivity and selectivity were studied and it was found that the oxidation mechanism is based on a multitude of comproportionation and disproportionation equilibria at low *pH*. A small but steadily replenished  $\text{HOBr}$  concentration is the source of the actual oxidant and effectively acts as a redox buffer. While the  $\text{NaHSO}_3/\text{NaBrO}_3$  reagent demonstrated excellent selectivities with the alcohol model systems, the oxidation of sugar substrates failed due to side-reactions occurring at the required low *pH*.

## Zusammenfassung

Die Oxidationsreaktionen von Zuckern zu den entsprechenden Zuckerlaktone sowie die selektive Oxidation von sekundären Zuckeralkoholfunktionen zu den entsprechenden Keto-Zuckern wurde anhand von Übergangsmetallkatalysatoren untersucht.

Shvos Wasserstofftransferkatalysator,  $[(\eta^4\text{-C}_4\text{Ph}_4\text{CO})(\text{CO})_2\text{Ru}]_2$ , oxidiert ungeschützte Zucker selektiv zu den  $\delta$ -Laktone unter sehr milden Reaktionsbedingungen. Dies ist die erste Methode zur Herstellung von  $\delta$ -D-Galactonolaktone, das erste Oxidationsprodukt des dritthäufigsten Zuckers.  $\delta$ -D-Galactonolaktone wurde mittels Konformationsanalyse auf der Basis von NMR Experimenten und theoretischen Rechnungen vollständig charakterisiert. Für die  $\delta \rightarrow \gamma$  Laktonisomerisierung schlagen wir einen Umlagerungsmechanismus vor, der in aprotischen, trockenen Lösungsmitteln über einen bizyklischen Übergangszustand führt.

Als Modellsystem für die selektive Oxidation der sekundären Alkoholgruppe in Zuckersubstraten zu Keto-Zuckern wurde die Oxidierung von *vicinalen* Diolen zu  $\alpha$ -Hydroxyketonen untersucht. Die Herausforderung bestand darin, eine Methode zu finden, die die selektive Oxidation von Diolen zu  $\alpha$ -Hydroxyketonen ermöglicht, jedoch die Überoxidierung zu Dienen oder Dicarbonsäuren verhindert. Mit der Annahme von bimolekularen Folgereaktionen wurde ein mathematisches Modell aufgestellt. Für eine praktische Versuchsvorschrift zur Synthese von  $\alpha$ -Hydroxyketonen müssen die Reaktionskonstanten für den ersten und zweiten Reaktionsschritt  $k_1(\text{Diol} \rightarrow \alpha\text{-OH Keton})$  und  $k_2(\alpha\text{-OH Keton} \rightarrow \text{Dion})$  ein Verhältnis von mindestens  $k_1 > 10 k_2$  besitzen.

Die bifunktionale Metall-Ligand Wasserstofftransferreaktionen von Shvos Katalysator und Noyoris  $\eta^6$ -Arene *N*-Tosyl-1,2-diaminoethan Ruthenium(II) Komplexen wurden anhand von Alkoholmodellsystemen untersucht. Für die Oxidierung von *vicinalen* Diolen sind sie aufgrund einer benachteiligenden Gleichgewichtslage unzureichend. Unter oxidierenden Bedingungen konkurrieren Wasserstofftransferreaktionen mit einer  $\beta$ -Hydrideliminierungsreaktion der

Ruthenium(II) 16 Elektronenkomplexe. Deshalb wurden degradierungsbeständige Liganden synthetisiert.

Die langsamen Oxidierungsreaktionen von Noyoris  $\eta^6$ -Arene *N*-Tosyl-1,2-diaminoethan Ruthenium(II) Komplexen unter oxidierenden Bedingungen, d.h. in Aceton oder Cyclohexanon als Lösungsmittel, wurden mit NMR und IR Methoden untersucht. Es wurde kein Beweis für eine kinetische Hemmung durch das Lösungsmittel gefunden. Es erscheint, dass die langsame Reaktionsgeschwindigkeit von einer hohen Aktivierungsenergie der Reaktion des 16-Elektronenrutheniumkomplexes mit einem Wasserstoffdonor abhängt und dass ein kinetisches Modell zwei effektiv verschiedene Oxidierungs- und Reduktionskatalystoren berücksichtigen muss. In einem Experiment, das gleiche Konzentrationen von Alkohol und Ketone beinhaltet, wurde ein linearer Zusammenhang zwischen Anfangsrate der Alkoholherstellung bzw. -konsumierung und  $\Delta G^\circ$  gefunden.

Bei Oxidierungen von Alkoholen mit Peroxiden als Oxidationsmittel werden die Probleme einer Gleichgewichtsreaktion umgangen, da das Gleichgewicht vollständig auf der Produktseite liegt. Die Oxidierung von Alkoholmodellsystemen mit mehreren Mo und W Katalysatoren sowie Peroxidverbindungen wurde untersucht. Durch die Bildung von Wasser- bzw. Hydroxidkomplexen werden die Katalysatoren deaktiviert. Die Produktverteilung der *trans*-1,2-Cyclohexandioloxidierung mit  $\text{MoO}_2(\text{acac})_2/\text{Na}_2\text{CO}_3 \times 1.5 \text{ H}_2\text{O}_2$  stimmte mit den theoretischen Berechnungen überein, jedoch das erzielte Reaktionskonstantenverhältnis von  $k_1 = 1.5 k_2$  ergab nur eine Maximalausbeute von 45 %  $\alpha$ -Hydroxycyclohexanon.

Die selektive Oxidierung von *vicinalen* Diolen war mit der  $\text{NiBr}_2$ / Benzoylperoxid Methode leider erfolglos, jedoch wurde die Oxidierungsreaktion von Monoalkoholen stark verbessert, wenn Wasser zur Reaktionsmischung zugegeben wurde. Als Reaktionsmechanismus schlagen wir vor, dass das eigentlich Oxidationsmittel der  $\text{NiBr}_2$ / Benzoylperoxid Methode  $[\text{Br}^+]$  ist, das aus dem Hydrolyseprodukt von Benzoylhypobromit, der unterbromigen Säure (HOBr), erzeugt wird.

Ishiis stöchiometrisches  $\text{NaHSO}_3/\text{NaBrO}_3$  Reagenz oxidiert *vicinale* Dirole selektiv zu  $\alpha$ -Hydroxyketonen ohne Überoxidierung. Der Oxidations-mechanismus wurde im Hinblick auf Substrat, Konzentration und  $\text{pH}$  Wert untersucht. Die Aktivität und Selektivität dieser Oxidierungsmethode basiert auf einem Netzwerk aus Komproportionierungs- und Disproportionierungs-gleichgewichten bei niedrigen  $\text{pH}$  Werten. Eine kleine, aber ständig erneuerte,  $\text{HOBr}$  Konzentration ist die Ursache für die Oxidation und verhält sich wie ein Redoxpuffer. Während das  $\text{NaHSO}_3/\text{NaBrO}_3$  Reagenz sehr gute Selektivitäten für die Alkoholmodellsysteme zeigt, scheitert es an der Oxidierung von Zuckern, da Nebenreaktionen unter den niedrigen  $\text{pH}$  Werten stattfinden.

## Abbreviations

AHA	alpha hydroxy acids
br	broad
calc.	calculated
CAS	chemical abstracts service
conc.	concentrated
COSY	correlation spectroscopy
cycl.	cyclization
d	doublet
dd	doublet of doublets
ddd	doublet of doublets of doublets
DFT	density functional theory
DMA	<i>N,N</i> -dimethylacetamide
DMF	<i>N,N</i> -dimethylformamide
DMSO	dimethylsulfoxide
dppp	1,3-bis(diphenylphosphino)propane
ee	enantiomeric excess
EI	electron impact
en	1,2-diamino-ethane
eq.	equivalent
Eq.	equation
equiv.	Equivalent
ESI	electrospray ionization
EtOAc	ethyl acetate
exp.	experimental
FID	flame ionization detector
FT-IR	Fourier transform-infra red spectroscopy
Gal	galactose
GC	gas chromatography
Glu	glucose
G98	Gaussian 98 program
HMPT	hexamethylphosphortriamide
HPLC	high pressure liquid chromatography
HSQC	heteronuclear single quantum coherence
<i>J</i>	coupling constant
Lit.	literature
m	multiplet
Man	mannose
<i>m</i> CPBA	<i>meta</i> -chloroperbenzoic acid
MS	mass spectrometry
n/a	not applicable
NAD <sup>+</sup>	nicotinamide adenine dinucleotide
NMP	<i>N</i> -methyl-2-pyrrolidinone
o	octuplet
p.	page

PC	personal computer
PEG	polyethyleneglycol
ppm	parts per million
q	quartet
qui	quintet
RI	refractive index
rpm	rounds per minute
Rxn	reaction
s	singlet
sept.	septet
SPC	sodium percarbonate
t	triplet
Tetracyclone	2,3,4,5-tetraphenyl-cyclopentadienone
THF	tetrahydrofuran
TLC	thin layer chromatography
TMS	trimethylsilyl
TOF	turn over frequency
TON	turn over number
Tos	<i>para</i> -toluene-sulfonyl
trityl	triphenylmethyl
UV/VIS	Ultra violet/ visible light spectroscopy
Vol%	volume %
vs.	versus
wt%	weight %

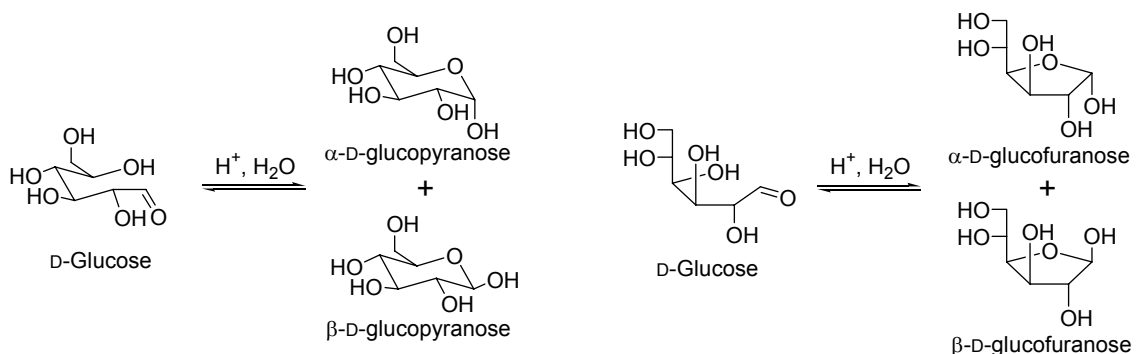
## Chapter 1 The Chemistry of Sugars, Transition Metal Catalysis and Research Motivation

### 1.1 General Significance and Features of Sugars and Their Oxidation Products

#### 1.1.1 Definitions and Properties of Sugars

Sugars are a class of organic compounds containing several hydroxy functional groups and a carbonyl group (aldehyde or ketone) with the capability of forming an intramolecular hemiacetal or hemiketal.<sup>1</sup> The nomenclature suffix “ose” is used to denote a sugar. The common usage of the word “sugar” signifies table sugar, which is a disaccharide (sucrose) containing one monosaccharide each of D-glucose and D-fructose. The monosaccharides also known as simple sugars possess the general formula  $C_nH_{2n}O_n$ . The name carbohydrate originates falsely from “carbon hydrate”  $[C(H_2O)]_n$  which one water molecule was said to be bound to carbon.<sup>1</sup> Despite this initial structural description, the name carbohydrate has been adopted in literature.

**Scheme 1.1** illustrates the formation of the hemiacetal using the D-glucose molecule. The intramolecular hemiacetal unit forms a six-membered pyranose and a five-membered furanose. In addition, each six or five membered hemiacetal ring can form an  $\alpha$ - or  $\beta$ - anomer at C1, commonly referred to as the anomeric centre.<sup>1</sup>



**Scheme 1.1** D-glucose transformation into  $\alpha$ - and  $\beta$ -D-glucopyranose and D-glucofuranose.



The monosaccharides are classified according to the number of carbon atoms they contain: triose ( $n = 3$ ), tetrose ( $n = 4$ ), pentose ( $n = 5$ ), hexose ( $n = 6$ ), heptose ( $n = 7$ ) etc.<sup>1</sup> The simplest basic building block is glyceraldehyde possessing only one asymmetric centre and therefore two enantiomers. Another type of classification of sugar compounds is by the nature of the carbonyl groups in their free, open chain form. A sugar containing an aldehyde is denoted “aldose” and one containing a ketone is denoted “ketose”. Based on the fundamental works of van't Hoff and Fischer, an aldopentose has eight isomers and an aldohexose has sixteen isomers.<sup>2,3</sup>

It is evident that there are a large number of sugars, beyond what is illustrated, exhibiting increasing structural complexity. The structural complexity increases further when consideration is given to combinations of monosaccharides leading to disaccharides, oligosaccharides and polysaccharides.<sup>1,4</sup>

Nature does not provide sugars in equal abundance. The most abundant monosaccharide is (+)-D-glucose, also commonly known as grape sugar, followed by (+)-D-mannose and (+)-D-galactose.<sup>1</sup> The least available monosaccharides are L-altrose, L- and D-idose as well L- and D-gulose, all of which are hexoses.<sup>1</sup>

As briefly mention before aldohexoses exist as different sixteen isomers, i.e. eight sets of enantiomeric pairs. Two diastereomers, which differ at only on one inverted asymmetric centre are called epimers. An overview of the epimeric relations starting from all-equatorial D-glucose and all-axial D-idose is outlined in **Figure 1.1**.

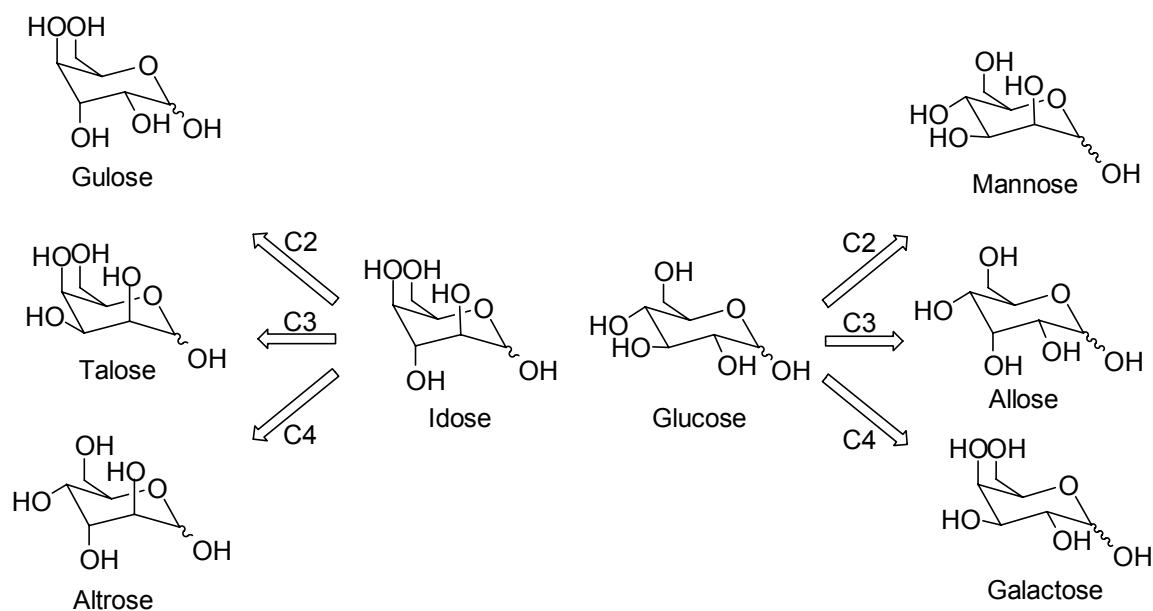


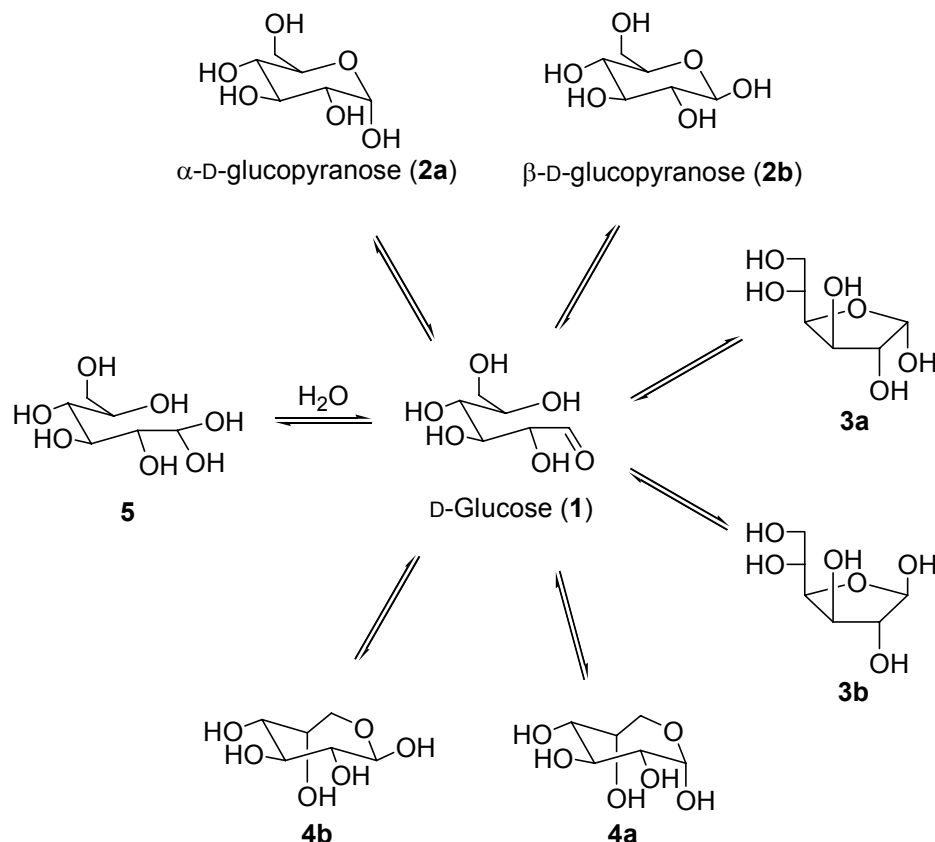
**Figure 1.1** Epimeric relations of  $\alpha$ - and  $\beta$ -D-glucopyranose and  $\alpha$ - and  $\beta$ -D-idopyranose. Arrows indicate epimerization at the respective carbon atom.

### 1.1.2 Equilibria and Mutarotation of Sugars

$\alpha$ -/ $\beta$ -D-Glucopyranose is very stable as a solid. However, isomerization occurs rapidly in aqueous solution through mutarotation as shown in **Scheme 1.2**.<sup>1,5</sup> In aqueous solution seven equilibria exist within the D-glucose system (**1**).<sup>1</sup> All products of these equilibria are isomers of D-glucose with the exception of **5**, which is a hydrated form. The transformation pathways to all products occur via the open chain form of D-glucose (**1**). The most predominant form is  $\alpha$ -D-glucopyranose (**2a**) followed by  $\beta$ -D-glucopyranose (**2b**).<sup>\*</sup> The two five membered ring forms are the D-glucofuranoses (**3a**) with  $\alpha$  configuration and (**3b**) with  $\beta$  respectively. The least stable seven membered forms **4a, b** play only a very minor role in the equilibria network. The hydrated species **5** is acyclic similar to **1**. Each of the equilibria constants vary with different solvent and temperature.

<sup>\*</sup> The descriptors “**a**” and “**b**” indicate here the  $\alpha$ - and  $\beta$ -forms, respectively.

Fortunately, in solution the pyranoses **2a**, **b** are predominately present and the other products can be neglected as their contents are less the 0.1%.<sup>1</sup>



**Scheme 1.2** Equilibria of glucose in aqueous solution.

### 1.1.3 Sugar Derivatives and Their Applications

Many derivatives of sugars are known.<sup>1,6</sup> One of the most commonly occurring derivatization of sugars is the substitution of a free hydroxyl group (**Figure 1.2**). The alcohol is transformed with the simplest substituent, hydrogen, into a deoxy sugar, e.g. 2-deoxy-ribose, which is a fundamental building block of DNA in biological systems. Another common substituent is an amino group, which e.g. can be found in glucosamine. Amino-deoxy sugar derivatives possess important biological functions, in particular *N*-acetyl glucosamine, which is a monomer in

the exoskeleton of insects, chitin. Halogenated sugars are an example of man-made derivatives. E.g. sucralose (Splenda®) contains three chlorine atoms and is used as an artificial sweetener without caloric content for humans.<sup>7</sup>

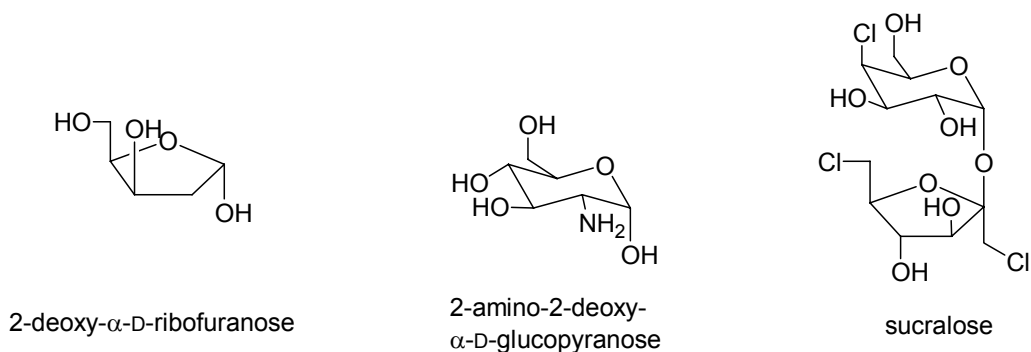
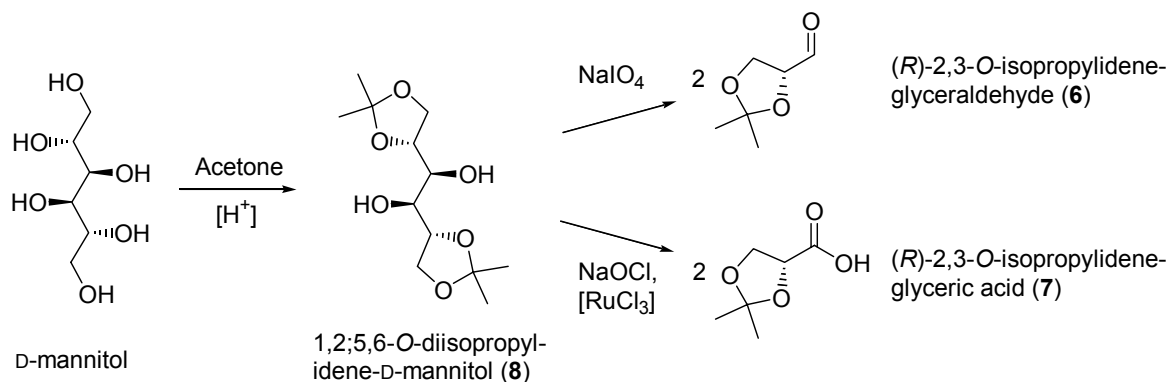


**Figure 1.2** Examples of simple sugar derivatives.

Carbohydrates and their derivatives are a readily available source of the chiral pool.<sup>6,8,9</sup> To highlight one example, D-mannitol is commonly used in the synthesis of enantiopure glyceraldehyde (**6**) and glyceric acid (**7**) derivatives as illustrated in **Scheme 1.3**.<sup>10</sup> D-(+)-Mannitol is optically pure and obtained from the reduction of D-(+)-mannose. When protected with isopropylidene (**8**) the C3-C4 carbon bond can be cleaved in a subsequent reaction step using sodium periodate or ruthenium catalysis with sodium hypochlorite as oxidant and yielding

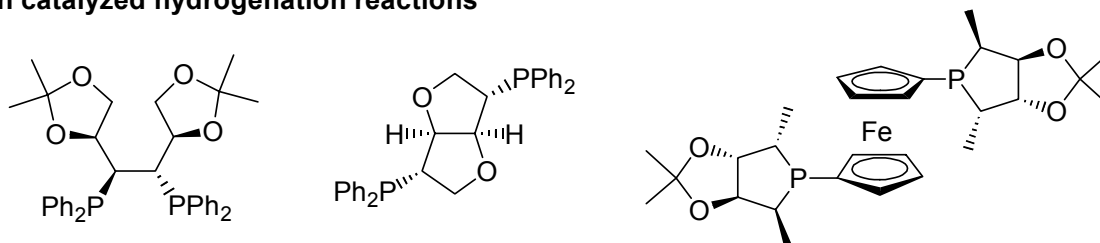


**Scheme 1.3** D-Mannitol as source for enantiopure glyceraldehyde and glyceric acid derivatives.

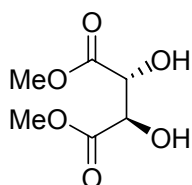
the aldehyde (**6**) or the acid (**7**). The  $C_2$  symmetry of D-mannitol makes this process synthetically very useful as two chiral products containing a 3-carbon backbone are produced.

Especially – but not exclusively – phosphine sugar derivatives have been used as chiral ligands for catalytic transformations such as hydrogenation, transition metal catalyzed cross-coupling reactions, epoxidation and addition reactions (**Figure 1.3**).<sup>8</sup>

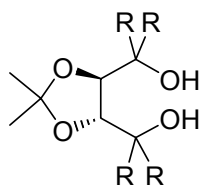
#### Rh catalyzed hydrogenation reactions



#### Ti catalyzed epoxidations



#### Ti catalyzed 1,2-additions to aldehydes



#### Ni catalyzed cross-coupling reactions

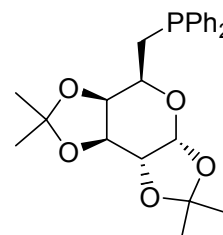


**Figure 1.3** Few highlights for sugar derived chiral ligands used in various chemical reactions.<sup>8</sup>

### 1.1.4 Oxidation Products of Sugars

Aldopyranoses and -furanoses possess three different alcohol functionalities: a primary alcohol, three secondary alcohol groups and one hemiacetal hydroxyl group. These hydroxyl functionalities are identified in **Figure 1.4** with  $\alpha$ -D-glucopyranose as an example.

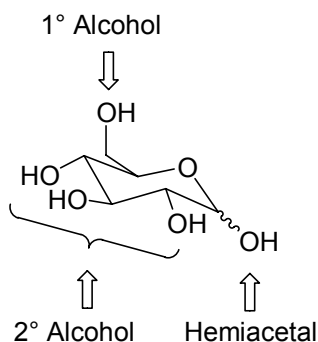
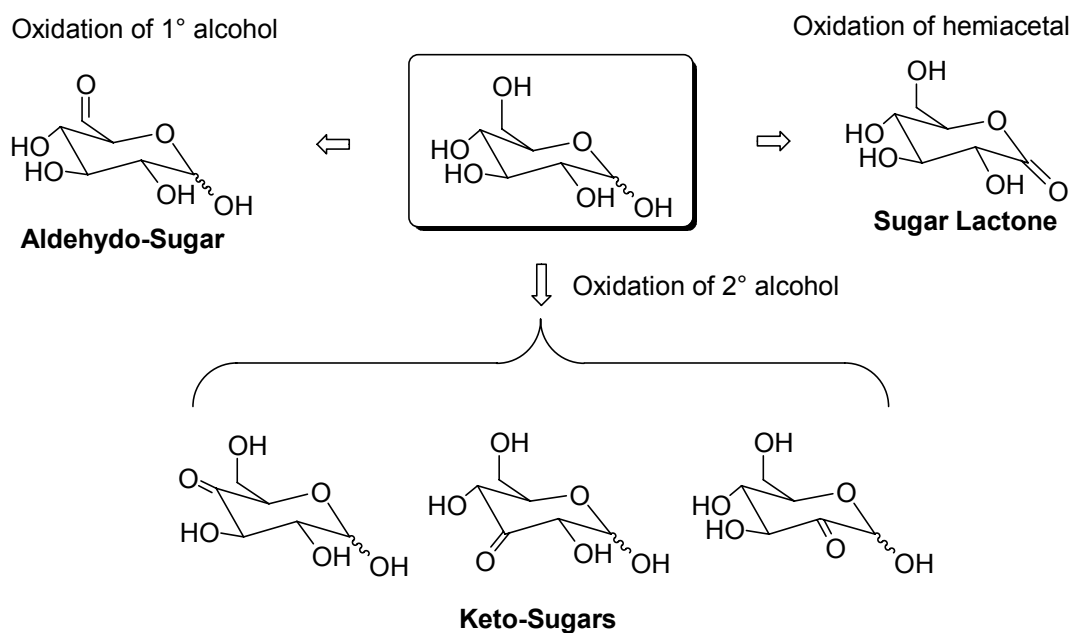


**Figure 1.4** Different hydroxyl groups of  $\alpha$ -D-glucopyranose.

Each of these OH groups can be oxidized to corresponding sugar derivatives as shown in **Scheme 1.4**. Sugar lactones can be generated by the oxidation at the C1 terminus. Three possible keto-sugars can be generated by oxidation of any of the secondary alcohol function. By oxidation of the primary alcohol an aldehydo-sugar is formed.



**Scheme 1.4** First oxidation products of glucopyranose.

### 1.1.4.1 Definition, Occurrence and Applications of Sugar Lactones

A sugar lactone, also known as aldonolactone, is defined as an intramolecular ester of a monosaccharide as shown in **Figure 1.5**.<sup>1</sup> The most common occurring sugar lactones are six-membered or five-membered rings. The six-membered lactones are also described as  $\delta$ -, pyrano- or 1,5-lactones. The five-membered lactones are known as  $\gamma$ - or furano- or 1,4-lactones.<sup>1</sup>

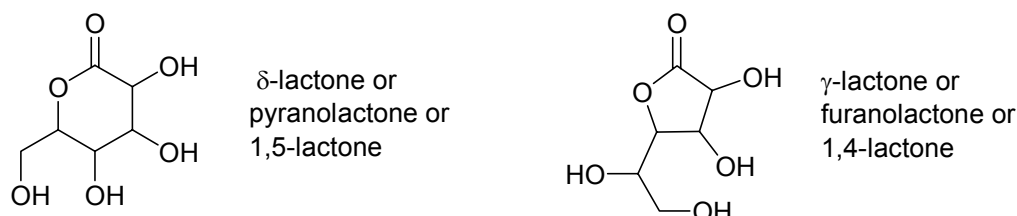


**Figure 1.5** Six-membered and five-membered sugar lactones derived from aldohexoses.

All  $\gamma$ -lactones of the three most abundant aldohexoses, glucose, mannose and galactose, have been known for almost a century.<sup>11-14</sup> The free  $\delta$ -lactones exist only from glucose and mannose.<sup>14</sup> There exists a CAS entry number for  $\delta$ -D-galactonolactone but it contains no synthetic preparation data. Only preparation for tetra-O-benzylated derivative of  $\delta$ -galactonolactone has been described.<sup>14,15</sup> An X-ray structure has been reported for  $\delta$ -gluconolactone.<sup>16</sup>

Sugar lactones do occur in nature.<sup>17</sup> They have been isolated from beans, alfalfa and clover and have been identified by their per-trimethylsilylated derivatives through exhaustive silylation of the plant extracts with TMSCl. The per-silylated derivatives have been separated and analyzed by GC-MS. Up to 20 different sugar derived acids and ten different sugar lactones were present in these natural product extracts.

The most commonly used sugar lactone is  $\delta$ -D-gluconolactone. It functions as leavening agent and preservative in baked goods.<sup>18,19</sup> Commercial production

values for  $\delta$ -D-gluconolactone reached  $20 \times 10^3$  t per year worldwide in 1997.<sup>18</sup> The white solids are also commercially available at chemical suppliers for approximately 16 Cdn\$ (~ 10 €) per 100 g.<sup>20</sup> The lactone undergoes a slow hydrolysis to its free acid, which will release continuously protons exhibiting its preserving properties. Hydrolysis studies and  $^{18}\text{O}$  label experiments have been reported for both free  $\gamma$ - and  $\delta$ -gluconolactones pointing to an intramolecular process based on the results of the lack of oxygen exchange of water solvent and the two lactone oxygen atoms during hydrolysis.<sup>21</sup>

Aldonolactones are also used and advertised in the cosmetic industry under the term "alpha-hydroxy acids" (AHA) in cosmetical products. The lactones exhibit properties of improving skin condition and antiaging effects.<sup>22</sup> 1,5-D-fuconolactone stimulates hair growth due to a glycosamine-glycanase inhibition as stated in a patent by the Unilever company.<sup>23</sup> Further, it is used as shampoo additive to decrease undesirable hair stickiness and stiffness.<sup>23</sup> A medical application for aldonolactones is as an additive in the administering of vitamin C.<sup>24</sup>

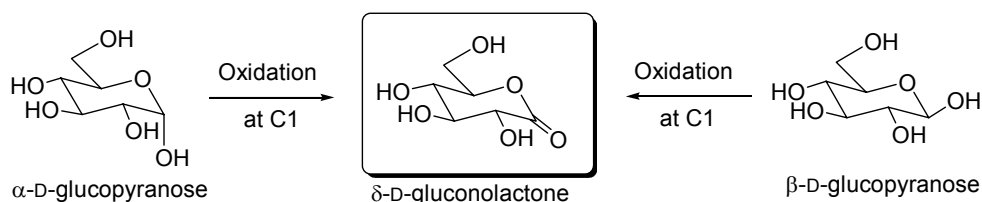
#### 1.1.4.2 Synthesis of Sugar Lactones

The ester functionality in the sugar lactone is generated by oxidation of the sugar at its C1 position. The generation of the lactone can be accomplished via two pathways. One pathway is the oxidation of the free aldehyde to the open chain sugar acid followed by a subsequent cyclization step, i.e. intramolecular esterification. In the other synthetic pathway the hemiacetal group of the cyclic sugar is directly oxidized to the lactone by a formal loss of hydrogen.

The free hemiacetal hydroxyl function in a reducing sugar will lose its stereochemical, chiral information upon oxidation; i.e. both, the  $\alpha$ - and  $\beta$ -anomer, are oxidized to the same sugar lactone (**Scheme 1.5**). The  $\alpha$ - and  $\beta$ -anomer are



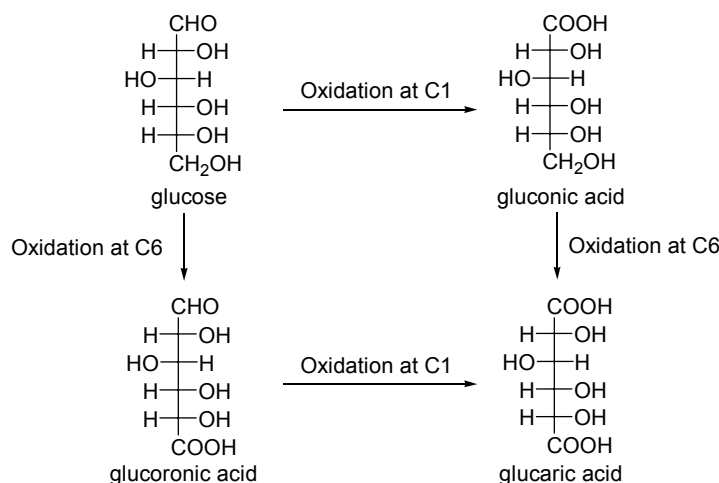
diastereomers and differ in their achiral properties which will intrinsically make them differently susceptible towards oxidation.<sup>1</sup> It was observed that the  $\beta$ -D-glucopyranose reacted 250 times faster than  $\alpha$ -D-under aqueous bromine oxidation condition.<sup>13</sup>



**Scheme 1.5** Oxidation of  $\alpha$ -D-glucopyranose and  $\beta$ -D-glucopyranose to  $\delta$ -D-gluconolactone.

The free sugar acids can be obtained by oxidation with aqueous bromine solutions or electrochemically from their corresponding free mono-saccharides.<sup>12,13,15</sup> Another access to aldonic acids is possible through the Kiliani method, in which the aldose sugar is reacted with cyanide and the resulting epimeric cyanohydrins are then hydrolyzed to the homologous aldonic acids.<sup>11,25</sup> In this case the carbon chain is of course lengthened by one atom, i.e. a hexose would yield a heptonic acid. Strong oxidants such as nitric acid oxidize also the primary alcohol to a carboxylic acid generating dicarboxylic acids. Possible oxidation reactions of glucose at C1 and C6 are summarized in

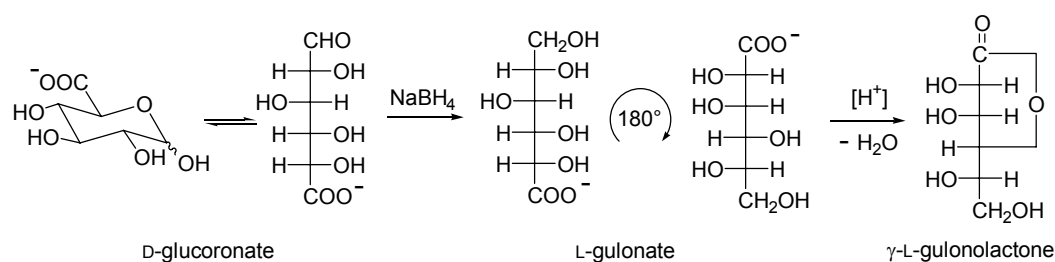
**Scheme 1.6.**<sup>25</sup>



**Scheme 1.6** Possible products in the oxidation at C1 and C6 terminus of glucose.

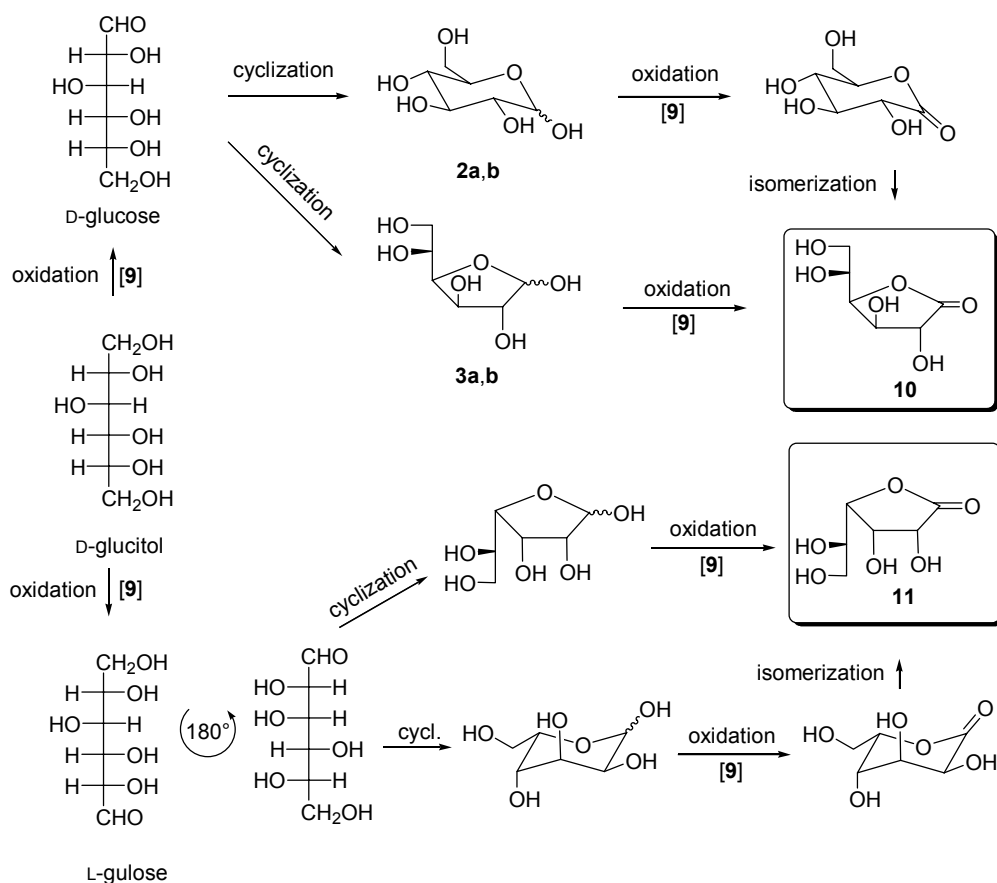
Depending on temperature and solvent,  $\delta$ - and  $\gamma$ -lactones are isolated from the aqueous reaction solutions in various proportions. The isolated lactones have been recrystallized from hot water/ dioxane solutions with respective seed crystals.<sup>12,13</sup> It has been noted that for the preparation of the  $\delta$ -lactones proper crystal seeds must be used and that the reaction should be conducted at lower temperature.  $\delta$ -Mannonolactone has to date only been isolated once through an elaborate sequence of fractional crystallizations using sodium and calcium oxalate while  $\delta$ -galactonolactone has never been isolated and only  $\gamma$ -galactonolactone is known.<sup>12</sup> The problem with this lactone preparation methodology is that the required crystallization seeds are not easily obtained. Absence of crystallization seeds produces syrupy substances and not crystalline products. At higher temperature and in presence of mineral acids the thermodynamically more stable  $\gamma$ -lactone is preferably formed over the  $\delta$ -lactone because of the lower ring strain energy of the  $\gamma$ -lactone.<sup>21,26-28</sup> In aqueous solution, apart from hydrolysis<sup>21</sup>, isomerization from the  $\delta$ -lactone to the  $\gamma$ -form occurs rapidly and mixtures of both lactones are obtained. Thus out of an equilibrated solution from mannonolactone only the  $\gamma$ -mannonolactone can be isolated.<sup>12</sup>

A preparation for L- $\gamma$ -galactonolactone and  $\gamma$ -L-gulonolactone was reported by Wolfrom *et al.* reducing the mixed calcium sodium salt of D-galacturonic acid and D-glucuronic acid with sodium borohydride under slightly basic conditions (**Scheme 1.7**).<sup>29</sup> Lactonization occurred when the product was passed through an ion exchange column. The resulting syrup was recrystallized from hot ethanol.



**Scheme 1.7** Synthesis of  $\gamma$ -L-gulonolactone from D-glucuronate by reduction with  $\text{NaBH}_4$  and lactonization.

Unprotected hexitols can also be transformed exclusively into  $\gamma$ -lactones by the transfer hydrogenation catalyst,  $\text{RhH}(\text{PPh}_3)_4$  (**9**), in DMF and benzylidenacetone as hydrogen acceptor.<sup>30,31</sup> For example, the rhodium complex **9** oxidizes D-glucitol to  $\gamma$ -D-gluconolactone (**10**) and  $\gamma$ -L-gulonolactone (**11**) in a ratio of 2.2 : 1 in 96 % overall yield.<sup>30,31</sup> The proposed reaction pathways are shown in **Scheme 1.8**.<sup>30</sup> Each of the two primary alcohols can be oxidized to the aldehyde and can cyclize to the glucose and gulose. Multiple pathways of oxidation of the furanose to the  $\gamma$ -lactone and pyranose to the  $\delta$ -lactone with subsequent isomerization to the respective  $\gamma$ -lactones were proposed by Isaak and co-workers.



**Scheme 1.8** Reaction pathways of D-glucitol to  $\gamma$ -D-gluconolactone and  $\gamma$ -L-gulonolactone.

On an industrial scale  $\delta$ -D-gluconolactone is produced by an enzymatic process using a glucose-dehydrogenase.<sup>18,19</sup>

As stated before  $\delta$ -D-galactonolactone has never been isolated and only been observed in solution by UV/VIS spectroscopy as a rapidly decaying intermediate in the enzymatic dehydrogenation by D-galactose dehydrogenase.<sup>32</sup> Under buffered, aqueous reaction conditions the *in situ* generated  $\delta$ -D-galactonolactone rapidly rearranges to the  $\gamma$ -D-galactonolactone with  $k = 1.0 \text{ min}^{-1}$ . The equilibrium constant between the  $\delta$  and  $\gamma$  lactones is  $K_{\text{eq}}(\gamma/\delta) > 100$  and is completely on the  $\gamma$ -D-galactonolactone product side.

#### 1.1.4.3 General Significance and Occurrence of Keto-sugars

Keto-sugars<sup>†</sup> – also known in literature as ‘oxo’-sugars or ulosiduloses<sup>9,33</sup> – have an additional keto functionality to their aldehyde/ hemiacetal or ketone/ hemiketal functional group. The keto-sugars can be prepared by the selective oxidation of one of the secondary alcohol functionalities of sugars. To date only limited information is available on the natural occurrence and biological function of the ulosiduloses.<sup>34,35</sup>

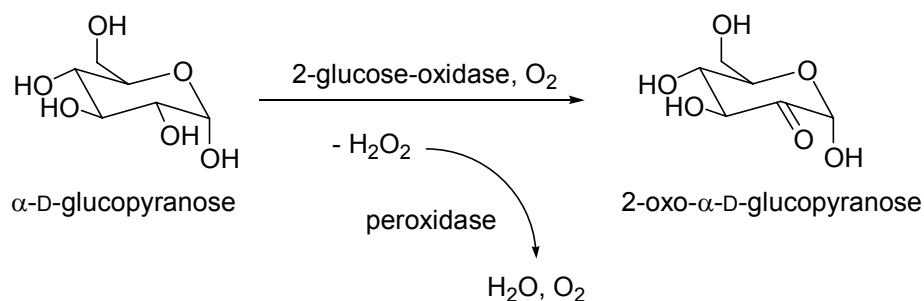
#### 1.1.4.4 Synthesis of Keto-sugars

Koepper and co-workers reported that the enzyme 2-glucose-oxidase catalyzed the oxidation of sugar substrates to 2-oxo-sugars as illustrated in **Scheme 1.9**.<sup>34-36</sup> The enzyme had been harvested from fungi. The proposed actual oxidant used by the enzyme was oxygen from the air generating hydrogen peroxide as by-product. The generated hydrogen peroxide was disproportionated to water and oxygen by a peroxidase in order to avoid undesired side reactions

---

<sup>†</sup> Note: A keto-sugar may not to be mistakenly seen as a ketose.

of hydrogen peroxide with the sugar products and enzyme present in the reaction solution.



**Scheme 1.9** Synthesis of 2-oxo- $\alpha$ -D-glucose from  $\alpha$ -D-glucose with an enzymatic process.

Unfortunately, 2-glucose-oxidase is very rare and must be isolated through a lengthy purification process.<sup>35</sup> However it is very impressive that a full characterization of the ulosiduloses was reported with such small<sup>‡</sup> quantities.<sup>35</sup> Possible hydrates of keto-sugars such as the hydrate of 2-oxo- $\alpha$ -D-glucopyranose have been identified in aqueous solutions (**Figure 1.6**).<sup>35</sup>

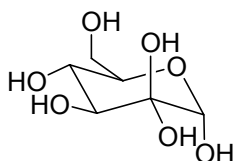


**Figure 1.6** Hydrate of 2-oxo- $\alpha$ -D-glucopyranose.

#### 1.1.4.5 Synthesis of Ulosiduloses

In contrast to the very rare free 2-oxo-sugars, much more is known about the synthesis and properties of ulosiduloses. Ulosiduloses are keto-sugars in which the anomeric hydroxyl group is bound to an alkyl or aryl group as illustrated in **Figure 1.7**. Various oxidation methods have been applied to partially

<sup>‡</sup> 2-oxo-sugars were synthesized in quantities of 3 mg.

protected monosaccharides containing one free, secondary hydroxyl, which can be oxidized to the corresponding ketone. For example, oxidation methods employed stoichiometric  $\text{RuO}_4$ ,<sup>37,38</sup> oxygen and a heterogeneous  $\text{Pt/C}$  catalyst,<sup>39</sup>  $\text{MoCl}_5$ <sup>40</sup> or Ru catalyzed oxidation with  $\text{NaOCl}$ .<sup>41</sup>

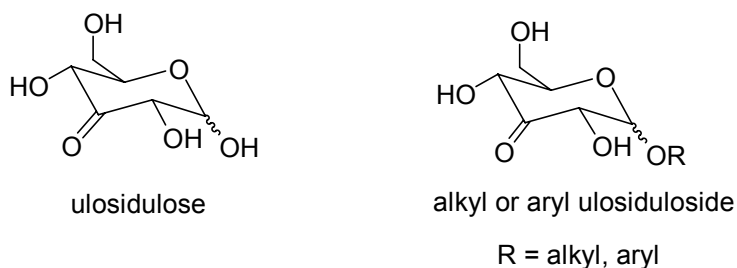


**Figure 1.7** Examples of a 3-ulosidulose and a 3-ulosidulose.

However, only oxidation reactions of unprotected monosaccharides were considered in the following literature survey.

As illustrated in **Figure 1.8**, a series of sixteen keto-sugars (**11 – 19**) has been reported by Tsuda and co-workers.<sup>9,33</sup> The tris-*n*-butyltin-oxide/ bromine method is based on a two step procedure: The first step is the selective stannylation of a *vicinal* diol functionality of the sugar substrate **20** to give a “stannyl ketal” (**Scheme 1.10**). This tin intermediate **21** was then reacted in a second reaction with  $\text{Br}_2$  resulting in the formation of the 3-keto-sugar compound **22**.

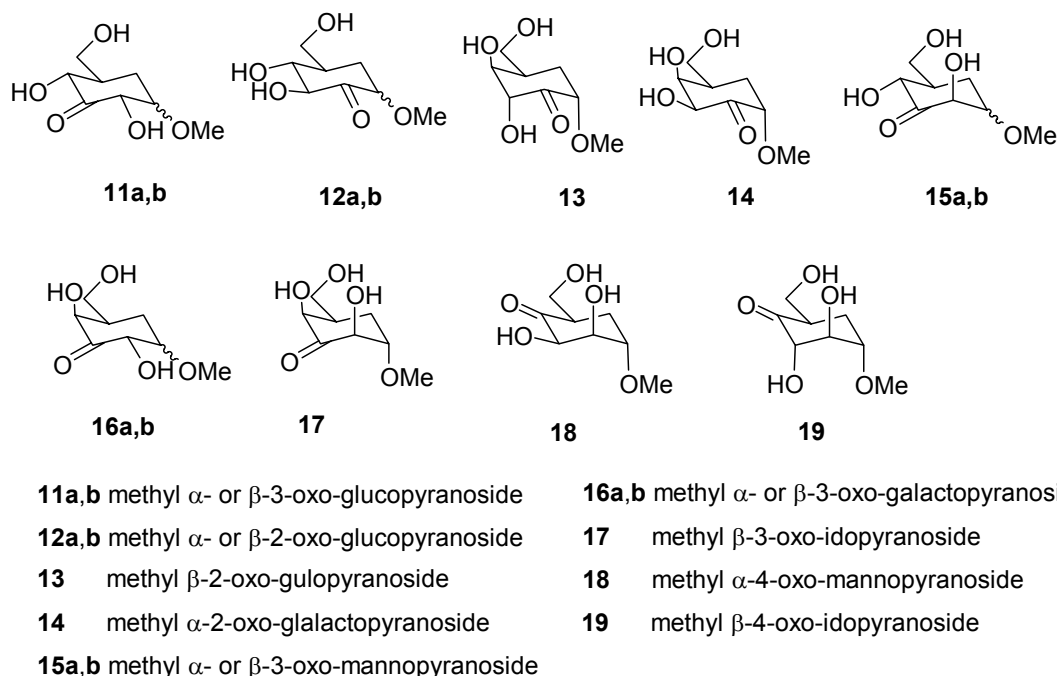
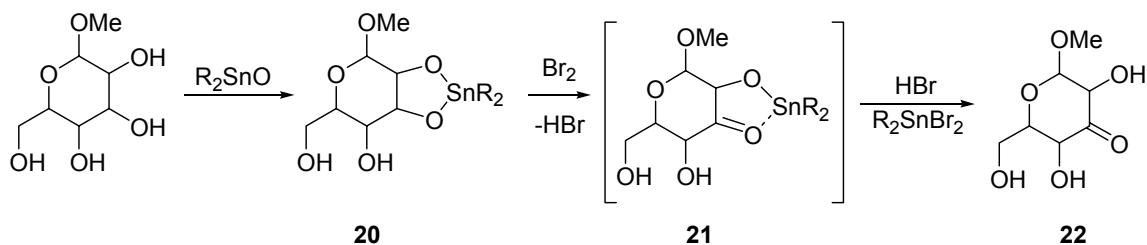


**Figure 1.8** Overview of synthesized keto-sugars by the tris-*n*-butyltin-oxide/ bromine method.<sup>9</sup>

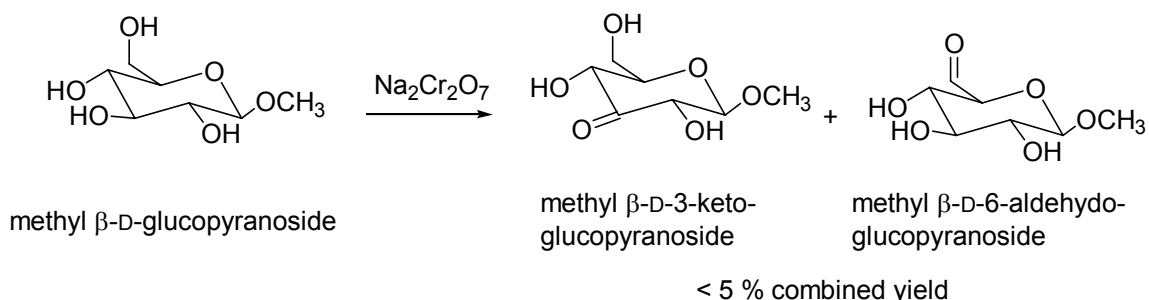


**Scheme 1.10** Schematic pathway of the tris-*n*-butyltin-oxide/ bromine method.<sup>9</sup>

Tsuda and co-workers reported two rules for this methodology: the “*cis*-glycol control” and the “anomeric control”.<sup>9</sup> The axial hydroxyl group is preferentially oxidized in *cis*-glycol systems and an axial anomeric ( $\alpha$ -) linkage directs oxidation to C4 while an equatorial anomeric centre ( $\beta$ -) directs oxidation to C3. Disadvantages of the tris-*n*-butyltin-oxide/ bromine method lie in the difficult experimental procedure especially the purification of the tin alkyl bromide by-product from the keto-sugar substrate. Despite the labour intensive purification

process, the use of tris-*n*-butyltin-oxide/ bromine method has been reported in literature.<sup>33,42-49</sup>

The first reported synthetic procedure for keto-sugars was by Theander *et al.* using dichromate as oxidant with the monosaccharide methyl  $\beta$ -D-glucopyranoside as illustrated in **Scheme 1.11**.<sup>50</sup> The oxidation was conducted in presence of oxalic acid at room temperature over a 20 h time period. The work-up procedure was very laborious and resulted in great loss of products due to work-up difficulties involving syrupy sugar mixtures. After purification with carbon celite column chromatography and fractional recrystallization methyl  $\beta$ -D-3-keto-glucopyranoside and methyl  $\beta$ -D-6-aldehydo-glucopyranoside were isolated in less than 5 % yield.



**Scheme 1.11** Oxidation of methyl  $\beta$ -D-glucopyranoside with sodium dichromate.

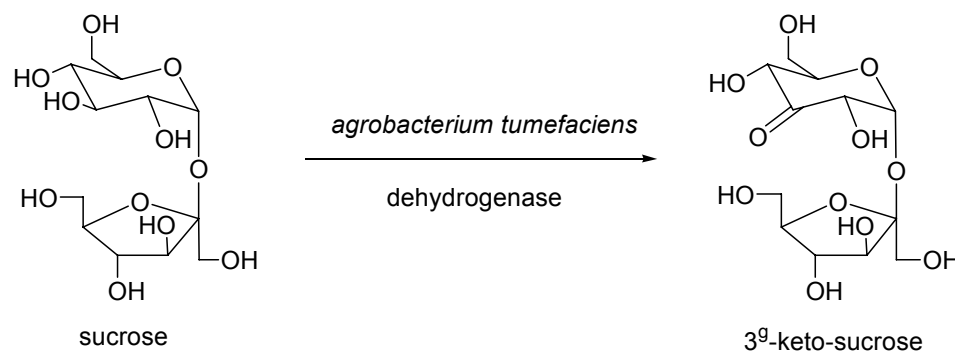
The identification of the two compounds was confirmed when subjected to reduction with Raney nickel. The reduction of methyl  $\beta$ -D-3-keto-glucopyranoside gave two products. One product was identical with the methyl  $\beta$ -D-glucopyranoside starting material and the other was determined as methyl  $\beta$ -D-allopyranoside.<sup>50</sup> Theander made further inroads into the field of keto-sugars using chromium trioxide as the oxidant.<sup>51</sup> The primary alcohol at C6 was protected with a triphenylmethyl group (trityl) in order to avoid unwanted oxidation. The investigated methyl 6-O-trityl-D-glucopyranosides have been



oxidized with chromium trioxide and produced 2-oxo, 3-oxo and 4-oxo derivatives in various amounts.

Another method for the oxidation of glycosides is the oxidation with  $\text{MnO}_2$ .<sup>52</sup> Through chromatographic methods a wide variety of oxidized sugar products was observed resulting in an intractable mixture of the individual components.

Apart from monosaccharides, the disaccharide sucrose was regiospecifically oxidized to 3<sup>g</sup>-ketosucrose with a dehydrogenase occurring in *agrobacterium tumefaciens* (**Scheme 1.12**).<sup>53</sup>



**Scheme 1.12** Synthesis of 3<sup>g</sup>-keto-sucrose from sucrose by an enzymatic process.

#### 1.1.4.6 Application of Keto-sugars in Reactions

The isolated keto-sugars can be subsequently reduced with lithium aluminum hydride, sodium borohydride or Raney nickel to obtain an epimeric mixture of the starting material as reported by Theander.<sup>9,50,51,53</sup> Thus, upon isolation and purification the epimers of uncommon sugars can be prepared from more abundant sugars. 1,2-5,6-O-di-isopropylidene-3-keto-fructose has been used as stoichiometric chiral oxidant when transformed into its dioxiran derivative (**Figure 1.9**).<sup>54</sup>

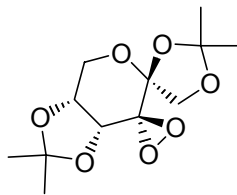
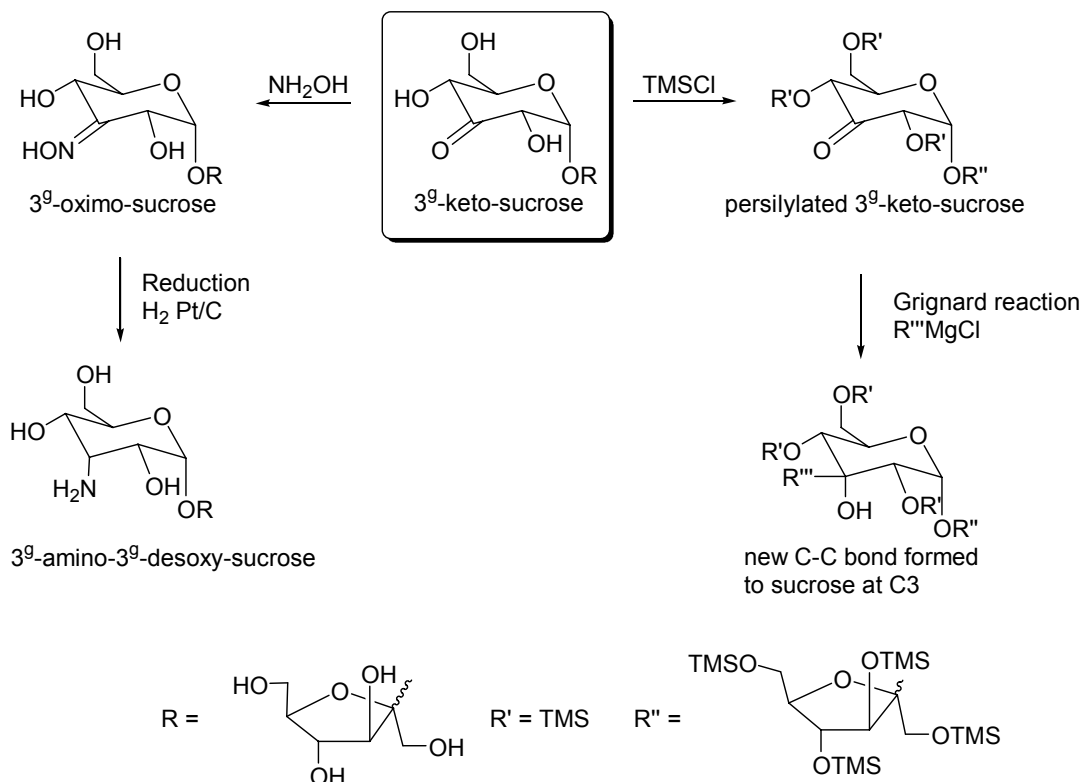


**Figure 1.9** Chiral stoichiometric oxidant based of fructose.

Despite the difficult accessibility of keto-sugars, some have been used as building blocks in synthetic chemistry.<sup>55,56</sup> The 3<sup>g</sup>-keto derivative of the disaccharide sucrose was reacted with hydroxylamine to yield the oxime as illustrated in **Scheme 1.13**.<sup>55</sup> This opens the pathway to the amino derivative through reduction of the oxime intermediate, or after persilylation of the free hydroxyl groups, a C-C bonds can be formed through Grignard reactions at the C3 position of the 3<sup>g</sup>-ketosucrose.<sup>55</sup>



**Scheme 1.13** Reaction pathways of 3<sup>g</sup>-ketosucrose.

#### 1.1.4.7 Aldehydo-Sugars

The synthesis of methyl 6-aldehydo- $\alpha$ -D-glucopyranoside was accomplished by Theander and co-workers when methyl  $\alpha$ -D-glucopyranoside was treated with dichromate as illustrated in **Scheme 1.11** (see page 17).<sup>50</sup> However the overall yield was low with less than 5% as the 6-aldehydo-sugars are very susceptible to further oxidation to glucuronic acids.<sup>1</sup>

#### 1.1.4.8 Other Sugar Oxidation Products

The oxidation of sugar compounds has been widely studied as there is a general interest to produce value-added chemical building blocks from feedstock other than petroleum based sources such as cellulose and starch.<sup>6,57-60</sup> E.g. the modification of cellulose is being studied as part of material science to create new compounds with improved physical properties such as high water absorption.

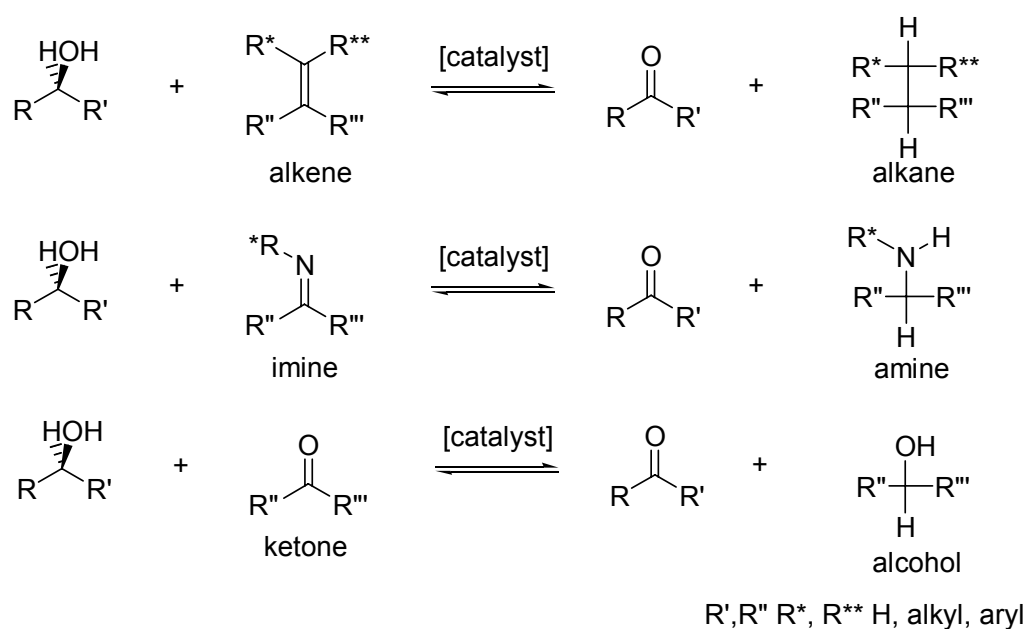
### 1.2 Transition Metal Catalyzed Transfer Hydrogenation Reaction as a Strategy for Sugar Transformations

The source of hydrogen in hydrogen transfer reactions are typically secondary alcohols. This immediately suggests that this type of reaction should in principle be applicable to sugars with one or several of the sugar hydroxyl functions acting as the hydrogen source while being transformed into a keto-sugar.<sup>61</sup> A brief overview of this type of reaction and typical catalysts system relevant to the work in this thesis is presented in the following paragraphs.

#### 1.2.1 Hydrogen Transfer Reactions

The principle of a hydrogen transfer reaction with alkenes, imines and ketones acting as the hydrogen acceptor and a secondary alcohols acting hydrogen

donor is illustrated in **Scheme 1.14**. In all three examples a catalyst is required to mediate the process and the secondary alcohol is oxidized to a ketone. Complementarily, the alkene is reduced to an alkane, the imine to an amine and the ketone to a secondary alcohol. An important feature of these reactions is that they are equilibrium reactions. As the position of the equilibrium depends on the relative free enthalpies and concentrations of reactants and products this can intrinsically limit the yield of the desired products.<sup>62</sup>



**Scheme 1.14** Generic equations of transfer hydrogen catalysis with alkene, imine and ketone.

The Noyori system shown in **Figure 1.10** is a prime example of a catalyst employed for hydrogen transfer reactions. The catalyst is a ruthenium(II)  $\eta^6$  arene ethylene diamine or  $\beta$ -amino ethanol system and can be added to the reaction mixture as either the 18-electron hydrogen loaded (**23** and **24**) or hydrogen deficient 16-electron complex (**25** and **26**).<sup>63-65</sup>

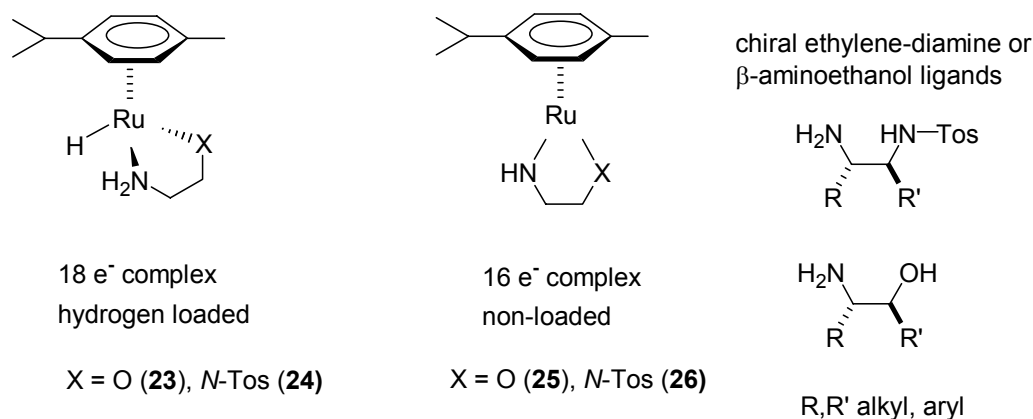
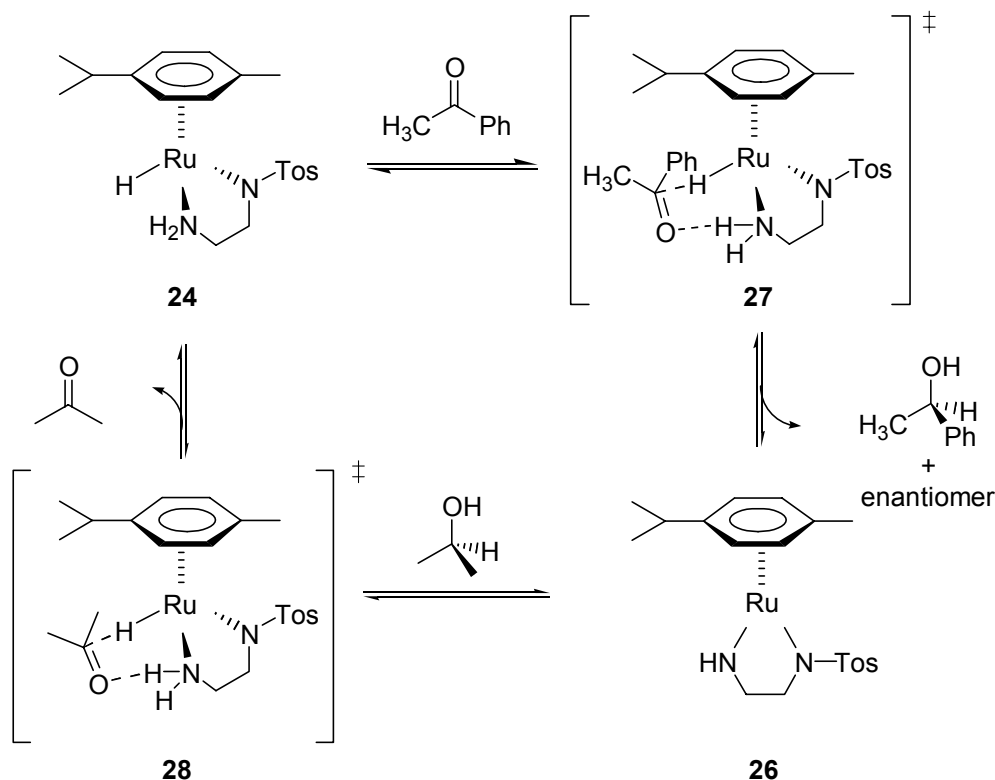


**Figure 1.10** Noyori's Ruthenium  $\eta^6$  arene based systems.<sup>65</sup>

The proposed reaction mechanism of the hydrogen transfer reaction to acetophenone from *iso*-propanol, which acts as both hydrogen donor and solvent is illustrated in **Scheme 1.15**.<sup>63-65</sup> The 18-electron hydride complex (**25**) can conveniently be prepared *in situ* by addition of [*p*-cymene RuCl<sub>2</sub>]<sub>2</sub>, *N*-tosyl-1,2-diaminoethylan ligand and an auxiliary base, e.g. KOH, in *iso*-propanol solvent at room temperature or individually prepared and isolated by reaction of the Ru precursor and *N*-tosyl-1,2-diamino-ethylene ligand with base in *iso*-propanol followed by recrystallization from dichloromethane and hexanes. The 16-electron complex **27** was prepared and isolated by addition of the Ru precursor, ligand and base in absence of protic solvents, e.g. in dichloromethane.

The reaction mechanism shown in **Scheme 1.15** is valid in all three different cases of catalyst preparation: *in situ* generation, addition of the 18-electron hydride complex (**24**) or 16-electron complex (**26**). When prepared *in situ*, the 18-electron hydride complex reacts with acetophenone via transition state **27**. A direct hydride transfer occurs from the metal bound hydride to the carbonyl carbon atom. Simultaneously, a proton is transferred from the amine functionality of the ligand to the oxygen atom in the carbonyl group. This reaction mechanism is an example for ligand-metal bifunctional catalysis, in which the ligand takes an active role in the reaction mechanism. The 16-electron complex containing a newly formed amide ligand reacts with an *iso*-propanol solvent

molecule via a similar transition state (**28**). The 18-electron hydride complex (**24**) is regenerated after the release of acetone. 66-68



**Scheme 1.15** Reduction of acetophenone to 1-phenyl-ethanol with the Noyori system.<sup>66</sup>

The reaction has been used in the enantioselective reduction of acetophenone and a plethora of other pro-chiral ketones by the use of (pseudo)  $C_2$  symmetric 1,2-diphenyl ethylene-bridged 1,2-diamino ligands. It was reported that only unsymmetrically *N*-tosylated 1,2-diamino-ethane ligands complexed to the Ru arene fragment possess catalytic activities.<sup>63-65</sup>

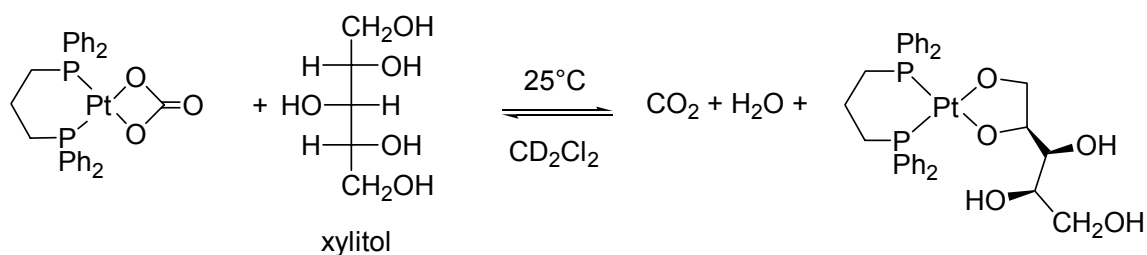
### 1.2.2 Other Metal Catalyzed Oxidation Reactions

Many metal catalyzed oxidation reactions of organic compounds other than transfer dehydrogenation are known and in contrast to the latter they are in most cases not equilibrium reactions, but are driven by the irreversible formation of

thermodynamically stable products.<sup>69</sup> E.g. when hydrogen peroxide is used as an oxidant water is generated. The driving force for the formation of water is so strong ( $\Delta G \ll 0$ ) that the oxidation reaction is completely irreversible. The use of peroxides as reactants is attractive and one of the focus points of “green” chemistry as the by-product water does not negatively affect the environment.<sup>70-72</sup>

### 1.2.3 Representative Examples of Metal Sugar Complexes

The coordinative binding of sugars to transition metal centres shows very high intrinsic regio-selectivities as shown in the example below.<sup>73-80</sup> The binding of the respective metals to the carbohydrates occurs typically through bidentate chelation by a *vicinal* diol unit forming five membered metallo-cycles as seen in **Scheme 1.15**.<sup>73</sup> Structures and complexation regioselectivities are illustrated in **Figure 1.11** for the reaction of mannitol and xylitol with (dppp)Pt(CO<sub>3</sub>) (dppp = 1,3-bis(diphenylphosphino)propane).



**Scheme 1.16** Formation of 1,2-xylitolato-platinum(II)-dppp in CD<sub>2</sub>Cl<sub>2</sub>.<sup>73</sup>

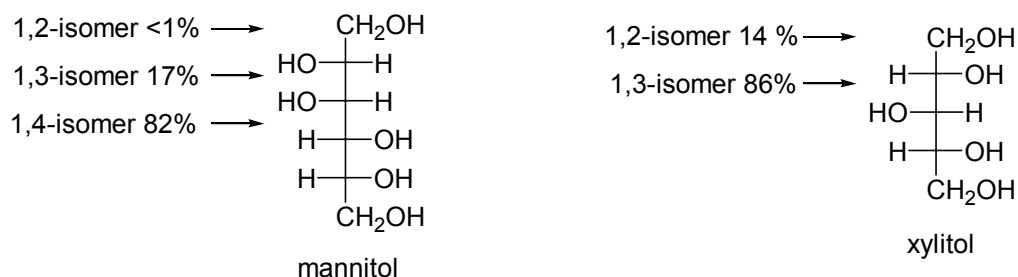


**Figure 1.11** Mannitol and xylitol structures and observed equilibrium complexation regio-selectivities for (dppp)Pt(alditolate) complexes in  $\text{CD}_2\text{Cl}_2$ .<sup>73</sup>

An example of a structure determined by X-ray crystallographical analysis in which two ethylenediamine palladium (II) fragments are coordinated to glucose is shown in **Figure 1.12**.<sup>75</sup>

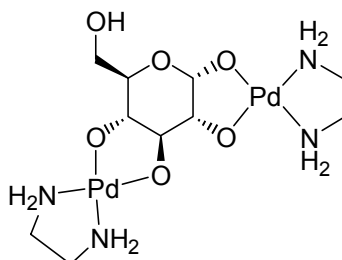


**Figure 1.12**  $[(\text{en})_2\text{Pd}_2(\alpha\text{-D-glucopyranose 1,2,3,4H}_4)]^{75}$

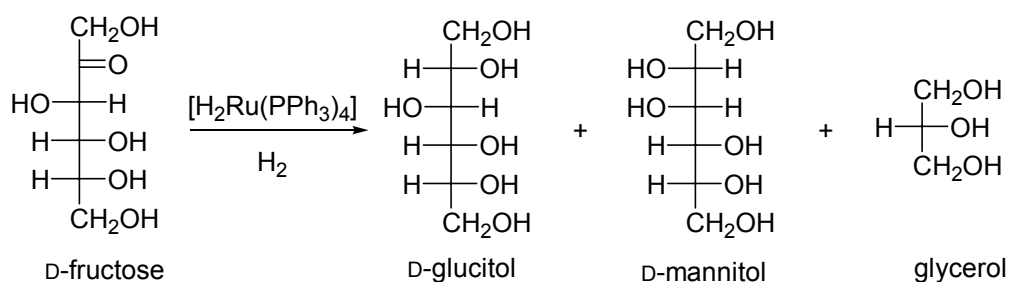
#### 1.2.4 Examples of Transition Metal Complex Catalyzed Transformations of Sugars

The established high coordination selectivities of sugar polyols to transition metal centres raise the intriguing possibility of exploiting this phenomenon in catalytic transformations. With the reasonable hypothesis that only those hydroxyl functions that actually complex to the metal centre will react, one could envision a catalytic chemo- and regio-selective transformation of polyols without the need for protecting groups. The transition metal catalyzed transformation of



unprotected sugar compounds has however been only marginally studied in the last two decades and there are thus relatively few examples of such reactions, none of which have demonstrated the concept presented above. As shown by Beaupere, Wilkinson's catalyst can chemoselectively give lactones from the unprotected free aldohexoses with benzylidene acetone acting as the hydrogen acceptor.<sup>30,31,81,82</sup> The selectivity of this reaction is however entirely dependent on the higher reactivity of the anomeric centre and not a catalyst induced kinetic effect.

Another example of a transition metal catalyzed sugar transformation is the ruthenium hydride mediated reduction of monosaccharides illustrated in **Scheme 1.17** with fructose as the substrate.<sup>83,84</sup> The reaction conditions reported were 100°C at 20 atm H<sub>2</sub> pressure in NMP solvent. The catalyst load was 1 mol% with respect to fructose. A wide range of polyol compounds was obtained; glucitol, mannitol and glycerol accounted for 77 % of the products. The formation of glycerol was rationalized through a retro-aldol reaction of fructose with subsequent hydrogenation of 1,3-dihydroxy-propanone and/ or 2,3-dihydroxy-propanal to glycerol.<sup>83</sup>



**Scheme 1.17** Hydrocracking of fructose with H<sub>2</sub>Ru(PPh<sub>3</sub>)<sub>4</sub>.<sup>83</sup>

An example of a transition metal complex mediated reaction of sugars in which carbon-carbon are broken is the non-catalytic reaction of stoichiometric amounts of RhH(PPh<sub>3</sub>)<sub>3</sub> with fructose, which results in decarbonylation products such as

five carbon atoms containing furfuryl alcohol and arabinol as well traces of four and less carbon atoms containing alcohol fragments.<sup>85</sup> While this reaction is conceptually interesting in the context of biomass conversion it has been pointed out that it would take only ~14 tons of glucose (i.e. a small truckload of corn sugar) to consume the entire planetary annual supply of rhodium (~ 8 tons).<sup>86</sup>

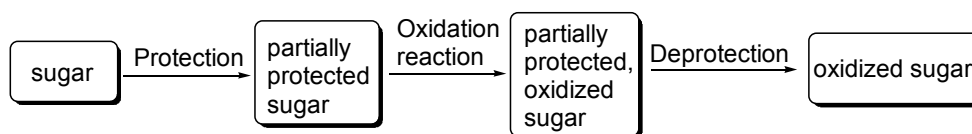
### 1.3 Motivation, Research Objectives and Potential Applications

#### 1.3.1 Motivation

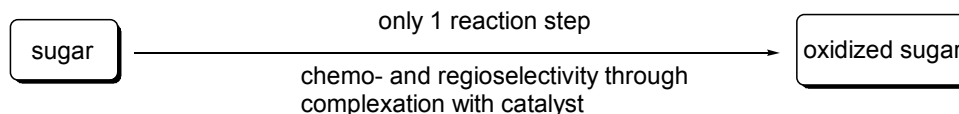
The motivation of this research project is to expand the body of knowledge on the selective oxidation of unprotected simple carbohydrates with homogeneous transition metal catalysis.

Access to first oxidation products of sugars, i.e. primarily the keto-sugars discussed above is presently very limited. They have however been synthesized by traditional carbohydrate chemistry, which uses sophisticated and – where necessary – iterative protection and deprotection protocols that make these syntheses very inefficient. As outlined in **Scheme 1.18** one single desired oxidation reaction requires a minimum of three reaction steps. This research project will attempt to utilize the selective binding properties of transition metals to carbohydrates and aims to investigate the direct oxidation of sugar compounds in only one reaction step. Particular interest lies in the investigation of the chemo- and regio-selectivity of those oxidation reactions.

#### Traditional Sugar Chemistry



#### This Research Project

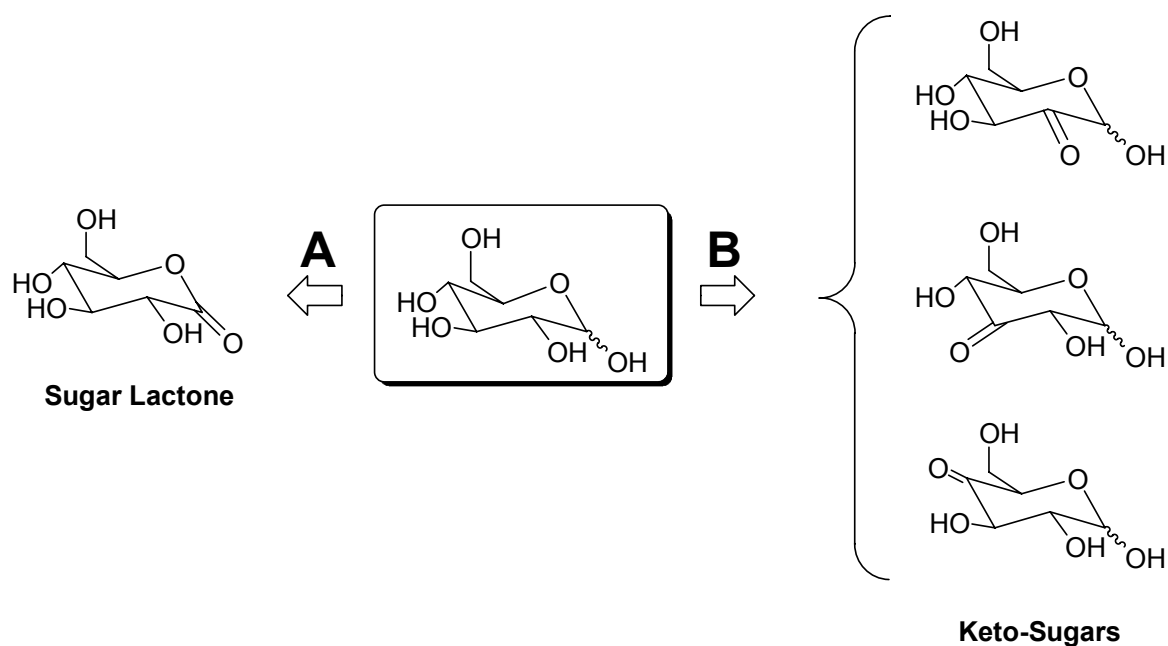


**Scheme 1.18** Motivation of this research project.

### 1.3.2 Research Objectives

Both fields, carbohydrate chemistry and transition metal catalysis, contain unlimited research opportunities regarding oxidation reactions, but this research project is focussed on the first oxidation products of simple carbohydrates through homogeneous transition metal catalysis. The research project is divided into two projects as outlined in **Scheme 1.19**.

- A)** the oxidation of the hemiacetal hydroxyl function to the corresponding sugar lactone
- B)** the oxidation of one secondary alcohol function to the corresponding keto-sugar



**Scheme 1.19** Objectives of this research project.

### 1.3.3 Potential Applications of Sugar Lactones and Keto-Sugars

A potential application for the synthesis of sugar lactones and keto-sugars is use as chemical building blocks in the pharmaceutical industry. E.g., the additional carbonyl function in a keto-sugar can open new pathways to chemical manipulations and transformations that are difficult to access by other means. A few transformations of keto-sugars such as stereo inversion or C-C bond generation have been reported but the research is limited to the rather difficult availability of the elusive keto-sugar substrates. If successful, the present research project would enable the creation of new tools for the synthesis of such compounds.

Sugar lactones and keto-sugars would also have an application in the field of enzyme research, in which they can act as inhibitors. This would allow the investigation of enzyme activity and mechanism studies. Possible reaction mechanisms and binding patterns found in the selective oxidation of sugars with transition metals might be adopted as model systems for enzymes to study their enzymatic activities.

## 1.4 References

- 1) Collins, P.; Ferrier, R. *Monosaccharides*; John Wiley & Sons, Ltd.: Chichester, UK, 1995.
- 2) Roth, K.; Höft-Schleeh, S. *Chem. in uns. Zeit* **2002**, 36, 390-402.
- 3) Fischer, E. *Ber.* **1891**, 24, 1836.
- 4) Bols, M. *Carbohydrate Building Blocks*; John Wiley & Sons, Inc.: New York, 1996.
- 5) Maple, S. R.; Allerhand, A. *J. Am. Chem. Soc.* **1987**, 109, 3168-3169.
- 6) Lichtenthaler, F. W.; Peters, S. *Chimie* **2004**, 7, 65-90.
- 7) *The Merck Index*; 13th Ed.; Merck & Co., Inc.: Whitehouse Station, NJ, 2001.
- 8) Dieguez, M.; Pamies, O.; Claver, C. *Chem. Rev.* **2004**, 104, 3189-3215.
- 9) Liu, H.-M.; Sato, Y.; Tsuda, Y. *Chem. Pharm. Bull.* **1993**, 41, 491-501.
- 10) Hollingsworth, R. I.; Wang, G. *Chem. Rev.* **2000**, 100, 4267-4282.
- 11) Kiliani, H. *Ann.* **1880**, 205, 182.
- 12) Isbell, H. S.; Frush, H. L. *B. S. Jour. Research* **1933**, 11, 649-664.
- 13) Isbell, H. S.; Frush, H. L. *Aldonic Acids and their Lactonization*, 1962; Vol. 2, 16-18.
- 14) *Dictionary of Organic Compounds*; Chapman & Hall: London, 1996.
- 15) Overkleeft, H. S.; Wiltenburg van, J.; Pandit, U. K. *Tetrahedron* **1994**, 50, 4215-4224.
- 16) Hackert, M. L.; Jacobson, R. A. *J. Chem. Soc., Chem. Comm.* **1960**, 1179.
- 17) Szczepanowska, E.; Kusmierz, J.; Szafranek, J.; Schramm, R. W. *Acta. Physiol. Plant.* **1989**, 11, 97-109.
- 18) Kirk-Othmer *Encyclopedia of Chemical Technology*; John Wiley & Sons: Toronto, 1998.
- 19) Kent, J. A. *Riegel's Handbook of Industrial Chemistry*; Chapman & Hall: Toronto, 1992, p. 945.
- 20) *Aldrich catalogue*, 2004/2005 Canadian Edition.
- 21) Pocker, Y.; Green, E. *J. Am. Chem. Soc.* **1974**, 96, 166-173.

- 22) Katsumata, M.; Kiuchi, K.; Uchikuga, S. JP 1994-56820.
- 23) Wiechers, J. W.; Lowry, M. R.; Wollers, J.; Pratley, S. K. EP 92-307962, Unilever Inc.
- 24) Markham, R. G. US 1990-459806.
- 25) Beyer, H.; Walter, W. *Lehrbuch der organischen Chemie*; S. Hirzel Verlag: Stuttgart, 1998.
- 26) Saiyasombat, W.; Molloy, R.; Nicholson, T. M.; Johnson, A. F.; Ward, I. M.; Poshyachinda, S. *Polymer* **1998**, 39, 5581-5585.
- 27) Dudev, T.; Lim, C. *J. Am. Chem. Soc.* **1998**, 120, 4450-4458.
- 28) Brown, J. M.; Conn, A. D.; Pilcher, G.; Leitao, M. L. P.; Yang, M. Y. *J. Chem. Soc., Chem. Commun.* **1989**, 23, 1817-1819.
- 29) Wolfrom, M. L.; Anno, K. *J. Am. Chem. Soc.* **1952**, 72, 5583-5584.
- 30) Isaac, I.; Stasik, I.; Beaupere, D.; Uzan, R. *Tetrahedron Lett.* **1995**, 36, 383-386.
- 31) Isaac, I.; Aizel, G.; Stasik, I.; Wadouachi, A.; Beaupere, D. *Synlett* **1998**, 475-476.
- 32) Ueberschaer, K.-H.; Blachnitzky, E.-O.; Kurz, G. *Eur. J. Biochem.* **1974**, 48, 389-405.
- 33) Tsuda, Y.; Hanajima, M.; Mastuhira, N.; Okuno, Y.; Kanemitsu, K. *Chem. Pharm. Bull.* **1989**, 39, 2344-2350.
- 34) Giffhorn, F.; Koepper, S.; Huwig, A.; Freimund, S. *Enzy. and Micro. Tech.* **2000**, 27, 734-742.
- 35) Freimund, S.; Huwig, A.; Giffhorn, F.; Koepper, S. *Chem. Eur. J.* **1998**, 4, 2442-2455.
- 36) Freimund, S.; Koepper, S. *Carbohydr. Res.* **1998**, 308, 195-200.
- 37) Nutt, R. F.; Arison, B.; Holly, F. W.; Walton, E. *J. Am. Chem. Soc.* **1965**, 87, 3273-3273.
- 38) Hall, R. H.; Bischofberger, K. *Carbohydr. Res.* **1978**, 65, 139-143.
- 39) Heyn, K.; Köll, P. *Methods in Carbohydr. Chem.* **1972**, 6, 342-347.
- 40) Dzhemilev, U. M.; Yur'ev, V. P.; Tolstikov, G. A. *Zhurnal Obshchei Khimii* **1970**, 41, 935-936.

- 41) Gonsalvi, L.; Arends, I. W. C. E.; Sheldon, R. A. *Org. Lett.* **2002**, *4*, 1659-1661.
- 42) Groneberg, R. D.; Miyazaki, T.; Stylianides, N. A.; Schulze, T. J.; Stahl, W.; Schreiner, E. P.; Suzuki, T.; Iwabuchi, Y.; Smith, A. L.; Nicolaou, K. C. *J. Am. Chem. Soc.* **1993**, *115*, 7593-7611.
- 43) White, J. D.; Jensen, M. S. *J. Am. Chem. Soc.* **1995**, *117*, 6224-6233.
- 44) Ueno, Y.; Okawara, M. *Tetrahedron Lett.* **1976**, 4597-4600.
- 45) Nicolaou, K. C.; Groneberg, R. D.; Miyazaki, T.; Stylianides, N. A.; Schulze, T. J.; Stahl, W. *J. Am. Chem. Soc.* **1990**, *112*, 8193-8195.
- 46) Fernandez-Mayoralas, A.; Bernabe, M.; Martin-Lomas, M. *Tetrahedron* **1988**, *44*, 4877-4882.
- 47) David, S.; Thieffry, A. *J. Chem. Soc., Perkin Trans. 1* **1979**, 1568-1573.
- 48) Kong, X.; Grindley, B. *J. Carbohydr. Chem.* **1993**, *12*, 557-571.
- 49) Nashed, M. A.; Anderson, L. *Tetrahedron Lett.* **1976**, 3503-3506.
- 50) Lindberg, B.; Theander, O. *Acta Chem. Scand.* **1954**, *8*, 1870-1874.
- 51) Theander, O. *Acta Chem. Scand.* **1957**, *11*, 1557-1564.
- 52) Bose, J. L.; Foster, A. B.; Stacey, M.; Webber, J. M. *Nature* **1959**, *184*, 1301-1303.
- 53) Stoppok, E.; Matalla, K.; Buchholz, K. *Appl. Microbiol. Biotechnol.* **1992**, *36*, 604-608.
- 54) Adam, W.; Saha-Moeller, C. R.; Zhao, C.-G. *Tetrahedron Asymm.* **1998**, *9*, 4117-4122.
- 55) Pietsch, M.; Water, M.; Buchholz, K. *Carbohydr. Res.* **1994**, *254*, 183-194.
- 56) Simiand, C.; Samain, E.; Martin, O. R.; Driguez, H. *Carbohydr. Res.* **1995**, *267*, 1-15.
- 57) Arts, S. J. H. F.; Mombarg, E. J. M.; Van Bakkum, H.; Sheldon, R. A. *Synthesis* **1997**, 597-613.
- 58) Arts, S. J. H. F.; van Rantwijk, F.; Sheldon, R. A. *J. Carbohydr. Chem.* **1996**, *15*, 317-329.
- 59) Emons, C. H. H.; Kuster, B. F. M.; Vekemans, J. A. J. M.; Sheldon, R. A. *Chim. Oggi.* **1992**, *1992*, 59-65.



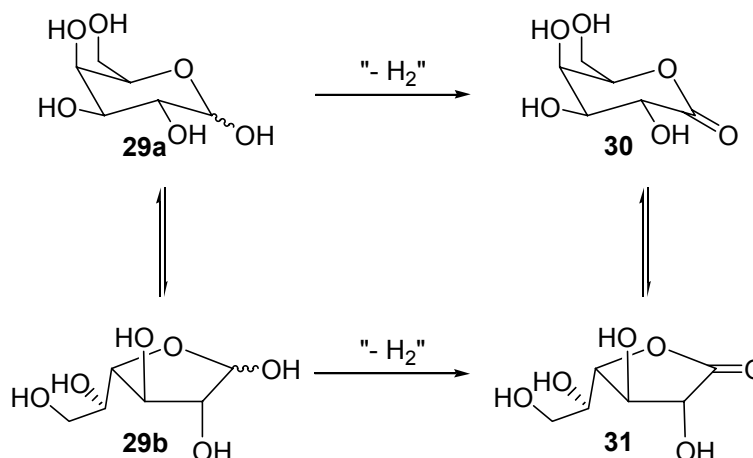
- 60) Boelrijk, A. E. M.; Dorst, J. T.; Reedijk, J. *Recl. Trav. Chim. Pays-Bas* **1996**, *115*, 536-541.
- 61) Shriver; Atkins *Inorganic Chemistry*; 3rd Ed.; Freeman: NY, 1999.
- 62) Adkins, H.; Eloffson, R. M.; Rossow, A. G.; Robinson, C. C. *J. Am. Chem. Soc.* **1949**, *71*, 3622-3629.
- 63) Noyori, R.; Hashiguchi, S. *Acc. Chem. Res.* **1997**, *30*, 97-102.
- 64) Hashiguchi, S.; Fujii, A.; Haack, K.-J.; Matsumura, K.; Ikariya, T.; Noyori, R. *Angew. Chem. Int. Ed. Engl.* **1997**, *36*, 288-290.
- 65) Haack, K.-J.; Hashiguchi, S.; Fujii, A.; Ikariya, T.; Noyori, R. *Angew. Chem. Int. Ed. Engl.* **1997**, *36*, 285-288.
- 66) Noyori, R.; Yamakawa, M.; Hashiguchi, S. *J. Org. Chem.* **2001**, *66*, 7931-7944.
- 67) Noyori, R.; Ohkuma, T. *Angew. Chem. Int. Ed.* **2001**, *40*, 40-73.
- 68) Noyori, R. *Angew. Chem. Int. Ed.* **2002**, *41*, 2008-2022.
- 69) Hudlicky, M. *Oxidations in Organic Chemistry*; Am. Chem. Soc. Monograph: Washington DC, 1990.
- 70) Sheldon, R. A.; Arends, I. W. C. E.; ten Brink, G.-J.; Dijkstra, A. *Acc. Chem. Res.* **2002**, *35*, 774-781.
- 71) ten Brink, G.-J.; Arends, I. W. C. E.; Sheldon, R. A. *Science* **2000**, *287*, 1636-1639.
- 72) Noyori, R.; Aoki, M.; Sato, K. *Chem. Commun.* **2003**, 1977-1986.
- 73) Andrews, M. A.; Voss, E. J.; Gould, G. L.; Klooster, W. T.; Koetzle, T. F. *J. Am. Chem. Soc.* **1994**, *116*, 5730-5740.
- 74) Kästle, X.; Klüfers, P.; Kunte, T. Z. *Anorg. Allg. Chem.* **2001**, *267*, 2042-2044.
- 75) Klüfers, P.; Kunte, T. *Angew. Chem. Intl. Ed.* **2001**, *40*, 4210-4212.
- 76) Herdin, S.; Klüfers, P.; Kunte, T.; Pootrowski, H. Z. *Anorg. Allg. Chem.* **2004**, *630*, 701-705.
- 77) Klüfers, P.; Kunte, T. Z. *Anorg. Allg. Chem.* **2004**, *630*, 553-557.
- 78) Klüfers, P.; Labisch, O. Z. *Naturforsch.* **2004**, *57b*, 1446-1453.

- 79) Klüfers, P.; Krotz, O.; Ossberger, M. *Eur. J. Inorg. Chem.* **2002**, 1919-1923.
- 80) Benner, K.; Klüfers, P. *Carbohydr. Res.* **2000**, 327, 287-292.
- 81) Beaupere, D.; Bauer, P.; Nadjó, L.; Uzan, R. *J. Organomet. Chem.* **1982**, 238, C12-C14.
- 82) Massoui, M.; Beaupere, D.; Goethals, G.; Uzan, R. *J. Mol. Catal.* **1985**, 33, 209-213.
- 83) Andrews, M. A.; Klaeren, S. A. *J. Am. Chem. Soc.* **1989**, 111, 4131-4133.
- 84) Andrews, M. A.; Klaeren, S. A. US 1991-5026927.
- 85) Andrews, M. A. *Organomet.* **1989**, 8, 2703-2708.
- 86) Personal communication with R. M. Bullock, B. N. L.

## Chapter 2 Selective Oxidation of Hemiacetals to Lactones

### 2.1 Synthesis and Properties of $\delta$ - and $\gamma$ -Sugar Lactones

Lactones are the first oxidation products of reducing sugars such as the naturally abundant aldohexoses D-glucose, D-mannose and D-galactose and are formally obtained by the dehydrogenation of their hemiacetal function. As illustrated for D-galactose (**29**) in **Scheme 2.1** two lactone isomers can – in principle – be obtained: The 1,5-pyrano or  $\delta$ -lactone (**30**) or the 1,4-furano or  $\gamma$ -lactone (**31**). Either isomer can – again in principle – be formed by either the direct oxidation of the pyranose (**29a**) or the furanose (**29b**) form or by the interconversion of the two lactone isomers following the initial oxidation of either form.

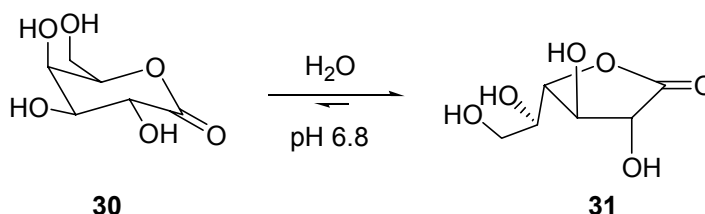


**Scheme 2.1** Possible pathways of the oxidation of galactose (**29**) to the lactones (**30** and **31**).

A complex equilibrium balance exists between the anomeric pyranose and furanose forms of these simple sugars.<sup>1</sup> Generally, the  $\alpha$ - and  $\beta$ -pyranose structures of monosaccharides are the predominant compounds in aqueous solutions. However, substantial amounts of furanose isomers can be present in the equilibrium with other solvents. E.g. the furanose contents of galactose, which have been determined by <sup>1</sup>H NMR of equilibrated solutions, are 15 % in dimethyl sulfoxide and 17 % in pyridine.<sup>2</sup>

$\alpha$ - and  $\beta$ -pyranoses have been shown to be the actual oxidation substrates in the preparation of  $\delta$ -aldonolactones.<sup>3</sup> The lactones are typically synthesized by oxidation with bromine followed by fractional crystallization.<sup>3,4</sup> For glucose the kinetic oxidation product  $\delta$ -gluconolactone is readily isolated,<sup>5</sup> but in all cases the  $\gamma$ -lactones are the thermodynamically stable oxidation product for aldohexoses.<sup>6-9</sup>  $\delta$ -D-Gluconolactone has been structurally fully characterized by X-ray crystallography.<sup>10</sup> It is finding widespread use as food additive and is produced on a technical scale by an enzymatic process.<sup>11,12</sup> The unprotected  $\delta$ -lactones of D-mannose and D-galactose are reportedly much less stable against isomerization to the  $\gamma$ -form, but  $\delta$ -mannonolactone has been isolated in moderate yield from a solution of calcium mannonate in aqueous oxalic acid by rapid fractional crystallization at low temperature.<sup>13</sup>

In contrast,  $\delta$ -D-galactonolactone has to our knowledge never been isolated or structurally characterized. § However,  $\delta$ -D-galactonolactone has been observed as the transient immediate product of the enzymatic dehydrogenation by D-galactose dehydrogenase.<sup>14</sup> As illustrated in **Scheme 2.2**  $\delta$ -galactonolactone rapidly rearranges to the  $\gamma$ -lactone with  $k = 1.0 \text{ min}^{-1}$  establishing a  $K_{\text{eq}}(\delta \text{ to } \gamma) > 100$  under the pH 6.8 buffered aqueous reaction conditions required by the enzyme.



**Scheme 2.2** Equilibrium of  $\delta$ -D-galactonolactone (**30**) and  $\gamma$ -D-galactonolactone (**31**) in aqueous buffered solution.

§ There exists a CAS registry number for  $\delta$ -D-galactonolactone but contains no synthetic preparation data.

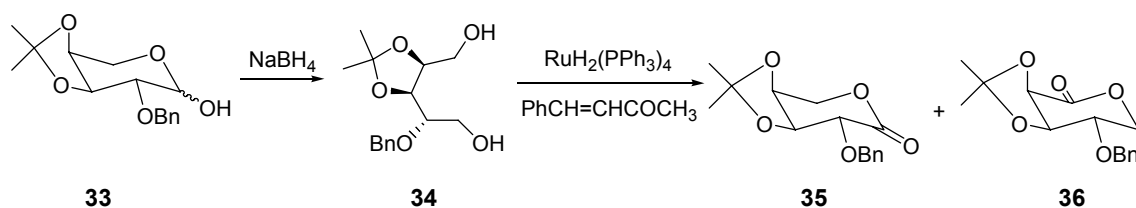
It was reported that the enzyme oxidized  $\beta$ -galactopyranose at a higher initial rate than its  $\alpha$ -galactopyranose anomer.<sup>14</sup> The enzyme was not catalytically active with  $\alpha$ - or  $\beta$ -galactofuranose, which was only oxidized when an aldose 1-epimerase was added to the reaction solution. The kinetic experiments were conducted in phosphate buffered aqueous solutions and the concentrations of the oxidizing agent,  $\text{NAD}^+$ , were photospectroscopically detected. Consumption of  $\text{NAD}^+$  was directly correlated with the generation of galactonolactone. In order to analyze the  $\delta$ - and  $\gamma$ - lactone contents, aliquots of the reaction mixture were taken and rapidly frozen with liquid nitrogen. The silylation agent, *N*-trimethylsilyl-imidazole, was added to the frozen samples and the reaction mixture was allowed to warm to room temperature. The persilylated lactones were quantitatively and qualitatively analyzed by gas chromatography methods.<sup>14</sup>

## 2.2 Transition Metal Catalysis

### 2.2.1 $\text{RuH}_2(\text{PPh}_3)_4$ and $\text{RhH}(\text{PPh}_3)_4$ in the Synthesis of Sugar Lactones

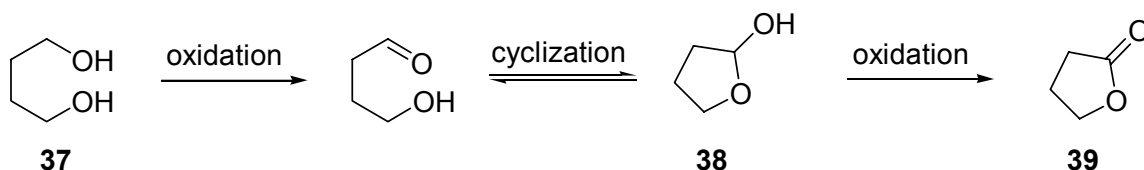
An alternative method for the preparation of sugar lactones are transition metal catalyzed transfer dehydrogenation reactions, which have been demonstrated for both protected and unprotected alditols as well as reducing sugars.<sup>15-18</sup>

As illustrated in **Scheme 2.3** 2,3,4-*O*-protected L-arabino and L-lyxono lactones can be prepared from the corresponding  $\alpha,\omega$ -diols with *cis*- $\text{RuH}_2(\text{PPh}_3)_4$  as the catalyst and benzalacetone (*trans*-4-phenyl-3-buten-2-one) as the hydrogen acceptor.<sup>18</sup> The  $\alpha,\omega$ -diol alditol (**33**) can be prepared by the reduction of 3,4-*O*-*iso*-propylidene-2-*O*-benzyl-L-arabinopyranose (**32**) with sodium borohydride. The oxidation of **33** with *cis*- $\text{RuH}_2(\text{PPh}_3)_4$  as catalyst produces the corresponding arabino-lactone **34** and lyxono-lactone **35** in approximately 2 : 1 ratio as determined by  $^1\text{H}$  NMR analysis. Depending on the size of the protecting group at C2 (here, benzyl) lyxono-lactone **35** is preferably formed over **34**.



**Scheme 2.3** Conversion of protected arabinose **33** with NaBH<sub>4</sub> and subsequent *cis*-RuH<sub>2</sub>(PPh<sub>3</sub>)<sub>4</sub> catalyzed oxidation of the arabinol intermediate **34** to the corresponding lactones (**35** and **36**).

A detailed mechanistic study of the oxidation of  $\alpha,\omega$ -diols and aldehydes to esters and lactones with *cis*-RuH<sub>2</sub>(PPh<sub>3</sub>)<sub>4</sub> and various hydrogen acceptors in mesitylene solvent at 180°C has been reported by Murahashi *et al.*<sup>19</sup> Lactones (**39**) are obtained from  $\alpha,\omega$ -diols (**37**) by a two step process as illustrated in **Scheme 2.4**. One primary alcohol of the  $\alpha,\omega$ -diol, here 1,4-butanediol, is oxidized to the corresponding aldehyde, i.e. 4-hydroxy-butanal. Then, the aldehyde and primary alcohol cyclize to form a hemiacetal (**38**), which is subsequently oxidized to the lactone, i.e.  $\gamma$ -butyrolactone (**39**).



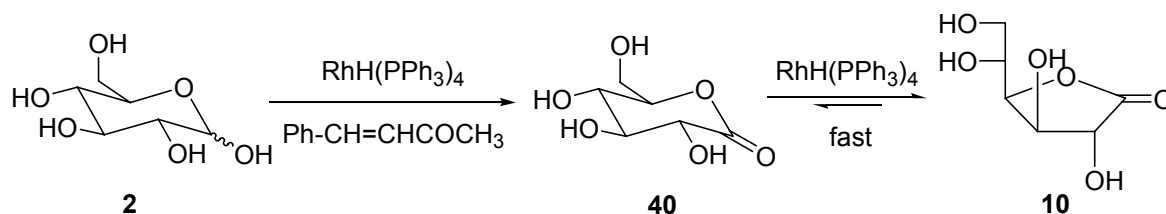
**Scheme 2.4** Reaction pathway from  $\alpha,\omega$ -diol (**37**) to lactone (**39**).

In the proposed catalytic reaction mechanism for the oxidation of primary alcohols to esters, the primary alcohol or hemiacetal adds oxidatively to coordinatively unsaturated Ru(PPh<sub>3</sub>)(L)<sub>3</sub> complex fragment (L = solvent or PPh<sub>3</sub>) to form a *cis*-hydrido-alkoxy complex.<sup>19</sup> After a  $\beta$ -elimination process a *cis*-dihydride Ru complex is generated and the aldehyde or lactone is cleaved. To regenerate the Ru catalyst, either hydrogen gas is released or, upon reaction

with a hydrogen acceptor, such as acetone or benzalacetone, the hydrogenated acceptor is released.

Using the same hydrogen acceptor, benzalacetone, Beaupère and coworkers employed  $\text{RhH}(\text{PPh}_3)_4$  as the catalyst in the dehydrogenation of a variety of  $\text{C}_4$ ,  $\text{C}_5$  and  $\text{C}_6$  reducing sugars and unprotected alditols under mild condition in DMF solvent in a temperature range of 60-80°C.<sup>20-22</sup> Yields ranging from 60 % to 96 % of the corresponding  $\gamma$ -lactones were obtained by this method, but in no case could the corresponding  $\delta$ -lactones be isolated.  $\text{C}_2$  symmetric alditols such as mannitol lead to formation of a single product, e.g.  $\gamma$ -mannonolactone from mannitol, as both primary alcohols are homotopic. In absence of  $\text{C}_2$  symmetry, two products are formed in various ratios depending on the relative orientation of the secondary alcohols.

NMR scale reactions in  $\text{DMF-d}^7$  with D-glucopyranose (**2**) established that the initial oxidation products are in fact the  $\delta$ -lactones, however control experiments with the easily accessible  $\delta$ -gluconolactone (**40**) showed that under the reaction conditions the rhodium catalyst,  $\text{RhH}(\text{PPh}_3)_4$ , rapidly isomerizes them to the thermodynamic  $\gamma$ -form (**10**) as shown in **Scheme 2.5**.<sup>20,22</sup> This leads in principle to the conclusion that the kinetic  $\delta$ -lactones can be exclusively synthesized under mild conditions when the isomerization to the thermodynamic more stable  $\gamma$ -lactones is suppressed.

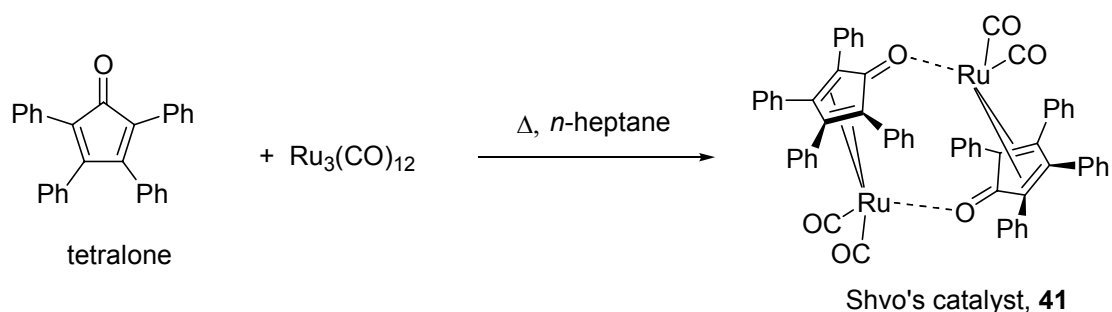


**Scheme 2.5** Oxidation and isomerization of D-glucose (**2**) to the  $\delta$ - and  $\gamma$ -lactone (**40** and **10**).

### 2.2.2 Shvo's Catalyst

The hydrogen transfer catalyst  $[(\eta^4\text{-C}_6\text{H}_4\text{CO})(\text{CO})_2\text{Ru}]_2$  (**41**), also known as Shvo's catalyst, has been shown to be an active catalyst for the dehydrogenation of primary alcohols to esters,<sup>23</sup> the disproportionation of aldehydes to esters<sup>24</sup> and the oxidation of secondary alcohols to ketones.<sup>25-27</sup>

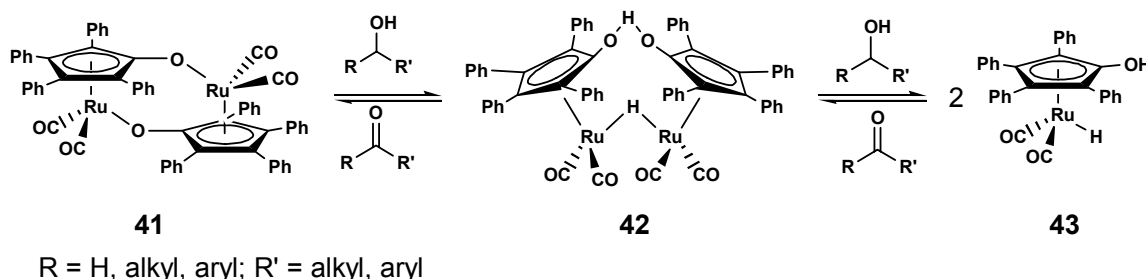
In preliminary studies Blum and Shvo showed that solutions of  $\text{Ru}_3(\text{CO})_{12}$  showed catalytic activity for the disproportionation of primary alcohols to esters and that the catalytic activity was highest when diphenylacetylene rather than ketones or aldehydes was added as the hydrogen acceptor.<sup>23</sup> Subsequently they established that the catalytically active species in the solution are in fact ruthenium tetracyclone (= tetraphenyl-cyclopentadienone) carbonyl complexes and isolated the dimeric complex  $[(\eta^4\text{-C}_6\text{H}_4\text{CO})(\text{CO})_2\text{Ru}]_2$  (**41**) as the resting state of the catalyst. The tetraphenyl-cyclopentadienone ligand was generated *in situ* through a [2+2+1] cycloaddition reaction with diphenylacetylene and carbon monoxide.<sup>23,28</sup> The dimeric ruthenium complex  $[(\eta^4\text{-C}_6\text{H}_4\text{CO})(\text{CO})_2\text{Ru}]_2$  (**41**) can also be synthesized directly by reacting  $\text{Ru}_3(\text{CO})_{12}$  with tetralone as shown in **Scheme 2.6**.<sup>24,29</sup>



**Scheme 2.6** Synthesis of  $[(\eta^4\text{-C}_6\text{H}_4\text{CO})(\text{CO})_2\text{Ru}]_2$  from  $\text{Ru}_3(\text{CO})_{12}$  and tetralone.

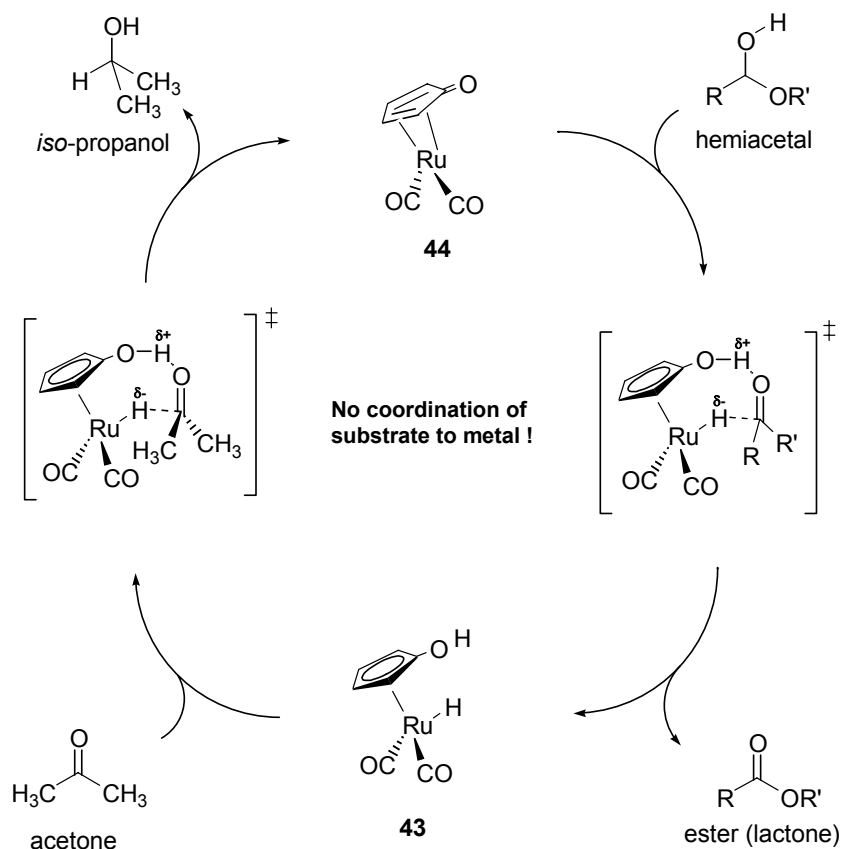


The complex  $[(\eta^4\text{-C}_4\text{Ph}_4\text{CO})(\text{CO})_2\text{Ru}]_2$  (**41**) reacts with alcohols to the hydrogen loaded dimer  $(\eta^5\text{-C}_4\text{Ph}_4\text{COHOCC}_4\text{Ph}_4)(\mu\text{-H})(\text{CO})_4\text{Ru}_2$  (**42**) and the monomeric ruthenium hydride complex  $(\eta^5\text{-C}_4\text{Ph}_4\text{COH})(\text{CO})_2\text{RuH}$  (**43**) (**Scheme 2.7**). All three complexes as well as the coordinatively unsaturated monomeric 16 electron complex  $(\eta^4\text{-C}_4\text{Ph}_4\text{CO})(\text{CO})_2\text{Ru}$  (**44**) have been shown to be part of the catalytic cycle, either as reactive intermediates (**42** and **44**) or catalyst resting states (**41** and **43**).<sup>30</sup>



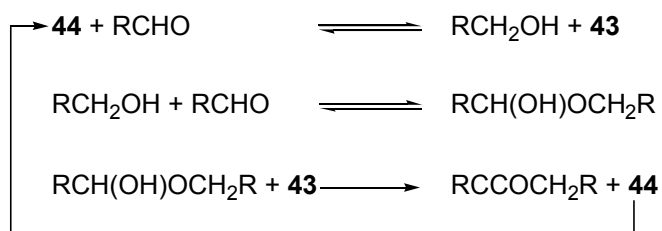
**Scheme 2.7** Hydrogen-transfer reaction of Shvo's catalyst (**42**).

The catalytic reaction mechanism of ruthenium complex  $[(\eta^4\text{-C}_4\text{Ph}_4\text{CO})(\text{CO})_2\text{Ru}]_2$  in the transfer (de-)hydrogenation of ketones to secondary alcohols is illustrated in **Scheme 2.8**. The dimeric ruthenium complex **41** is a precatalyst, as only the monomeric fragments **43** and **44** are catalytically active. In a first step, the unsaturated  $\text{Ru}^0$  complex **44** reacts with secondary alcohols to the hydrogen loaded  $\text{Ru}^{\text{II}}$  complex **43**. The ligand takes an active part in the catalytic cycle and thus, the mechanism is an example of ligand-metal bifunctional catalysis. In a second step, *iso*-propanol is generated from acetone by a direct transfer of a hydride from Ru to the carbonyl carbon atom and a proton from the phenol-type ligand to the oxygen atom in acetone. Upon releasing *iso*-propanol, the  $\text{Ru}^0$  complex is regenerated. In this reaction mechanism, neither ketone nor alcohol substrate bind directly to the Ru metal centre of **43** and **44**. A formation of alkoxy complexes similar to  $\text{RuH}_2(\text{PPh}_3)_4$  reaction mechanism is not observed.



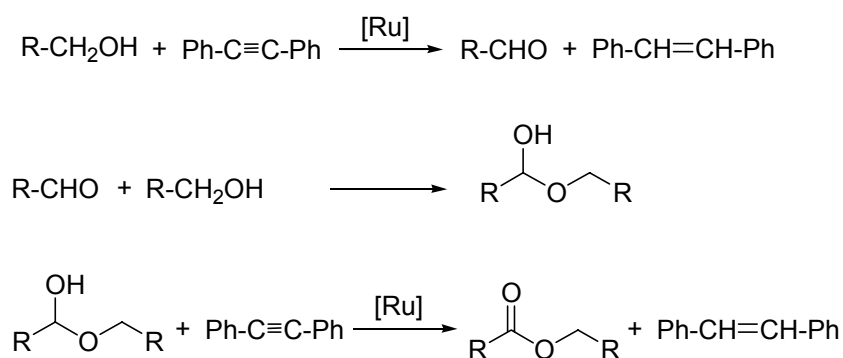
**Scheme 2.8** Dehydrogenation reaction mechanism of Shvo's catalyst.

The disproportionation of aldehydes to esters by the Shvo catalyst system follows the steps shown in **Scheme 2.9**,<sup>24</sup> i.e. involves the formation of hemiacetals as intermediates.



**Scheme 2.9** Reaction pathway of primary alcohols to corresponding ester.

Similarly to the aldehyde disproportionation reaction an ester can be prepared in the oxidation reaction of two primary alcohols using diphenylacetylene as hydrogen acceptor as shown in **Scheme 2.10**. A primary alcohol is transformed into the corresponding aldehyde by hydrogen transfer reaction to diphenylacetylene to produce *cis*-diphenylethene. The aldehyde generated then reacts with a second primary alcohol forming a hemiacetal, which is then oxidized to the ester in a second hydrogen transfer reaction, again with diphenylacetylene as hydrogen acceptor.



**Scheme 2.10** Transformation of primary alcohols to esters by Shvo's catalyst with diphenyl-acetylene as hydrogen acceptor.

## 2.3 Results and Discussion

### 2.3.1 Rationale for the Selection of Catalyst and Reaction Conditions

On the basis of the literature known reactions discussed above, we postulated that Shvo's catalyst would also be a highly effective catalyst for the oxidation of hemiacetal function in reducing sugars, possibly under very mild conditions. This hypothesis was tested by a simple NMR scale experiment. Shvo catalyst dimer **41** (0.020 mmol = 0.040 mmol ruthenium) is dissolved in 1.5 mL DMF- $d_7$  to give a clear orange-yellow solution, the  $^1\text{H}$  NMR spectrum of displays only the previously reported signals of the phenyl protons of **41**.<sup>29</sup> Addition of 0.20 mmol  $\alpha$ -D-glucose (5-fold excess with respect to ruthenium) to this solution at room-

temperature leads to an instantaneous colour change to deep red. The  $^1\text{H}$  NMR of this solution shows two singlets intensity 1:1 at 10.2 and  $-9.7$  ppm assigned to the hydroxyl proton and hydride ligand of the hydrogenated monomer complex **43** along with the overlapping signals of a mixture of **2** and **40**. Addition of 0.2 mmol of benzalacetone to the sample and heating to  $100^\circ\text{C}$  for 6 h resulted in a colour change back to orange-yellow and the disappearance of the peaks assigned to **43** indicating that the equilibrium in **Scheme 2.7** had been shifted back to complex **41**. Due to the presence of the large amount of hydrogen acceptor the other regions of the  $^1\text{H}$  NMR of the resulting solution do not lend themselves to a detailed  $^1\text{H}$  NMR analysis. However, the  $^{13}\text{C}$  NMR spectrum shows that judging from the signals for the C1 carbon atoms at 172.0 and 175.7 ppm, respectively, that an 8:1 mixture of  $\delta$ - and  $\gamma$ -gluconolactone had formed with no starting material remaining. The sugar was quantitatively converted to the  $\delta$ -lactone with only a marginal amount of subsequent isomerization to the  $\gamma$ -lactone occurring. In addition, a control experiment in which a solution of authentic  $\delta$ -gluconolactone in  $\text{DMF-d}^7$  and 10 mol% **41** was heated for 2 h did not result in any measurable formation of  $\gamma$ -lactone. From these experiments it was evident that the Shvo system is indeed a viable hydrogen transfer catalyst for the transformation of pyranose sugars into their corresponding  $\delta$ -lactones, but – in contrast to  $\text{RhH}(\text{PPh}_3)_4$  – does not or only marginally catalyze their isomerization to the  $\gamma$ -lactones.

## 2.3.2 Synthesis and Isolation of $\delta$ -Lactones

### 2.3.2.1 Variation in Hydrogen Acceptor

$\delta$ -/  $\gamma$ -mixtures of the lactones can be isolated from reaction mixtures as the one described above by removal of the catalyst, DMF solvent and benzalacetone through solvent evaporation in high vacuum and sonication with chloroform for extended periods of time ( $> 12$  h). Filtration and drying *in vacuo* at elevated temperature leaves the lactones as white solids. However the yields of

gluconolactone isolated (< 60 %) as well as the  $\delta$ : $\gamma$ -ratios (between 4:1 to 1:1) were unsatisfactory. We therefore evaluated a series of alternative hydrogen acceptors to optimize both. The investigated hydrogen-acceptors are listed in **Figure 2.1**.

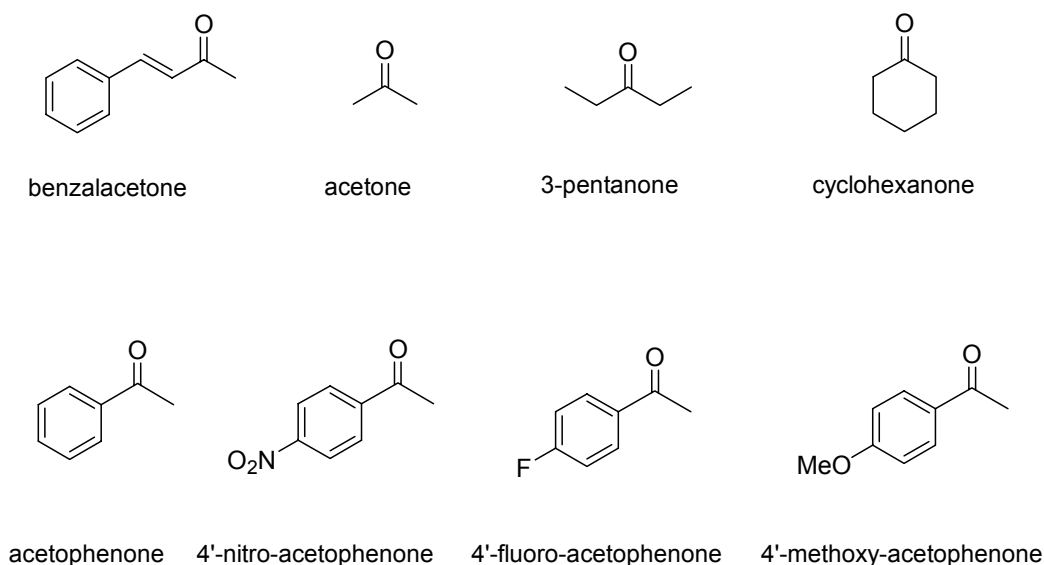


**Figure 2.1** List of investigated hydrogen-acceptor molecules.

Based on the original works of Beaupere,<sup>20,22</sup> which used benzalacetone as hydrogen acceptor, a series of aromatic acetophenone derivatives was investigated. The reaction time varied from 2 h to over 10 weeks with different hydrogen-acceptors in anhydrous DMF at 45 °C. The results of the oxidation experiments of  $\alpha$ -D-glucose are summarized in **Table 2.1**. The influence of an electron rich carbonyl function, i.e. *para*-methoxy electron donating substituent, and electron poor carbonyl function, i.e. *para*-nitro substituent, reduced the reactivity of the oxidation reaction by orders of magnitude compared to benzalacetone as the reference. In the case of *para*-nitro-acetophenone the solution turned black after 4 weeks indicating a degradation of Shvo's catalyst.

**Table 2.1** Oxidation of glucose with Shvo's catalyst (**42**) with various hydrogen-acceptors.<sup>a</sup>

Entry	Hydrogen-acceptor	Equiv. <sup>b</sup>	Reaction time	Ratio of $\gamma$ : $\delta$ lactone <sup>c</sup>	Conversion <sup>d</sup>
1	Benzylidenacetone	15	67 h	3 %: 97 %	95 %
2	Benzylidenacetone	2	18 d	18 % : 82 %	>99 %
3	4'-nitro-acetophenone	2	>10 weeks	Only $\gamma$ -lactone	50 % <sup>e</sup>
4	4'-fluoro-acetophenone	2	9 weeks	Only $\gamma$ -lactone	> 99 %
5	4'-methoxy-acetophenone	2	> 8 weeks	Only $\gamma$ -lactone	60 %

<sup>a</sup>  $\alpha$ -D-Glucose (265 mg, 1.47 mmol), Shvo's catalyst (20 mg, 0.018 mmol = 2.5 mol% with respect to substrate) and hydrogen-acceptor in anhydrous DMF (10 mL) at room temperature. Naphthalene as internal GC standard.<sup>b</sup> Molar equivalents of hydrogen-acceptor with regard to glucose. <sup>c</sup> Determined by <sup>1</sup>H NMR of isolated material. <sup>d</sup> Conversion of  $\alpha$ -D-glucose determined by quantitative GC measurements of consumed hydrogen acceptor. <sup>e</sup> Black colour after 4 weeks.

The results in **Table 2.1** show that benzalacetone as hydrogen-acceptor is much more effective than the *para*-acetophenone compounds. An increase in the amount of hydrogen acceptor dramatically reduced the reaction time and produced a favourable ratio of  $\gamma$  :  $\delta$ - gluconolactone. 15 equivalents of benzalacetone (= 3.2 g, 22 mmol) are the maximum amount, which dissolves at room temperature in 10 mL anhydrous DMF, i.e. a saturated solution. Under these conditions the oxidation reaction is to 95 % completed within less than 3 d compared to 3 weeks (**Table 2.1, Entries 1 and 2**). Observing such a vast reactivity increase, the focus was on utilizing an excess of hydrogen-acceptor. The reaction of Shvo's catalyst **41** with sugar hemiacetal produced an instantaneous colour change suggesting that the proposed rate determining step of the catalytic mechanism is the reaction of the hydrogen loaded intermediate **43** with hydrogen acceptor. Using an excess of hydrogen-acceptor should therefore accelerate the oxidation reaction. In order to avoid saturation limit effects of the hydrogen-acceptor, liquid hydrogen acceptors were investigated. The four chosen hydrogen acceptors are miscible with DMF at room temperature and are listed in **Table 2.2**. The reaction conditions were designed for the complete

dissolution of the sugar substrate in the DMF/acceptor mixture rather than a true comparison of thermodynamic and kinetic parameters. The transfer hydrogenation equilibrium is based on molar equivalents and a clear trend emerges from the data: the shorter the reaction time the higher the amount of  $\delta$ -lactone obtained. This is congruent with the notion that – just as for the other oxidation methods described above – the  $\delta \rightarrow \gamma$  isomerization follows the initial oxidation of the pyranose to the  $\delta$ -lactone. The different reaction times observed possibly reflect different degrees of steric interactions between the acceptor and **43** affecting the rate of the hydrogen transfer reaction from **43** to the acceptor. E.g., the conformationally flexible 3-pentanone results in the slowest while the conformationally rigid and effectively “smaller” cyclohexanone gives the fastest reaction. Considering the release of ring strain energy in the hydrogenation of cyclohexanone to cyclohexanol, a linear free enthalpy relationship may also be in effect here.<sup>8,31</sup>

**Table 2.2** Effectiveness of excess hydrogen acceptors for the catalytic dehydrogenation of D-glucose in DMF by **41**.<sup>a</sup>

Entry	Acceptor	Amount	Reaction time [h]	$\gamma$ : $\delta$ - Lactone ratio <sup>b</sup>
1	Cyclohexanone	5 mL = 33 eq.	2	3 %: 97 %
2	Acetone	5 mL = 46 eq.	18	7 %: 93 %
3	3-pentanone	5 mL = 32 eq.	312	12 %: 88 %
4	Acetophenone	5 mL = 29 eq.	18	10 %: 90 %

<sup>a</sup> Reaction conditions: D-glucose (265 mg = 1.47 mmol) in 7 mL dry DMF, 45°C, 1.25 mol % **41** (20 mg = 0.018 mmol). <sup>b</sup> Determined by <sup>1</sup>H NMR of isolated materials.

### 2.3.2.2 Variation of Co-solvent

A variation in aprotic polar amide solvents from DMF to DMA and NMP was conducted in order to investigate solvent activity in the oxidation of glucose to  $\delta$ -gluconolactone with Shvo's catalyst. The oxidation reactions were monitored by GC analysis of the tracking of the cyclohexanol content, which was equal to total gluconolactone content formed. The reaction conditions were 1.47 mmol  $\alpha$ -D-glucose, 1.25 mol% Shvo's catalyst (= 2.5 mol% ruthenium per substrate)

and 2.94 mmol benzalacetone at 45°C in 10 mL of the respective amide solvent (Figure 2.2).

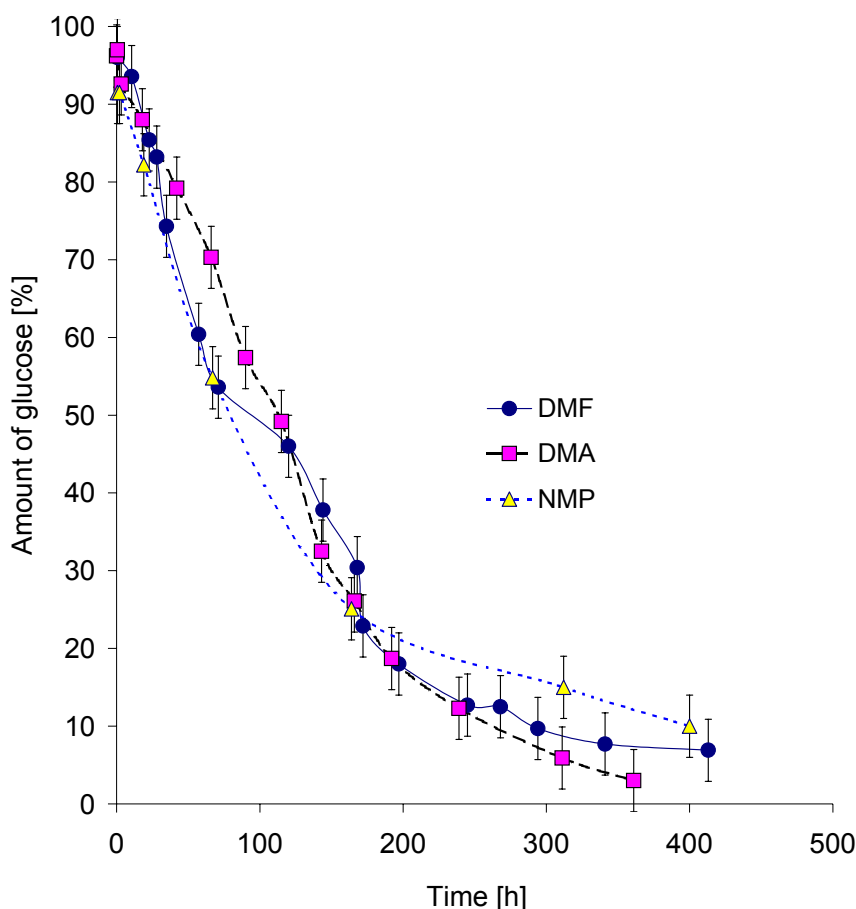


**Figure 2.2** Shvo's catalyst **41** (20 mg, 2.5 mol% per Ru),  $\alpha$ -D-glucose (1.47 mmol) and benzalacetone (2.94 mmol) at 45 °C in 10 mL of solvent monitored by GC of produced cyclohexanol.

Within the range of accuracy of the quantitative GC measurements, there is no significant difference in reaction rate between the three amide solvents. The  $\gamma$  :  $\delta$  gluconolactone ratios, which were determined by NMR analysis of the isolated products were identical in all three solvents. Solubility of catalyst and sugar substrate also was not measurably different. Not surprisingly removal of the solvent by evaporation *in vacuo* was found to take longer with the higher boiling solvents DMA and NMP compared to the lowest boiling DMF solvent, possibly negatively affecting the  $\gamma$  :  $\delta$ -ratio during work-up. For further oxidation reaction experiments DMF was therefore the chosen as co-solvent.



### 2.3.2.3 Oxidation Reactions without Co-solvent

A yellow to dark orange colour change of Shvo's catalyst was observed when  $\alpha$ -D-glucose, Shvo's catalyst and cyclohexanone were mixed and *before* DMF had been added. The orange colour indicated that oxidation of the sugar substrate occurred generating the hydrogen loaded form **43**, which is dark orange coloured, and suggesting that  $\alpha$ -D-glucose is sufficiently soluble in cyclohexanone for the reaction to occur.

Thus a series of reactions were carried out, in which glucose, mannose and galactose were oxidized with cyclohexanone with and without the presence of amide solvent.

Typical profiles of these reactions were obtained by tracking the amount of cyclohexanol produced as determined by GC and disregarding the  $\delta$  :  $\gamma$  ratio of the lactones formed and are shown in **Figure 2.3**. Under the reaction conditions no other products resulting from the oxidation of the secondary or primary hydroxyl functions in the sugar are detectable, i.e. the amount of cyclohexanol is equimolar to the amount of lactone present. In order to ensure reproducible results, the dispersions of sugar in cyclohexanone solvent were vigorously stirred.

The oxidation of the monosaccharides glucose, mannose and galactose in cyclohexanone are slower without DMF co-solvent than with DMF co-solvent as shown in **Figure 2.3**. In principle, the oxidation reaction can occur in solution, on the surface of the solid particles, or both. If the reaction occurs on the surface only, the observed reaction rates would only be marginally different, as approximately similar surface areas should be available to the catalyst for all three sugar substrates. However, the observed reaction rates are different, which therefore must reflect the different solubilities of the respective sugars in cyclohexanone solvent. In analogy, the solubility in aqueous solutions scales in

the order  $\alpha$ -D-glucose >  $\alpha$ -D-mannose >  $\alpha$ -D-galactose.<sup>1</sup> Further evidence for a solution phase oxidation is that the reaction temperature had to be raised to 45°C in order to observe an oxidation reaction for mannose and galactose. In contrast, the conversion of  $\alpha$ -D-glucose was approximately 20 % after 24 h at ambient temperature.

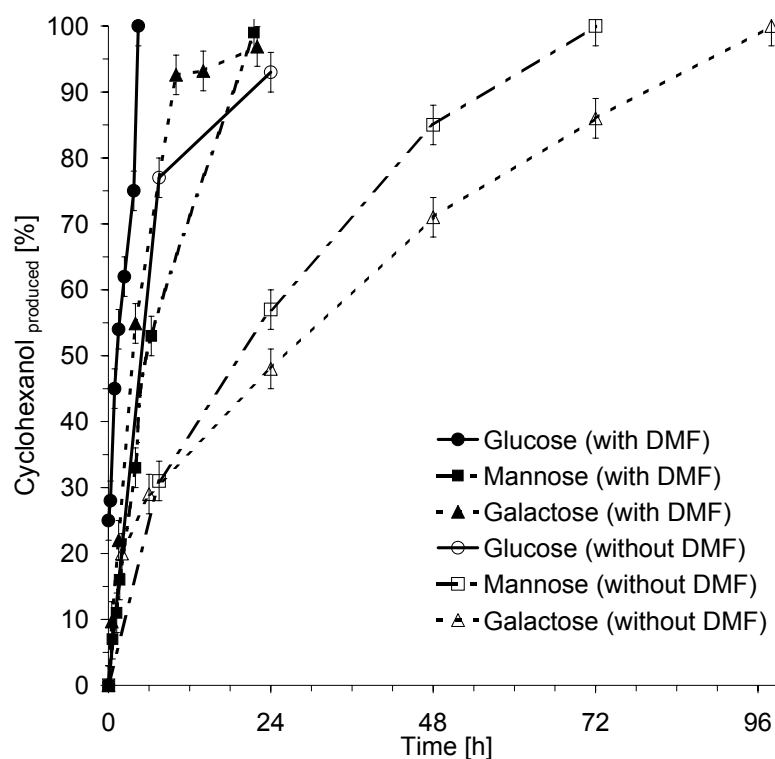


**Figure 2.3** Oxidation of sugars with Shvo's catalyst. Reaction conditions: a) **with DMF** (solid symbols): 132 mg sugar, 10.0 mg Shvo' catalyst **41**, 3.5 mL cyclohexanone, 2.5 mL DMF, naphthalene as internal standard, 45°C. b) **without DMF** (empty symbols): 132 mg sugar, 10.0 mg Shvo catalyst **41**, 5 mL cyclohexanone, naphthalene as internal standard, 45°C.

In these reactions the lactone content in the glucose oxidation is exclusively  $\delta$ -gluconolactone. In contrast, the  $\gamma$ -lactones were predominantly obtained in the oxidation of mannose and galactose with only traces of  $\delta$ -lactone due to the elevated temperature of 45°C and the prolonged reaction times of 72 h and 96 h, respectively.

As illustrated in **Figure 2.4**, the undissolved, solid glucose and gluconolactone compounds established an equilibrium between the gluconolactone and glucose produced based on their respective solubility constants in cyclohexanone solvent.

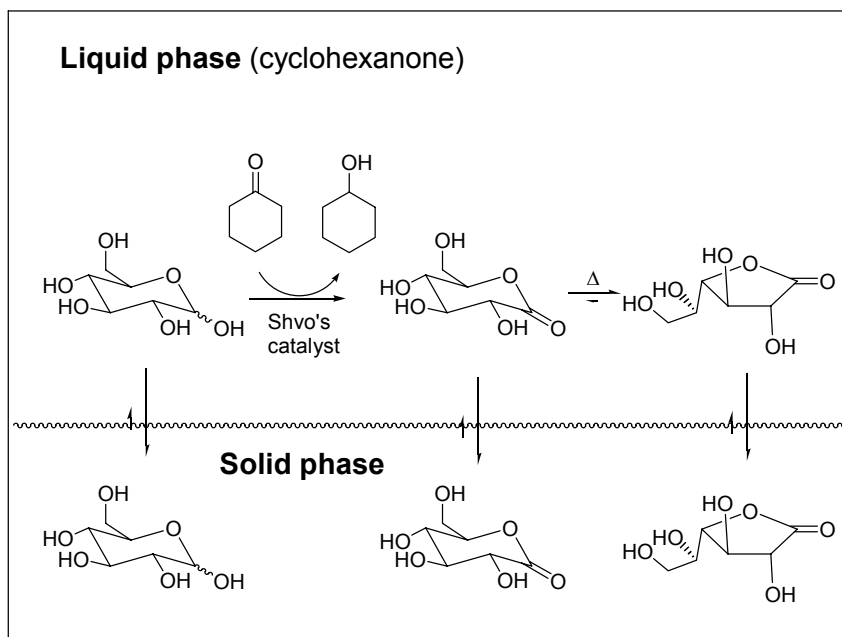
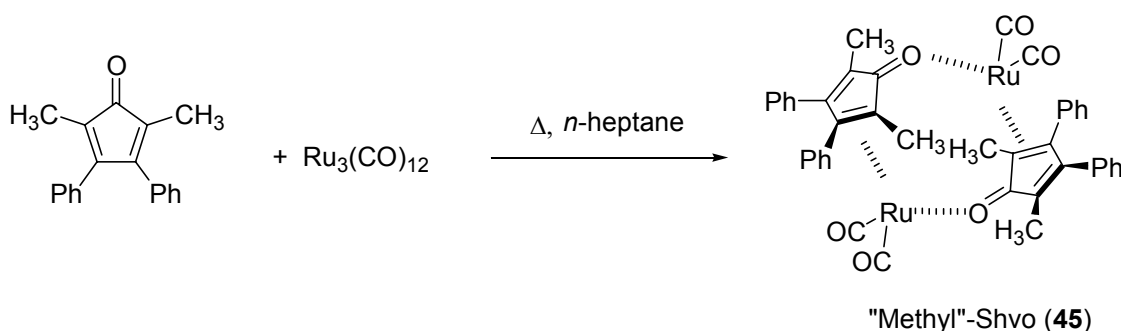


**Figure 2.4** Oxidation of  $\alpha$ -D-glucose to  $\delta$ -D-gluconolactone with Shvo's catalyst in cyclohexanone solvent without DMF co-solvent.

An increase in oxidation reactivity was anticipated by raising the polarity of the cyclohexanone solvent. However, when *N*-tetraalkylammonium bromide (10 mol%) was added to the dispersion reaction no increase in oxidation rate was detected. A change of morphology of the monosaccharides by using finely powdered starting materials from different commercial source also had no measurable impact on the reaction rates.

### 2.3.2.4 Modification of Catalyst

The ligand of the Shvo catalyst is actively involved in the hydrogen transfer reaction, thus modifications of the cyclopentadienone moiety should affect its catalytic activity. The effect can derive from either a steric or electronic aspect. The effect of ligand modification on catalytic activity was explored by synthesis of the analogue (**45**) from commercially available 2,5-dimethyl-3,4-diphenyl-cyclopentadienone and  $\text{Ru}_3(\text{CO})_{12}$  according to published procedures in 65 % yield (**Scheme 2.11**).<sup>29</sup>



**Scheme 2.11** Synthesis of "Methyl"-Shvo catalyst (**45**).

The catalytic activity of the "Methyl"-Shvo catalyst **45** (1.25 mol%) was tested under the standard reaction conditions of **41** with the three monosaccharides  $\alpha$ -D-glucose,  $\alpha$ -D-mannose and  $\alpha$ -D-galactose in 7 mL DMF and 5 mL cyclohexanone solution as well without amide solvent in 12 mL cyclohexanone at 45°C. In comparison to the tetraphenyl substituted parent catalyst **41**, the "Methyl"-Shvo catalyst (**45**) is approximately half reactive in cyclohexanone dispersion and DMF/cyclo-hexanone solvent mixture reactions. This observation can be rationalized by the steric volume of the 2,5-dimethyl substituents compared to that of the 2,5-diphenyl ligands. Compared to the tripodal methyl groups, the phenyl ligands are relatively "flat" and when oriented perpendicular to

the cyclopentadienone moiety would experience substantially less interactions with an incoming substrate than the rotationally invariant “footprint” of methyl groups in the same position. Possible other analogs in which substituents would lower or raise the electron density of the cyclopentadienone moiety by substitution of electron with more electron withdrawing or electron donating groups were initially considered, but dismissed as the required starting materials were not readily available.

### 2.3.2.5 Optimized Reaction Conditions

On the basis of the results listed in **Table 2.2**, cyclohexanone was adopted as the hydrogen acceptor for all subsequent experiments. Reaction and isolation procedures based on decantation and centrifugation designed to minimize thermal stress on the material and hence the  $\delta \rightarrow \gamma$  ratios and are detailed in the experimental section.

**Table 2.3** summarizes the isolated yields and  $\delta \rightarrow \gamma$  ratios of the lactones for the oxidation of glucose, mannose and galactose using these protocols (*Method A* and *B*). *Method A* carried out at room temperature (21°C) constitutes an empirically determined compromise between the reaction rate of oxidation and the rate of  $\delta \rightarrow \gamma$  isomerization and is optimized for the maximum amount of labile  $\delta$ -lactones **5a** and **6a** present in the isolated material rather than yield.

**Table 2.3** Oxidation of sugars with the Shvo’s catalyst system and cyclohexanone as the hydrogen acceptor at 45 °C.

Entry	Sugar	Method <sup>a</sup>	Time [h]	T [°C]	Conversion <sup>b</sup> [%]	Isolated yield [%]	$\delta/\gamma$ ratio of isolated product <sup>c</sup>
1	Glu	B	16	45	98	86	99.9 : 0.1
2	Man	A	87	21	91	41	94 : 6
3	Gal	A	87	21	92	54	93 : 7

<sup>a</sup> See Experimental section. <sup>b</sup> By quantitative GC of cyclohexanol formed with naphthalene as internal standard; estimated error  $\leq 5\%$ . <sup>c</sup> Determined by <sup>1</sup>H NMR of isolated product.

As *method B* specifies the oxidations can in fact be carried out in a cyclohexanone suspension without DMF solvent by exploiting the marginal solubilities of the sugars in the acceptor itself. The method is however only practical for the oxidation of glucose, as for mannose and galactose the oxidation reactions at 21°C without DMF solvent are very slow while at 45°C the  $\gamma$ -mannonolactone (**46**) and  $\gamma$ -galactonolactone (**31**) dominate the product distribution.

**Table 2.4** Comparison of the NMR Data for  $\delta$ -D-galactonolactone (**30**) with those of  $\delta$ -D-gluconolactone (**40**) and  $\delta$ -D-mannonolactone (**47**) in DMSO- $d_6$ .

<sup>1</sup> H δ [ppm]	H-2	H-3	H-4	H-5	H-6	H-6'	OH-2	OH-3	OH-4	OH-6	
Glu	3.79 dd	3.54 m	3.54 m	4.00 m	3.65 ddd	3.56 m	5.81 d	5.43 m	5.43 m	4.89 t	
Glu (Lit.) <sup>a</sup>	3.79 m	3.53 m	3.51 m	4.01 o	3.65 q	3.55 m	b	b	b	b	
Man	4.45 dd	3.81 m	3.54 m	4.01 ddd	3.63 ddd	3.50 m	5.36 d	5.31 d	5.52 d	4.89 t	
Man (Lit.) <sup>a</sup>	4.93 dd	4.31 dd	4.03 dd	4.49 o	4.12 q	3.98 q	b	b	b	b	
Gal	4.01 dd	3.71 ddd	3.89 q (br)	4.21 t (br)	3.55 m	3.55 m	5.72 d	5.32 d	5.24 d	4.88 dd	
J [Hz]	<sup>3</sup> J <sub>2,3</sub>	<sup>3</sup> J <sub>3,4</sub>	<sup>3</sup> J <sub>4,5</sub>	<sup>3</sup> J <sub>5,6</sub>	<sup>3</sup> J <sub>5,6'</sub>	<sup>2</sup> J <sub>6,6'</sub>	<sup>4</sup> J <sub>2,5</sub>	<sup>3</sup> J <sub>2,OH2</sub>	<sup>3</sup> J <sub>3,OH3</sub>	<sup>3</sup> J <sub>4,OH4</sub>	<sup>3</sup> J <sub>6,OH6</sub>
Glu (Lit.) <sup>a</sup>	8.5 <sup>a</sup>	7.5 <sup>a</sup>	8.1 <sup>a</sup>	2.5 <sup>a</sup>	4.4 <sup>a</sup>	−12.2 <sup>a</sup>	0.5 <sup>a</sup>	5.6	m	m	5.6
Man (Lit.) <sup>a</sup>	3.4 <sup>a</sup>	1.2 <sup>a</sup>	8.3 <sup>a</sup>	2.6 <sup>a</sup>	5.4 <sup>a</sup>	−12.6 <sup>a</sup>	0.5 <sup>a</sup>	6.3	3.5	5.6	5.8
Gal	9.8	2.5	1.5	6.2 <sup>c</sup>	6.2 <sup>c</sup>	−11.0 <sup>c</sup>	< 0.5	6.2	5.2	4.4	5.628; 5.738
<sup>13</sup> C δ [ppm]	C-1	C-2	C-3	C-4	C-5	C-6					
Glu	172.0	72.5	67.9	73.9	81.4	60.2					
Glu (Lit.) <sup>a</sup>	172.2	71.4	73.6	67.8	81.4	60.3					
Man	173.0	69.9	68.4	75.2	80.8	61.0					
Man (Lit.) <sup>a</sup>	172.4	69.7	74.9	68.1	80.7	60.8					
Gal	172.6	69.9	71.8	69.9	79.8	67.6					

<sup>a</sup> Same value as reported by Walaszek *et al.*<sup>32</sup> and measured in the presence of CF<sub>3</sub>CO<sub>2</sub>H. <sup>b</sup> Not reported by the authors.<sup>32</sup> <sup>c</sup> Determined from Spinworks 2.2 simulation.<sup>33</sup>

### 2.3.3 NMR and Conformational Analysis

$^1\text{H}$  and  $^{13}\text{C}$  NMR spectra of  $\delta$ -D-galactonolactone (**30**) isolated in > 95 % isomeric purity (**Table 2.3**) were recorded in DMSO- $d_6$  at 400 MHz and 100 MHz, respectively. The combination of COSY, HSQC and APT techniques allows the unambiguous assignment of all resonances. **Table 2.4** lists the NMR data of all three  $\delta$ -lactones of glucose, mannose and galactose as obtained from this work at 294 K and the literature.<sup>32</sup> The slight differences in chemical shifts for **40** and **47** between those given by the literature and observed by us are due to the fact that the former were recorded in the presence of  $\text{CF}_3\text{COOH}$ , which presumably also precluded the authors from reporting the shifts and coupling constants of the protons of the hydroxyl functions. At the same time a spectrum of **30** cannot be obtained in the presence of  $\text{CF}_3\text{COOH}$ , as even traces of acid or base lead to a rapid isomerization **30**  $\rightarrow$  **31**.

The conformations of **40** and **47** in DMSO- $d_6$  have previously been determined by the calculation of dihedral bond angles using various forms of the Karplus equation.<sup>32</sup> This analysis suggested that the conformational equilibrium lies strongly in favor of a  $^4\text{H}_3(\text{gg})$  halfchair for **40**, essentially the same conformation as in the solid state determined by single-crystal X-ray crystallography<sup>10</sup> and a  $\text{B}_{2,5}(\text{gg})$  boat conformation for **47**.

We hypothesize that the molecular shape of the individual  $\delta$ -lactones in solution determines the pronounced differences in their stabilities with respect to the  $\delta \rightarrow \gamma$  isomerization and therefore carried out a conformational analysis of **30** on the basis of the NMR data obtained following the same rationale as Walaszek *et al.*<sup>32</sup> In order to verify the coupling constants obtained from the experimental spectrum and extract coupling constants (as listed in **Table 2.4**) for the broad resonances for H-5 at 4.21 ppm, H-4 at 3.89 ppm and the multiplet for H-6 and H-6' at 3.55 ppm we first simulated the spectrum of **30** using the *Spinworks* program by Marat.<sup>33</sup>



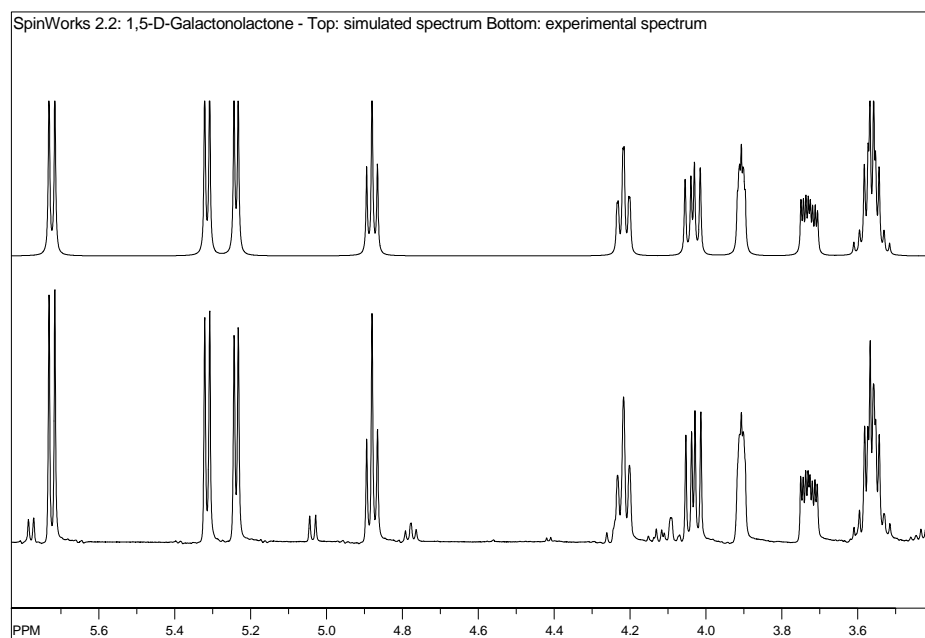


**Figure 2.5** Simulated and experimental  $^1\text{H}$  NMR spectrum of **30**.

**Figure 2.5** shows the simulated (top) and experimental (bottom) spectrum. The small additional peaks in the experimental spectrum represent small amount of the  $\gamma$ -lactone **31**<sup>34</sup> formed on the time-scale of the NMR experiment. With the experimental constants for  $J_{2,3}$  and  $J_{3,4}$  and the simulation derived coupling constant for  $J_{4,5}$  we determined the dihedral angles for these pairs of protons in **40**, **30** and **47** using the classical Karplus<sup>35,36</sup> as well as the Altona-Haasnoot equation.<sup>37</sup> The latter takes into account the effect of the chemical nature of substituents and their relative orientation to each other on the observed coupling constants through purely empirically derived position dependent substituent constants rather than group electronegativities.<sup>\*\*</sup> While the Altona-Haasnoot equation is mathematically only uniquely defined to express  $J$  as a function of the associated dihedral angle  $\phi$ , values for  $\phi$  as a function of the observed  $J$  value can easily be determined through a numeric analysis using standard spreadsheet programs.

<sup>\*\*</sup> Values for Altona-Haasnoot: OH = 1.34, C(=O)R = 0.51, OC(=O)R = 1.17 and CH(OH)  $\approx$  CH<sub>3</sub>.

We also determined the energy minimum structures of the lactones through Gaussian 98/03 calculations using the *mPW1PW91* method<sup>38</sup> with the 6-31(d,p) basis set and a continuous solvent sphere model in DMSO as implemented in the Gaussian 98/03 program.<sup>39-41</sup> With these geometries we carried out the “reverse” calculations, i.e. determined the coupling constants *J* from the dihedral angles that define the geometry of the pyranose ring. **Table 2.5** summarizes this data for all three  $\delta$ -lactones.

Making the reasonable assumption that the solid state structure of **40** is the true energy minimum of the pyranose ring or very close to it, the X-ray data for **40** provides a reference point for a comparison and quality assessment of the of the angles obtained from the Karplus and Altona-Haasnoot analysis on one hand and the quantum mechanical calculations on the other. The data in **Table 2.5** shows that the dihedral angles obtained from the DFT calculation provide a better overall fit to the X-ray structure than the ones calculated from the NMR coupling constants pointing to either the limitations of the Karplus and Altona methods or as suggested by Walaszek *et al.*<sup>32</sup> an equilibrium with other conformers of the lactone in solution or even more likely – both. By extension we postulate with high confidence that the same is true for the structures of **30** and **47**, i.e. the geometries obtained from the DFT calculation represent energy minima that in solution are in equilibrium with other minor conformers whose presence impacts the observed *J* values and hence the dihedral angles calculated from them. **Figure 2.6** shows the geometries of all three  $\delta$ -lactones as determined by the DFT calculations.

**Table 2.5** Calculated dihedral angles and coupling constants for  $\delta$ -lactones **40**<sup>34</sup>, **47**<sup>32</sup> and **30**.

$J_{xy}$	$J$ [Hz] exp.	$[\theta]$ X-ray	$[\theta]$ calc. by G98 <sup>a</sup>	$[\theta]$ calc. from $J$ Karplus	$[\theta]$ calc. from $J$ Altona <sup>b</sup>	$J$ [Hz] calc. from X-ray $[\theta]$ Karplus	$J$ [Hz] calc. from X-ray $[\theta]$ Altona	$J$ [Hz] Calc. from G98 $[\theta]$ Karplus	$J$ [Hz] Calc. from G98 $[\theta]$ Altona
<b>Glu</b>									
<b>2,3</b>	8.5	167.3	176.7	164.0	147.0	8.8	9.7	9.2	9.5
<b>3,4</b>	7.5	178.3	175.7	154.8	164.0	9.2	8.8	9.2	8.6
<b>4,5</b>	8.1	170.9	176.8	159.9	158.0	9.0	8.9	9.2	9.1
<b>Man</b>									
<b>2,3</b>	3.4	n/a	45.7	49.0	53.0	n/a	n/a	3.9	4.3
<b>3,4</b>	1.2	n/a	135.9	113.0	81.0	n/a	n/a	4.6	3.7
<b>4,5</b>	8.3	n/a	177.7	162.0	160.0	n/a	n/a	9.2	9.1
<b>Gal</b>									
<b>2,3</b>	9.8	n/a	176.4	n/a <sup>c</sup>	168.8 <sup>d</sup>	n/a	n/a	9.2	9.6
<b>3,4</b>	2.5	n/a	54.2	55.0	57.0	n/a	n/a	2.6	2.8
<b>4,5</b>	1.5	n/a	35.0	63.0	78.0	n/a	n/a	5.4	6.3

<sup>a</sup> Geometry and frequency optimized using the mPW1PW91 method with the 6-31(d,p) basis set and a continuous solvent sphere model in DMSO. <sup>b</sup> Calculated numerically. <sup>c</sup> Mathematically not defined. <sup>d</sup> Mathematically maximum possible value equivalent to 9.7 Hz.

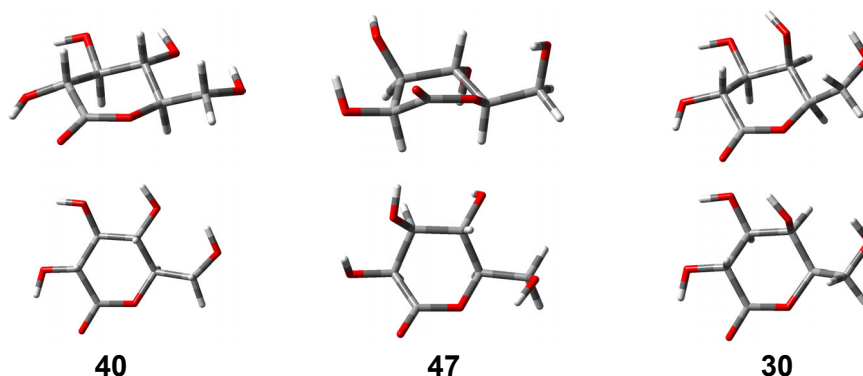


**Figure 2.6** “Side” and “top” view of the minimum energy conformations  $\delta$ -gluco (**40**),  $\delta$ -manno (**47**) and  $\delta$ -galactono (**30**) lactones determined by DFT (*mPW1PW91/6-31(d,p)*) calculations.

The DFT calculations recreate the  ${}^4H_3$  conformation for **4a** and the  $B_{2,5}$  conformation for **47** previously determined by a Karplus analysis<sup>32</sup> and result in a  ${}^4H_3$  for **30** congruent with the combined results of the Karplus and Altona analysis for this compound. The comparatively large discrepancies between the DFT and NMR results for the 3,4 dihedral angle in **47** and 4,5 dihedral angle in **30** point to the contribution in solution of a twist conformer for **47** and a somewhat more flattened halfchair for **30**, but do not change the overall geometry preference of the pyranose rings. The top view of the lactones (bottom row of structures in (**Figure 2.6**) reveals an ordered arrangement of the hydroxyl functions in **30** and **40** and to a lesser extent in **47** that – at least in the reference frame of the solvent model used – suggests the presence of a weak intramolecular hydrogen bond network at the static energy minimum determined by the DFT calculation. Since the energies involved in such bonds are on the order of 2-4 RT ( $\sim 5 - 10 \text{ kJ mol}^{-1}$ ) the situation is more dynamic in DMSO solution and only a small portion of the lactones will display this type of network. SIMPLE (i.e. H/D isotope exchange) and variable temperature NMR studies on monosaccharides by Angyal, Christofides and Vasella and co-workers<sup>42-44</sup> estimate that at any given time only 5 to 10 % of the sugar is internally hydrogen bonded with other C-O-H and C<sup>5</sup>-C<sup>6</sup>H<sub>2</sub>-O-H rotamers dominating, whose

energies are accessible by thermal molecular motion at 294 K. This explains why the DFT minimum energy structures of **30** and probably **40** do not represent the *gg* conformation proposed to dominate for the C<sup>5</sup>-C<sup>6</sup> bond.<sup>32</sup> We can however not make a definite statement for **30**, as the reported coupling constant of 6.2 Hz is derived from the simulation and the same for both  $J_{5,6}$  and  $J_{5,6'}$ . The true constants could be significantly different, but we are unable to extract them from the current data, as the signal for H-5 at 4.21 ppm is a broad pseudo-triplet and the simulated spectrum already provides an excellent match with the second order multiplet at 3.55 ppm for H-6/H6', i.e. the amount of information obtainable from the simulation is exhausted.

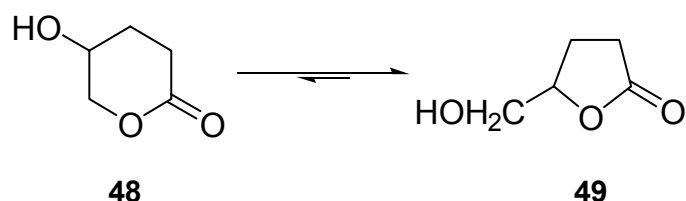
In summary, the DFT derived structures as well as the comparison of NMR coupling constants between **40/47** and **30** suggest that the  $\delta$ -D-galactonolactone (**30**) assumes the same <sup>4</sup>H<sub>3</sub> conformation as  $\delta$ -D-gluconolactone (**40**), a fact intimately related to its rapid isomerization to the  $\gamma$ -isomer (**31**) that to date had precluded its structural characterization.

### 2.3.4 $\delta$ to $\gamma$ Lactone Rearrangement

#### 2.3.4.1 Thermodynamic Considerations

Considering the parent compounds  $\gamma$ -butyrolactone and  $\delta$ -valerolactone as models, the pronounced greater stability of the  $\gamma$ -lactones over the  $\delta$ -lactones can be rationalized on the basis of a difference in ring strain between the pyrano and furano lactones – uniquely for alicyclic compounds larger for the 6- than the 5-membered ring.<sup>9</sup> Matching the conformational behavior of sugar lactones **30** and **40**,  $\delta$ -valerolactone also has a high preference for the half-chair conformation while  $\gamma$ -butyrolactone exists as a single conformer. The ring strains in  $\gamma$ -butyrolactone and  $\delta$ -valerolactone have been determined to 36.8 and 46.8 kJ mol<sup>-1</sup>, respectively, resulting in a  $K_{eq} = [\delta]/[\gamma] \approx 60$  on the basis of the release in ring strain alone. Similar behavior has been inferred in the equilibrium of the

model compounds 4-hydroxy- $\delta$ -valero-lactone (**48**) and 4-hydroxymethyl- $\gamma$ -butyro-lactone (**49**) (**Scheme 2.12**).<sup>31,45</sup> In addition for the lactones **30** and **40** there is an unfavorable steric interaction between the equatorial substituent on C-2 and the ester functionality in the  $^4H_3$  conformation adopted by these lactones (**Figure 2.6**).<sup>46</sup>



**Scheme 2.12** Equilibrium between 4-hydroxy- $\delta$ -valero-lactone (**48**) and 4-hydroxymethyl- $\gamma$ -butyrolactone (**49**).

The actual equilibrium  $\delta \rightarrow \gamma$  ratios of the three lactones in dry DMSO- $d_6$  were determined by the integration average of their sharp and well separated hydroxyl  $^1H$  NMR resonances. To ensure that equilibrium had been attained, individual samples were heated to 333 K for several days (**40/10**, **30/31**) or weeks (**47/46**) and slowly cooled to 294 K before the spectra were acquired. **Table 2.6** lists the experimentally determined ratios and free enthalpies calculated by van't Hoff's equation for the  $\delta \rightarrow \gamma$  isomerization. In addition **Table 2.6** compares the data to thermally and zero-point corrected energies obtained by DFT calculations for both isomers. It should be noted that the experimentally determined isomer distributions presented here cannot be directly compared to any previously published data,<sup>14,46,47</sup> as all of them were obtained in (buffered) aqueous solutions and thus include hydrolysis to the free aldonic acids, which is not observed in the dry DMSO medium employed in our study.

**Table 2.6** Experimental and DFT calculated  $\gamma$  :  $\delta$  ratios of the lactones in DMSO at 294 K.

Lactone ( $\gamma$ : $\delta$ ratio)	Experi- mental (+/- 2) <sup>a</sup>	$\Delta G_{\text{exp.}}$ ( $\delta \rightarrow \gamma$ ) [kJ mol <sup>-1</sup> ] <sup>b</sup>	mPW1PW91 6-31G (d,p) <sup>c</sup> (optimized)	$\Delta G_{\text{DFT}}$ ( $\delta \rightarrow \gamma$ ) [kJ mol <sup>-1</sup> ] <sup>b</sup>	mPW1PW91 6-311G (d,p) (single point) <sup>c</sup>	$\Delta G_{\text{DFT}}$ ( $\delta \rightarrow \gamma$ ) [kJ mol <sup>-1</sup> ] <sup>b</sup>
Glucono- lactone	89 : 11	- 5.1	3 : 97	8.5	4 : 96	7.7
Mannono- lactone	54 : 46	- 0.4	55.5 : 44.5	-0.5	38 : 62	1.2
Galactono- lactone	100 : 0	< - 9.5 <sup>d</sup>	0.9 : 99.1	11.5	34 : 66	1.6

<sup>a</sup> By integration of <sup>1</sup>H NMR signals. <sup>b</sup> By  $\Delta G = -RT \ln K$  <sup>c</sup> Reaction field solvent model in DMSO.  
<sup>d</sup> Based on an assumed maximum NMR integration error of  $\pm 2$  % resulting in  $\delta$  :  $\gamma$  = 98 : 2.

The discrepancies between the experimental data and those obtained from the DFT calculations are small in terms of total energies (1 – 12 kJ mol<sup>-1</sup>), but have a large impact on the  $\delta$  :  $\gamma$  equilibrium distribution and are thus instructive in pointing out the limitations of the computational method in the context of the current problem: While the DFT optimized structures provide a very good match with those derived by the Karplus/Altona and – in one case – X-ray analysis, the energy differences between the two isomers are too small to be accurately recreated *in silico*. Allinger has pointed out that the relative energies of monosaccharide conformers, in particular the energy differences between pyranose and furanose forms and  $\alpha/\beta$  anomers are more reliably obtained using larger basis sets.<sup>48</sup> Following his suggestion we therefore expanded the basis set to 6-311<sup>++</sup>(2d,2p) and calculated the single point energies of the lactones at this level using the minimized structures and thermal energy corrections obtained with the 6-31g(2d,2p) basis set. However as the last column in **Table 2.6** shows this also does not mirror the experimental data. While further calculations designed to explore the conformational potential energy surface, e.g. especially those incorporating other rotamers about the C(5)-C(6) bond (*i.e.*, various *gg*, *gt*, *tg* conformers) and C-O-H bonds may yet lead to a better match between theory and experiment, we believe the errors to be primarily associated with the limitations of the solvent model employed.

The calculated energy differences between conceivable conformers<sup>48</sup> are of the same order of magnitude as those of hydrogen bonds ( $10 - 40 \text{ kJ mol}^{-1}$ )<sup>44</sup> and those of the experimentally determined energy differences between  $\delta$ - and  $\gamma$ -lactones (**Table 2.6**). In the DMSO- $d^6$  solvent intermolecular and intramolecular hydrogen bonding competes (see **Figure 2.6**), however from the available experimental data there is no information on the number or relative orientation of the solvating DMSO molecules, i.e. no model of the structure of the solvent sphere, potential intermolecular hydrogen bonds and their influence on the relative energies of the isomers is available. While such a specific solvent cage model should in principle be open to a computational investigation, it constitutes a formidable challenge beyond our present capabilities.

#### 2.3.4.2 Mechanistic Considerations

The  $\delta \rightarrow \gamma$  isomerizations of the lactones in dry DMSO- $d^6$  (water content  $\ll 0.01$  eq./lactone by  $^1\text{H}$  NMR) follow simple 1<sup>st</sup> order kinetics. Dissolving 10 mg of the  $\delta$ -lactones in 0.6 mL of DMSO- $d^6$  rate constants of  $k_{\text{obs}} = 1.41 \times 10^{-4} \text{ s}^{-1}$  and  $k_{\text{obs}} = 1.73 \times 10^{-4} \text{ s}^{-1}$  are observed at 333 K for **40** and **30**, respectively, while **47** isomerizes too slowly for  $k$  to reliably measured by  $^1\text{H}$  NMR. Experimentally the equilibrium distributions in **Table 2.6** are reached within 7 h for **30/31** and 10 h for **40/10** (i.e., 7 half-lives each), while **47/46** requires weeks to attain the equilibrium. Overall, the isomerization process in DMSO- $d^6$  is orders of magnitudes slower than the value of  $k = 1 \text{ min}^{-1} = 1.67 \times 10^{-2} \text{ s}^{-1}$  observed for **30** in aqueous solution buffered at  $\text{pH} = 6.8$ ,<sup>14</sup> suggesting that in aqueous solution the isomerization is susceptible to general acid/base catalysis that is also observed in the hydrolysis of the lactones and precludes the isolation of **30** from aqueous solution.<sup>49</sup> Also, the relative rate of isomerization for the lactones **40** and **47** observed by us in DMSO- $d^6$  are opposite from those previously noted in the literature. This is probably because the only known previous preparation of **47** was carried out by dissolving calcium mannonate in excess aqueous oxalic



acid solution, i.e. under conditions of general acid catalysis and probably following a mechanism involving the free aldonic acid thus providing an alternative rapid isomerization pathway.<sup>13</sup>

The fact that there is essentially no water and no free acid present in the solutions investigated by us and that first order kinetics are observed, immediately suggest an intramolecular  $\delta \rightarrow \gamma$  rearrangement mechanism involving a nucleophilic attack of OH-4 on the carbonyl carbon as originally proposed for **40/10** by Jermyn.<sup>47</sup> In addition Überschär *et al.* have determined that – even in buffered aqueous solution – the  $\delta \rightarrow \gamma$  rearrangement of **30** to **31** is faster than the hydrolysis of **30** to free galactonic acid.<sup>14</sup> **Figure 2.7** depicts the three ester *hemi*-ketals that can be postulated to occur as intermediates on the reaction coordinate in order to effect the change from the  $\delta$ -1,5- to the  $\gamma$ -1,4-linkage.

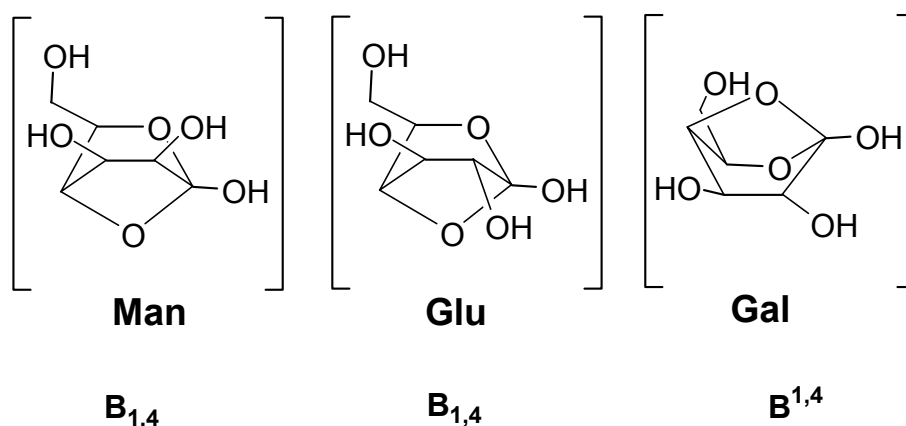


**Figure 2.7** Structures of the proposed bicyclic intermediates in the  $\delta \rightarrow \gamma$  isomerization reactions of mannono-, glucono- and galactonolactone.

Starting from the known dominant conformations of **40** and **47**<sup>32</sup> and the newly determined conformation of **30** (this work, see **Table 2.5**), applying the *principle of least molecular motion* and assuming that the formation of the bicyclic intermediates is the rate-determining elementary step, it is then evident that the

experimentally observed order of isomerization rates  $k_{\text{Gal}} > k_{\text{Glu}} \gg k_{\text{Man}}$  is a direct consequence of the relative structural similarity or dissimilarity between the postulated ester *hemi*-ketal intermediates and the native conformation of the  $\delta$ -lactones in DMSO- $d^6$ . The  ${}^4\text{H}_3$  conformation of **30** (Figure 2.6) is structurally most closely related to that of the  $\text{B}^{1,4}$  conformation of the intermediate requiring only motion of the  $\text{C}(1)=\text{O}$  (and to a lesser extent  $\text{C}(3)-\text{OH}-3$ ) group from below to above the plane defined by atoms  $\text{C}(2)-\text{C}(5)-\text{O}$ , i.e. the  $\delta$ -galactonolactone is structurally “set-up” to attain the geometry required to isomerize to the  $\delta$ -form resulting in a low activation barrier for this process. Starting from the same  ${}^4\text{H}_3$  conformation, the equatorial position of  $\text{OH}-4$  in **40** requires that the 1,4-linkage is established below the  $\text{C}(2)-\text{C}(5)-\text{O}$  plane to give a  $\text{B}_{1,4}$  conformation, requiring motion of both  $\text{C}(1)$  and  $\text{C}(4)$  thus leading to a higher activation barrier and a slower rearrangement. In comparison a yet much more extensive molecular motion is required for the  $\text{B}_{2,5} \rightarrow \text{B}_{1,4}$  conformational change that **47** has to undergo in order to establish the 1,4-linkage. In addition there is an unfavorable *cis*-interaction between  $\text{OH}-2$  and  $\text{OH}-3$  present in the ester *hemi*-ketal intermediate that we also assume to be present in the actual transition state of similar structure further raising the activation barrier resulting in the comparatively very slow rate of the **47**  $\rightarrow$  **46** rearrangement in DMSO- $d^6$ .

## 2.4 Conclusions

$\delta$ -D-Galactonolactone can be prepared and isolated from DMF solutions by transfer dehydrogenating D-galactopyranose with Shvo's catalyst and cyclohexanone as the hydrogen acceptor. In DMSO- $d^6$   $\delta$ -D-galactonolactone predominantly exists in the  ${}^4\text{H}_3$  conformation, a structure closely related to a bicyclic ester *hemi*-ketal postulated to be the intermediate in its rearrangement to the corresponding  $\gamma$ -lactone explaining its instability against this isomerization. In comparison  $\delta$ -glucono- and  $\delta$ -mannonolactone are much more stable against this isomerization as their native conformations do not or less closely resemble the shape of their corresponding ester *hemi*-ketal intermediates.

## 2.5 Experimental section

NMR spectra (400 MHz/ $^1\text{H}$ ; 100 MHz/ $^{13}\text{C}$ ) were measured in DMSO- $\text{d}_6$  with DMSO ( $\delta$  2.49,  $^1\text{H}$ ;  $\delta$  39.5,  $^{13}\text{C}$ ) and deuterated chloroform ( $\delta$  7.24,  $^1\text{H}$ ;  $\delta$  77.0,  $^{13}\text{C}$ ) as the internal reference. DMSO was stored inside a dry-box under argon atmosphere over 4 Å activated molecular sieves. For variable temperature measurements the spectrometer temperature controller unit was calibrated using a bimetal thermometer directly inserted into the probe.  $\delta/\gamma$ -ratios of the lactones were determined by integration of their  $^1\text{H}$  signals. NMR simulations were carried out using the SpinWorks program (Version 2.2).<sup>33</sup> DFT calculations were carried out on a PC using the Gaussian 98 and Gaussian 03 suite of programs. GC analyses were performed on a 30 m  $\times$  0.25 mm PEG column. The GC-FID was calibrated for cyclohexanol with naphthalene as an internal standard. All experimental preparations were conducted in a dry-box under argon atmosphere and/or with usual Schlenk technique on a vacuum line. Acetone, cyclohexanone and *n*-heptane were dried by distillation under argon from anhydrous  $\text{CaCl}_2$ , anhydrous  $\text{MgSO}_4$  and potassium, respectively, degassed and stored under argon. *N,N*-Dimethylformamide was dried over BaO and distilled under reduced pressure, then degassed and stored under Ar atmosphere. Cyclohexanol, cyclohexanone, 2,5-dimethyl-3,4-diphenyl-cyclopentadienone,  $\alpha$ -D-galactose,  $\alpha$ -D-glucose,  $\alpha$ -D-mannose, naphthalene, tetraphenyl-cyclopentadienone, acetone, chloroform, *n*-heptane,  $\text{Ru}_3(\text{CO})_{12}$  were purchased from commercial sources. All chemicals were reagent grade and used as obtained without further purification unless otherwise noted. Shvo's catalyst (**41**) and its dimethyl analog (**45**) was prepared according to literature procedures.<sup>29,50</sup> Best results were obtained when the synthesis was carried out inside the dry-box. Oil-pump vacua applied in the isolation of the lactones were  $\leq 30$  mTorr.

**General procedure A; oxidation of  $\alpha$ -D-galactose:** In a 50 mL Schlenk-flask under Ar atmosphere,  $\alpha$ -D-galactose (396 mg, 2.20 mmol), Shvo's catalyst (1.25 mol%, 30 mg), dry cyclohexanone (20 mL) and dry DMF (10 mL) were combined.

Naphthalene (50 mg) was added as internal GC standard. The reaction was stirred at 21°C and monitored by GC following the appearance of a peak for cyclohexanol. After completion the reaction mixture was transferred to a 50 mL one necked flask and the solvents evaporated under oil-pump vacuum at  $\leq 45^\circ\text{C}$ . Anhydrous acetone (10 mL) was added to the remaining solids, the mixture sonicated for 1 min, transferred to a centrifuge tube and centrifuged at 2500 rpm for 3 min. The supernatant solution was carefully removed with a Pasteur pipette. The acetone extractions was repeated usually three times until the supernatant solution was colourless. The residual white solid was dried under oil-pump vacuum to constant weight. The reaction can be scaled to 1/3 or 2/3 of the above stated and carried out analogously for  $\alpha$ -D-mannose. See text for isolated yields and  $\delta/\gamma$  ratios.

**General procedure B; oxidation of  $\alpha$ -D-glucose:** In a 15 mL Schlenk-tube under Ar atmosphere,  $\alpha$ -D-glucose (132 mg, 0.73 mmol), Shvo's catalyst (1.25 mol%, 10 mg) and dry cyclohexanone (10 mL) were combined. Naphthalene (50 mg) was added as internal GC standard. The suspension was stirred at 45°C and monitored by GC following the appearance of a peak for cyclohexanol. After completion the reaction mixture was transferred to a centrifuge tube and centrifuged at 2500 rpm for 1 min. The supernatant orange solution was carefully removed with a Pasteur pipette and the residual white solid dried under oil-pump vacuum. If the solids are slightly coloured anhydrous acetone (10 mL) was added and the extraction procedure repeated. See text for isolated yields and  $\delta/\gamma$  ratios.

**General procedure for NMR experiments.** Sugar lactone (10 mg) was dissolved in 0.6 mL DMSO- $d_6$  (stored over 4 Å activated molecular sieves). The  $^1\text{H}$ -NMR spectra were recorded at the desired temperature after allowing the solution to equilibrate for approximately 10 min at each temperature.

## 2.6 References

- 1) Collins, P.; Ferrier, R. *Monosaccharides*; John Wiley & Sons, Ltd.: Chichester, UK, 1995.
- 2) Mackie, W.; Perlin, A. S. *Can. J. Chem.* **1966**, *44*, 2039-2049.
- 3) Isbell, H. S.; Hudson, C. S. *Bureau of Standards Journal of Research* **1932**, *8*, 327-338.
- 4) Kiliani, H. *Ann.* **1880**, *205*, 182.
- 5) Isbell, H. S.; Frush, H. L. *Aldonic Acids and their Lactonization*, 1962; Vol. 2, 16-18.
- 6) Brown, H. C.; Brewster, J. H.; Shechter, H. *J. Am. Chem. Soc.* **1954**, *76*, 467-474.
- 7) Saiyasombat, W.; Molloy, R.; Nicholson, T. M.; Johnson, A. F.; Ward, I. M.; Poshyachinda, S. *Polymer* **1998**, *39*, 5581-5585.
- 8) Dudev, T.; Lim, C. *J. Am. Chem. Soc.* **1998**, *120*, 4450-4458.
- 9) Brown, J. M.; Conn, A. D.; Pilcher, G.; Leitao, M. L. P.; Yang, M. Y. *J. Chem. Soc., Chem. Commun.* **1989**, *23*, 1817-1819.
- 10) Hackert, M. L.; Jacobson, R. A. *J. Chem. Soc., Chem. Comm.* **1960**, 1179.
- 11) Kent, J. A. *Riegel's Handbook of Industrial Chemistry*; Chapman & Hall: Toronto, 1992, p. 945.
- 12) Kirk-Othmer *Encyclopedia of Chemical Technology*; John Wiley & Sons: Toronto, 1998.
- 13) Isbell, H. S.; Frush, H. L. *B. S. Jour. Research* **1933**, *11*, 649-664.
- 14) Überschar, K.-H.; Blachnitzky, E.-O.; Kurz, G. *Eur. J. Biochem.* **1974**, *48*, 389-405.
- 15) Descotes, G.; Sinou, D. *Tetrahedron Lett.* **1976**, 4083-4086.
- 16) Descotes, G.; Sabadie, J.; Sinou, D. *Tetrahedron Lett.* **1978**, 3351-3354.
- 17) Descotes, G.; Praly, J. P.; Sinou, D. *J. Mol. Catal.* **1979**, *5*, 415-423.
- 18) Saburi, M.; Ishii, Y.; Kaji, N.; Aoi, T.; Sasaki, I.; Yoshikawa, S.; Uchida, Y. *Chem. Lett.* **1989**, 563-566.
- 19) Murahashi, S.-I.; Naota, T.; Ito, K.; Maeda, Y.; Taki, H. *J. Org. Chem.* **1987**, *52*, 4319-4327.

- 20) Isaac, I.; Aizel, G.; Stasik, I.; Wadouachi, A.; Beaupere, D. *Synlett* **1998**, 475-476.
- 21) Beaupere, D.; Bauer, P.; Nadjo, L.; Uzan, R. *J. Organomet. Chem.* **1982**, 238, C12-C14.
- 22) Isaac, I.; Stasik, I.; Beaupere, D.; Uzan, R. *Tetrahedron Lett.* **1995**, 36, 383-386.
- 23) Blum, Y.; Shvo, Y. *Isr. J. Chem.* **1984**, 24, 144-148.
- 24) Menashe, N.; Shvo, J. *Organometallics* **1991**, 10, 3885-3891.
- 25) Wang, G.-Z.; Andreasson, U.; Bäckwall, J. E. *J. Chem. Soc., Chem. Commun.* **1994**, 1037-1038.
- 26) Almeida, M. L. S.; Beller, M.; Wang, G.-Z.; Bäckwall, J.-E. *Chem. Eur. J.* **1996**, 2, 1533-1536.
- 27) Pamies, O.; Bäckwall, J.-E. *Chem. Eur. J.* **2001**, 7, 5052-5058.
- 28) Washington, J.; McDonald, R.; Takats, J.; Menashe, N.; Reshef, D.; Shvo, Y. *Organometallics* **1995**, 14, 3996-4003.
- 29) Mays, M. J.; Morris, M. J.; Raithby, P. R.; Shvo, Y. *Organometallics* **1989**, 8, 1162-1167.
- 30) Casey, C. P.; Singer, S. W.; Powell, D. R.; Hayashi, R. K.; Kavana, M. J. *Am. Chem. Soc.* **2001**, 123, 1090-1100.
- 31) Wiberg, K. B.; Waldon, R. F. *J. Am. Chem. Soc.* **1991**, 113, 7697-7705.
- 32) Walaszek, Z.; Horton, D.; Ekiel, I. *Carbohydr. Res.* **1982**, 106, 193-201.
- 33) Marat, K., Winnipeg, University of Manitoba, *Spinworks*, 2003.
- 34) Walaszek, Z.; Horton, D. *Carbohydr. Res.* **1982**, 105, 131-143.
- 35) Karplus, M. *J. Chem. Phys.* **1959**, 30, 11-15.
- 36) Karplus, M. *J. Am. Chem. Soc.* **1963**, 85, 2870-2871.
- 37) Altona, C.; Francke, R.; Haan, R. d.; Ippel, J. H.; Daalsmans, G. J.; Hoekzema, A. J. A. W.; Wijk, J. v. *Magn. Reson. Chem.* **1994**, 32, 670-678.
- 38) Adamo, C.; Barone, V. *J. Chem. Phys.* **1997**, 108, 664-675.
- 39) Kirkwood, J. G. *J. Chem. Phys.* **1934**, 2, 351.
- 40) Onsager, L. *J. Chem. Phys.* **1936**, 58, 1486-1493.

- 41) Wong, M. W.; Frisch, M. J.; Wiberg, K. B. *J. Am. Chem. Soc.* **1991**, *113*, 4776-4782.
- 42) Christofides, J. C.; Davies, D. B. *J. Chem. Soc., Perkin Trans. 2* **1987**, 97-100.
- 43) Angyal, S. J.; Christofides, J. C. *J. Chem. Soc., Perkin Trans. 2* **1996**, 1485-1491.
- 44) Bernet, B.; Vasella, A. *Helv. Chim. Acta* **2000**, *83*, 995-1021.
- 45) Abraham, R. J.; Ghersi, A.; Petrillo, G.; Sancassan, F. *J. Chem. Soc., Perkin Trans. 2* **1997**, 1279-1286.
- 46) Capon, B. *Chem. Rev.* **1969**, *69*, 407-498.
- 47) Jermyn, M. A. *Biochim. et Biophys. Acta* **1960**, *37*, 78-92.
- 48) Lii, J.-H.; Ma, B.; Allinger, N. L. *J. Comp. Chem.* **1999**, *20*, 1593-1603.
- 49) Pocker, Y.; Green, E. *J. Am. Chem. Soc.* **1973**, *96*, 166-173.
- 50) Shvo, Y.; Czarkie, D.; Rahamim, Y. *J. Am. Chem. Soc.* **1986**, *108*, 7400-7402.

## Chapter 3 Oxidation of 2° Alcohols in Unprotected Sugars

### 3.1 General Overview and Research Strategy

#### 3.1.1 Chemical Properties of Keto-Sugars

As described in **Chapter 1** keto-sugars can only be prepared by a few oxidation methods such as Cr(VI) oxidations<sup>1,2</sup>, the bis-tri-*n*-butyl-tin-oxide method<sup>3,4</sup> and enzymatic processes.<sup>5-7</sup>

The most important chemical property of keto-sugars is their propensity to form hydrates and a multitude of isomers. The hydrate of 2-keto-D-allopyranose is shown as an example in **Figure 3.1**.

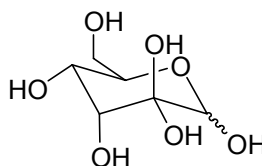
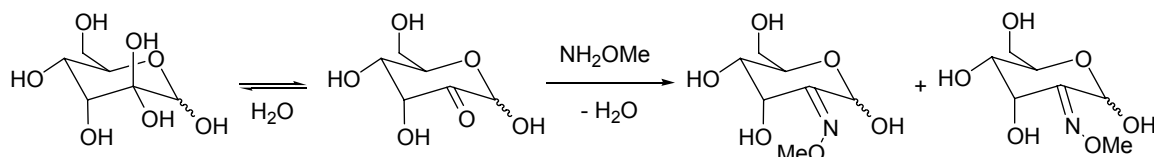


**Figure 3.1** Hydrated form of 2-keto-D-allopyranose.

It was reported that some keto-sugar “derivatives even form as much as 15 different isomers in aqueous solution”.<sup>5</sup> The observation of such a large number of isomers of a given keto-sugars obfuscates the structural analysis, especially by NMR methods. For analytical purposes keto-sugars are therefore generally chemically transformed with hydroxylamine into their oxime derivatives (**Scheme 3.1**), which do not undergo isomerization reactions as readily as the keto-sugars containing a carbonyl group. The two possible E/Z oxime derivatives can be separated with chromatography methods and the isolated oxime compounds can be structurally analyzed, e.g. by NMR methods.

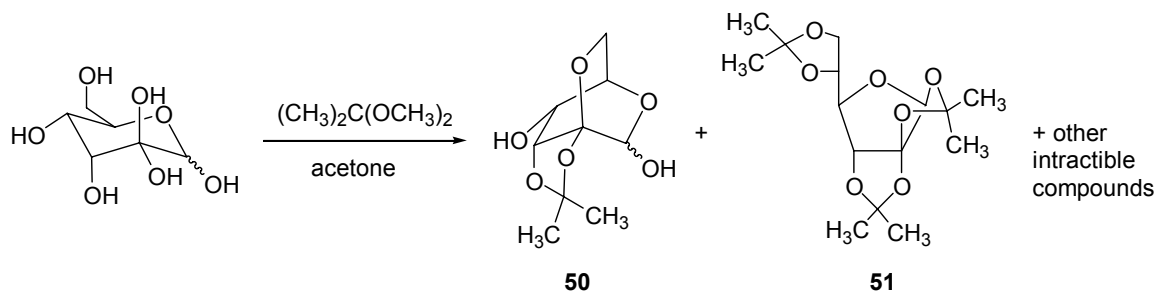




**Scheme 3.1** Preparation of the O-methyl oxime derivatives of 2-keto-D-allopyranose.

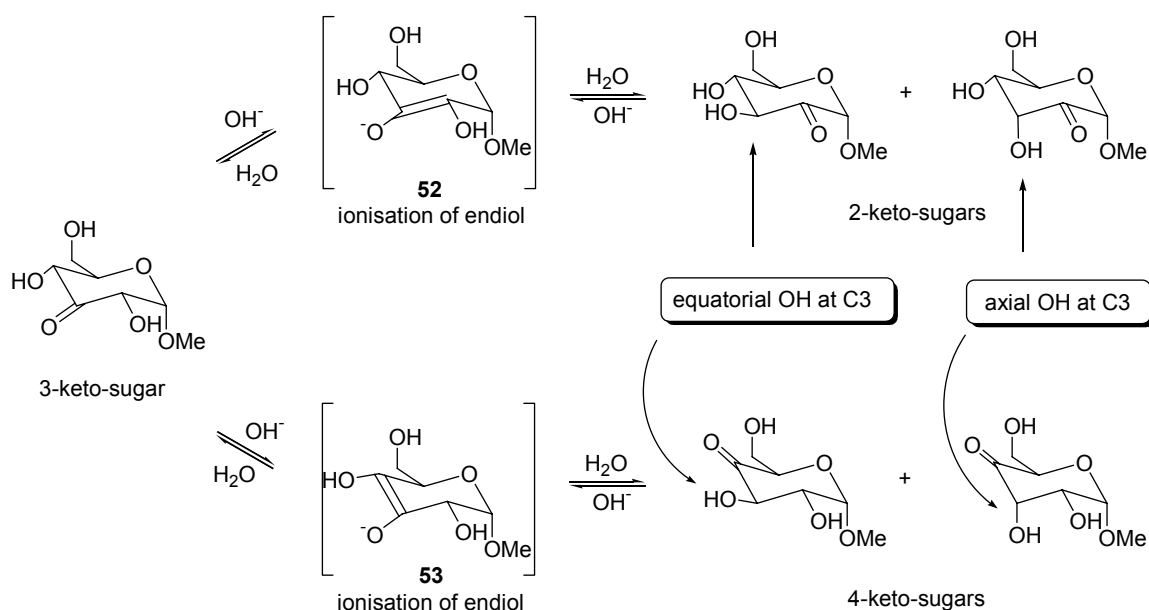
Another method that avoids isomerization reactions of the keto-sugar substrates is the protection of the remaining free hydroxyl functions with e.g. an isopropylidene ketal group. As shown in **Scheme 3.2** isopropylidenation of 2-keto-D-allopyranose produced a mixture of compounds of which the monoisopropylidene **50** and the triisopropylidene **51** derivative were isolated in 38 % and 4 % yield, respectively.<sup>5</sup> In an intramolecular cyclization reaction that is similar to the preparation of anhydro-sugars, the primary alcohol and the axially oriented OH at C2 of the monoisopropylidene derivative (**50**) formed the ether-linked second ring of the bicyclic structure.

The triisopropylidene derivative (**51**) can however only be formed, when the pyranose sugar rearranges to its furanose form. This triisopropylidation reaction can only occur through a rather long multi-step reaction pathway explaining the low yield of 4 %.



**Scheme 3.2** Preparation of isopropylidene derivatives of 2-keto-D-allopyranose.

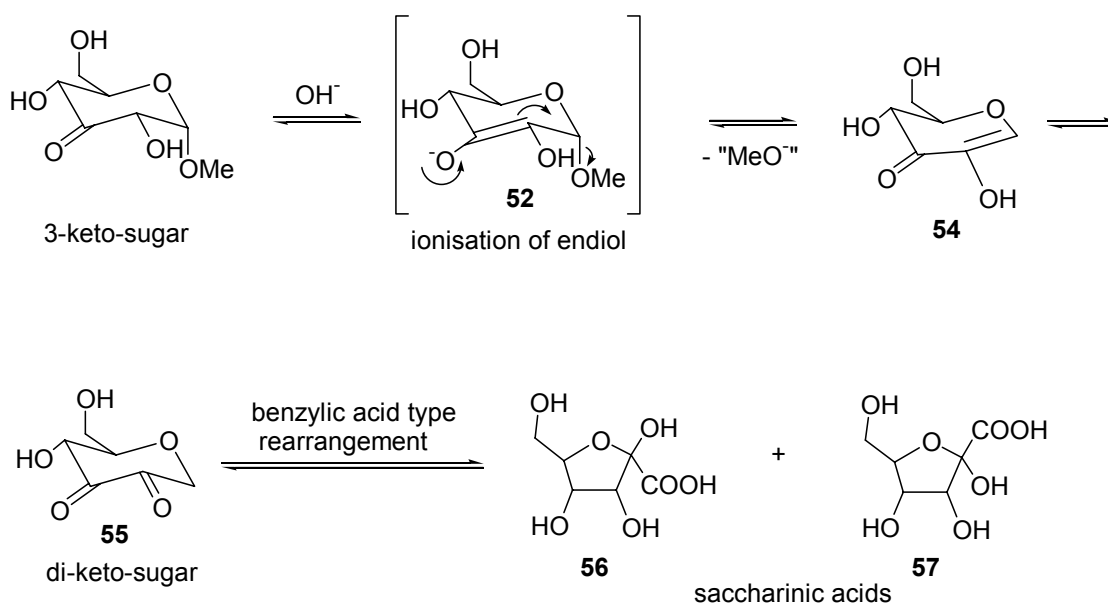
Possible isomerization side-reactions of keto-sugars are illustrated in **Scheme 3.3** using methyl 3-keto- $\alpha$ -D-glucoside as an example.<sup>8</sup> In a basic, aqueous environment the 3-keto-sugar can be deprotonated at either  $\alpha$ -position of the carbonyl group forming the enediol anion intermediates **52** or **53**. Upon re-protonation of **52** or **53** the endiol can isomerize into the 2-keto or 4-keto isomer. The newly generated hydroxyl function at C3 can assume an equatorial or axial position in both regio-isomers with the ratio of its orientation depending on the relative thermodynamic stability of the formed keto-sugar epimers.<sup>8</sup> In addition to the shown isomerization reaction under basic condition, keto-sugars can also isomerize in acidic medium. In acidic solution, the carbonyl function is protonated at the oxygen terminus. The respective two  $\alpha$ -positions of the carbonyl moiety are deprotonated and the generated en-diol intermediates tautomerize to the 2-keto- and 4-keto regio-isomers – again both in their C3 epimeric mixtures.



**Scheme 3.3** Isomerization of methyl 3-keto- $\alpha$ -glucopyranoside to its 2-keto and 4 keto isomers in basic environment.

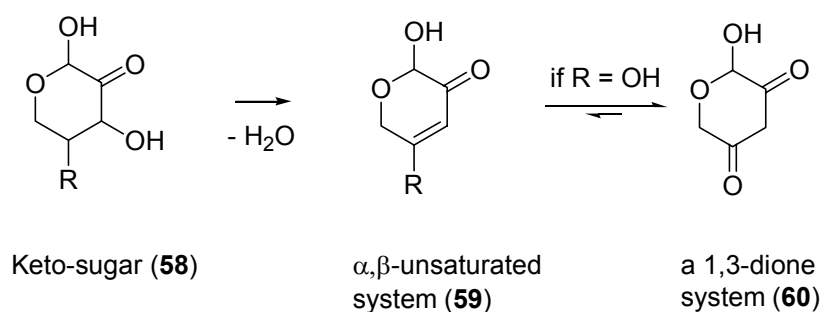
An equilibrium of 16 isomeric keto-sugars, i.e. eight in the  $\alpha$ -pyranose and eight in the  $\beta$ -pyranose form, is established from any one keto-pyranose substrate via the described isomerization pathways, when the isomerization of the pyranose to the furanose form is not considered. In principle, *all* keto- and aldehydo-sugars possessing the sum formula  $C_6H_{10}O_6$  can thus be formed starting from only one keto-sugar substrate.

In addition to isomerization reactions keto-sugars can exhibit other side-reactions such as elimination reactions. As shown in **Scheme 3.4** the endiol anion intermediate **52** can undergo an elimination reaction, in which the methoxy ligand at the anomeric centre is cleaved.<sup>8</sup> The released methoxide reacts immediately in the aqueous solution to form methanol and hydroxide. The highly reactive  $\alpha,\beta$ -unsaturated carbonyl intermediate **54** tautomerizes readily to the dicarbonyl compound **55**. **55** itself is very reactive and can undergo subsequent reactions such as a benzylic acid type rearrangement to the saccharinic acid derivatives **56** and **57**.<sup>8,9</sup>



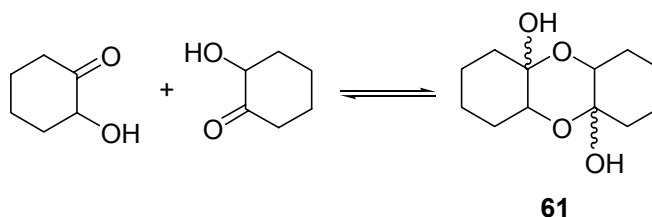
**Scheme 3.4** Degradation of methyl  $\alpha$ -D-3-oxo-glucopyranoside to saccharinic acids in basic medium.<sup>8</sup>

A special case of an elimination reaction is the dehydration reaction. The acid catalyzed dehydration reaction of sugars is commonly known as caramelization and is illustrated for the keto-sugar **58** in **Scheme 3.5**.<sup>10</sup> Acid catalyzed dehydration generates an  $\alpha$ - $\beta$ -unsaturated carbonyl system (**59**), which is thermodynamically favoured as a conjugated system. In the case where R is not hydrogen or an alkyl group but an alcohol group, the generated enol tautomerizes to the more thermodynamically stable ketone resulting in a 1,3-dicarbonyl system **60**.



**Scheme 3.5** Dehydration reaction of a 2-keto-sugar.

Dimerization of the keto-sugars has also been observed.<sup>4</sup> As illustrated in **Scheme 3.6**,  $\alpha$ -hydroxy-cyclohexanone dimerizes to form a tricyclic structure **61** of which the compound **61a** is the thermodynamically most stable. The stability of the di-hemiketal (**61a**) is based on the *cis*-annulation of both cyclohexane rings minimizing steric repulsion, i.e. 1,3-diaxial interaction, of the cyclohexane ring and the axial hydrogen compared to the *trans*-annulated system **61b** (**Figure 3.2**)



**Scheme 3.6** Dimerization of  $\alpha$ -hydroxy-cyclohexanone.

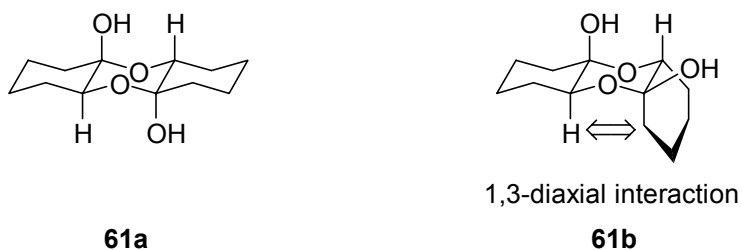


**Figure 3.2** *Cis*- and *trans*-annulated dimerized  $\alpha$ -hydroxy-cyclohexanone.

### 3.1.2 Catalyst and Reaction Condition Requirements

The objective of this research project is the selective oxidation of sugar substrates at one of their secondary alcohol function to produce keto-sugars by means of transition metal catalysis. The high reactivity of the keto sugars described above imposes some severe restrictions on the tolerable reaction conditions, which are discussed in detail in the following.

#### 3.1.2.1 Reaction Medium

The reaction must be neutral ( $pH$  7), as acid or basic conditions allow undesired side reactions (i.e. isomerization, elimination) of the sugar substrate formed as described on 3.1.1. If the  $pH$  7 condition cannot be achieved in a given oxidation method, the environment should at least only be mildly acidic or basic, i.e. not exceed the range of  $pH$  6 to  $pH$  8.

Neutral conditions will also allow the developed methodology to have a maximum compatibility with other functional groups present in the substrate, e.g. ester protecting groups that could be cleaved under acidic and basic conditions.<sup>10</sup>

### 3.1.2.2 Solubility

Sugar, oxidant and catalyst have to be soluble under the same reaction condition. The choice of solvents is limited to very few – especially when the sugar substrates are unprotected and contain predominantly polar hydroxy functions. Suitable solvents are aprotic polar amides such as *N,N*-dimethylformamide (DMF), *N,N*-dimethylacetamide (DMA) and *N*-methyl-2-pyrrolidinone (NMP). Other possible solvents are water, methanol and acetonitrile. The listed solvents are all miscible with each other and binary solvent mixtures can be used to dissolve sugar substrate, oxidant and the transition metal catalyst.

A two-phase liquid-liquid system can be employed if the use of non-polar solvents such as diethyl ether, tetrahydrofuran (THF) or dichloromethane is necessary for the oxidation reaction. In this instance, phase transfer catalysts like tetraalkylammonium salts could be added to the reaction mixture to facilitate permeation of the polar and non-polar solvent boundary by reactants and/or catalysts between.

### 3.1.2.3 Reaction Temperature

As it is known that sugars will undergo unselective condensation reactions such as caramelization under temperatures higher than 100°C,<sup>10</sup> the transition metal catalyzed oxidation reaction of sugars substrate to keto-sugars should preferably take place at ambient temperature. Additionally, the reaction set-up at room temperature is simple and convenient without the need for a cooling bath or heating unit. Elevated reaction temperatures up to ~60°C are tolerable to the sugar substrates for 24 h as undesired dehydration reactions at neutral medium only occur marginally under those conditions.<sup>10</sup>

### 3.1.2.4 Transition Metal Catalyst

A transition metal catalyst will be required for the selective oxidation reaction to the keto-sugar to occur under mild conditions (see above).<sup>11</sup> The selectivity of any oxidation method using only sugar substrates and an oxidant will only be dependent on the direct interactions of the oxidant and the substrate. Regioselectivity may be induced either if the oxidant is selectively coordinating to the substrate (kinetic control) or by the relative stability of two or more possible alternative oxidation products (thermodynamic control).<sup>12,13</sup> The latter is of course only possible if the oxidation is reversible, i.e. occurs under equilibrium conditions. In the presence of a catalysts another possibility arises: reasonably postulating that only hydroxyl functions that directly interact with – i.e. coordinate to – a catalytic metal centre will be oxidized, it is evident that this coordination selectivity may be exploited to induce a regio-selective oxidation of poly-hydroxy substrates. In light of the well established high coordination selectivity of polyols to metal centre (see above and literature) this is an intriguing prospect.<sup>14-20</sup>

The transition metal catalyst should thus contain ligands that can be modified to “fine-tune” the coordination behaviour of the catalysts to a specific poly-hydroxy substrate and consequently affect the selectivity of the oxidation reaction. A specific example in the current context would be the incorporation of hydrogen bond acceptors into the ligand backbone that could interact with hydroxyl functions not coordinated to the metal. However, before such studies can be undertaken a simpler “parent” catalyst system that is in fact active and chemoselective for the desired diol to  $\alpha$ -hydroxy ketone transformation must be identified.

### 3.1.2.5 Mediator

In some instances the oxidation strength of the oxidizing agent may be so strong that the reaction proceeds further than single oxidation and thus multioxidation

and even C-C bond cleavage can occur. A mediator can be employed to avoid overoxidation. The mediator is affecting the thermodynamic parameters of the reaction while the catalyst is affecting the kinetic parameters.<sup>11</sup>

The mediator adjusts the thermodynamic energy level of the reaction being actually involved in the oxidation mechanism. It acts as an oxidizing shuttle lowering the redox potential from the stoichiometrically employed oxidizing agent.<sup>21,22</sup> Examples for mediator systems are *N*-hydroxyphthalimide<sup>23</sup> and Br-radicals<sup>24-26</sup>. Mediators may in particular be useful, if a cheap, readily available and environmentally friendly stoichiometric oxidant, e.g. H<sub>2</sub>O<sub>2</sub>, is to be used, but that oxidant is too powerful for the desired reaction.

#### 3.1.2.6 Reaction Time Scale

The preferential reaction time window for the transition metal catalyzed selective sugar oxidations is 10<sup>1</sup> – 10<sup>3</sup> min. If the oxidation reaction rate is too high, the rate can be lowered by decreasing the reaction temperature. Lowering the temperature may also result in an increase of regio- and chemo-selectivity. In contrast, a slow reaction can be accelerated by an increase in reaction temperature. However, loss of selectivity due to undesired side-reactions at higher temperatures must be considered.

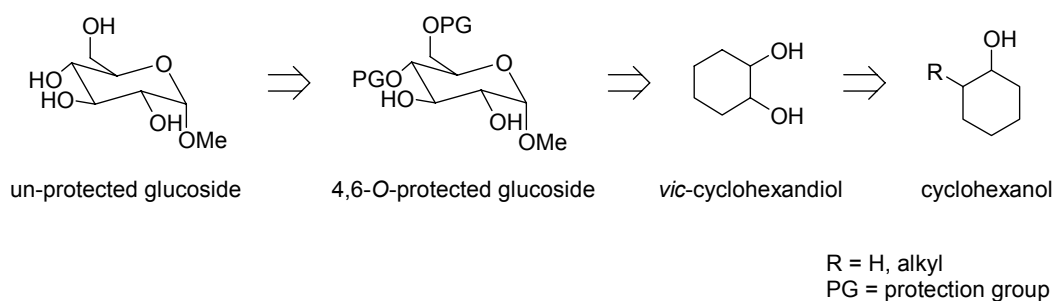
#### 3.1.2.7 Other Factors

If there is a choice of oxidation methods or reactants, the less dangerous system is chosen. Possible explosive or highly toxic substances should be avoided. This is e.g. true for use of *N,N,N',N',N'',N''*-hexamethyl-phosphortriamide (HMPT) as the solvent.<sup>27</sup> Other amide solvents DMF, DMA, NMP are adequate enough to dissolve sugar compounds and exhibiting a far less toxicity than HMPT.



### 3.1.3 Research Strategy and Model Systems

The research strategy for selective oxidation of sugars at their secondary alcohols to keto-sugars illustrated in **Scheme 3.7**. The targeted sugar substrates contain a variety of hydroxy functions, which allow unwanted side reaction pathways and obstruct the chemical manipulation and handling.<sup>††</sup> Our initial approach therefore employed model systems. The first reduction in complexity is to investigate partially protected sugar substrates (e.g. 4,6-O-protected sugars) before investigations are focussed on un-protected sugars. The targeted functional group in the protected and un-protected sugar substrates are *vicinal* diols, which is oxidized to an  $\alpha$ -hydroxy ketone. Therefore, an isolated *vicinal* diol of a cyclic compound such as 1,2-cyclohexanediol is a good model system for the selective oxidation of secondary alcohols of sugar substrates. The complexity is further reduced if the diol is deduced to a mono-alcohol, e.g. cyclohexanol. Mono-alcohols such as cyclohexanol and its derivatives are the simplest model systems in the transition metal catalyzed selective oxidation of secondary alcohols to keto-sugars.

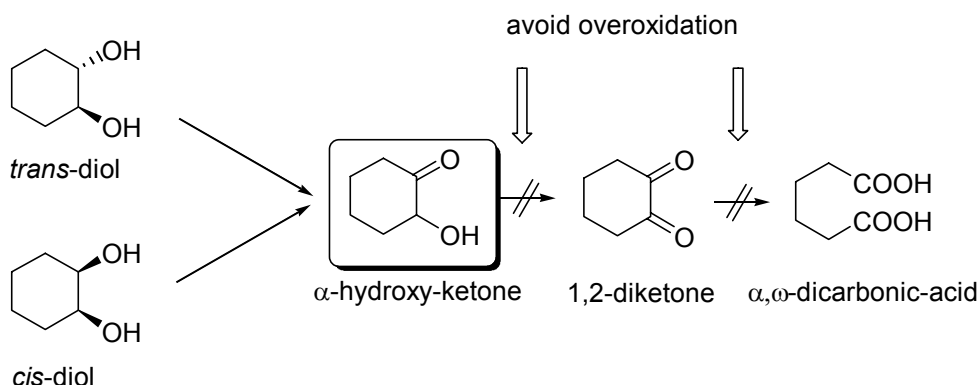


**Scheme 3.7** Deduction of complex sugar substrates to simple model systems.

<sup>††</sup>Letter of Emil Fischer to his mentor Adolf von Baeyer on January 12<sup>th</sup>, 1889: “Unfortunately, the experimental difficulties in this (sugar) group are so great, that a single experiment takes more time in weeks than other classes of compounds takes in hours, so only rarely is a student found who can be used for this work.”<sup>10</sup> M.B. would like to share his sympathy with Fischer.

### 3.1.3.1 Vicinal Diols

The difficulty in the selective oxidation of a *vicinal* diol to the corresponding  $\alpha$ -hydroxy ketone is the prevention of overoxidation to a *vicinal* dione or – after carbon-carbon bond cleavage – dicarboxylic acid (**Scheme 3.8**).



**Scheme 3.8** *Vicinal* diol oxidation at the example of cyclohexane 1,2-diol.

### 3.1.3.2 Thermodynamic and Kinetic Parameters

For any process to occur spontaneously the free energy must be negative, i.e.  $\Delta G < 0$ .<sup>28</sup> As illustrated for the present reaction in **Figure 3.3** and **Figure 3.5** the relative energy levels of the reactants must be higher than the energy levels of the products. However, the relative free energies are not only determined by the relative energies of diol,  $\alpha$ -hydroxy ketone and dicarbonyl compound alone but also the oxidizing agent and its reduced form and are shown for the diol  $\rightarrow$   $\alpha$ -hydroxy ketone and  $\alpha$ -hydroxy ketone  $\rightarrow$  dione reaction.

$$E_A^1 < E_A^2$$

In case 1 the diol is reacted with an oxidant in an uncatalyzed reaction. As illustrated in **Figure 3.3** the activation energy,  $E_A^1$ , for the diol  $\rightarrow$   $\alpha$ -hydroxy ketone reaction is proposed to be smaller than the activation energy,  $E_A^2$ , for the  $\alpha$ -hydroxy ketone  $\rightarrow$  dione oxidation. In this theoretical case, the formation of

$\alpha$ -hydroxy cyclohexanone is preferred and overoxidation to 1,2-cyclohexanedione compound is suppressed.

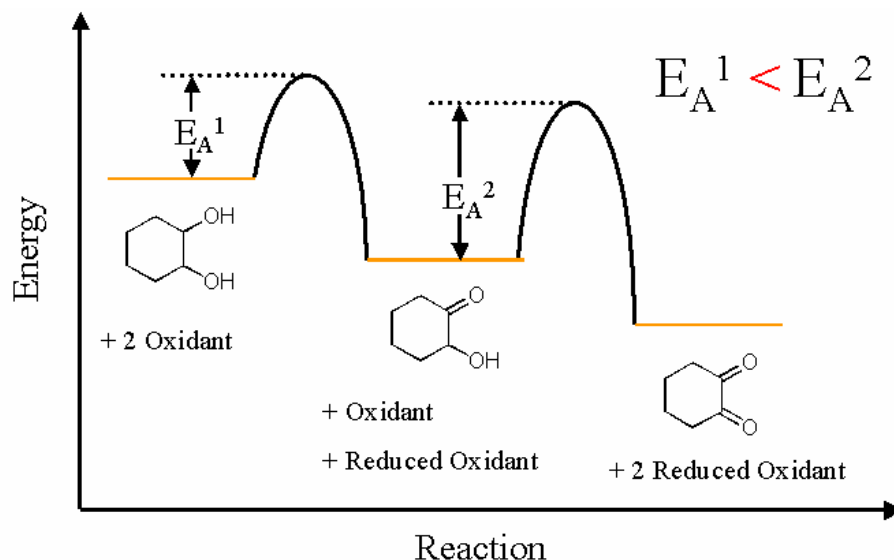


**Figure 3.3** Energy diagram of case 1 in the oxidation of diol to  $\alpha$ -hydroxy ketone.

In order to improve the selectivity of the diol  $\rightarrow$   $\alpha$ -hydroxy ketone reaction a transition metal catalyst can be introduced. Ideally a catalyst will decrease  $E_A^1$  more than  $E_A^2$  compared to the uncatalyzed oxidation as illustrated in **Figure 3.4** allowing the isolation of more  $\alpha$ -hydroxy ketone product.

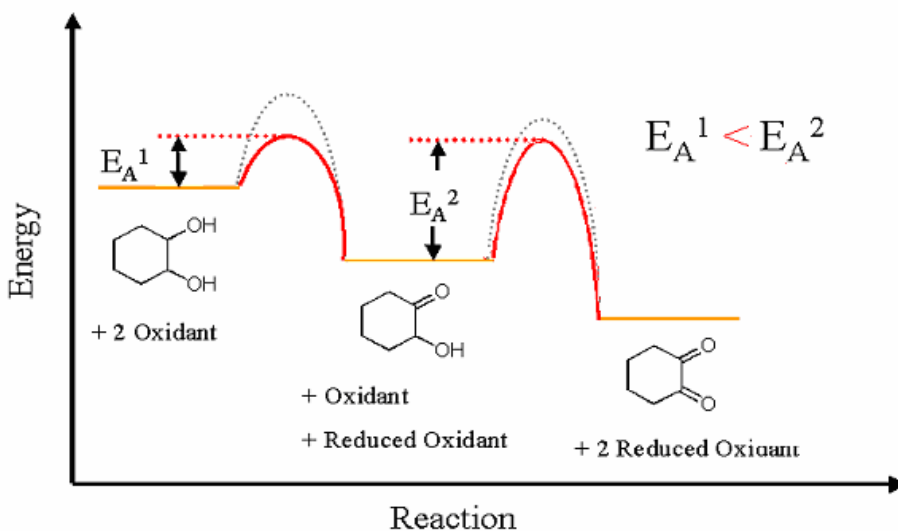


**Figure 3.4** Energy diagram of case 1 in the oxidation of diols to  $\alpha$ -hydroxy ketone (uncatalyzed reaction is dotted, catalyzed reaction is solid).

$$E_A^1 > E_A^2$$

In case 2 the activation energy,  $E_A^1$ , of the first oxidation step is proposed to be larger than the activation energy,  $E_A^2$ , of the second oxidation step as shown in **Figure 3.5**.

In this case the second oxidation reaction is favoured generating 1,2-cyclohexanedione as the thermodynamic product. The 1,2-cyclohexanedione possesses a very reactive *vicinal* di-ketone group and can undergo further reactions notably cleavage of the carbon-carbon bond to generate dicarboxylic acids. This system would therefore not be useful for the synthesis of  $\alpha$ -hydroxy ketones unless a kinetic solution, i.e. transition metal catalyst that relatively lowers  $E_A^1$  and raises  $E_A^2$  so that  $E_A'^1 < E_A'^2$ , is found.

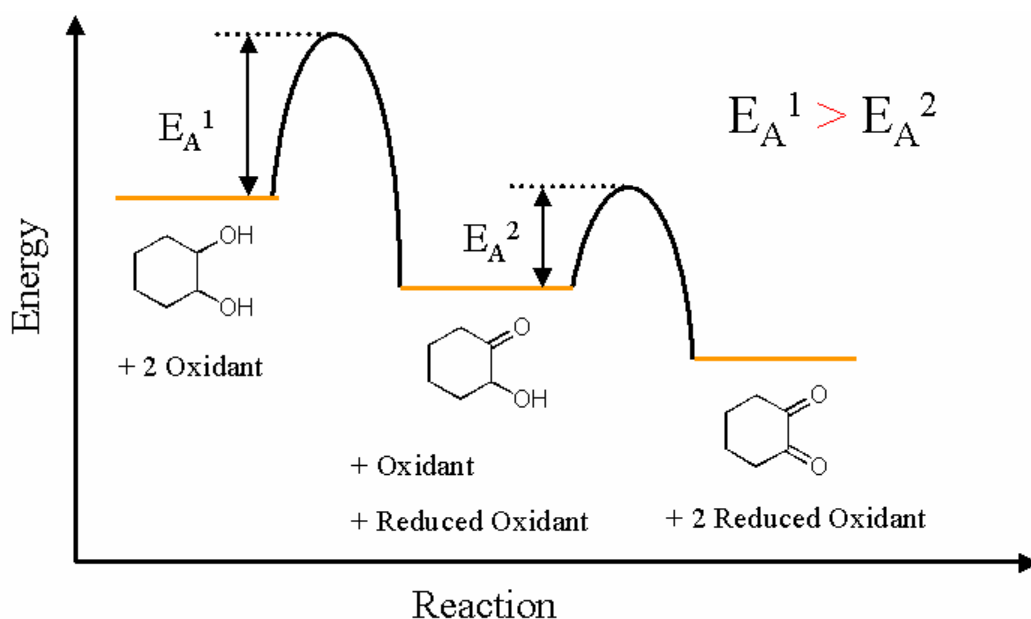
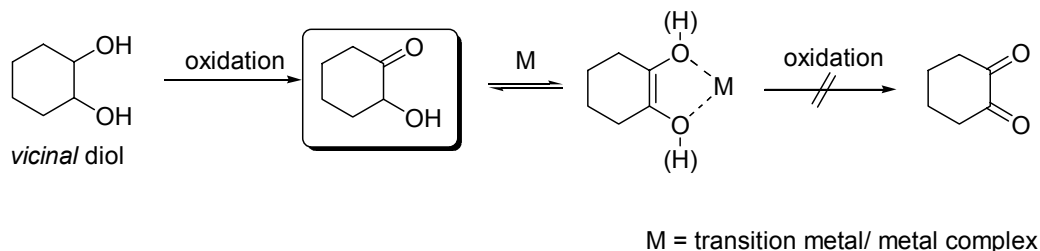


**Figure 3.5** Case 2 of the postulated energy diagram for the oxidation of cis/trans 1,2-cyclohexane-diol.

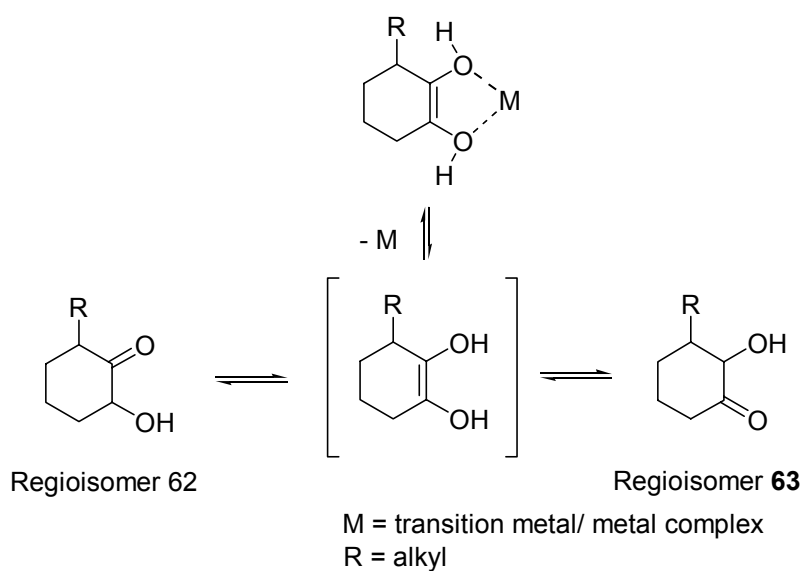
Another solution for the preparation of  $\alpha$ -hydroxy ketones from *vicinal* diols than the discovery of a catalyst, is to trap the produced  $\alpha$ -hydroxy-cyclohexanone intermediate as outlined in **Scheme 3.9**. A stoichiometric amount of transition metal complexes is added to the oxidation reaction to form a transition metal

enediol complex with the  $\alpha$ -hydroxy cyclohexanone intermediate. The generated metal-enediol complex does not undergo further oxidations.<sup>29</sup>



**Scheme 3.9** Trapping of  $\alpha$ -hydroxy-cyclohexanone by complexing with transition metal of the tautomeric enediol form.

Removal of the transition metal results in the isolation of the  $\alpha$ -hydroxy cyclohexanone. In the case of symmetrical diol substrate the two possible  $\alpha$ -hydroxy-cyclohexanone regioisomers are degenerate and only one product is formed. However, the decomplexation reaction becomes more complicated if the  $\alpha$ -hydroxy-ketone is asymmetric (**Scheme 3.10**). The substituted enediol intermediate can tautomerize into the two possible regioisomers **62** and **63**, which are each a mixture of two diastereomers. The relative ratio of regioisomer **62** to **63** depends on the relative thermodynamic energy levels of both isomers.

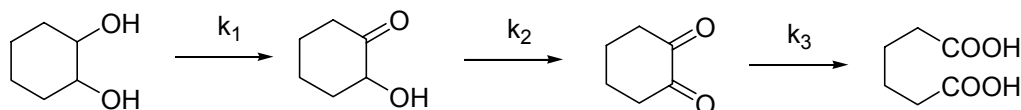


**Scheme 3.10** Possible regioisomers after decomplexation of metal-endiol complex.

The produced mixture of regio-isomers after decomplexation of the metal complex might cause a problem for optimization of regioselectivity in the oxidation reaction of the sugar substrate. However, the relative energies of the two regioisomers can be in some cases so different that upon decomplexation one product is obtained exclusively. Therefore, any mixtures of the two regioisomers formed during the oxidation process would be transformed to one regioisomer during the trapping of the  $\alpha$ -hydroxy ketone intermediate and thus enhancing the selectivity of the (overall) oxidation reaction. However, synthesis of the opposite regioisomer would not be possible through this oxidation-endiol trapping-decomplexation method.

### 3.1.3.3 Theoretical Calculations of Diol Oxidations

As stated above, the key problem in the selective oxidation of *vicinal* diols to  $\alpha$ -hydroxy ketones is the prevention of overoxidation to the diketone and after C-C cleavage to dicarboxylic acids (**Scheme 3.11**).



**Scheme 3.11** Oxidation of *vicinal* diol.

Each of the oxidation steps involves a net loss of two electrons, which are received by the oxidizing agent, i.e. oxidant. Assuming a bimolecular reaction, the following reaction rate laws can be postulated:

$$\frac{d}{dt} [\alpha\text{-OH ketone}] = k_1 [\text{diol}] [\text{oxidant}] \quad \text{Eq. 1}$$

$$\frac{d}{dt} [\text{dione}] = k_2 [\alpha\text{-OH ketone}] [\text{oxidant}] \quad \text{Eq. 2}$$

$$\frac{d}{dt} [\text{dicarboxylic acid}] = k_3 [\text{dione}] [\text{oxidant}] \quad \text{Eq. 3}$$

It is assumed in **Eq. 3** that the water required is not part of the rate determining step when the reactions is carried out in aqueous medium.

In all three equations there is a dependence on the concentration of [oxidant], and all three reactions occur in the same reaction vessel. Thus, to simplify the mathematical equations the [oxidant] expression can be dropped by formally normalizing all rates to this concentration. The resulting mathematical expressions are now 1<sup>st</sup> order rate laws (**Eq. 4-6**).

The mathematical ‘trick’ is that the oxidant concentration is treated as constant and does not change during the oxidation reaction. However, in the oxidation reaction the oxidant concentration will not be constant but decrease and lower the rates of oxidation reaction. The model is however still conceptually valid, as the overall effect of this simply an elongation of any resulting graphs of the 1<sup>st</sup> order curves along the time axis without any impact on the actual ratios of diol,  $\alpha$ -hydroxy ketone, dione and dicarboxylic acid present at any point during the reaction.

$$\frac{d}{dt} [\alpha\text{-OH ketone}] = - \frac{d}{dt} [\text{diol}] = k_1 [\text{diol}] \quad \text{Eq. 4}$$

$$\frac{d}{dt} [\text{dione}] = - \frac{d}{dt} [\alpha\text{-OH ketone}] = k_2 [\alpha\text{-OH ketone}] \quad \text{Eq. 5}$$

$$\frac{d}{dt} [\text{dicarboxylic acid}] = - \frac{d}{dt} [\text{dione}] = k_3 [\text{dione}] \quad \text{Eq. 6}$$

Analytical solutions for the equation system above are available from the literature and with  $k_1$  and  $k_2$  for diol and  $\alpha$ -hydroxy ketone concentration are presented in **Eq. 7** and **8**.<sup>28</sup>

$$[\text{diol}] = [\text{diol}]_0 e^{-k_1 t} \quad \text{Eq. 7}$$

$$[\alpha\text{-OH ketone}] = \frac{k_1}{k_2 - k_1} [\text{diol}]_0 (e^{-k_1 t} - e^{-k_2 t}) \quad \text{Eq. 8}$$

In order to simulate three consecutive 1<sup>st</sup> order reactions, a numerical solution was produced using a spread-sheet program.<sup>‡‡</sup> The following graphs contain the calculated results with various  $k_1$ ,  $k_2$  and  $k_3$  ratios.

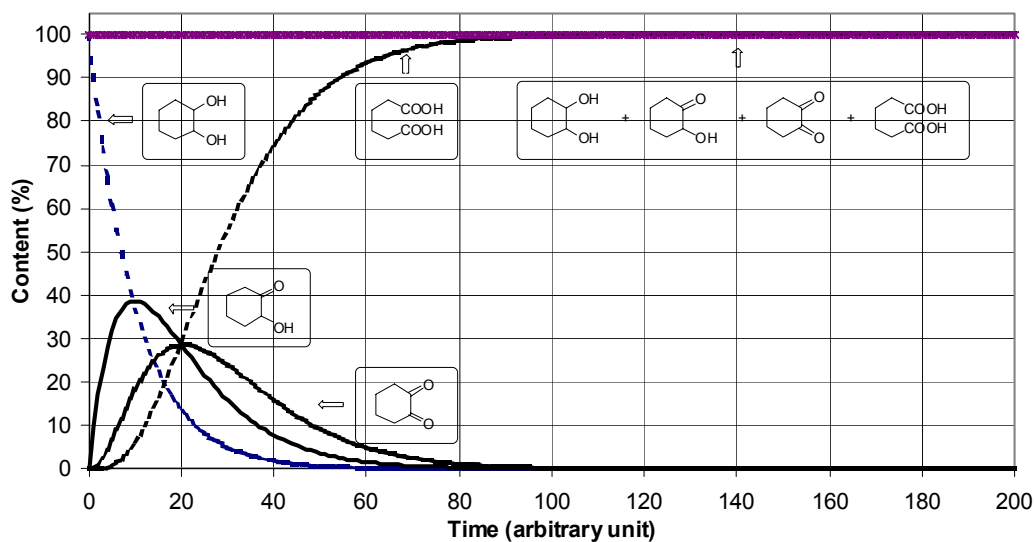


**Figure 3.6** Theoretical product distribution when  $k_1 = k_2 = k_3$ .

<sup>‡‡</sup> See appendix for further information.



In **Figure 3.6** the distribution of the reactant and products is displayed in which all three rate constants have the same value, i.e.  $k_1 = k_2 = k_3$ . The maximum  $\alpha$ -hydroxy ketone content is 38 %. At this point, the diol starting material content is 35 % along with 22 % dione and 5 % dicarboxylic acid. The total amount of consumed oxidant is 0.95 equivalents, which is based on amount of diol starting material.<sup>§§</sup> Explicitly, any two consecutive reactions which do not differ in their rate constants and are a function of the expressed rate laws **Eq. 1** and **2** will produce a maximum amount of 38 % of the intermediate compound, i.e. in this case the  $\alpha$ -hydroxy ketone.

The oxidation reaction can be stopped by quenching of the reaction with reducing agent, when the  $\alpha$ -hydroxy ketone compound reached 38 % yield. However, the  $\alpha$ -hydroxy ketone content must be constantly monitored and quantitatively measured (e.g. GC analysis). Another method to stop the reaction at the maximum  $\alpha$ -hydroxy ketone yield is the use of the stoichiometric amount of oxidant consumed. This amount can be determined from the calculated graphs, i.e. 0.95 equivalents in the case of  $k_1 = k_2 = k_3$ . However, the oxidation reaction with a set amount of consumable oxidant is slower than the quenching of the reaction employing excess of oxidant, as the oxidant concentration approaches zero asymptotically during the reaction resulting in a reaction rate decrease.

If the second reaction step – the subsequent oxidation of the  $\alpha$ -hydroxy ketone to the dione – is ten times slower than the oxidation of the diol, i.e.  $k_1 = k_3$  and  $k_1 = 10 \times k_2$  as illustrated in **Figure 3.7** the relative product distribution changes dramatically compared to the case 1. The maximum  $\alpha$ -hydroxy ketone content is now 78 % with a diol content of 7 %, dione content of 7 % and dicarboxylic acid content of 8 %. The total amount of oxidant consumed is 1.16 equivalents.

---

<sup>§§</sup> The amount of oxidant is calculated by multiplication of  $\alpha$ -hydroxy ketone content by 1, dione content by 2 and dicarboxylic acid content by 3:  
amount oxidant =  $[\alpha\text{-OH}] + 2 \times [\text{dione}] + 3 \times [\text{dicarboxylic acid}]$

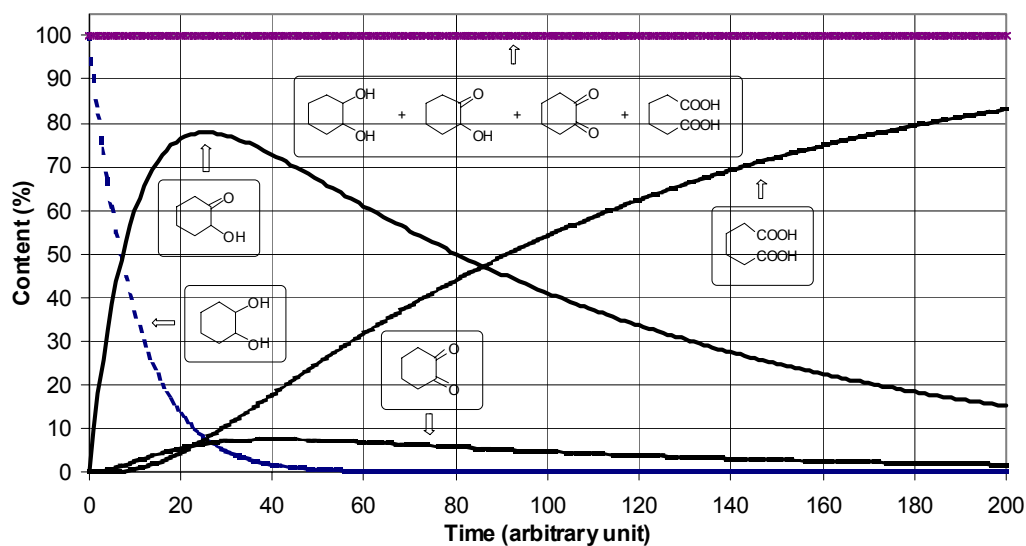


**Figure 3.7** Theoretical product distribution when  $k_1 = 10 k_2 = k_3$ .

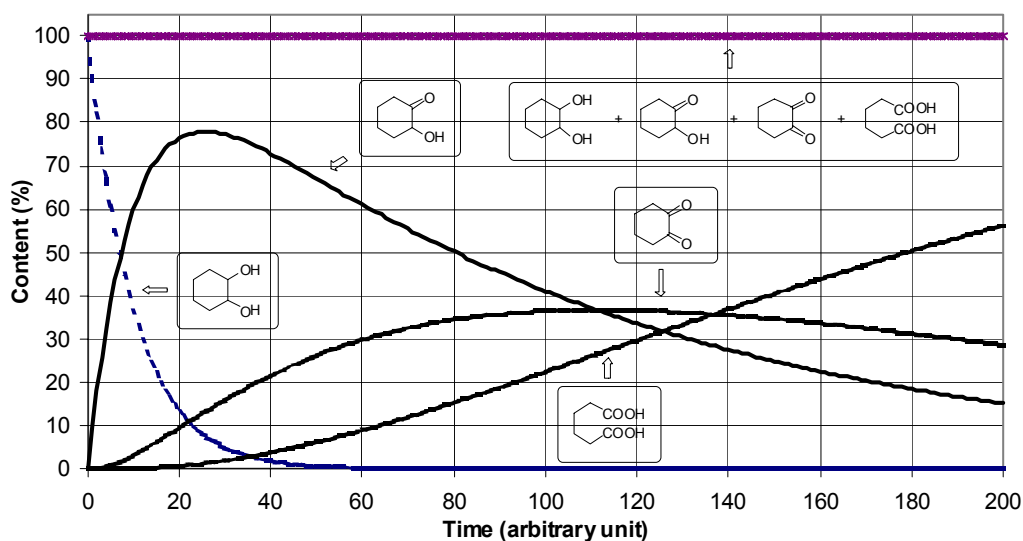


**Figure 3.8** Theoretical product distribution when  $0.1 k_1 = k_2 = k_3$ .

The distribution of the diol reactant and oxidation products for the theoretical calculation using  $k_2 = k_3 = 0.1 \times k_1$  as the relative rate constants is shown in **Figure 3.8**. The maximum  $\alpha$ -hydroxy ketone content is unchanged at 78 % compared to **Figure 3.7** where  $k_1 = k_3 = 0.1 \times k_2$ . When the third oxidation step

( $k_3$ ) is 10 fold slower than the previous case, the dione and dicarboxylic acid content are 13 % and 2 %.

This is a very crucial result as only the ratio of the first two reactions,  $k_1$  and  $k_2$ , are of importance in the synthesis of  $\alpha$ -hydroxy ketones from the selective oxidation of diols.

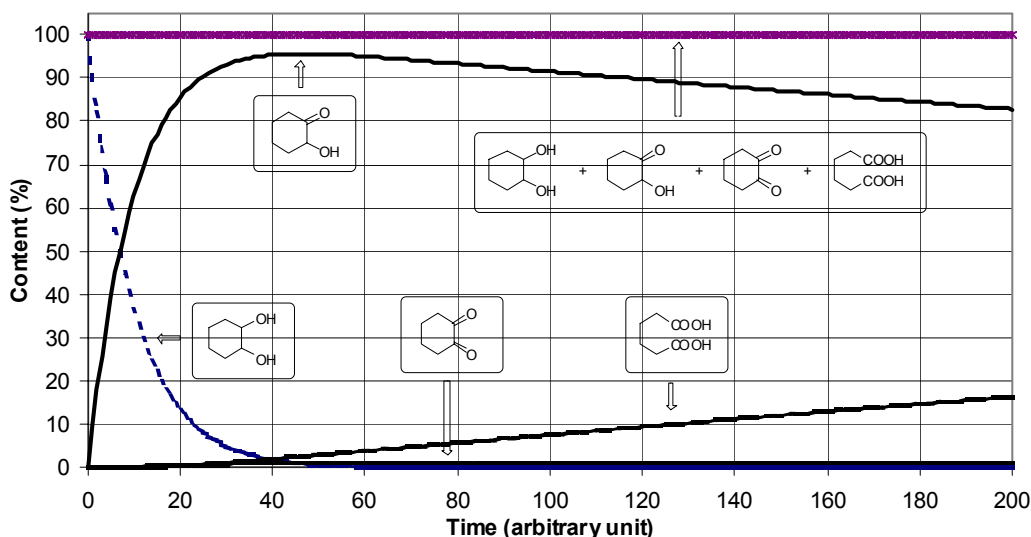


**Figure 3.9** Theoretical product distribution when  $0.01 k_1 = k_2 = k_3$ .

When the second reaction step is 100 fold slower than the first reaction step, i.e.  $k_2 = 0.01 \times k_1$ , the maximum  $\alpha$ -hydroxy ketone content is 95 % with a diol content of 1.5 %, dione 1 % and 2.5 % dicarboxylic acid as shown in **Figure 3.9**.

In conclusion, for synthetically useful results the ratio between the rate of the first oxidation step, i.e.  $k_1$  (diol  $\rightarrow$   $\alpha$ -hydroxy ketone), and that of the second oxidation step, i.e.  $k_2$  ( $\alpha$ -hydroxy ketone  $\rightarrow$  dione), must be at least 10 (**Table 3.1**). Any subsequent oxidation reaction does not affect the maximum  $\alpha$ -hydroxy ketone content.

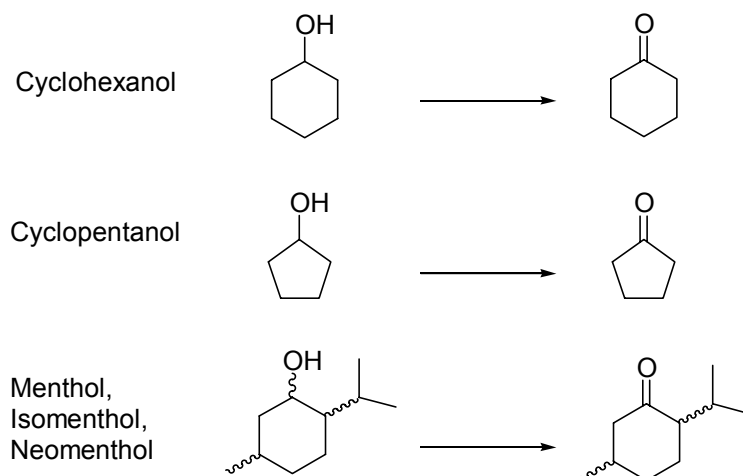
**Table 3.1** Maximum  $\alpha$ -hydroxy ketone content based on the ratio of  $k_1$  (diol  $\rightarrow$   $\alpha$ -hydroxy ketone) and  $k_2$  ( $\alpha$ -hydroxy ketone  $\rightarrow$  dione) obtained from the calculated reaction profiles.

Ratio of $k_1 : k_2$	Maximum $\alpha$ -hydroxy ketone content
1000 : 1	99.3 %
100 : 1	95.5 %
10 : 1	78.5 %
5 : 1	67.5 %
2 : 1	51.2 %
1 : 1	38.3 %
1 : 2	27.6 %
1 : 5	17.1 %
1 : 10	12.2 %

#### 3.1.3.4 Mono-alcohol Model Systems

The simplest model systems for the selective oxidation of sugars at their secondary alcohol functions are mono-alcohols (**Scheme 3.12**). Cyclohexanol is the model systems for a 6-membered ring, i.e. pyranose, and cyclopentanol for the 5-membered ring, i.e. furanose. The secondary alcohols can be oxidized to the corresponding ketone exclusively without formation of side products.

The simplicity of the model systems is convenient to establish reaction conditions, which are congruent with the postulated conditions for synthesis of keto-sugars. Another advantage of the mono-alcohol and diol model systems is their facile qualitative and quantitative analysis by GC-MS and GC.



**Scheme 3.12** Variety of mono-alcohols as test system for oxidation reaction condition.

The diastereomeric alcohols menthol, isomenthol and neomenthol can be used for the investigation of steric effects of a neighboring alkyl in the oxidation of a secondary alcohol (**Figure 3.10**). In menthol all substitutes of the cyclohexane ring system are in equatorial positions, while the lowest energy conformation of isomenthol is a twisted half-chair resulting in an intermediate axial-equatorial position of the hydroxyl group. In neomenthol the hydroxyl group is in an axial position.

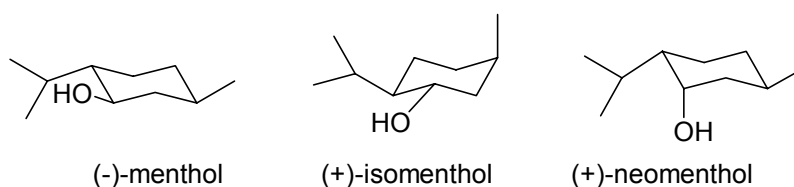


**Figure 3.10** Stereoisomers (-)-menthol, (+)-isomenthol and (+)-neomenthol.

The “menthol-series” thus allows to investigate the influences on the rate of oxidation from the relative orientation of neighboring isopropyl group and the position of the OH group, i.e. axial or equatorial.

### 3.1.3.5 Diol Model Systems

Upon optimization of the oxidation conditions of mono-alcohols investigations focus on the diol systems. A variety of commercially available cyclic diols is shown in **Figure 3.11**.

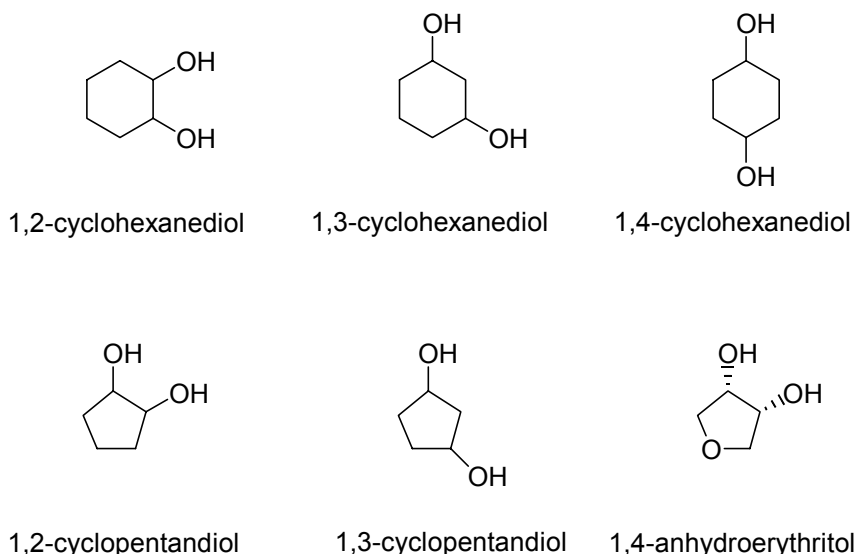


**Figure 3.11** Overview of diol model systems (*cis* and *trans* configurations).

The diols can be grouped into three different categories:

- **vic** and **non-vic**: The diols of our interest are the *vicinal* 1,2-diols as this is the key functional group moiety in sugar substrate targets.
- **5-membered** and **6-membered systems**: The diol compounds can be divided into systems containing 5 or 6 membered ring systems reflecting furanose and pyranose systems, respectively. 1,4-anhydroerythritol is even a better model system for a furanose as it contains an oxygen atom in its ring.
- **cis** and **trans configuration**: In any diol the relative configuration of the hydroxy groups can be distinguished by *cis* or *trans*.

It is important to point out that in the 1,2-diol systems the relation of a *cis* configuration reflects an axial/equatorial positioning of the hydroxy groups. The possible equatorial/axial positioning is energetically degenerate unless there are other substitutes on the ring. An axial or equatorial position of any ring substituent is truly correct in cyclohexane derivatives only, while the positions in 5-membered rings are strictly speaking pseudo-axial and pseudo-equatorial. The *trans* configuration reflects an axial/axial or equatorial/equatorial position in *vicinal* diol substrates. Without any other substitutes on the cyclic ring the thermodynamically more stable equatorial/equatorial conformer is the only occurring species. In contrast to the 1,2-diol system, the relation of the hydroxy groups as axial/axial or equatorial/equatorial is *cis* in a 1,3-diol system. Once again, the equatorial/equatorial relation is the thermodynamically more stable conformer than the axial/axial conformer. The *trans* configuration in the 1,3-diol system is an axial/equatorial relation and energetically degenerate with respect to the equatorial/axial relation. The 1,4-diol system has the same stereo relations of *cis* and *trans* configuration as in the 1,2-diol system.

It is necessary to divide the diols into the three categories and evaluate the data from the oxidation reactions for each group. The insights gained from the data can then be applied to more complex sugar substrates.

### 3.1.4 Reaction Monitoring

#### 3.1.4.1 Monitoring of Model Systems

Simple mono-alcohols and diols were chosen as model systems, because they are easy to handle, inexpensive and commercially available. Also, in contrast to sugars they are volatile enough to be directly monitored by GC without any need for sample derivatization. Quantification of the GC analysis is also easily achieved through multi-level multi-compound calibration against authentic

samples of all reactants and anticipated products with reference to an internal standard.

The internal standard must not affect the oxidation reaction, and thus should be inert, possess a relatively high mass for easy measurability, be pure and air and water stable and dissolve in the used solvents. Preliminary test demonstrated that naphthalene, NMP and *cis*-decalin are appropriate internal standards for quantitative GC monitoring of the oxidation reactions carried out in the context of this project.

In addition possible products of the oxidation of diols (e.g. *cis*- or *trans*-1,2-cyclohexanediol) can be identified by GC-MS, provided that they are volatile enough. This excludes  $\alpha,\omega$ -dicarboxylic acids (e.g. adipic acid potentially formed from 1,2-cyclohexanediol). The content of  $\alpha,\omega$ -dicarboxylic acids must therefore be calculated as difference from the mass balance of other reactants and products present.

#### 3.1.4.2 Monitoring of Sugar Substrate Systems

In strong contrast to the mono-alcohol and diol model systems, the partially protected or free sugar substrates and potential oxidation products cannot be detected and separated by GC methods due to their thermal instability and involatility. However, sugars can be monitored using thin layer chromatography, which is a good qualitative and semi-quantitative method.

Sugars and their derivatives can be quantitatively analyzed and detected by HPLC. The detection of the sugar substrates can be conducted through UV/VIS or through the change in refractive index (RI). The RI detector must be employed in case the sugar substrate is lacking a chromophore such as phenyl group. If isolation of keto-sugars is very difficult preparative HPLC can be conducted with 20 – 100 mg of compound.



Another possible method is to monitor the oxidation reaction of sugars with NMR methods *in situ*. The oxidation reaction is conducted in deuterated solvent inside a NMR tube and the  $^1\text{H}$  or  $^{13}\text{C}$  NMR spectra are recorded. Integration of signals in NMR spectra can be used for determination of relative product ratios.

A labour intensive protocol in the monitoring of sugar oxidation is to work up aliquots of the reaction mixture, and then analyze and characterize the obtained products. This monitoring method is only useful when the reaction are conducted on a large scale so that sufficient amounts of sugar compounds can be isolated and purified for the structural analysis with NMR, IR, and elemental analysis methods.

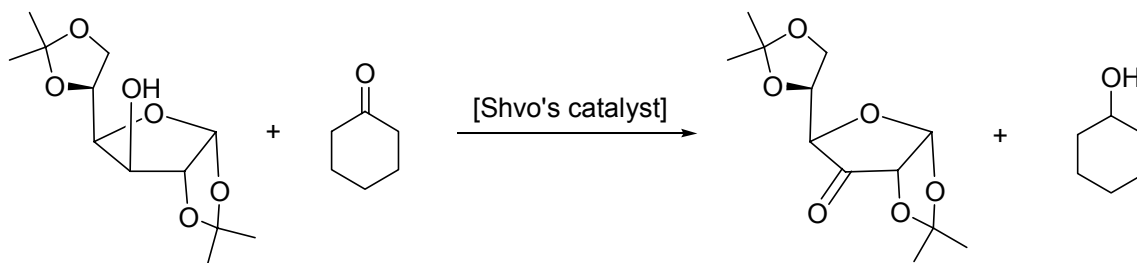
## 3.2 Catalytic Hydrogen Transfer Reactions Investigated

### 3.2.1 Shvo's Catalyst

#### 3.2.1.1 Shvo's System in the Oxidation of Secondary Alcohols

As described in **Chapter 2** Shvo's catalyst,  $[(\eta^4\text{-C}_4\text{Ph}_4\text{CO})(\text{CO})_2\text{Ru}]_2$ , has been successfully used for the oxidation of hemiacetals to sugar lactones in cyclohexanone solvent.<sup>30</sup>

Shvo's ruthenium complex is a transfer hydrogenation catalyst that operates at very mild conditions as required for the synthesis of keto-sugars through the oxidation of secondary alcohol functions in sugar substrates.<sup>30-37</sup> The catalyst was tested in the selective oxidation of 1,2;5,6-*O*-diisopropylidene  $\alpha$ -D-glucopyranoside (diacetone-glucose) with acetone or cyclohexanone as hydrogen acceptor as illustrated in **Scheme 3.13**.



**Scheme 3.13** Oxidation of 1,2;5,6-O-diisopropylidene α-D-glucopyranan with Shvo's catalyst and cyclohexanone as hydrogen-acceptor.

At room temperature, no oxidation of diacetone-glucose was observed with either acetone or cyclohexanone as the hydrogen-acceptor as no *iso*-propanol or cyclohexanol by-product, respectively, was detected by GC. With acetone as the solvent and hydrogen-acceptor a colour change of the reaction mixture from dark orange to bright yellow was observed after 15 min at 56°C. This colour change is indicative of the generation of the hydrogen loaded form of Shvo's catalyst by dehydrogenation of the alcohol substrate. The amount of produced *iso*-propanol, which assuming a clean reaction by necessity must be equivalent to the 1,2;5,6-O-diisopropylidene 3-keto-α-D-glucopyranan produced, was however less than 5 % after 24 h and still less than 7 % after 48 h. Using cyclohexanone as hydrogen-acceptor and solvent the conversion to cyclohexanol was approximately 15 % after 48 h at 100°C, however multiple side-products were observed by GC analysis.

Shvo's catalyst thus shows only limited reactivity in the oxidation of secondary alcohol functions in sugar substrate such as diacetone-glucose. While there is an immediate colour change in the oxidation of an hemi-acetal the colour change occurs in the oxidation reaction of diacetone-glucose only after 15 min. We propose that the lower dehydrogenation reactivity of Shvo's catalyst is based on both the steric repulsion of the *ortho*-phenyl groups of the cyclopentadienone moiety by the bulky sugar substrate and the higher redox potential of a secondary alcohol/ketone pair compared to a hemi-acetal/lactone pair, which is

more favoured as a resonance stabilized system is formed.<sup>38</sup> Raising the reaction temperature to 100°C in order to compensate for the apparent lower reactivity, a significant amount of decomposition of the sugar substrate was observed.

Subsequent research therefore focussed on identifying a more reactive hydrogen transfer catalyst system that would operate at lower temperatures thus avoiding thermal decomposition of the sugar substrate.

### 3.2.1.2 Experimental Section

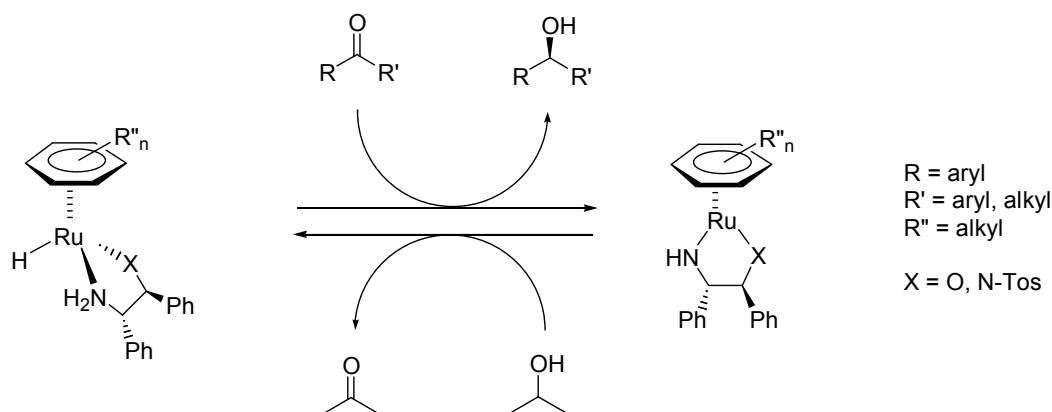
GC analyses were performed on a Varian CP-3800 equipped with a 30 m × 0.25 mm PEG column. The GC FID was multi-level calibrated for alcohol and ketone substrates using solutions of authentic samples with naphthalene as the internal standard. All experimental preparations were conducted in a dry-box under argon atmosphere and/or with usual Schlenk technique on a vacuum line. Alcohol and ketone substrates, naphthalene and common solvents were purchased from commercial sources. All chemicals were reagent grade and used without further purification unless otherwise stated. Acetone, cyclohexanone and *iso*-propanol were dried by distillation under argon from anhydrous CaCl<sub>2</sub> or anhydrous K<sub>2</sub>CO<sub>3</sub> containing LiAlH<sub>4</sub> degassed by freeze/thaw cycles and stored under argon. The synthesis of Shvo's catalyst was conducted as described in literature.<sup>31,32</sup>

**Typical oxidation procedure using Shvo's catalyst.** Inside a glove-box under Ar atmosphere, a 15 mL Schlenk flask was charged with and 1,2;5,6-O-diisopropylidene α-D-glucofuranoside (260 mg, 1.0 mmol) and naphthalene (~75 mg) and the solids dissolved in 5.0 mL degassed acetone. After addition of Shvo's catalyst (13.5 mg, 0.0125 mmol) the Schlenk flask was stirred at 45°C and the reaction was monitored by GC.

### 3.2.2 Noyori System

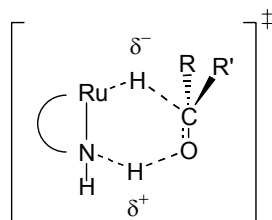
#### 3.2.2.1 Introduction to Metal-Ligand Bifunctional Catalysis and Motivation

Noyori's chiral diamine based ruthenium (II) complexes are very active hydrogen transfer catalysts for the enantioselective reduction of prochiral ketones in high *ee* values. The catalysts employ *iso*-propanol as both the solvent and the hydrogen source and show high TON and TOF under mild conditions, i.e. at ambient temperatures (**Scheme 3.14**).<sup>39-46</sup>



**Scheme 3.14** Hydrogen transfer reaction of acetophenone in *iso*-propanol catalyzed by chiral ruthenium complex.

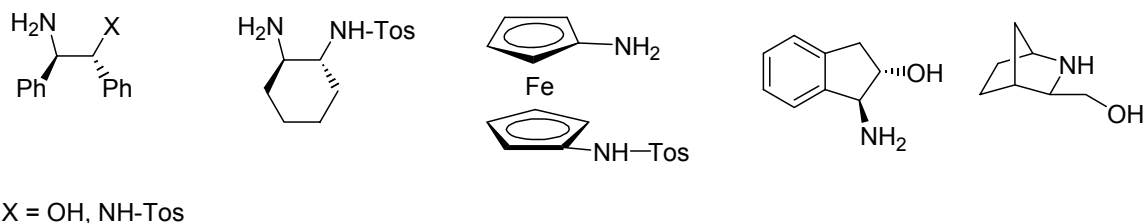
One key feature of these catalyst systems is that they operate by what has been termed a metal-ligand bifunctional mechanism (**Figure 3.12**),<sup>46</sup> in which both the metal centre and the ligand are actively involved in the catalytic cycle. For the Noyori system a hydrogenation of a ketone is effected by a simultaneous transfer of a hydride from Ru-H and a proton from NH<sub>2</sub> to the carbonyl function of the substrate occurs via a pericyclic transition state. This particular bi-functional catalysis mechanism has also been named “NH-effect”.<sup>46</sup>



pericyclic transition state

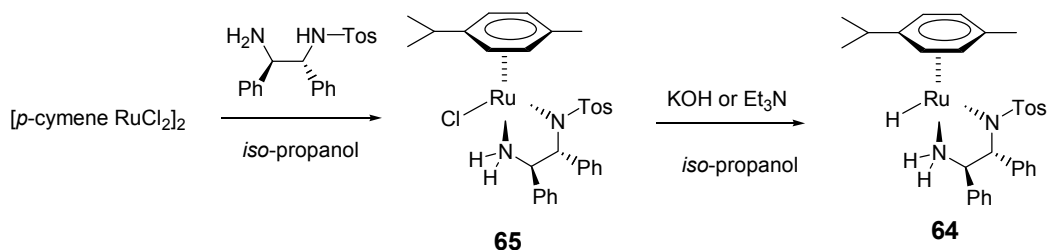
**Figure 3.12** “NH-effect”

A brief overview of  $\beta$ -aminoethanol and 1,2-diamino-ethane derived ligands used in the enantioselective reduction of prochiral ketones is shown in **Figure 3.13**. A common theme is the application of (pseudo-)  $C_2$  symmetrical ligands, which enhance the enantioselectivity compared to the  $C_s$  symmetrical ligands.<sup>47</sup> The most commonly used ligands are the *anti*-1,2-diphenyl-ethylene based ligands,<sup>40,41,43</sup> but 1,2-diamino-cyclohexane and 1,1'-diaminoferrocene derivatives<sup>48,49</sup> and indane- and bicyclic- $\beta$ -aminoethanol ligands have also been reported to be active chiral auxiliaries in the  $\eta^6$ -arene ruthenium catalyzed reduction of aromatic ketones in *iso*-propanol solvent.<sup>47</sup> However, only the  $\beta$ -aminoethanol and *N*-tosyl-1,2-ethylenediamine complexes showed catalytic activity in the hydrogenation of non-activated ketones to secondary alcohols. In comparison the complexes of the symmetric ligands 1,2-diamino-ethane and *N,N'*-ditosyl-1,2-diamino-ethane gave no – or only marginal – hydrogen transfer activity. <sup>40,41,46</sup>

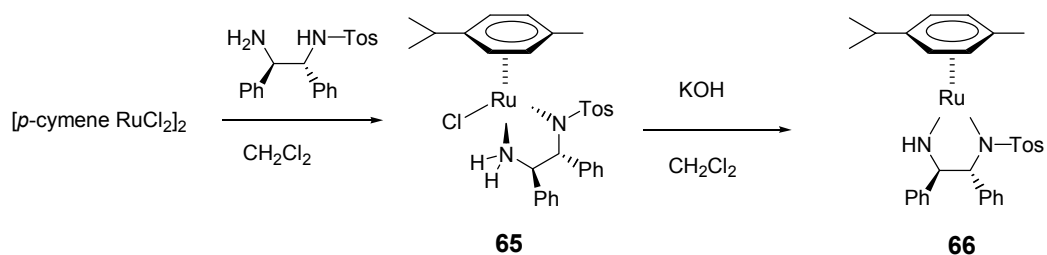
**Figure 3.13**  $\beta$ -Aminoethanol and 1,2-diamino-ethane ligands used in the enantioselective reduction of prochiral ketones.

Regardless of which ligand is employed, there are three ways to introduce the ruthenium catalyst to the reaction mixture (**Scheme 3.15**): (i) *In situ* generation of an  $\eta^6$ -arene ruthenium (II) *N*-tosyl 1,2-diaminoethane hydride complex **64** by reaction of the  $\eta^6$ -arene ruthenium dichloride dimer precursor  $[(p\text{-cymene})\text{RuCl}_2]_2$ <sup>50</sup>, ethylene ligand and an auxiliary base, e.g. KOH, in *iso*-propanol solvent. (ii) Direct addition of the 18-electron Ru-hydride complex **64**, which can separately be prepared from the ruthenium chloride complex **65** in *iso*-propanol solvent under the influence of base. (iii) Direct addition of the 16-electron ruthenium amide complex **66**, which can separately be prepared from the ruthenium chloride complex **65** under basic conditions in aprotic solvents such as dichloromethane.

**Procedure (i) and (ii)**



**Procedure (iii)**

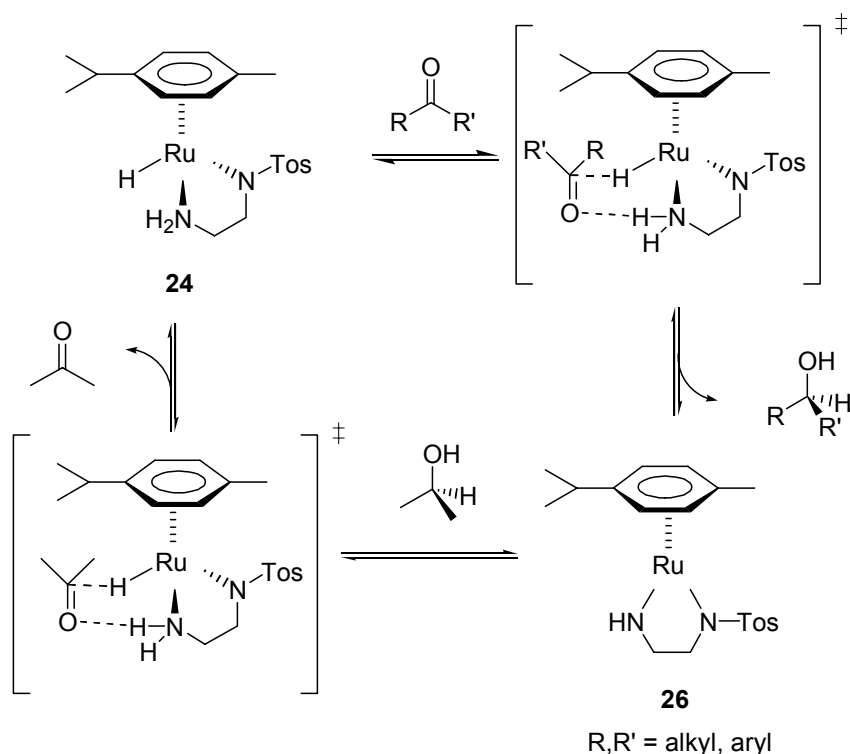


**Scheme 3.15** Synthesis of ruthenium catalysts.

The advantage of procedure (i) is its synthetic simplicity as the catalyst is generated *in situ* from the readily available, air-stable precursor compounds, *p*-cymene ruthenium dichloride dimer and 1,2-diaminoethane ligand in presence of a base. However, if the substrates are base sensitive, as anticipated for keto-sugars, procedures (ii) and (iii) are of interest as both the isolated 18-electron Ru-hydride **64** and 16-electron Ru complex **66** can be added directly to the

hydrogen transfer reaction *without* necessity of having base present in the reaction medium. Thus, reduction reactions can be conducted in pH neutral *iso*-propanol solvent under mild conditions.<sup>51</sup>

The proposed reaction mechanism for the hydrogen transfer reaction catalyzed by these systems hinges on the already introduced pericyclic metal-ligand bifunctional transition state and is illustrated in its entirety in **Scheme 3.16**.<sup>46</sup>



**Scheme 3.16** Proposed mechanism of a hydrogen transfer reaction in metal-ligand bifunctional catalysis.

The hydride-proton transfer occurs from the hydrogen-loaded 18-electron complex **24** to the ketone substrate producing alcohol and the 16-electron complex **26**. The 16-electron complex **26** then reacts with the *iso*-propanol solvent to give acetone while regenerating the 18-electron hydrogen-loaded complex **24** via a similar transition state.

Based on the principle of microreversibility the transfer hydrogenation reactions can in principle be conducted under “forward” conditions, i.e. reduction of ketone substrate in *iso*-propanol solvent or under “reverse” conditions, i.e. oxidation of secondary alcohols in acetone solvent.

Noyori and co-workers demonstrated that the  $\eta^6$ -arene diamine ruthenium (II) based catalysts can be successfully employed under oxidizing conditions for the kinetic resolution of racemic benzylic or allylic alcohols achieving high ee values (92 % to 99 %) at 50 % conversion within 6 to 36 h at 28°C.<sup>52</sup> Another result supporting the reversibility of the  $\eta^6$ -arene diamine Ru(II) catalyzed hydrogen transfer reactions is the fact that the optical activity of a chiral benzylic alcohol solution decreases after extended reaction time and high ketone concentrations.<sup>39,40,42,53</sup>

On the basis of these known facts and concepts we postulated that the Noyori system should be a suitable catalyst for the chemoselective oxidation of sugar and other polyol substrates to keto-sugars and  $\alpha$ -hydroxy-ketones, respectively under exceedingly mild thermal conditions at neutral pH. To our knowledge only benzylic and allylic alcohols have been oxidized under the kinetic resolution condition<sup>52</sup>, but the oxidation of aliphatic alcohols or *vicinal* diols has not been reported in literature.

#### 3.2.2.1.1 Selection of Catalyst System and Oxidation Substrates

The most active ruthenium catalysts for “forward” reactions, i.e. reductions of ketones in *iso*-propanol solvents were obtained with  $\beta$ -amino-ethanol and *N*-tosyl-1,2-diaminoethane as the ligands.<sup>41</sup> Presumably the resulting complexes allow the most facile access of substrates to the catalytically active centre because of the least amount of steric repulsion with the ethane backbone.<sup>40,41,46</sup>



Cyclopentanol, cyclohexanol and 1,2;5,6-*O*-diisopropylidene  $\alpha$ -D-glucopyranoside (diacetone-glucose) (**Figure 3.14**) were chosen as model systems for sugar substrates in order to test the  $\beta$ -amino-ethanol and *N*-tosyl-1,2-diaminoethane *p*-cymene ruthenium complexes in hydrogen transfer reactions under oxidizing conditions, i.e. in acetone or cyclohexanone solvent .

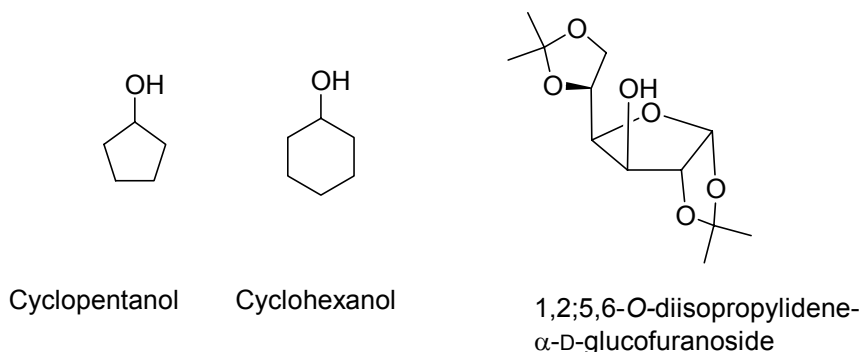


**Figure 3.14** Model systems for oxidation of secondary alcohols in sugar substrates.

### 3.2.2.2 Results and Discussion

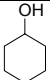
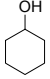
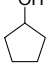
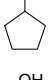
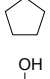
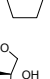
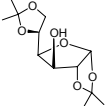
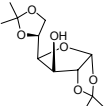
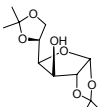
#### 3.2.2.2.1 Oxidation Reactions with Known Systems

The results of the oxidation of cyclopentanol, cyclohexanol and diacetone-glucose with the  $\beta$ -aminoethanol *p*-cymene-ruthenium hydride complex, which was synthesized according to literature procedure<sup>40</sup>, are shown in **Table 3.2**. The oxidation reactions were monitored by GC using NMP as internal standard. The experimental technique and actual activity of the catalyst was verified in a control experiment by the quantitative reduction of acetophenone to 1-phenyl-ethanol in *iso*-propanol after 6 h at room temperature using an authentic catalyst sample from the same synthesis batch.<sup>53</sup>

In all oxidation reactions, the initial colour of the reaction solution is purple but turned to dark brown containing black precipitate after 24 h to 48 h indicating the formation of ruthenium(0) as by-product of catalyst decomposition. Even at the

high catalyst load of 10 mol% the room temperature oxidation of cyclohexanol and cyclopentanol in acetone solvent was very slow yielding less than 15 % conversion after 24 to 48 h (**Entries 1,3,5**). An increase in temperature to 56°C increased the conversion of cyclopentanol and cyclohexanol to 15 % and 46 %. A higher temperature was reached when the ketone solvent was cyclohexanone, which is not only preferred as higher boiling solvent but also releases ring strain energy by formation of cyclohexanol.<sup>54,55</sup> The loss of ring strain energy favoured the oxidation direction as seen with Shvo's catalyst in **Chapter 2**. With cyclohexanone as hydrogen-acceptor, cyclopentanol was oxidized to cyclopentanone in 70 % after 24 h at 100°C (**Entry 6**). Diacetone-glucose was not oxidized with acetone as the hydrogen-acceptor at 56°C but oxidation occurred with cyclohexanone at 100°C and 150°C with 12 % and 71 % of cyclohexanol produced, which as a first approximation should be equivalent to the amount of diacetone-glucose oxidized. However, isolation attempts of the diacetone-glucose reaction (**Entry 9**) failed as NMR analysis of the recovered solids revealed an intractable mixture of organic compounds generated through undefined thermal side-reactions at 150°C.

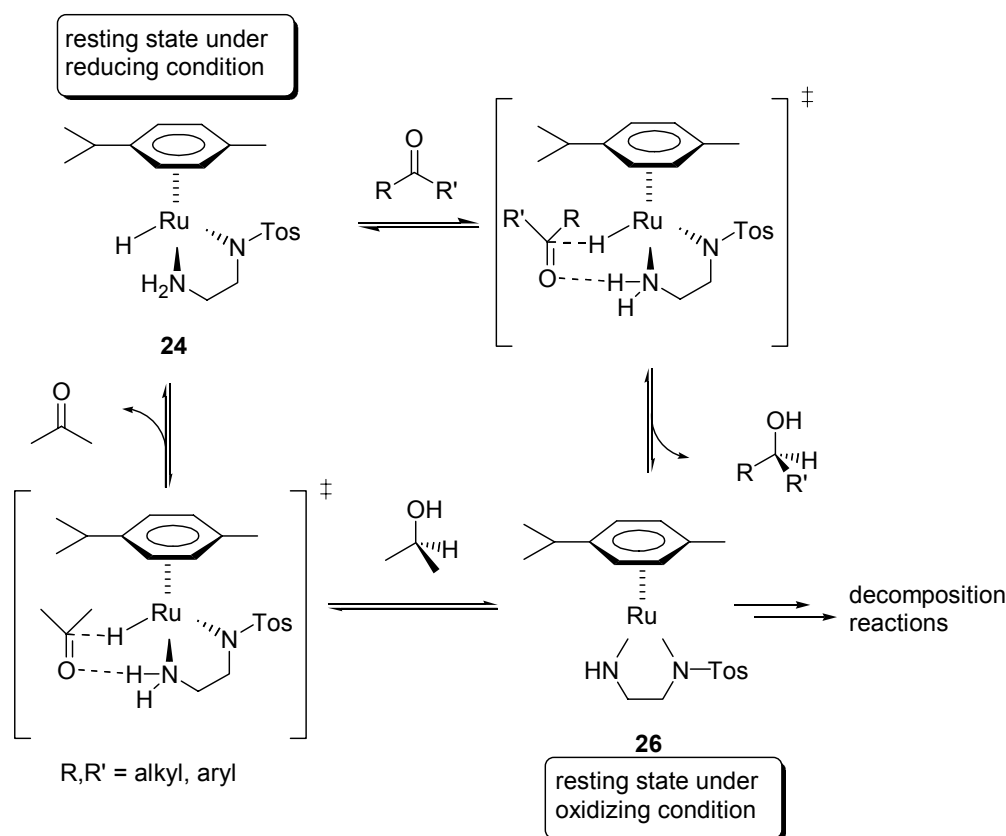
**Table 3.2** Oxidation of secondary alcohols with *p*-cymene-Ru- $\beta$ -aminoethanol hydride (**23**) as catalyst.<sup>a</sup>

Entry	Substrate	Solvent	Temperature	Time	GC-Conversion <sup>b</sup>
1 <sup>c</sup>		Acetone	25°C	48 h	<2%
2 <sup>c</sup>		Acetone	56°C	24 h	15 %
3 <sup>c</sup>		Acetone	25°C	48 h	<10 %
4 <sup>c</sup>		Acetone	56°C	24 h	46 %
5		Cyclohexanone	25°C	48 h	40 %
6		Cyclohexanone	100°C	24 h	70 %
7		Acetone	56°C	24 h	0 % <sup>d</sup>
8		Cyclohexanone	100°C	24 h	12 % <sup>e</sup>
9		Cyclohexanone	150°C	24 h	71 % <sup>e,f</sup>

<sup>a</sup> 1.0 mmol alcohol substrate, 0.1 mmol *p*-cymene  $\beta$ -aminoethanol ruthenium hydride and NMP (~100 mg) in 10 mL ketonic solvent under Ar. <sup>b</sup> Production of ketone substrate determined by GC with NMP as internal standard. <sup>c</sup> *In situ* generation of catalyst with additional 0.30 mmol KOH. <sup>d</sup> Produced *iso*-propanol measured. <sup>e</sup> Produced cyclohexanol measured. <sup>f</sup> Isolation of sugar product failed.

Important insights into the relative stability of the Noyori catalyst under reducing and oxidizing conditions and the apparent decomposition of the catalysts in acetone or cyclohexanone solvent originate from the following observations: Under reducing conditions in *iso*-propanol solvent the reaction mixture is yellow-orange coloured, which indicates that the resting state is the 18-electron ruthenium hydride complex **24** as illustrated in **Scheme 3.17**. However, under

oxidizing conditions in acetone or cyclohexanone solvent, the deep purple colour demonstrates that the 16-electron complex **26** is the resting state.



**Scheme 3.17** Different resting states of catalyst under reducing and oxidizing condition.

It therefore appeared to be logical to attempt to directly use the 16-electron complex **26** as the catalyst, as addition of this complex to the reaction mixture would possibly have a positive effect on the reaction rate as the initial step is the dehydrogenation of the alcohol substrate. Furthermore this would also ensure a base-free reaction environment.

The syntheses of the 16-electron  $\beta$ -aminoethanol and *N*-tosyl-1,2-diaminoethylene-*p*-cymene ruthenium complexes **25** and **26** (**Figure 3.15**) were conducted in analogy to the reported synthetic procedure.<sup>53</sup> However, the syntheses and isolation of both 16-electron complexes **25** and **26** failed. In

solution the purple colour of each 16-electron complex was briefly observed after addition of KOH but the reaction mixture turned black within minutes and undefined solids were obtained. We rationalized this result by proposing that the 16-electron complex undergoes a  $\beta$ -hydride elimination reaction forming imine and aldehyde based ligands **67** to **70** as proposed intermediates (**Scheme 3.18**), which would then be followed by reductive elimination of the ligand leading to the complete disintegration of the complexes and formation of ruthenium(0). GC-MS analysis of the dark brown reaction mixture was however inconclusive as even with mild chemical ionization methods (acetonitrile) the presence of the very reactive imine and aldehyde intermediates could not be unambiguously determined.

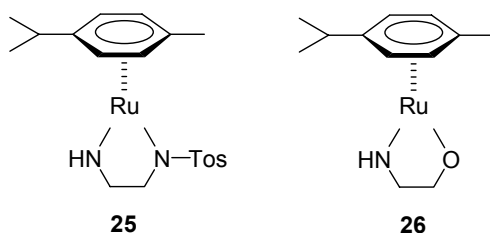
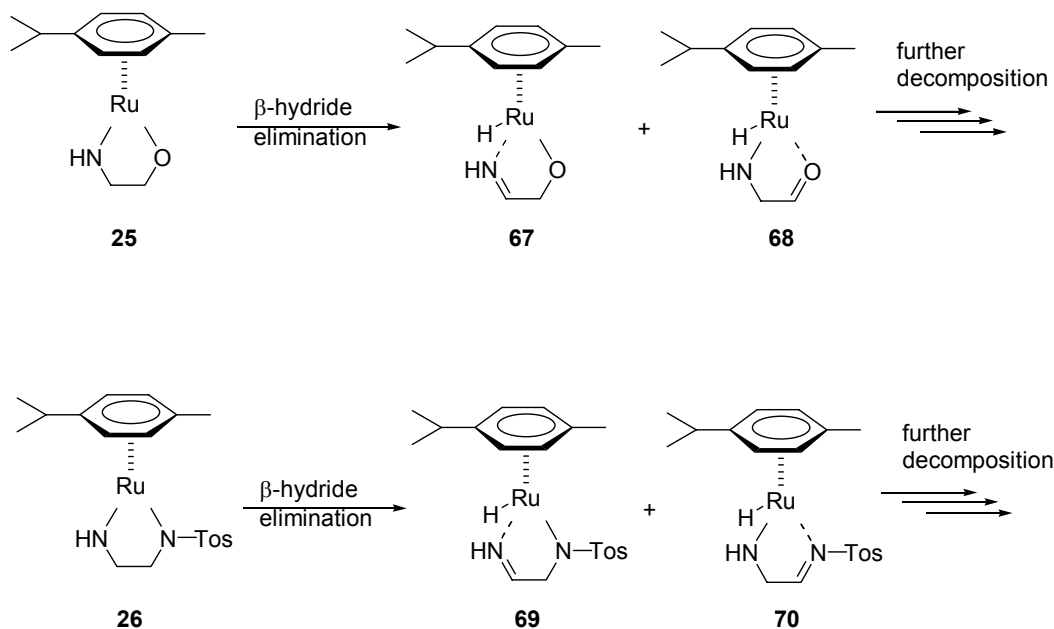


**Figure 3.15** *N*-tosyl-1,2-diaminoethane and  $\beta$ -amino-ethanol *p*-cymene-ruthenium(II).



**Scheme 3.18** Possible decomposition products of 16-electron complexes **25** and **26** through  $\beta$ -hydride elimination.

We thus propose that the  $\beta$ -hydride elimination process is the key problem in the oxidation of secondary alcohols with Noyori's ruthenium catalysts as the 16-electron ruthenium complex is the resting state under oxidizing conditions (**Scheme 3.17**). The 16-electron ruthenium complex undergoes decomposition reactions based on  $\beta$ -hydride elimination processes cleaving all ligands and precipitation of black metallic ruthenium(0) occurs. In contrast, the 18-electron hydride complex is the resting state under reducing conditions in *iso*-propanol solvent. It does not undergo a  $\beta$ -hydride elimination but is stable under the reducing conditions. Implicit in these realizations is that in *iso*-propanol solvent the hydrogenation of the 16-electron complexes **25** and **26**, which by necessity must also be formed as reactive intermediates under reducing conditions, must be a lot faster than the  $\beta$ -hydride elimination process.

### 3.2.2.2 Rational Design and Synthesis of Oxidation Resistant Ligands

To avoid  $\beta$ -hydride elimination, a rational synthesis of oxidation resistant ethylene diamine ligands, which contained no  $\beta$ -hydrides or disfavour a  $\beta$ -hydride elimination, was planned and executed.

The three target ligands *N*-tosyl-*ortho*-diaminobenzene (**71**), *N*-tosyl-1,2-diamino-1,1,2,2-tetramethylethane (**72**) and racemic *N*-tosyl-*meso*-diphenyl-1,2-diaminoethane (**73**), are shown in **Figure 3.16**.

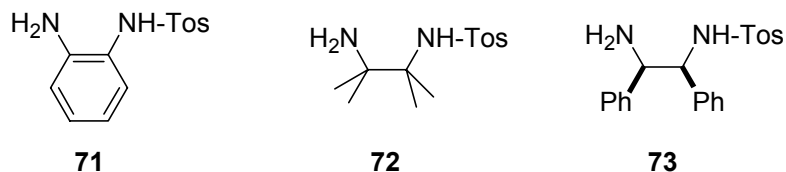


**Figure 3.16** Degradation resistant ligands.

While the diamino compounds **71** and **72** do not contain any  $\beta$ -hydrides, the *meso*-1,2-diphenyl ligand (**73**) contains two  $\beta$ -hydrogen atoms. A  $\beta$ -hydride elimination from a 16-electron ruthenium complex is however not preferred as the four membered transition state required for a  $\beta$ -hydride elimination process is energetically unfavoured due to steric repulsion of the phenyl substituents.

It was reported that *syn*-disubstituted 1,2-diaminoethane ligands preferably coordinate to the ruthenium centre in an *exo*-conformation rather than an *endo*-conformation as illustrated in **Figure 3.17**.<sup>47</sup> In the *exo*-position the phenyl ligands point away from the reactive catalytic centre thus enabling a more facile access of an alcohol. The catalytic reactivities of the *syn*- and *anti*-disubstituted ligand are comparable but the enantioselectivity of reduction of aromatic ketones was generally decreased with *syn*-disubstituted ethylene ligands in  $\eta^6$ -arene ruthenium complexes compared to those in the *anti*-configuration.<sup>47</sup>

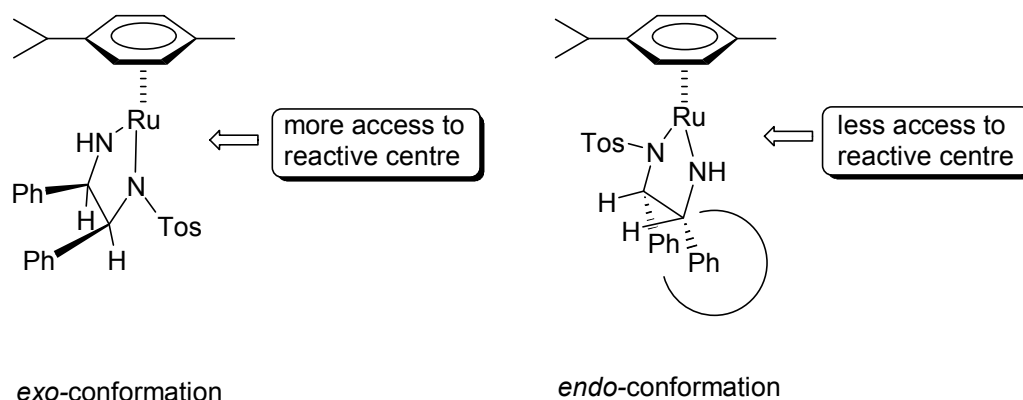
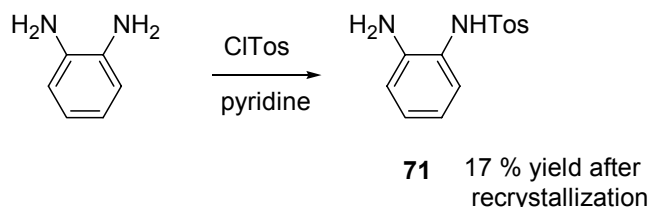


**Figure 3.17** *Exo*- and *endo*-conformation of *syn*-disubstituted 1,2-diaminoethane 16-electron ruthenium(II) complexes.

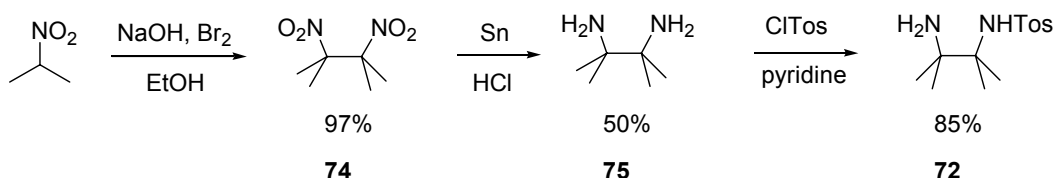
The synthesis of *N*-tosyl-*ortho*-diaminobenzene (**71**) was accomplished by tosylation of *o*-amino-aniline as illustrated in **Scheme 3.19**.<sup>56</sup> The tosylation was conducted in pyridine solvent with *para*-toluylsulfonyl chloride and an oily residue was afforded, which produced a white solid in 17 % yield upon recrystallization in

ethanol. This reaction was not improved as the reactants were inexpensive and sufficient quantities of **71** were obtained.



**Scheme 3.19** Synthesis of *N*-tosyl-*ortho*-diaminobenzene (**71**).

*N*-tosyl-1,2-diamino-1,1,2,2-tetramethylethane (**72**) was prepared by a three step synthesis as shown in **Scheme 3.20**. The first step was the oxidative fusion of 2-nitro-propane to the 1,2-dinitro-tetramethylethane **74** in ethanol solvent with elemental bromine under basic condition in 97 % yield.<sup>57</sup> Subsequent reduction of the nitro groups to primary amines (**75**) was conducted with tin metal in acidic medium. The resulting white solids were purified by steam distillation. Tosylation of the diamine compound **75** with substoichiometric *p*-toluyl-sulfonyl chloride in pyridine solvent yielded **72** in 85 %.

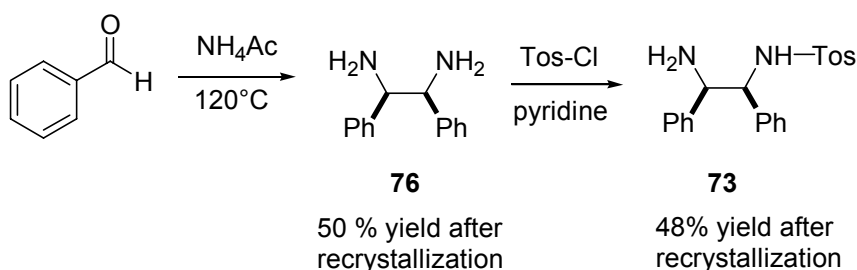


**Scheme 3.20** Synthesis of *N*-tosyl-1,2-diamino-1,1,2,2-tetramethylethane (**72**).

As outlined in **Scheme 3.21** the precursor to the third ligand, *meso*-1,2-diphenyl-1,2-diaminoethane (**76**) was synthesized from the reaction of neat benzaldehyde and ammonium acetate under refluxing condition with 50 % after recrystallization from methanol.<sup>58</sup> The obtained *meso*-1,2-diphenyl-1,2-diaminoethane compound was subsequently monotosylated with substoichiometric amounts of *p*-toluyl-



sulfonyl chloride in pyridine to give *N*-tosyl-*meso*-1,2-diphenyl-1,2-diaminoethane (**73**) in 48 % yield.<sup>\*\*\*</sup>



**Scheme 3.21** Synthesis of *N*-tosyl-*meso*-1,2-diphenyl-1,2-diaminoethane (**73**).

### 3.2.2.2.3 Synthesis and Properties of New Noyori Type Complexes

The three *N*-tosyl-1,2-diamine ligands **71** to **73** were then used to synthesize the corresponding 16 electron  $\eta^6$  *p*-cymene ruthenium complexes **77** to **79** shown in **Figure 3.18**.

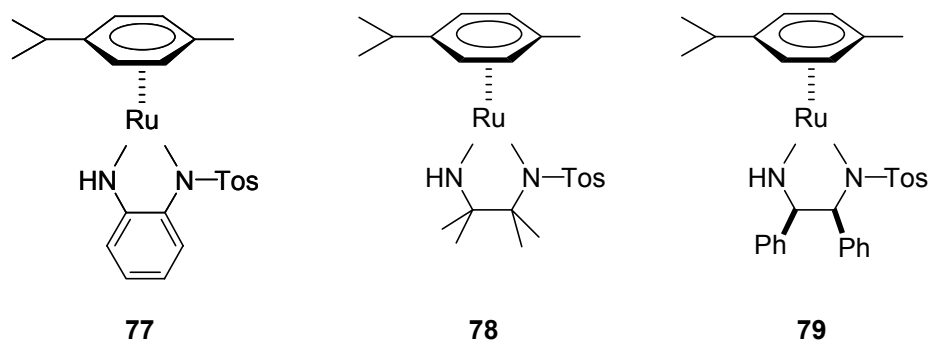


**Figure 3.18** Synthesized 16-electron ruthenium (II) complexes.

All three complexes were synthesized in analogy to published literature procedures.<sup>40,43,44,53</sup> The [*p*-cymene RuCl<sub>2</sub>]<sub>2</sub> precursor,<sup>50</sup> synthesized from

<sup>\*\*\*</sup> A four step enantioselective synthesis of *N*-(*p*-toluyl-sulfonyl)-(1*S*,2*R*)-1,2-diphenyl-1,2-diaminoethane from enantiopure (1*S*,2*R*)-1,2-diphenyl-β-aminoethanol is described in literature.<sup>47</sup>

$\alpha$ -pinene and ruthenium (III) chloride hydrate in refluxing ethanol, is reacted with one equivalent *N*-tosyl-diamino ligand at room temperature in degassed dichloromethane under Ar atmosphere and yielded 82 % (**77**), 94 % (**78**) and 92 % (**79**), respectively.<sup>†††</sup> Addition of solid KOH, produced a bright red coloured reaction mixture with **77** and **79** and deep purple colour with **78**. The compounds **77** and **78** are new and **79** has only recently been published as the pure (1*S*,2*R*)-enantiomer.<sup>47</sup>

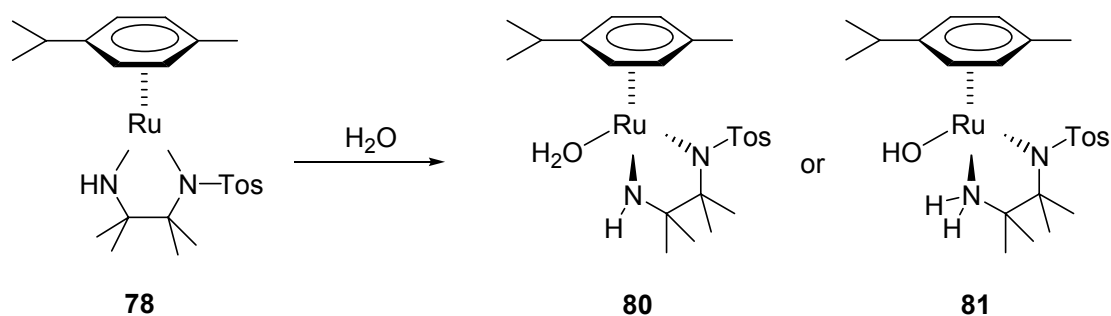
The *ortho*-diaminobenzene complex (**77**) is red coloured and air-stable. The tetramethyl complex (**78**) and *meso*-diphenyl complex (**79**) are deep purple and dark red coloured and are extremely air-sensitive when dissolved in organic solvents.

A unique chemical property of the tetramethyl complex **78** is that it dissolved immediately in oxygen-free water turning the purple solids into a yellow solution (**Scheme 3.22**). After 5 min a bright yellow precipitate formed, which was stable in air. When the yellow solids were dried under vacuum, the colour of the solids turned immediately purple suggesting that aquo-complexes were formed (**80** or **81**) containing weakly bound water. After exposure of the solids to moist air, the yellow colour occurred again. This process was reversible and was repeated several times until a brown solid was formed after 4 to 5 days. The brown solids were probably the decomposition products derived from the reaction of the very reactive and oxygen sensitive purple 16-electron complex with air.

In theory water can coordinate to the ruthenium centre (**80**) either as an actual aquo ligand or the bifunctional catalysis takes effect and a hydroxide amine ligand is produced **81** as illustrated in **Scheme 3.22**.

---

<sup>†††</sup> The 16-electron ruthenium(II) complexes are usually highly oxygen sensitive and reactions must be conducted under Ar atmosphere and degassed solvents.



**Scheme 3.22** Two possible aquo complexes **80** and **81**.

Analysis of this elusive complex was however very difficult as the yellow solids were not soluble in deuterated benzene or other available non-coordinating deuterated solvents, but a purple solution of the 16-electron complex **78** was formed another indication that the postulated water ligand is only weakly bound to the ruthenium complex.

In an attempt to gather further evidence for the existence of the aquo complexes an NMR experiment was carried out (**Figure 3.19**). Approximately 2 mg purple tetramethyl complex **78** were dissolved in degassed  $\text{D}_2\text{O}$  (0.6 mL) resulting in a pale yellow solution. The  $^1\text{H}$  NMR was recorded with large number of scans (i.e. 1024) due to the very low solubility of the yellow solids in water. The sample concentration was too weak to obtain a  $^{13}\text{C}$  NMR in a reasonable time window. The signal integration in the 7.0 to 8.0 ppm (*p*-toluyl sulfonyl group) and 5.0 to 5.5 ppm range (*p*-cymene ligand) indicate that there is an approximately 1 : 1 mixture of two compounds in solution possibly **80** and **81**. However, other processes such as dimerization of the complexes cannot be unambiguously excluded.

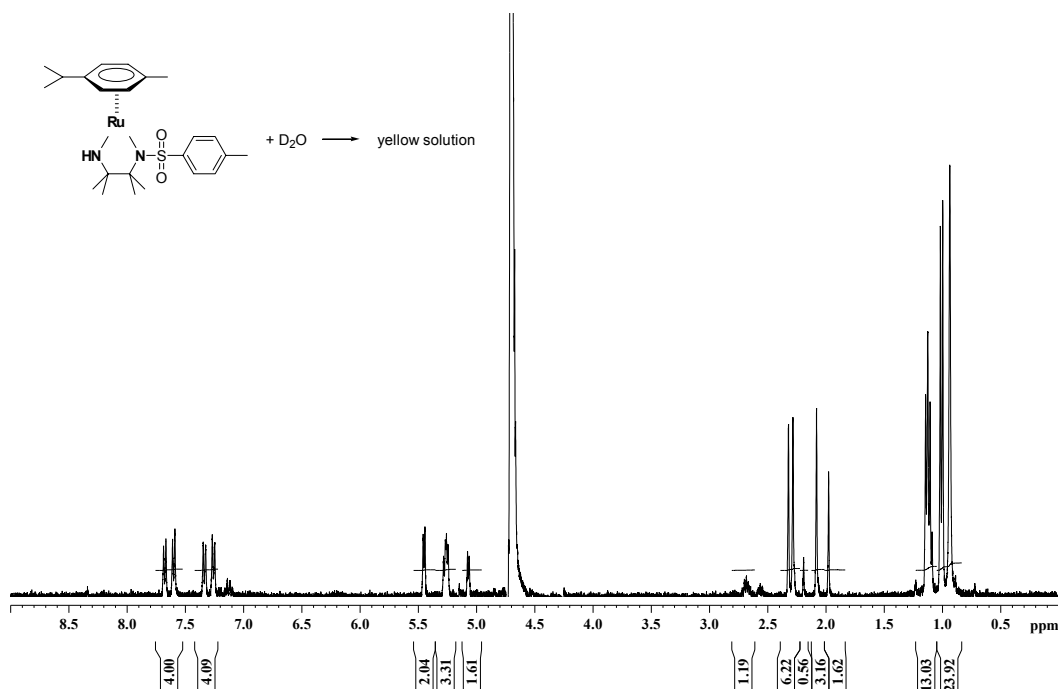
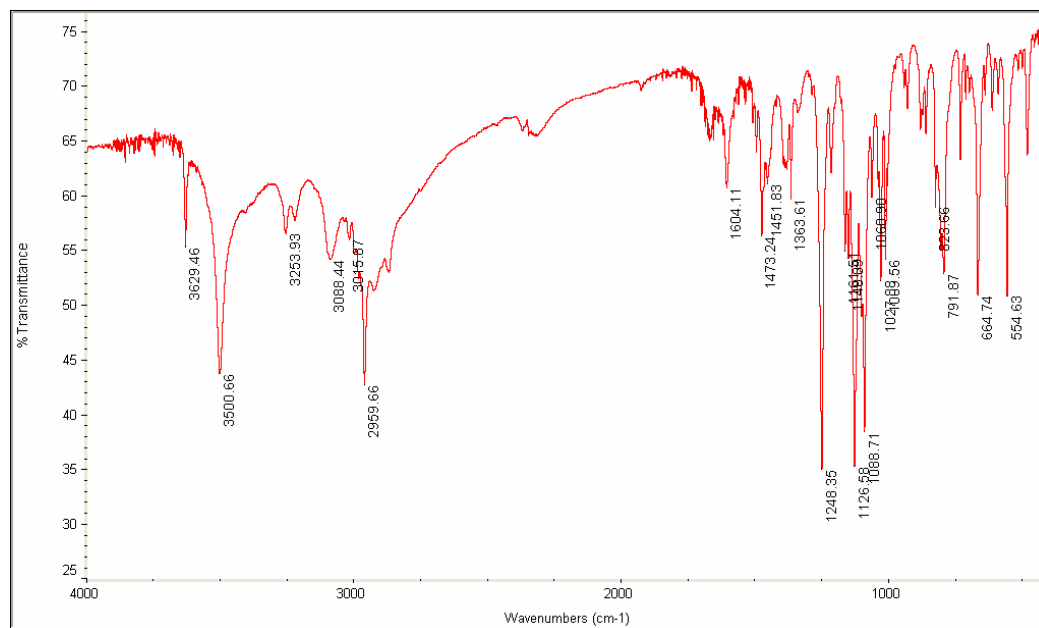


Figure 3.19  $^1\text{H}$ -NMR of **78** in  $\text{D}_2\text{O}$  solvent.

Better evidence is provided by the IR spectrum of the yellow precipitate, which is shown in **Figure 3.20**. All observed bands are basically identical with the 16-electron complex **78** and the yellow solid. However, one distinct feature is a strong band at  $3500\text{ cm}^{-1}$ , which does not occur in the 16-electron ruthenium complex **78**. The  $3500\text{ cm}^{-1}$  band is fairly strong and the medium broad signal is indicative of an  $\nu_{\text{OH}}$ . However, the yellow solids could only be dried through frit-filtration open to air as a vacuum would generate purple solids. Therefore this band could in principle also originate from traces of non-bound water that remained after air-drying at ambient pressure. Visual inspection of the consistency of the resulting yellow powder however suggested that this is not the case and the aquo complex was in fact obtained.



**Figure 3.20** IR (KBr) of yellow solids of tetramethyl Ru complex (**80** or **80**).

Compared to the hydrogen transfer reaction of **78** in *iso*-propanol to produce the yellow coloured hydride complex, which takes about 15 to 30 min at room temperature, the reaction of **78** with water occurred instantaneously. This water-adduct reaction of **78** is very unique and intrinsic to this complex, as the analog complexes **77** and **79** do not dissolve or react in water.

#### 3.2.2.2.4 Hydrogen Transfer Reactions with New Ruthenium Systems

The catalytic transfer hydrogenation activity of the *ortho*-diaminobenzene ruthenium complex **77** was investigated under both oxidizing and reducing conditions. A typical reaction was the oxidation of 1-phenyl-ethanol (1.0 mmol, 0.20 M) in 5.0 mL degassed acetone with 0.010 mmol ruthenium complex **77** *cis*-decalin as internal GC standard at ambient temperature and Ar atmosphere. No catalytic activity of **77** was observed with 1-phenyl-ethanol and cyclohexanol after 7 days. After 4 weeks, the contents of acetophenone and cyclohexanone were only 1 %.

For investigation of catalytic hydrogenation activity under reducing conditions, similar concentrations as the oxidation condition were employed with acetophenone (1.0 mmol, 0.20 M), 0.010 mmol ruthenium complex **77** and *cis*-decalin in 5.0 mL degassed *iso*-propanol solvent at room temperature and under Ar atmosphere. Again the phenylene complex **77** showed no catalytic activity in reducing acetophenone to 1-phenyl ethanol (0 %) and only very marginal activity for the conversion of cyclohexanone to cyclohexanol (11 % after four weeks).

We attribute the low reactivity to the *ortho*-diaminobenzene ligand acting as a non-innocent ligand that stabilizes the Ru complex through an *ortho*-quinone type system (**82**) as illustrated in **Figure 3.21**. The aromatic hydrogens of the cymene ligand have a chemical shift of 5.17 and 5.05 ppm in the tetramethyl-ruthenium compound **78** but in the *ortho*-diaminobenzene compound **77** the proton resonances are shifted downfield by approximately 0.5 ppm to 5.67 ppm and 5.63 ppm, which indicates a higher ring current and thus more electron density donate towards the  $\pi^*$ -orbitals of the cymene moiety. This electron density must originate from a more electron rich ruthenium centre than in the tetramethyl ruthenium complex, which in turn can be rationalized through the resonance structure on the right of **Figure 3.21**, which postulates a ruthenium(0) centre.

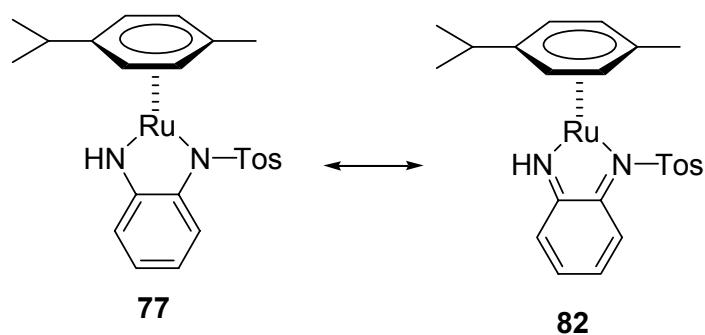


**Figure 3.21** *Ortho*-diaminobenzene as a non-innocent ligand.

Another observation supporting the non-innocent nature of this ligand and its effects is the stability of **77** in air. Even when dissolved in organic solvents such

as acetone or *iso*-propanol the red colour does not change and the complex is stable. Heating to 50°C does not decompose the complex.

As the phenylene ruthenium complex **77** is not useful for the catalytic hydrogen transfer reaction of alcohols and ketones and further investigations focussed on the other two ruthenium complexes **78** and **79**.

Hydrogen transfer reaction under reducing and oxidizing conditions were carried out with a series of representative secondary alcohol/ketone pairs and the tetramethyl complex (**78**) as the catalyst. Standard oxidation conditions involved alcohol (1.0 mmol, 0.20 M) in 5.0 mL degassed acetone with 0.010 mmol ruthenium complex **78** at ambient temperature and Ar atmosphere and *cis*-decalin as the internal GC standard (**Figure 3.22**). The reducing conditions used similar concentrations as the oxidizing condition with ketone substrate in *iso*-propanol solvent (**Figure 3.23**). Under reducing conditions with *iso*-propanol as solvent and hydrogen source, the reaction mixture was yellow. In contrast, under oxidizing conditions the colour was deep purple.

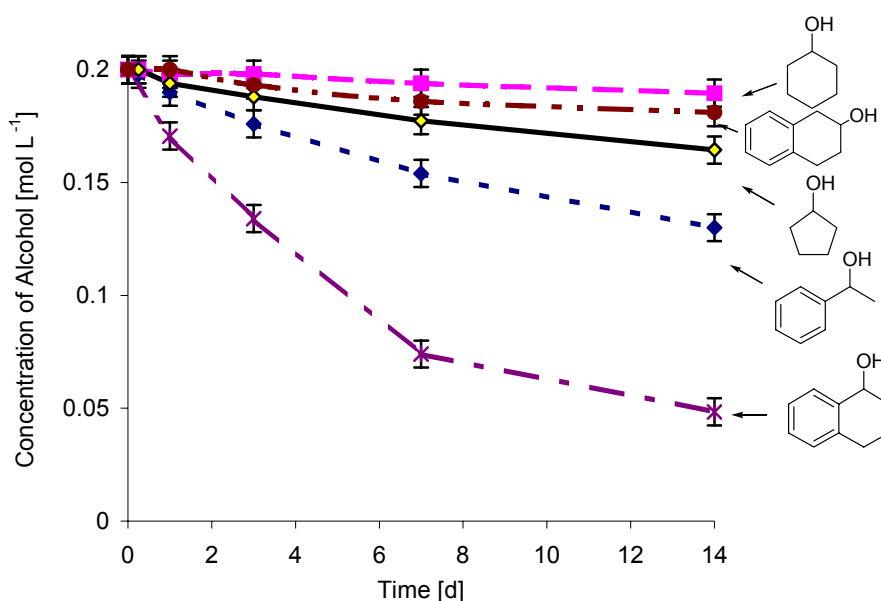


**Figure 3.22** Time dependence of alcohol content. Conditions 1.0 mmol alcohol in 5.0 mL acetone, 0.010 mmol tetramethyl catalyst (**78**), 50 mg *cis*-decalin as internal GC standard.

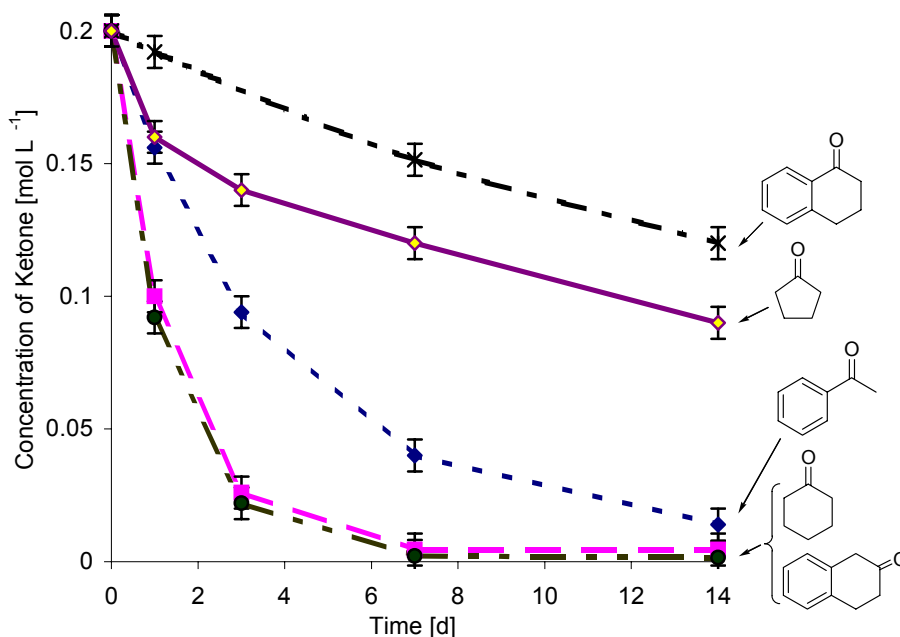


**Figure 3.23** Time dependence of ketone content. Conditions 1.0 mmol ketone in 5.0 mL *iso*-propanol, 0.010 mmol tetramethyl catalyst (**78**), 50 mg *cis*-decalin as internal GC standard.

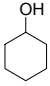
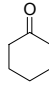
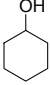
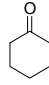
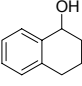
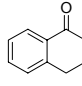
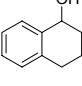
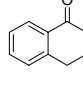
The catalytic hydrogen transfer activity of **78** under reducing condition is much lower compared to the TON and TOF reported by Noyori and co-workers, which reported quantitative reduction of 1-phenyl-ethanol within 24 h.<sup>40,41</sup> As seen in **Figure 3.23**, cyclohexanone and  $\beta$ -tetralone were quantitatively reduced to their corresponding alcohols within 5 d at room temperature and 1 mol% **78** in *iso*-propanol solvent. After 14 d acetophenone reacted to 95 %, cyclopentanone 52 % and  $\alpha$ -tetralone 37 % to their corresponding alcohols. Under oxidizing conditions as seen in **Figure 3.22**, the order of oxidation is reversed compared to the reducing conditions and the catalytic activity is even lower and no quantitative oxidation was observed even after 14 d. The 1-phenyl-ethanol content after 14 d is 69 % compared to 82 % of cyclopentanol.

In order to investigate the temperature dependency of the reaction of **78** with the cyclohexanone/ cyclohexanol and  $\alpha$ -tetralone/ $\alpha$ -tetralol substrate reactions at room temperature and 50°C were carried out as shown in **Table 3.3**. Under both



oxidizing and reducing conditions the overall conversions of alcohol or ketone starting material of the hydrogen transfer reactions as well as the conversion after 24 h were increased at the elevated temperature. However, cyclohexanol, the model system for pyranose sugars, was despite an almost one fold increase in conversion only to 5 % converted after 7 d at 50°C compared to 3 % after 7 d at room temperature.

**Table 3.3** Ruthenium catalyst **78** under oxidizing and reducing conditions at different temperatures.

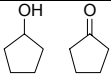
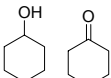
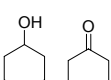
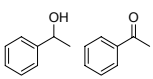
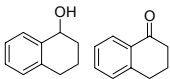
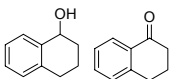
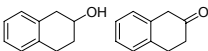
Entry	Alcohol <sup>a</sup>	Temp.	Conv. % <sup>c</sup>	Entry	Ketone <sup>b</sup>	Temp.	Conv. % <sup>d</sup>
1		RT	1 % (24 h) 3 % (7 d)	5		RT	50 % (24 h) 98 % (7 d)
2		50°C	2 % (24 h) 5 % (7 d)	6		50°C	75 % (24 h) 96 % (48 h)
3		RT	15 % (24 h) 63 % (7 d)	7		RT	4 % (24 h) 24 % (7d)
4		50°C	29 % (24h) 85 % (7 d)	8		50°C	4 % (24 h) 28 % (7 d)

<sup>a</sup> 1.0 mmol alcohol, 0.010 mmol **23** and *cis*-decalin (~50 mg) in 5.0 mL acetone under Ar atmosphere. <sup>b</sup> 1.0 mmol ketone, 0.010 mmol **23** and *cis*-decalin (~50 mg) in 5.0 mL *iso*-propanol under Ar atmosphere. <sup>c</sup> Determined by GC of produced corresponding ketone. <sup>d</sup> Determined by GC of produced corresponding alcohol.

Noyori and co-workers reported that the reduction of ketone substrates in *iso*-propanol solvent is in first order with regards to the ketone.<sup>52</sup> Similarly, the oxidation of allylic and benzylic alcohols in acetone solvent was first order in alcohol.<sup>52</sup> Thus we assumed a pseudo first order rate law in alcohol under oxidizing condition and pseudo first order rate law in ketone under reducing condition and determined the corresponding rate constants from the concentration vs. time plots of the substrates as determined by quantitative GC (**Figure 3.22** and **Figure 3.23**). Comparing the rate constants of the respective alcohol and ketone substrate pairs shows that the rates of the reductions are generally one to two magnitudes greater than compared to the rate constants of

reduction. The exception is  $\alpha$ -tetralol/  $\alpha$ -tetralone pair for which the oxidation reaction is markedly faster than the reduction, as fact that must be related to the formation of a benzylic conjugated carbonyl function upon oxidation of the alcohol. The implications of this phenomenon are discussed in greater detail in later sections (*vide infra*).

**Table 3.4** Rate constants assuming a 1<sup>st</sup> order rate law in alcohol or ketone substrate, respectively with ruthenium catalyst **78**.

Entry	Alcohol/Ketone	Temperature	Rate constant Oxidation [s <sup>-1</sup> ]	Rate constant Reduction [s <sup>-1</sup> ]
1		RT	$9.4 \times 10^{-8}$	$6.4 \times 10^{-7}$
2		RT	$2.3 \times 10^{-8}$	$6.3 \times 10^{-6}$
3		50°C	$9.9 \times 10^{-8}$	$1.9 \times 10^{-5}$
4		RT	$1.9 \times 10^{-7}$	$1.4 \times 10^{-6}$
5		RT	$5.5 \times 10^{-7}$	$2.3 \times 10^{-7}$
6		50°C	$3.6 \times 10^{-6}$	$5.7 \times 10^{-7}$
7		RT	$4.5 \times 10^{-8}$	$1.7 \times 10^{-6}$

<sup>a</sup> 1.0 mmol alcohol, 0.010 mmol **78** and *cis*-decalin (~50 mg) in 5.0 mL acetone under Ar atmosphere. <sup>b</sup> 1.0 mmol ketone, 0.010 mmol **78** and *cis*-decaline (~50 mg) in 5.0 mL *iso*-propanol under Ar atmosphere. <sup>c</sup> Determined from GC measurements and semi natural logarithmic plot of ln (concentration of product) vs. time [s].

The tetramethyl complex **78** was also tested in the oxidation of *cis*- and *trans*-1,2-cyclohexanediol as the substrate (1.0 mmol) in 5.0 mL acetone and cyclohexanone solvent at room temperature under Ar atmosphere. However, after 7 d only trace amounts (< 2 %) of *iso*-propanol or cyclohexanol as well  $\alpha$ -hydroxy-cyclohexanone substrate were detected. The reactivity of the diol substrate was in the same range as the oxidation of the cyclohexanol model system and thus improvement of catalytic activities were focussed on the oxidation of the cyclohexanol model system first.

The third 16-electron complex **79** containing the *N*-tosyl-*meso*-1,2-diphenyl-1,2-diaminoethane ligand was also tested with cyclohexanol/ cyclohexanone and  $\alpha$ -tetralol/  $\alpha$ -tetralone under oxidizing and reducing conditions and the standard concentration of 0.2 M substrate in 5.0 mL solvent. All reactions were monitored by quantitative GC measurements using *cis*-decalin as internal standard.

Cyclohexanol was oxidized to cyclohexanone with **79** after 24 h only in trace amounts (<1 %) and a 2 % content was detected after 14 d at room temperature. In contrast, with the same catalysts under reducing conditions 68 % of cyclohexanone were reduced to cyclohexanol after 24 h, 88 % after 48 and 95 % after 72 h at room temperature.

Under oxidizing conditions,  $\alpha$ -tetralol was oxidized to  $\alpha$ -tetralone in 20 % after 24 h and 84 % after 14 d at room temperature. In contrast, the reduction of  $\alpha$ -tetralone yielded no reaction after 24 h and only 14 % after 14 d.

While the tetramethyl complex **78** is stable in solution for 3 to 4 weeks the diphenyl complex **79** decomposes and brown precipitate occurs after 1 to 2 weeks. This is probably based on the existence of  $\beta$ -hydrogens, through the high energy four-membered transition state with a relatively low, but finite possibility for a  $\beta$ -hydride elimination.

#### 3.2.2.2.5 Investigations into the Kinetic Inhibition of 16 Electron Complexes

We hypothesized that one possible reason for the slower oxidation reaction could be a coordinative inhibition of the catalysts (**78** and **79**) under oxidizing conditions through coordination of acetone or cyclohexanone solvent towards the Ru metal centre or amide/amine functionality of the catalyst (**Figure 3.24**). Coordination of acetone can in principle occur through an  $\eta^1$  or  $\eta^2$  coordination of the C=O function, both of which have been shown to occur at various metal centre,<sup>59,60</sup> or by enolization of the acetone and cooperative coordination of the resulting C=C double bond and hydroxyl function.

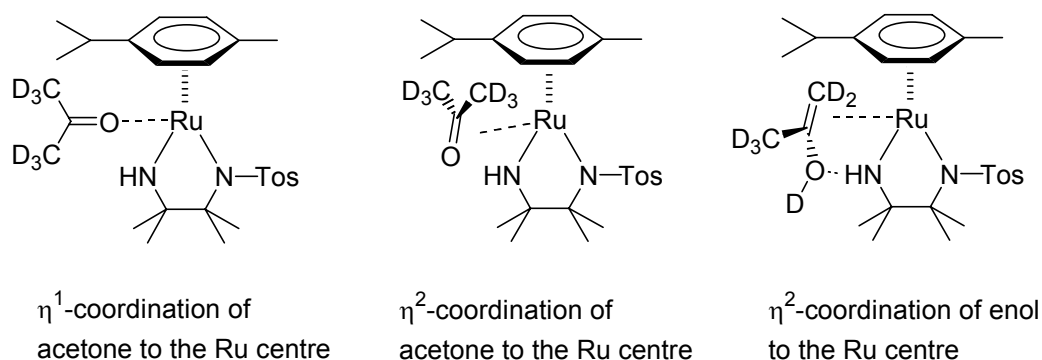


**Figure 3.24** Possible inhibition of the catalyst through acetone- $d^6$  coordination.

This hypothesis was investigated by NMR experiments. A 16-electron complex sample (**78**) was carefully prepared under Ar using degassed and anhydrous deuterated solvents. In acetone- $d^6$  scrambling of the amide proton (7.3 ppm) was observed at ambient temperature in less than 24 h. In benzene- $d^6$  and  $CD_2Cl_2$  solvent no scrambling was observed. All three solutions remained purple in a sealed NMR tube for over 2 months at ambient temperature and decomposition was not observed. In  $CDCl_3$  the complex decomposed to black precipitate after one week at room temperature. The scrambling of the amide proton can be explained through a rapid D/H exchange of acetone- $d^6$  with the amide through ketone-enol tautomerism of acetone in solution or through a possible  $\eta^2$  coordination of the acetone enol to the Ru and NH moiety as shown in **Figure 3.24**.

To further test this hypothesis, a low temperature  $^2H$  NMR experiment with **78** was carried out in acetone- $d^6$  solvent at 400 MHz aiming to observe any olefinic signals of the complexed enol form of acetone. The sample was cooled to  $-80^\circ C$  and was continuously shimmed observing the  $^2H$  solvent signal. The sample was allowed to thermally equilibrate at  $-80^\circ C$  for 15 min and the  $^2H$  spectrum was recorded however no olefinic  $^2H$  signals were observed in the 3 to 6 ppm range. This means that either there is no exchange of D/H with the amide function

through the postulated  $\eta^2$  coordination mechanism or it occurs so rapidly that even at  $-80^\circ\text{C}$  that the exchange of formed enol-Ru complex and surrounding acetone is still too fast to be observed on the time scale of the NMR experiment.

To test for coordination of the non-enolized form of a ketone solvent, a  $^{13}\text{C}$  NMR experiment were carried out with the same sample as well as cyclohexanone and complex **78**. For the second sample 30 mg of the 16-electron complex **78** was dissolved in 0.6 mL  $\text{CD}_2\text{Cl}_2$ , one equivalent and ten equivalents of cyclohexanone were added under careful exclusion of oxygen and the  $^{13}\text{C}$  NMR spectra recorded at room temperature. Even with lengthy recording times (4000 scans) no carbonyl resonances shifted from those of free cyclohexanone (211.5 ppm) could be observed in both experiments. It was reported that the  $^{13}\text{C}$  NMR resonance of a carbonyl carbon complexed to a metal centre occurred in the normal downfield range of carbonyl resonances for  $\eta^1$  coordination but the resonances for  $\eta^2$  coordinated carbonyl groups were observed in the upfield range of 45 to 110 ppm.<sup>60</sup>

In conclusion, all experimental NMR evidence suggests that the exchange of the NH-proton occurs very rapidly at room temperature and even  $-80^\circ\text{C}$ , i.e. it is too fast to be observed on the NMR time scale. In the  $^{13}\text{C}$  and low temperature  $^2\text{H}$  NMR experiment, no additional signals other than the free ketone were observed. We thus have no experimental NMR evidence for any kinetic inhibition of the 16-electron complex of **78** and **79** under oxidizing conditions.

In a corresponding IR experiment the  $\nu_{\text{C=O}}$  stretching frequency of acetone can be used as a sensitive probe for coordination of a acetone in a  $\eta^1$  or  $\eta^2$  fashion,<sup>59,60</sup> however  $\eta^1$  coordination of a ketone to a metal centre lowers the  $\nu_{\text{C=O}}$  usually less than  $100\text{ cm}^{-1}$ . In contrast, with  $\eta^2$  coordination of ketone to a metal centre the  $\nu_{\text{C=O}}$  is observed in the range of 1017 to  $1160\text{ cm}^{-1}$  due to the loss in bond order in carbon-oxygen bond.<sup>60</sup>

IR experiments with the 16-electron complex (**78**) were also conducted with the careful exclusion of oxygen. One to ten equivalents of acetone were added to a dichloromethane solution containing complex **78** in a CaF<sub>2</sub> cell with 0.2 mm optical path length. A shift of the  $\nu_{\text{C=O}}$  frequency was not observed when comparing the IR spectrum to acetone or complex **78** dichloromethane reference IR spectra.

In another IR experiment complex **78** (10 mg) was dissolved in neat acetone (0.5 mL) and the IR spectrum was recorded using a cell with a very small (15  $\mu\text{m}$ ) optical path length. Even with this very short optical path length, the intensity of the  $\nu_{\text{C=O}}$  stretching frequency was too strong so that the maximum bottomed out between 1707 and 1715  $\text{cm}^{-1}$ . However, a shifted signal in the 1600 to 1700  $\text{cm}^{-1}$  range or lower than 1600  $\text{cm}^{-1}$  was not observed.

We therefore conclude based on NMR and IR evidence that the Ru centre of **78** is inert towards coordination with the acetone solvent and that the observed lower catalytic activity of the tetramethyl Ru complex (**78**) in the oxidation reaction cannot be attributed to an inhibition of the 16-electron species by the surrounding ketone solvent.

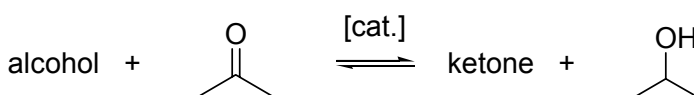
#### 3.2.2.2.6 Thermodynamic Discussion

In the absence of evidence for any coordinative inhibition of the catalysts under oxidizing conditions, our investigations focussed on a thermodynamical approach in order to explain the slower oxidation rates compared to the reduction rates as other factors must affect these reaction rates.

A kinetic approach to gaining further insights into the reaction parameters was not attempted on the basis of the following considerations: As illustrated in **Scheme 3.17**, there exist two distinct resting states of the catalysts system in solution, the 16-electron complex (**26**) and 18 electron complex (**24**). Effectively, there are therefore two different catalysts at different concentrations present in solution at any given time, the relative concentrations of which are a function of

redox potential of the participating alcohol/ketone pairs (both substrate and solvent). This constitutes a major challenge for developing any kinetic model and to our knowledge no complete kinetic model and rate law is available for the Noyori system.

In consequence we focussed on thermodynamic considerations only beginning with thermochemical calculations of the free reaction enthalpies of the isodesmic hydrogen transfer reactions. The energies of the participating alcohol and ketone substrate with acetone and *iso*-propanol were determined through Gaussian 03 calculations by density functional theory B3LYP the 6-31g(d) level in the gas phase at 298 K.<sup>61</sup> The values obtained are listed in **Table 3.5**. The standard free energy, i.e.  $\Delta G^\circ$ , was calculated for the generic reaction (**Scheme 3.23**) from the sum of the minimum energies of *iso*-propanol and ketone substrate subtracted by the sum of the minimum energies of acetone and alcohol substrate reactants. The equilibrium constants were calculated from  $\Delta G^\circ = -RT \ln K$  at 298 K. All energies are corrected for zero point energies and no imaginary frequencies were observed in any of the calculations.



**Scheme 3.23** Generic hydrogen-transfer reaction for calculation of  $\Delta G^\circ$ .

**Table 3.5** Results of DFT calculations of alcohol and ketone substrates with B3LYP/6-31g(d) level in gas phase at 298 K.

Entry	Alcohol	Energy [Hartree]	Ketone	Energy [Hartree]	$\Delta G^\circ$ [kJ mol <sup>-1</sup> ] <sup>a</sup>	Equilibrium constant $K^b$
<b>1</b>	iso-propanol	-194.270049	acetone	-193.099579	0	1
<b>2</b>	3-pentanol	-272.845606	3-pentanone	-271.67093	11.04	0.01
<b>3</b>	cyclopentanol	-271.650446	cyclopentanone	-270.480041	-0.17	1.07
<b>4</b>	cyclohexanol	-310.943474	cyclohexanone	-309.770014	7.85	0.04
<b>5</b>	1-phenyl-ethanol	-385.959161	acetophenone	-384.790127	-3.77	4.57
<b>6</b>	$\alpha$ -tetralol	-463.347962	$\alpha$ -tetralone	-462.183585	-15.99	634
<b>7</b>	$\beta$ -tetralol	-463.351359	$\beta$ -tetralone	-462.17749	8.92	0.02
<b>8</b>	<i>trans</i> -4- <i>tert</i> .-butyl- cyclohexanol	-468.088098	4- <i>tert</i> .-butyl- cyclohexanone	-466.913025	12.08	0.007
<b>9</b>	<i>cis</i> -4- <i>tert</i> .-butyl- cyclohexanol	-468.087456	4- <i>tert</i> .-butyl- cyclohexanone	-466.913025	10.39	0.01
<b>10</b>	<i>cis</i> -2-methyl- cyclohexanol	-350.232537	2-methyl- cyclohexanone	-349.059162	7.62	0.04
<b>11</b>	<i>trans</i> -2-methyl- cyclohexanol	-350.233855	2-methyl- cyclohexanone	-349.059162	11.08	0.011

(continued below)



Entry	Alcohol	Energy [Hartree]	Ketone	Energy [Hartree]	$\Delta G^\circ$ [kJ mol <sup>-1</sup> ]	Equilibrium constant K
<b>12</b>	1-buten-3-ol	-232.341623	1-buten-3-one	-231.173626	-6.49	13
<b>13</b>	cyclo-2-hexen-ol	-309.734163	cyclo-2-hexen-one	-308.568087	-11.53	104
<b>14</b>	3-methyl-cyclo-2-hexen-ol	-349.028352	3-methyl-cyclo-2-hexen-one	-347.863644	-15.12	446
<b>15</b>	cis-cyclohexane-1,2-diol	-386.154987	$\alpha$ -hydroxy cyclohexanone	-384.964225	53.27	$4 \times 10^{-10}$
<b>16</b>	trans-cyclohexane-1,2-diol	-386.1552	$\alpha$ -hydroxy cyclohexanone	-384.964225	53.83	$4 \times 10^{-10}$
<b>17</b>	$\alpha$ -hydroxy cyclohexanone	-384.964225	cyclohexan-1,2-dione	-383.787724	15.83	0.001

<sup>a</sup> Calculated from the metathesis reaction of alcohol + acetone  $\rightleftharpoons$  ketone + *iso*-propanol. <sup>b</sup> Calculated from  $\Delta G^\circ = -RT \ln K$  at 298 K.

In order to correlate the calculated  $\Delta G^\circ$  results from **Table 3.5** with the reaction actually carried out,  $\Delta G_{\text{reaction}}$  was calculated for the conditions using the equations shown in **Figure 3.25**. The initial concentration of alcohol substrate was 0.2 M and acetone solvent possesses a 13.6 M. Plots of  $\Delta G_{\text{reaction}}$  versus the concentration of produced ketone are shown in **Figure 3.26**.

$$\Delta G_{\text{reaction}} = \Delta G^\circ + RT \ln Q$$

$$Q = \frac{[\text{ketone}] [\text{isopropanol}]}{[\text{alcohol}] [\text{acetone}]} = \frac{x^2}{[0.2-x] [13.6-x]}$$

$$[\text{ketone}]_{\text{produced}} = [\text{isopropanol}]_{\text{produced}} =: x$$

$$[\text{alcohol}]_{\text{initial}} = 0.2 \text{ M}$$

$$[\text{acetone}]_{\text{initial}} = 13.6 \text{ M}$$

$$T = 298 \text{ K}$$

**Figure 3.25** Mathematical calculation of  $\Delta G_{\text{reaction}}$  in systems investigated.

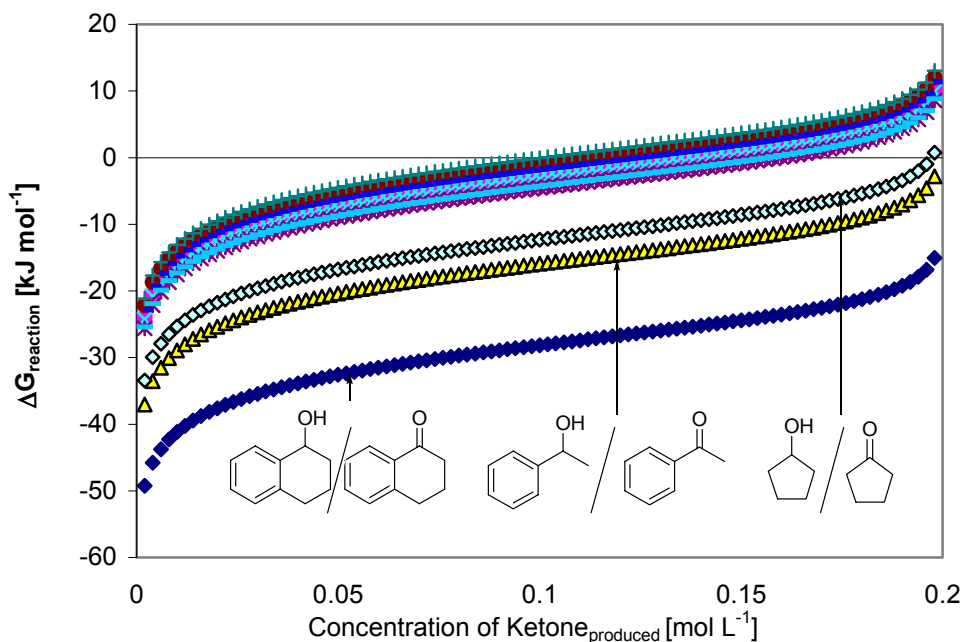


**Figure 3.26**  $\Delta G_{\text{reaction}}$  calculated from DFT calculations as a function of produced ketone in acetone solvent from the corresponding alcohols.

The  $\Delta G_{\text{reaction}}$  values for the majority of the alcohol and ketone substrate pairs pass through and cluster around the zero-line, i.e. are essentially thermoneutral. However the values for the  $\alpha$ -tetralol/ $\alpha$ -tetralone, 1-phenyl-ethanol/acetophenone and cyclopentanol/cyclopentanone pairs are distinctively more negative suggesting that the equilibrium constitutes a quantitative oxidation of the alcohol to the corresponding ketone. These results are in principle congruent with the experimental values shown in **Figure 3.22**, however the equilibrium had not been reached after 14 d.

The results of the DFT calculations of  $\Delta G_{\text{reaction}}$  for the reaction involving the reduction of ketones (0.2 M) in 5.0 mL *iso*-propanol (13.1 M) are displayed in **Figure 3.27** and also show a good correlation to the experimental data (**Figure 3.23**). The reduction of  $\alpha$ -tetralone is thermodynamically unfavoured and only a marginal  $\alpha$ -tetralol content can be obtained at the equilibrium. However, while the reduction of cyclopentanone and acetophenone are not as favoured as the other calculated ketone substrate, the plots suggest that eventually a quantitative conversion can be obtained at equilibrium.

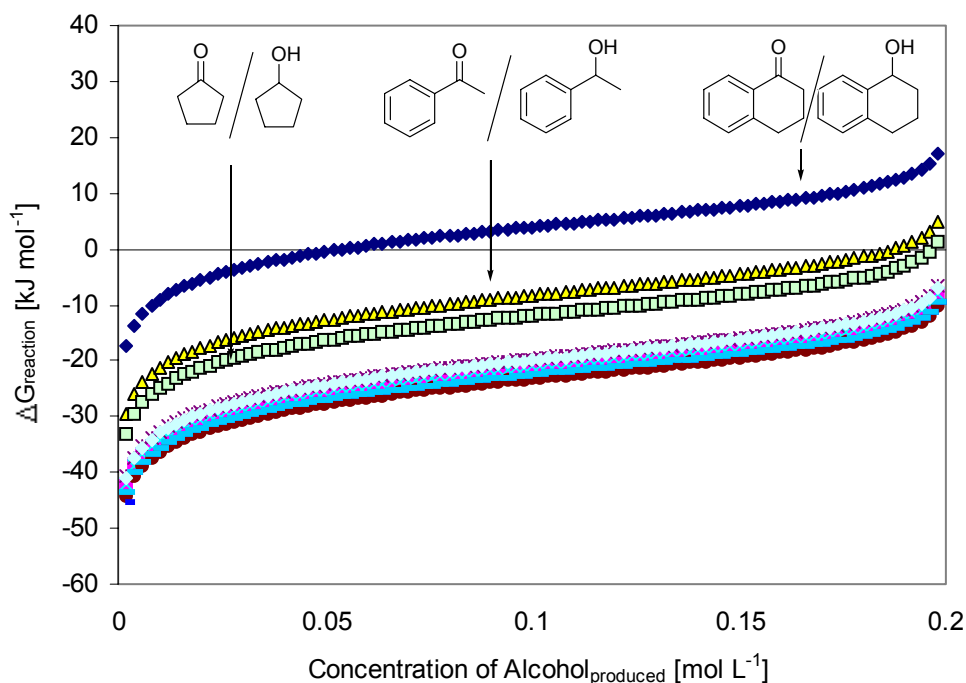


**Figure 3.27**  $\Delta G_{\text{reaction}}$  calculated from DFT calculations as a function of produced alcohol in *iso*-propanol solvent from the corresponding ketone.

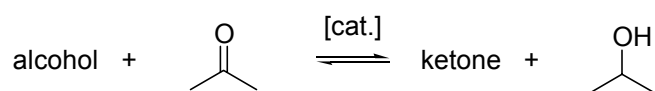
The DFT calculations have been conducted on 6-31/g(d) level in the gas phase and a finite error must be attributed to the calculated values. In solution hydrogen bonding does occur especially in *iso*-propanol solvent which further affects the minimum energies and will influence the  $\Delta G_{\text{reaction}}$  values. However since the calculation of the  $\Delta G_{\text{reaction}}$  values involves taking the differences of the absolute  $\Delta G$  values for an isodesmic reaction, it is reasonable to assume that the errors cancel out at least partially and therefore only marginally affect the relative results.

From the experimental data (**Table 3.4** and **Table 3.5**) it is apparent that the reactions possessing a very negative  $\Delta G^\circ$  value in either oxidation or reduction direction were faster than those with lower  $\Delta G^\circ$  values. This observation suggests a relationship similar to the Hammond postulate, i.e. for the hydrogen transfer reaction under investigation,  $\Delta G^\ddagger$  is correlated to  $\Delta G^\circ$ .<sup>13</sup>

With our observation that the resting state of the catalyst is dependent on the redox environment of the reaction partners involving solvents and alcohol and ketone substrate the actual rate of reaction is then a superposition of the oxidation and reduction parameters for each of the two catalytically active species, i.e. one would expect substantially different rates for the forward and reverse reaction. As mentioned previously we refrained from trying to develop a full kinetic model for the Noyori system, as it would require the knowledge of the actual relative concentrations of the two active catalysts species, which experimentally is difficult to realize. Instead we limited our kinetic data analysis to determining the initial rates for the reaction, for which in a first approximation the reactant concentrations are known. Within this ultimately thermodynamic approach to the problem, there is fortunately one single situation where there is no need in knowing the actual kinetic law of the reaction in order to determine a correlation between  $\Delta G^\circ$  and initial rates. This situation arises, when both the oxidized and reduced substrate as well as the oxidizing and reducing solvent are

present in equal concentrations.<sup>†††</sup> At time = 0 this is a condition easily realized experimentally. As expressed by the equations in **Figure 3.28**,  $\Delta G_{\text{reaction}}$  equals  $\Delta G^\circ$  at  $t_{\text{initial}} = 0$ , when the concentration of ketone and alcohol substrate as well the concentrations of acetone and *iso*-propanol solvent are set to be equal. Through cancellation of the respective concentration values  $Q$  is 1 and hence  $\ln Q$  is zero. The combined ketone and alcohol concentration was set to 0.2 M with 0.010 mmol ruthenium catalyst in order to be able to compare results with the experimental and calculated data for the oxidation or reduction reactions. Another advantage of the equal concentration experiment is the direct experimental determination of  $\Delta G^\circ$  from the substrate and reactant concentration (by quantitative GC analysis) once the equilibrium has been established. The error margin for this determination is low as neither the nominator nor the denominator of the equilibrium constant equation  $K$  is close to zero.

**Equation:**



$$\Delta G_{\text{reaction}} = \Delta G^\circ + RT \ln Q$$

$$Q = \frac{[\text{ketone}] [\text{isopropanol}]}{[\text{alcohol}] [\text{acetone}]} = 1 \quad \begin{array}{l} [\text{ketone}]_{\text{initial}} = [\text{alcohol}]_{\text{initial}} = 0.1 \text{ M} \\ [\text{isopropanol}]_{\text{initial}} = [\text{acetone}]_{\text{initial}} = 7.4 \text{ M} \end{array}$$

$$\Rightarrow \ln Q = 0$$

$$\Rightarrow \boxed{\Delta G_{\text{reaction}} = \Delta G^\circ}$$

**Figure 3.28** Mathematical derivation of  $\Delta G_{\text{reaction}}$  under equal concentration experiment.

For the special situation of equal initial concentrations of all redox substrate pairs, it can also be assumed that the rate law for the forward reaction (**Eq. 9**) and the rate law of the backward reaction (**Eq. 10**) are only a function of the

<sup>†††</sup> By using equal concentration for all reactants including solvents, the reaction is said to set-up “in the middle”. Thus pending on its  $\Delta G^\circ$  value the reaction itself “determines” if it “wants” to proceed into an oxidizing or reducing direction.

concentrations of ketone and alcohol and catalyst in its hydrogen loaded for and unloaded form, respectively.

**Eq. 9**  $r_{\text{forward}}(t = 0) = k_{\text{forward}} \times [\text{ketone}]_{\text{initial}} \times [\text{cat-H}_2]$

**Eq. 10**  $r_{\text{reverse}}(t = 0) = k_{\text{reverse}} \times [\text{alcohol}]_{\text{initial}} \times [\text{cat}]$

In this situation, the free energy of the hydrogen transfer reaction of a given alcohol/ketone substrate pair can therefore be visualized experimentally.

The overall direction of the hydrogen transfer reaction can easily be determined by quantitative GC measurements of the alcohol/ ketone substrate concentration (**Figure 3.29**). The standard free energy,  $\Delta G^\circ$  can be determined experimentally through calculation of the equilibrium constant  $K$  when the hydrogen transfer reaction has reached its equilibrium stage, i.e. the concentrations of the reactant do no longer change with time. For cyclohexanol the equilibrium concentration was 0.171 M and 0.029 M for cyclohexanone. The acetone concentration at equilibrium was thus 6.40 M + 0.071 M = 6.47 M and 6.40 M – 0.071 M = 6.33 M for *iso*-propanol. The equilibrium constant  $K$  was 0.166 resulting in an experimental  $\Delta G^\circ$  value of 4.4 kJ mol<sup>-1</sup> using  $\Delta G^\circ = -RT \ln K$  equation at 298 K.

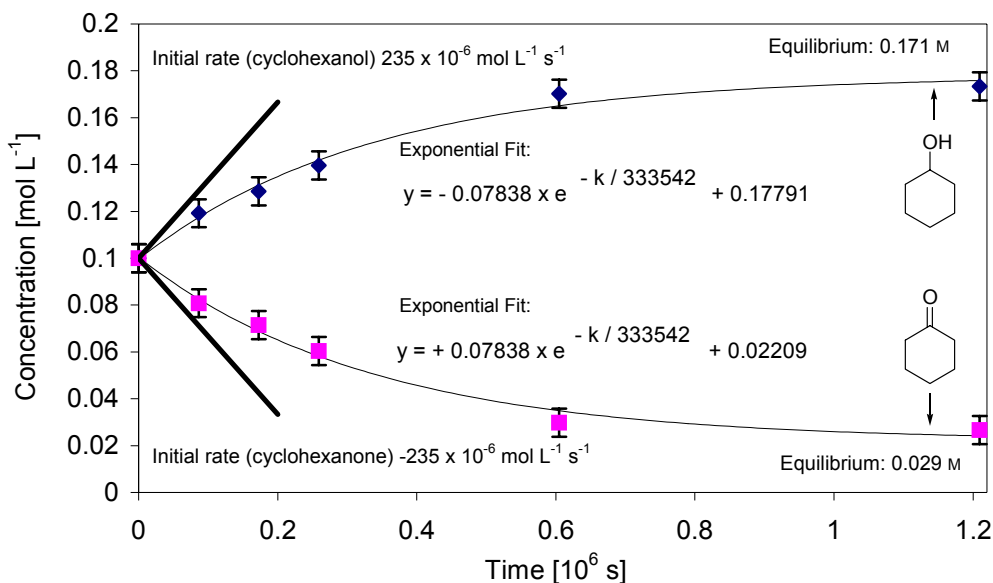


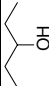
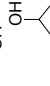
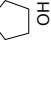
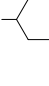
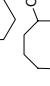
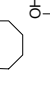
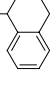
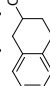
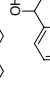
**Figure 3.29** Determination of initial rates and equilibrium concentrations of alcohol and substrate from concentration vs. time graphs.

The GC data were carefully evaluated if equilibrium had been reached because a degradation of the catalyst could prevent reaching the equilibrium stage. In cases when the concentrations of the reactants and products were still changing the final concentrations were determined by fitting the GC data to an 1<sup>st</sup> order exponential approximation which gave results of high numerical confidence level, i.e.  $R^2$  between 0.92 and 0.97.

A variety of aliphatic and aromatic, cyclic and acyclic, allylic and benzylic alcohol and ketone substrate pairs were investigated by this method. The standard equal concentration experiment used 0.50 mmol alcohol substrate, 0.50 mmol corresponding ketone substrate, 32 mmol acetone (2.5 mL), 32 mmol *iso*-propanol (2.6 mL), *cis*-decalin (~50 mg) and 0.010 mmol ruthenium complex **78** at RT under Ar atmosphere. The numerical results obtained from this study are shown in **Table 3.6**.

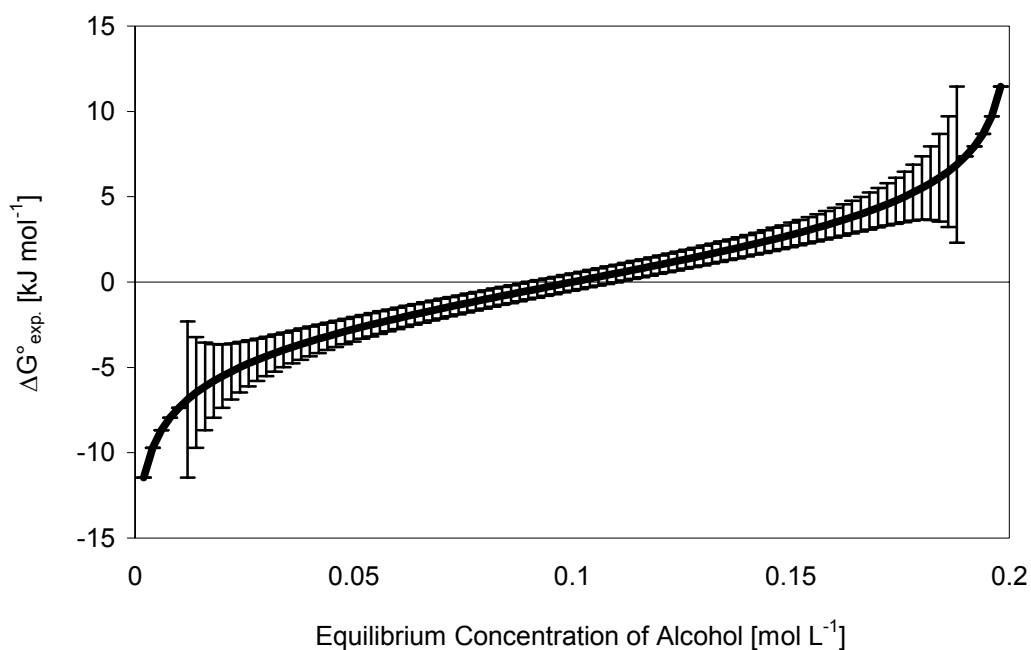
In order to estimate the error margin of the calculated  $\Delta G^\circ_{\text{exp}}$  the maximum error in the quantitative GC was allowed to be 5 %.  $\Delta G^\circ_{\text{exp}}(\text{error})$  was then calculated based on a worst case scenario in which both nominator concentrations were set to be 5 % too high and the denominator concentrations were set to be 5 % too low. The difference of 5 % error based  $\Delta G^\circ_{\text{exp}}(\text{error})$  and  $\Delta G^\circ_{\text{exp}}$  was determined as error margin and was purposefully set relatively high in order to have a very conservative and trustable result. At extreme low or high concentration, the error increases dramatically, which is an effect of a mathematical singularity. The distribution of error margin as a function of equilibrium concentration of alcohol is shown in **Figure 3.30**.

**Table 3.6** Results of equal concentration experiments with ruthenium catalysts **78** and **79**.<sup>a</sup>

Alcohol/Ketone	Tetramethyl catalyst (78)				Diphenyl catalyst (79)			
	$c_{T=\infty}$ alcohol [mol L <sup>-1</sup> ] <sup>e</sup>	$c_{T=\infty}$ ketone [mol L <sup>-1</sup> ] <sup>e</sup>	$\Delta G^{\circ}_{\text{exp}}$ ± 5% Error in $\Delta G^{\circ}_{\text{exp}}$ [kJ mol <sup>-1</sup> ] <sup>d</sup>	$\Delta G^{\circ}_{\text{exp}}$ ± 5% Error in $\Delta G^{\circ}_{\text{exp}}$ [kJ mol <sup>-1</sup> ] <sup>d</sup>	$c_{T=\infty}$ alcohol [mol L <sup>-1</sup> ] <sup>e</sup>	$c_{T=\infty}$ ketone [mol L <sup>-1</sup> ] <sup>e</sup>	$\Delta G^{\circ}_{\text{exp}}$ ± 5% Error in $\Delta G^{\circ}_{\text{exp}}$ [kJ mol <sup>-1</sup> ] <sup>d</sup>	$\Delta G^{\circ}_{\text{exp}}$ ± 5% Error in $\Delta G^{\circ}_{\text{exp}}$ [kJ mol <sup>-1</sup> ] <sup>d</sup>
	0.099	0.101	-0.03 ± 0.50		0.093	0.107	-0.35 ± 0.51	
	0.123	0.077	1.18 ± 0.52		0.121	0.079	1.05 ± 0.52	
	0.171	0.029	4.45 ± 0.87		0.173	0.027	4.66 ± 0.91	
	0.080	0.120	-1.01 ± 0.54		0.089	0.111	-0.56 ± 0.51	
	0.003	0.197	-10.32 ± 4.58		0.042 <sup>c</sup>	0.958 <sup>c</sup>	-3.33 ± 0.83	
	0.153	0.047	2.96 ± 0.65		0.119	0.0881	0.97 ± 0.52	
	0.068	0.132	-1.69 ± 0.59		0.096	0.104	-0.20 ± 0.50	
	0.002 <sup>b</sup>	0.198	-11.46 ± 4.58		0.066 <sup>c</sup>	0.134 <sup>c</sup>	-1.78 ± 0.59	
	0.002 <sup>b</sup>	0.198	-11.46 ± 4.58		0.018 <sup>c</sup>	0.182 <sup>c</sup>	-5.72 ± 1.86	

<sup>a</sup> Equal concentration experiment with 0.50 mmol alcohol, 0.50 mmol ketone, 32 mmol acetone (2.3 mL), 32 mmol *iso*-propanol (2.4 mL), *cis*-decalin (~50 mg) and 0.010 mmol **78** or **79** at room temperature under Ar atmosphere. <sup>b</sup> Quantitative conversion, minimum concentration set to GC detection limit (0.002 M). <sup>c</sup> Catalyst decomposition observed after 7 d. <sup>d</sup> For error calculation see **Figure 3.30**. <sup>e</sup>  $c_{T=\infty}$  concentration at equilibrium.



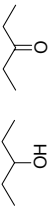
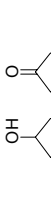
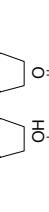
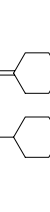
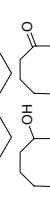
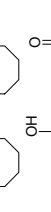
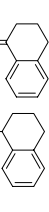
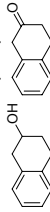
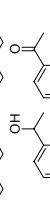
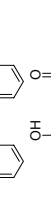


**Figure 3.30** Calculation of  $\Delta G^\circ_{\text{exp}}$  with error margin based on cumulative 5 % error in GC.

The initial rates obtained from the equal concentration experiments are listed in **Table 3.7** and are based on the observed production or consumption of alcohol substrate, i.e. under overall reducing condition ketone substrate reacts to the corresponding alcohol substrate. Thus the initial rate is  $> 0$ . A negative initial rate in alcohol substrate indicates that the overall reaction favours the consumption of alcohol, i.e. oxidation of the alcohol substrate occurs.

To evaluate the reliability of the initial rate constant, the standard deviation of the 1<sup>st</sup> order exponential fit of alcohol contents were used to calculate the error margins of the initial rates with a very conservative confidence interval.

**Table 3.7** Initial rates and  $\Delta G^\circ_{\text{exp}}$  of equal concentration reactions with ruthenium catalysts **78** and **79**.

Entry	Alcohol/Ketone	Tetramethyl catalyst (78)			Entry	Diphenyl catalyst (79)		
		$\pm 5\% \Delta G^\circ_{\text{exp}} [\text{kJ mol}^{-1}]^b$	$\Delta G^\circ_{\text{exp}} [\text{kJ mol}^{-1}]^b$	Initial rate $[10^{-9} \text{ mol L}^{-1} \text{ s}^{-1}]^c$		$\pm 5\% \Delta G^\circ_{\text{exp}} [\text{kJ mol}^{-1}]^b$	$\Delta G^\circ_{\text{exp}} [\text{kJ mol}^{-1}]^b$	Initial rate $[10^{-9} \text{ mol L}^{-1} \text{ s}^{-1}]^c$
<b>1</b>		$-0.03 \pm 0.50$		$-1.3 \pm 0.5$	<b>11</b>	$-0.35 \pm 0.51$		$-4.6 \pm 12$
<b>2</b>		$1.18 \pm 0.52$		$76 \pm 10$	<b>12</b>	$1.05 \pm 0.52$		$229 \pm 22$
<b>3</b>		$4.45 \pm 0.87$		$127 \pm 14$	<b>13</b>	$4.66 \pm 0.91$		$235 \pm 35$
<b>4</b>		$-1.01 \pm 0.54$		$-37 \pm 10$	<b>14</b>	$-0.56 \pm 0.51$		$-46 \pm 11$
<b>5</b>		$-10.32 \pm 4.58$		$-223 \pm 16$	<b>15</b>	$-3.33 \pm 0.83$		$-257 \pm 40$
<b>6</b>		$2.96 \pm 0.65$		$158 \pm 27$	<b>16</b>	$0.97 \pm 0.52$		$103^d \pm 30$
<b>7</b>		$-1.69 \pm 0.59$		$-24 \pm 10$	<b>17</b>	$-0.20 \pm 0.50$		$-2.6 \pm 6.0$
<b>8</b>		$-11.46 \pm 4.58$		$-281 \pm 14$	<b>18</b>	$-1.78 \pm 0.59^e$		$-150 \pm 10$
<b>9</b>		$-10.80 \pm 4.57$		$-153 \pm 48$	<b>19</b>	$-1.13 \pm 0.54^e$		$-6.9 \pm 5$
<b>10</b>		$-11.46 \pm 4.58$		$-332 \pm 20$	<b>20</b>	$-5.72 \pm 1.86$		$-476 \pm 10$

<sup>a</sup> Equal concentration experiment with 0.50 mmol alcohol, 0.50 mmol ketone, 32 mmol acetone (2.3 mL), 32 mmol *iso*-propanol (2.4 mL), *cis*-decalin (~50 mg) and 0.010 mmol **78** or **79** at room temperature under Ar atmosphere. <sup>b</sup> For error calculation see **Figure 3.30** <sup>c</sup> Error determined from 1<sup>st</sup> order exponential approximation. <sup>d</sup> Approximated by first two data points. <sup>e</sup> Catalyst decomposition after 7 d.

The initial rates were plotted against the experimental  $\Delta G^\circ$  value in order to visualize a potential linear relationship as shown in **Figure 3.31**. A linear regression was calculated for both ruthenium catalysts (**23** and **24**) possessing a correlation factor,  $R^2$ , of 0.92 and 0.89 respectively.

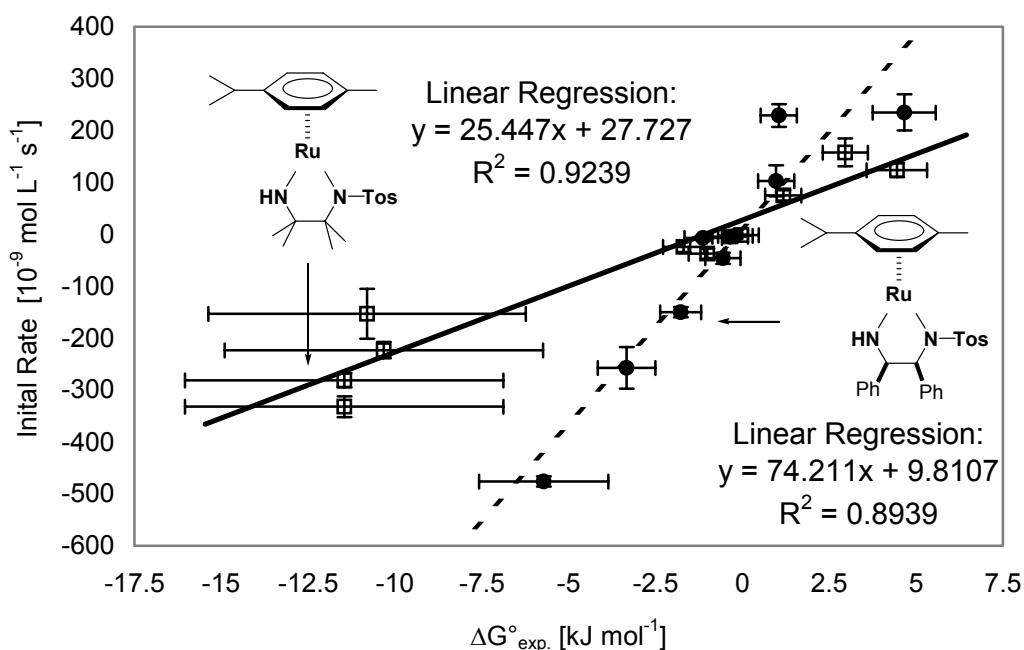


**Figure 3.31** Graph of initial rate versus  $\Delta G^\circ_{\text{exp}}$  of equal concentration experiment with ruthenium catalysts **78** and **79**.

The graphs in **Figure 3.31** suggest a trend between the initial rates and  $\Delta G^\circ$  values, however no clear mathematically well defined linear relationship between the rate constants (**Table 3.4**) or the natural logarithm with the  $\Delta G^\circ$  values was found and in the absence of a kinetic model a further quantitative interpretation or prediction of any relationship is very difficult.

In order to at least qualitatively detect the relative concentration of **78** in its 16-electron or 18-electron hydrogen loaded form, a simple experiment was carried out inside a glove-box under Ar atmosphere. Three solutions of **78** (5.0

mg) were prepared using (A) 5.0 mL acetone, (B) 5.0 mL *iso*-propanol and (C) a mixture of *iso*-propanol (2.5 mL) and acetone (2.5 mL).

The acetone solution (A) was deep blue-purple coloured. The *iso*-propanol solution (B) was orange-yellow coloured after approximately 15 min at room temperature and the 1:1 acetone : *iso*-propanol mixture (C) was dark red-purple coloured.

After addition of *iso*-propanol (1.0 mL) to (A) the colour changed slightly to a reddish-purple similar to the solution (C). A similar colour resulted in addition of acetone (1.0 mL) to (B). After addition of 15 mL of *iso*-propanol i.e. a 1:20 mixture acetone: *iso*-propanol, the colour intensity reduces due to concentration effect but there is no change back to a yellow colour. Addition of 15 mL acetone to (A) produced a deep purple solution with a taint of red.

We therefore concluded that the 16-electron complex is the predominant species in any *iso*-propanol/ acetone solvent mixture.

### 3.2.2.3 Conclusions

Noyori's  $\eta^6$ -arene *N*-tosyl 1,2-diaminoethane based ruthenium(II) complexes can be used not only in the oxidation of allylic and benzylic alcohols but also in the oxidation of aliphatic and cyclic secondary alcohols in acetone solvent under mild conditions albeit with low yields. The 16-electron amide complex is the resting state under oxidizing condition and the 18-electron hydride complex under reducing condition. A coordinative inhibition of the Ru or NH moiety of acetone solvent in an  $\eta^1$ -or  $\eta^2$ -fashion does not exist based on NMR and IR experiment evidence and is not the cause for the lower reactivity under oxidizing condition.

In an equal concentration experiment the initial rates of the alcohol consumption or alcohol production gives an approximately linear relationship with the  $\Delta G^\circ$  of

the participating alcohol/ketone pair. The slope of this relationship is dependent of the catalyst employed. A likely explanation for the lower activity of the catalysts under oxidizing conditions compared to reducing condition is that there is a relatively high barrier of activation associated with the rearrangement of the 16-electron complex to a conformation required for hydrogen transfer and formation of the 18-electron hydride complex. Under oxidizing conditions, i.e. in excess ketone solvent, this formation of the 18-electron hydride complex becomes the rate determining step, while under reducing conditions, i.e. in excess alcohol solvent, the rate determining step occurs between the ketone substrate and the hydrogen loaded complex. Thus even though the overall reaction is a genuine equilibrium, the presence of two distinct active catalysts for the forward and reverse reactions gives rise to distinct reaction pathways with different activation barriers explaining the marked differences in reactivity in oxidation vs. reduction hydrogen transfer reactions. This difference in reactivity as well as an apparent inverse correlation between the initial rates of oxidation with the  $\Delta G_{\text{reaction}}$  for hydrogen transfer reactions under oxidizing conditions, renders the Noyori type system unsuitable for the catalytic synthesis of  $\alpha$ -hydroxy-ketones from *vicinal* diols.

#### 3.2.2.4 Experimental Section

NMR spectra (400 MHz/ $^1\text{H}$ ; 100 MHz/ $^{13}\text{C}$ ) were measured in DMSO- $\text{d}_6$  with DMSO ( $\delta$  2.49,  $^1\text{H}$ ;  $\delta$  39.5,  $^{13}\text{C}$ ) and deuterated chloroform ( $\delta$  7.24,  $^1\text{H}$ ;  $\delta$  77.0,  $^{13}\text{C}$ ) as the internal reference. DMSO was stored inside a dry-box under argon atmosphere over 4 Å activated molecular sieves. For variable temperature measurements the spectrometer temperature controller unit was calibrated using a bimetal thermometer directly inserted into the probe. DFT calculations were carried on a PC using the Gaussian 98 and Gaussian 03 suite of programs. GC analyses were performed on a 30 m  $\times$  0.25 mm PEG column. The GC FID was calibrated for alcohol and ketone substrates with *cis*-decalin as an internal standard. GC MS experiments were performed on a Varian 3800, Saturn 2000 a

30 m  $\times$  0.25 mm PEG column with 70 V electron impact ionization or acetonitrile chemical ionization technique. IR spectra were recorded with a Bomen FT-IR using a 1.0 mm and 2.0 mm CaF<sub>2</sub> liquid cell or a 15  $\mu$ m cell containing a Teflon® washer (15  $\mu$ m) between two BaF<sub>2</sub> cell windows. The IR cells were filled with the oxygen sensitive 16-electron complexes inside glove box and carefully sealed from air atmosphere. Electron impact (EI) mass spectrometry was conducted on a JEOL HX110 double focussing mass spectrometer ionizing at 70 eV with source temperature at 200°C. Electrospray ionization (ESI) mass spectrometry was conducted on a micromass QTOF Global Mass spectrometer in a positive ionization mode (3.5 kV spray voltage) at atmospheric pressure in acetonitrile. All experimental preparations were conducted in a dry-box under argon atmosphere and/or with usual Schlenk technique on a vacuum line. Acetone, *iso*-propanol and CH<sub>2</sub>Cl<sub>2</sub> were dried by distillation under argon from anhydrous CaCl<sub>2</sub>, anhydrous K<sub>2</sub>CO<sub>3</sub> containing LiAlH<sub>4</sub> and K<sub>2</sub>CO<sub>3</sub>, respectively, degassed and stored under argon. Alcohol and ketone substrates, *cis*-decalin and common solvents were purchased from commercial sources. All chemicals were reagent grade and used after degassing through repetitive freeze-dry technique.

***N*-(*p*-tolyl-sulfonyl)-1,2-diaminoethane.**<sup>62</sup> *p*-toluylsulfonyl chloride (19.1 g, 0.10 mol) in 75 mL benzene was added dropwise to a solution of 1,2-diamino-ethane (20.0 mL, 0.30 mol) in 40 mL benzene and was stirred vigorously for 3 h. A white precipitate appeared and was filtered and treated with 1 M hydrochloric acid (~ 50 mL). The remaining solid was filtered and filtrate made strongly basic with addition of NaOH (~10 g). A white crystalline solid appeared, was filtered and washed with 10 mL cold water. Yield 18.3 % (12.4 g, 54 mmol). C<sub>9</sub>H<sub>16</sub>N<sub>2</sub>O<sub>2</sub>S, MM = 226 g mol<sup>-1</sup>. <sup>1</sup>H-NMR (CDCl<sub>3</sub>; 7.24 ppm)  $\delta$  7.71 (d, *J* = 8.4 Hz, 2 ), 7.26 (d, *J* = 8.4 Hz, 2H), 2.92 (t, *J* = 5.2 Hz, 2H), 2.82 (s, br, 3H), 2.75 (t, *J* = 5.2 Hz, 2H), 2.38 (s, 3H). <sup>13</sup>C NMR (CDCl<sub>3</sub>; 77.0 ppm)  $\delta$  143.3, 136.9, 129.7, 127.0, 45.2, 40.8, 21.4. IR (KBr, cm<sup>-1</sup>)  $\nu$  3361, 3298, 1594, 1498, 1401, 1360, 1313, 1300, 1200, 1150, 1106, 1055, 1016, 943, 874, 818, 774, 708, 658, 572, 553, 537.

***N*-(*p*-toluyl-sulfonyl)-*ortho*-diaminobenzene (71).**<sup>56</sup> In a 250 mL round bottle flask, *o*-phenylene-diamine (10.8 g, 100 mmol) was dissolved in 45 mL pyridine. To this reaction mixture *p*-toluyl-sulfonyl chloride (17.7 g, 93 mmol) in 10 mL pyridine was added dropwise. After stirring at room temperature for 30 min, the reaction was quenched carefully with 2 M HCl (~50 mL) and afforded an oily red residue, which turned to an orange solution after treatment of the reaction mixture in ultrasound bath. The aqueous layer was extracted with 3 x 50 mL dichloromethane. The combined organic layers were dried over anhydrous NaHCO<sub>3</sub> and the solvent was evaporated under reduced pressure. The orange oil was dissolved in warm ethanol (40 mL), producing a off-white solid upon cooling, which was isolated by filtration and dried *in vacuo*. Yield 17 % (4.12 g, 15.8 mmol). C<sub>13</sub>H<sub>14</sub>N<sub>2</sub>O<sub>2</sub>S, MM = 262 g mol<sup>-1</sup>. <sup>1</sup>H-NMR (CDCl<sub>3</sub>) δ 7.62 (d, *J* = 8.4 Hz, 2H), 7.25 (d, *J* = 8.4 Hz, 2H), 7.06 (t, *J* = 7.4 Hz, 1H), 6.73 (d, *J* = 7.4 Hz, 1H), 6.51 (m, 1H), 6.22 (s, br, 1H), 4.08 (s, br, 2H), 2.42 (s, 3H). <sup>13</sup>C NMR (CDCl<sub>3</sub>) δ 144.5, 143.9, 135.9, 129.6, 128.9, 128.6, 127.5, 121.0, 118.5, 117.1, 25.4. IR (KBr, cm<sup>-1</sup>) ν 3481, 3385, 3209, 2800, 1916, 1623, 1597, 1497, 1463, 1408, 1322, 1290, 1265, 1150, 1092, 1030, 946, 917, 813, 753, 726, 676, 548.

**1,2-dinitro-1,1,2,2-tetramethylethane (74).**<sup>57</sup> In a 250 mL round bottle flask with ice-bath cooling, 2-nitropropane (45 mL, 0.50 mol) was dissolved in 6 M sodium hydroxide solution (85 mL). Bromine (12.5 mL, 0.25 mol) in ethanol (165 mL) was added dropwise to the cold reaction mixture. The resulting yellow solution was heated to reflux for 3 h. Upon cooling with an ice-bath, the product precipitated as a white solid, was filtered and dried *in vacuo*. White solid 97 % yield (42.7 g, 0.24 mol). C<sub>6</sub>H<sub>12</sub>N<sub>2</sub>O<sub>4</sub>, MM = 176 g mol<sup>-1</sup>. <sup>1</sup>H-NMR (CDCl<sub>3</sub>) δ 1.66 (s, 12H). <sup>13</sup>C NMR (CDCl<sub>3</sub>) δ 93.1, 15.7.

**1,2-diamino-1,1,2,2-tetramethylethane (75).**<sup>57</sup> In a 250 mL round bottle flask equipped with reflux condenser solid 1,2-dinitro-1,1,2,2-tetramethylethane (17.6 g, 0.10 mol) was added to a vigorously stirred conc. HCl solution (150 mL) at 60°C. Through a powder funnel granular tin (75 g, 0.64 mol) was added slowly

and the reaction mixture was refluxed for 20 min. Upon cooling to 0°C, NaOH (~75 g) was added portion wisely to the cold reaction mixture. The colour of the solution turned grayish-black. Steam distillation of the reaction mixture afforded approximately 500 mL of aqueous solution. The aqueous layer was extracted with 3 x 50 mL diethyl ether. The combined organic layers were dried over anhydrous MgSO<sub>4</sub>, filtered and the organic solvent was evaporated under reduced pressure. The resulting 2,3-dimethyl-2,3-diamine is a white, crystalline powder 82 % yield (9.5 g, 0.082 mol). C<sub>6</sub>H<sub>16</sub>N<sub>2</sub>, MM = 116 g mol<sup>-1</sup>. <sup>1</sup>H-NMR (CDCl<sub>3</sub>) δ 1.15 (s, 12H). <sup>13</sup>C NMR (CDCl<sub>3</sub>) δ 66.5, 23.3.

***N*-(*p*-toluyl-sulfonyl)-1,2-diamino-1,1,2,2-tetramethylethane (72).** In a 250 mL round bottle flask and ice cooling, 1,2-diamino-1,1,2,2-tetramethylethane (9.5 g, 82 mmol) was dissolved in benzene (25 mL) and a solution of *p*-toluyl-sulfonyl chloride (5.2 g, 27 mmol) dissolved in 50 mL benzene was added drop-wise. After addition, the reaction mixture was kept at 40 °C for 3 h, then increased to refluxing temperature for 30 min. After cooling to ambient temperature, white solids precipitated, which were filtered and dried *in vacuo* yielding 8.2 g of crude product. The product was dissolved in 1 M HCl (50 mL), filtered through celite and the remaining clear solution was cooled to 0°C and 6 M NaOH (50 mL) was added carefully. The white precipitate was filtered and dried *in vacuo*. 85 % yield (6.2 g, 23 mmol). C<sub>13</sub>H<sub>22</sub>N<sub>2</sub>O<sub>2</sub>S, MM = 270 g mol<sup>-1</sup>. <sup>1</sup>H-NMR (DMSO-d<sub>6</sub>; 2.49 ppm) δ 7.56 (d; *J* = 8.0 Hz; 2H), 7.11 (d; *J* = 8.0 Hz; 2H), 2.28 (s, br, 3H), 0.93 (s, 6H), 0.90 (s, 6H). <sup>13</sup>C NMR (DMSO-d<sub>6</sub>; 39.5 ppm) δ 142.1, 138.0, 128.2, 126.1, 59.7, 55.7, 25.9, 23.6, 20.8. IR (KBr, cm<sup>-1</sup>) ν 3383, 3246, 2979, 2427, 1910, 1598, 1579, 1457, 1387, 1362, 1299, 1218, 1180, 1151, 1107, 1048, 1015, 915, 810, 777, 687, 651, 557.

***meso*-1,2-diphenyl-1,2-diaminoethane (76).**<sup>62</sup> In a 250 mL round bottle flask with reflux condenser, ammonium acetate (70 g, 91 mmol) was added to freshly distilled benzaldehyde (40 mL, 46 mmol). The reaction mixture was kept at reflux temperature for 2 h. The clear solution turned yellow. After cooling to ambient



temperature, a white solid precipitated and was filtered, washed with ethanol (100 mL), and dried *in vacuo*. To a 500 mL round bottle flask containing 350 mL of 10 % sulfuric acid the white solid was added and the reaction mixture was kept at refluxing temperature for 1 h. The reaction mixture was allowed to cool to ambient temperature and produced white crystal needles. The cold reaction mixture was made strongly basic ( $\text{pH} > 13$ ) upon careful addition of solid NaOH (~ 10 g). The aqueous layer was extracted with 3 x 75 mL dichloromethane. The combined organic layers were dried over anhydrous  $\text{Na}_2\text{SO}_4$ , filtered and the organic solvent was evaporated under reduced pressure. The light green precipitate was recrystallized in hot MeOH (10 mL). White crystalline solid, 50 % yield (4.8 g, 23 mmol).  $\text{C}_{14}\text{H}_{16}\text{N}_2$ , MM = 212 g mol<sup>-1</sup>.  $^1\text{H}$ -NMR ( $\text{CDCl}_3$ ; 7.24 ppm)  $\delta$  7.35 (m, 10H), 4.02 (s, 2H), 1.30 (s, br, 3H).  $^{13}\text{C}$  NMR ( $\text{CDCl}_3$ ; 77.0 ppm)  $\delta$  142.9, 128.8, 128.3, 128.2, 127.6, 62.8. IR (KBr, cm<sup>-1</sup>)  $\nu$  3346, 3276, 3081, 3028, 2907, 2874, 1960, 1592, 1492, 1451, 1350, 1196, 1157, 1075, 1057, 1027, 1001, 902, 790, 758, 698, 582, 525.

***N*-(*p*-tolyl-sulfonyl)-*meso*-1,2-diphenyl-1,2-diaminoethane (73).**<sup>62</sup> *p*-toluyl-sulfonyl chloride (0.64 g, 3.3 mmol) in 75 mL benzene was added dropwise to a solution of *meso*-1,2-diphenyl-1,2-diaminoethane (2.12 g, 10 mmol) in 40 mL benzene and was stirred vigorously for 3 h. A white precipitate appeared and was filtered and treated with 1 M hydrochloric acid (~ 50 mL). The remaining solid was filtered and filtrate made strongly basic with addition of NaOH (~4 g). A white crystalline solid appeared, was filtered, washed with 10 mL cold water and recrystallized from benzene/ hexanes mixture. Yield 48 % (1.75 g, 4.8 mmol).  $\text{C}_{21}\text{H}_{22}\text{N}_2\text{O}_2\text{S}$ , MM = 366 g mol<sup>-1</sup>.  $^1\text{H}$ -NMR ( $\text{CDCl}_3$ ; 7.24 ppm)  $\delta$  7.38 (d,  $J$  = 7.8 Hz, 2H), 7.25-6.85 (m, 10H), 6.76 (d,  $J$  = 7.8 Hz, 2H), 5.60 (s, br, 1H), 4.39 (d,  $J$  = 5.6 Hz, 1H), 4.04 (d,  $J$  = 5.6 Hz, 1H), 2.24 (s, 3H), 1.57 (s, br, 2H).  $^{13}\text{C}$  NMR ( $\text{CDCl}_3$ ; 77.0 ppm)  $\delta$  142.9, 140.9, 137.1, 136.7, 129.2, 128.3, 128.2, 127.8, 127.7, 127.0, 126.9, 60.8, 63.4, 25.4. IR (KBr, cm<sup>-1</sup>)  $\nu$  3057, 3020, 2962, 1599, 1493, 1447, 1382, 1261, 1080, 1071, 953, 811, 698, 666, 573, 545.

**( $\eta^6$ -1-isopropyl-4-methyl-benzene)*N*-*p*-tosyl-*ortho*-diaminobenzene**

**ruthenium(II) (77).** [*p*-cymene RuCl<sub>2</sub>]<sub>2</sub> (306 mg, 0.50 mmol) and *N*-(*p*-tolyl-sulfonyl)-*ortho*-diaminobenzene (248 mg, 1.0 mmol) were transferred into a 30 cm long Schlenk tube with a stir bar. The Schlenk flask was evacuate and re-filled with Ar three times and 15 mL dry, under Ar distilled dichloromethane was added with syringe. The red/orange solution was stirred for 10 min at room temperature and finely ground potassium hydroxide (0.5 g) was added. The reaction mixture was red coloured and stirred for additional 45 min at room temperature. Then, 15 mL of oxygen free water (freshly prepared as heated under Ar atmosphere) was added via syringe and the white solid and excess KOH were dissolved. The greenish aqueous solution was removed via a canula and the remaining dichloromethane solution was dried with CaH<sub>2</sub> (~0.4 g) until hydrogen gas evolution stopped. The solution was filtered under Ar with a Schlenk frit and the remaining solids. The solvent of the filtrate was evaporated under reduced pressure and a red solid was obtained in 82 % yield (406 mg, 0.82 mmol). C<sub>23</sub>H<sub>25</sub>N<sub>2</sub>O<sub>2</sub>SRu, MM = 495 g mol<sup>-1</sup>. Properties: The red complex is stable in air as solid and in solution; soluble in dichloromethane, benzene, *iso*-propanol and acetone. <sup>1</sup>H-NMR (CD<sub>2</sub>Cl<sub>2</sub>; 5.31 ppm)  $\delta$  9.49 (s, br, 1H), 7.74 (d, *J* = 8.0 Hz, 2H), 7.58 (d, *J* = 8.0 Hz, 2H), 7.21 (d, *J* = 8.0 Hz, 2H), 6.97 (dd, *J* = 7.6, 1.2 Hz, 1H), 6.74 (m, 2H), 5.67 (d, *J* = 6.4 Hz, 2H), 5.63 (d, *J* = 6.4 Hz, 2H), 2.57 (sept., *J* = 7.2 Hz, 1H), 2.35 (s, 3H), 2.22 (s, 3H), 1.24 (d, *J* = 6.8 Hz, 6H). <sup>13</sup>C-NMR (CD<sub>2</sub>Cl<sub>2</sub>; 53.7 ppm)  $\delta$  151.5, 141.2, 139.5, 138.3, 128.1, 125.4, 119.0, 117.4, 116.3, 113.4, 100.6, 90.2, 79.6, 76.3, 30.9, 22.6, 20.1, 19.1. IR (KBr, cm<sup>-1</sup>)  $\nu$  3299, 2962, 2360, 1476, 1456, 1321, 1307, 1140, 1086, 1036, 929, 847, 825, 665, 566.

**( $\eta^6$ -1-isopropyl-4-methyl-benzene)-*N*-(*p*-tolyl-sulfonyl)-1,2-diamino-1,1,2,2-tetramethyl-ethane ruthenium(II) (78).** [*p*-cymene RuCl<sub>2</sub>]<sub>2</sub> (612 mg, 1.0 mmol) and *N*-(*p*-tolyl-sulfonyl)-1,2-diamino-1,1,2,2-tetramethyl-ethane (540 mg, 2.0 mmol) were transferred into a 30 cm long Schlenk tube with a stir bar. The Schlenk flask was evacuate and re-filled with Ar three times and 30 mL of dry,

under Ar distilled dichloromethane was added with syringe. The red/orange solution was stirred for 10 min at room temperature and finely ground potassium hydroxide (1.0 g) was added. The reaction mixture turns immediately deep purple and was stirred for additional 15 min at room temperature. Then, 15 mL of oxygen free water (freshly prepared as heated under Ar atmosphere) was added via syringe and the white solid and excess KOH were dissolved. The greenish aqueous solution was removed via a canula and the remaining dichloromethane solution was dried with  $\text{CaH}_2$  (~0.8 g) until hydrogen gas evolution stopped. The purple solution was filtered under Ar with a Schlenk frit and the remaining solids were washed with 10 mL degassed dichloromethane. The solvent of the purple filtrate was evaporated under reduced pressure and a purple solid was obtained in 91 % yield (914 mg, 1.82 mmol).  $\text{C}_{23}\text{H}_{34}\text{N}_2\text{O}_2\text{SRu}$ , MM = 503 g mol<sup>-1</sup>. Properties: The purple solid is stable in air (~ 24 h), however, in solution the complex decomposes instantaneously upon exposure to air; soluble in dichloromethane, benzene, *iso*-propanol and acetone. <sup>1</sup>H-NMR ( $\text{C}_6\text{D}_6$ ; 7.15 ppm)  $\delta$  8.13 (d,  $J$  = 7.3 Hz, 2H, CH-Tosyl), 6.94 (d,  $J$  = 7.3 Hz, 2H, CH-Tosyl), 6.85 (s, br, 1H, N-H), 5.17 (d,  $J$  = 5.1 Hz, 2H), 5.05 (d,  $J$  = 5.1 Hz, 2H), 2.30 (sept.,  $J$  = 6.8, 1H), 2.00 (s, 3H), 1.90 (s, 3H), 1.25 (s, 6H), 1.11 (d,  $J$  = 6.4 Hz, 6H), 0.73 (s, 6H). <sup>13</sup>C-NMR ( $\text{C}_6\text{D}_6$ ; 128.1 ppm)  $\delta$  147.6, 139.4, 128.7, 127.2, 98.7, 87.5, 82.5, 78.7, 74.1, 67.0, 32.0, 26.8, 24.6, 23.8, 21.1, 19.9. IR (KBr, cm<sup>-1</sup>)  $\nu$  3281, 2960, 1598, 1492, 1470, 1387, 1352, 1254, 1127, 1087, 1052, 1025, 931, 807, 816, 791, 657, 561. High resolution MS (EI, 70 eV;  $m/z$  of parent ion; normalized) 498.1378 (1.19%), 501.1364 (2.92%), 502.1380 (3.70%), 503.1543 (5.35%), 504.1441 (8.33%), 505.1348 (2.79%), 506.1399 (5.01%), 507.1598 (1.46%).

**( $\eta^6$ -1-isopropyl-4-methyl-benzene)-*N*-(*p*-tolyl-sulfonyl)-1,2-diamino-meso-1,2-diphenyl-ethane ruthenium(II) (79).** [*p*-cymene  $\text{RuCl}_2$ ]<sub>2</sub> (612 mg, 1.0 mmol) and *N*-(*p*-tolyl-sulfonyl)-1,2-diamino-meso-1,2-diphenyl-ethane (728 mg, 2.0 mmol) were transferred into a 30 cm long Schlenk tube with a stir bar. The Schlenk flask was evacuate and re-filled with Ar three times and 30 mL of dry, under Ar distilled dichloromethane was added with syringe. A bright red-orange

precipitate formed after 5 min at room temperature and finely ground potassium hydroxide (1.0 g) was added. The red-orange precipitate dissolved and the reaction mixture was dark-red coloured. After additional stirring for 45 min at room temperature, 15 mL of oxygen free water (freshly prepared as heated under Ar atmosphere) was added via syringe and the white solid and excess KOH were dissolved. The brownish aqueous solution was removed via a canula and the remaining dichloromethane solution was dried with  $\text{CaH}_2$  (~0.8 g) until hydrogen gas evolution stopped. The dark-red solution was filtered under Ar with a Schlenk frit and the remaining solids were washed with 10 mL degassed dichloromethane. The solvent of the dark-red filtrate was evaporated under reduced pressure and a red solid was obtained in 94 % yield (1.12 g, 1.87 mmol).  $\text{C}_{31}\text{H}_{34}\text{N}_2\text{O}_2\text{SRu}$ , MM = 599 g mol<sup>-1</sup>. Properties: The red solid is stable in air, however, a solution of complex decomposed upon exposure to air; soluble in dichloromethane, benzene, *iso*-propanol and acetone.

Several recrystallization-isolation attempts of **79**, which possesses four stereocentres and exists in principle in up to 16 different diastereomers, failed and produced an intractable mixture observed in <sup>1</sup>H NMR. In the <sup>13</sup>C NMR spectrum a multitude of signals was observed which however coincide with chemical shifts of the other ruthenium complexes **77** and **78**.

<sup>13</sup>C NMR (acetone-d<sub>6</sub>, 206.68 ppm, 29.92 ppm) 150–135, 124.7–122.1, 22.6, 20.1, 19.1. IR (KBr, cm<sup>-1</sup>)  $\nu$  3057, 2961, 1917, 1598, 1494, 1447, 1382, 1261, 1081, 1071, 951, 811, 698, 664, 573, 545. High resolution MS (ESI, 3.5 kV spray voltage, m/z of M+1, normalized) 595.1025 (5%), 598.0909 (28%), 599.0887 (40%), 600.0873 (50%), 601.0767 (100%), 602.0969 (15%), 603.0881 (40%), 604.1102 (5%).

**( $\eta^6$ -1-isopropyl-4-methyl-benzene)-*N*-(*p*-tolyl-sulfonyl)-1,2-diamino-1,1,2,2-tetramethylethane ruthenium(II) aquo complex.** In 100 mL Schlenkflask under Ar atmosphere, ( $\eta^6$ -1-isopropyl-4-methyl-benzene)-*N*-(*p*-tolyl-sulfonyl)-1,2-diamino-1,1,2,2-tetramethyl-ethane ruthenium(II) (100 mg, 0.20 mmol) was

dissolved in freshly prepared, de-oxygenated water (20 mL) and stirred at room temperature. The solution turns immediately bright yellow with a few undissolved purple solids. The reaction mixture was sonicated for 5 min and after approximately 10 min a bright yellow precipitate was formed. The precipitate was filtered in air with Hirsch funnel and 95 mg off-yellow solids were obtained after drying at ambient pressure. The yellow solid was very sensitive towards vacuum and turned bright purple, which turned yellow again in moist air after 2 h. The process was reversible but after 24 h only a brown coloured solid was obtained.  $^1\text{H}$  NMR ( $\text{D}_2\text{O}$ , 4.68 ppm) 7.68 (d,  $J = 8.0$  Hz, 2H), 7.60 (d,  $J = 8.0$  Hz, 2H), 7.43 (d,  $J = 8.0$  Hz, 2H), 7.27 (d,  $J = 8.0$  Hz, 2H), 5.45 (d,  $J = 6.4$  Hz, 2H), 5.25 (m, 4H), 5.08 (d,  $J = 6.4$  Hz, 2H), 2.68 (m, 1 H), 2.55 (m, 1 H), 2.32 (s, 3H), 2.30 (s, 3 H), 2.08 (s, 3H), 1.97 (s, 3H), 1.16 (m, 12H), 1.05 (s, 6H), 1.00 (s, 6H), 0.94 (s, 12H). IR (KBr  $\text{cm}^{-1}$ )  $\nu$  3629, 3500, 3253, 3083, 2959, 1640, 1473, 1363, 1248, 1126, 1088, 1061, 1027, 823, 792, 664, 554.

### Kinetic experiments

The following reaction procedures must be conducted under *strict* exclusion of oxygen. All solvents such as *iso*-propanol and acetone were purified under Ar atmosphere and degassed. The liquid alcohol and ketone substrates were degassed using the freeze-thaw technique (three times) before usage. Solid alcohol and ketone substrates were used without purification. The set-up of the reactions is in a 7 mL screw top vial equipped with a stir bar inside a glovebox under Ar atmosphere. GC-monitoring was conducted typically after 6 h, 24 h, 48 h, 72 h, 7 d and 14 d by direct injection of the crude reaction mixture.

**Typical procedure under oxidizing condition.** Inside a glove box with Ar atmosphere alcohol substrate (1.0 mmol), 16-electron ruthenium catalyst (0.010 mmol) and *cis*-decaline (~50 mg) are dissolved in 5.0 mL degassed acetone in a 7 mL vial and stirred at room temperature. The reaction was monitored by quantitative GC using *cis*-decalin as the internal standard.

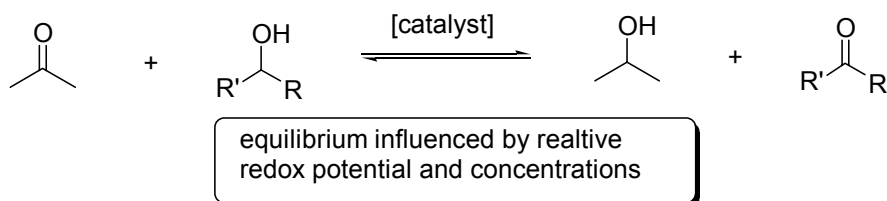
**Typical procedure under reducing condition.** Inside a glove box with Ar atmosphere, ketone substrate (1.0 mmol), 16-electron ruthenium catalyst (0.010 mmol) and *cis*-decaline (~50 mg) are dissolved in 5.0 mL degassed *iso*-propanol in a 7 mL vial and stirred at room temperature. The reaction was monitored by quantitative GC using *cis*-decalin as the internal standard.

**Typical procedure for equal-concentration experiments:** Inside a glove box under Ar atmosphere, alcohol substrate (0.50 mmol), ketone substrate (0.50 mmol) and *cis*-decalin (~50mg) were dissolved in 2.4 mL acetone (2.4 mL) and *iso*-propanol (2.5 mL). Then, 16-electron ruthenium complex (0.010 mmol) was added and the reaction mixture was stirred at RT. The reaction was monitored by quantitative GC using *cis*-decalin as the internal standard.

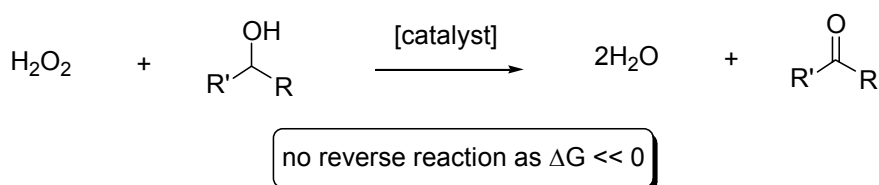
### 3.3 Investigated Transition Metal Catalyzed Peroxide Oxidations

In hydrogen transfer reaction an equilibrium is established between reactants and products. Therefore the formation of the desired ketone is based on the relative redox potential of the reactants and the products as well their relative concentrations.<sup>38</sup> In contrast, oxidation reactions using peroxides as oxidants result in the formation of water as the by-product as shown in **Scheme 3.24**. The reverse reaction from products back to the reactants does not occur as the formation of water is thermodynamically strongly favoured and the reaction is not an equilibrium, i.e.  $\Delta G \ll 0$ .<sup>63</sup>

#### Hydrogen transfer reaction



#### Peroxide oxidation



**Scheme 3.24** Hydrogen transfer reactions and peroxide oxidation reactions.

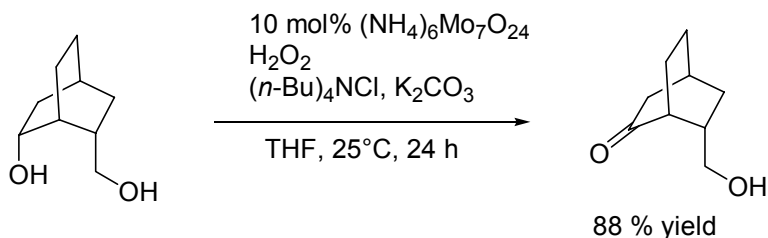
### 3.3.1 Molybdenum/ Tungsten Peroxide Systems

#### 3.3.1.1 Oxidations with $(\text{NH}_4)_6\text{Mo}_7\text{O}_{24}$ and $\text{Na}_2\text{MoO}_4$

##### 3.3.1.1.1 Background of $(\text{NH}_4)_6\text{Mo}_7\text{O}_{24}$ Catalyzed $\text{H}_2\text{O}_2$ Oxidations

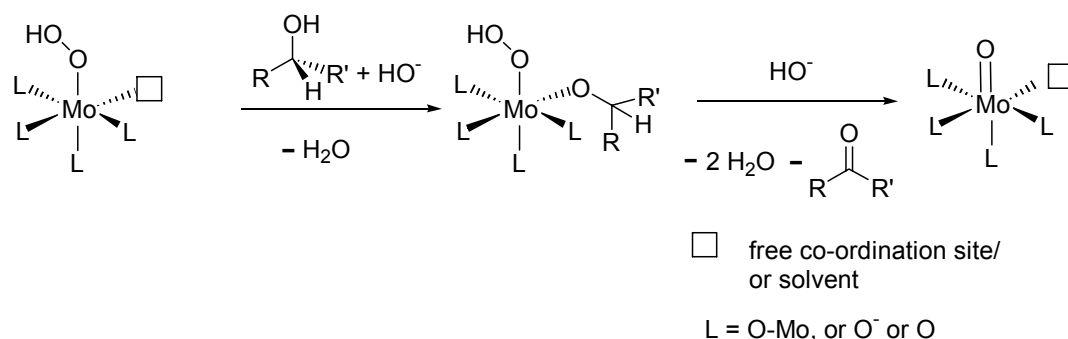
Molybdenum complexes have previously been used for the catalytic oxidation of alcohols, but their use in selective oxidation of *vicinal* diols has been studied only marginally.<sup>64-68</sup>

The selective oxidation of secondary alcohols to ketones in the presence of primary alcohols was realized with hydrogen peroxide using the  $(\text{NH}_4)_6\text{Mo}_7\text{O}_{24}$  complex as catalyst under basic conditions as shown in **Scheme 3.25**.<sup>69</sup> Only the secondary alcohol function in the [2.2.2]-bicyclo-octane structure was selectively oxidized in 88 % yield after 24 h at room temperature. As illustrated in **Scheme 3.26** the proposed reaction step of the secondary alcohol oxidation mechanism is base dependent. A base deprotonates the geminal hydrogen of the secondary alkoxide, ligand, releasing the ketone product and hydroxide from the peroxide ligand. The molybdenum oxide species generated is then re-oxidized with hydrogen peroxide to close the catalytic cycle.<sup>69</sup>



**Scheme 3.25** Selective oxidations with hydrogen peroxide catalyzed by  $(\text{NH}_4)_7\text{Mo}_7\text{O}_{24}$ .





**Scheme 3.26** Base dependent oxidation step of secondary alcohol to corresponding ketone.<sup>69</sup>

### 3.3.1.1.2 Results and Discussion

The (NH<sub>4</sub>)<sub>6</sub>Mo<sub>7</sub>O<sub>24</sub>/ H<sub>2</sub>O<sub>2</sub> oxidation method was validated in a control experiment using (+)-menthol under the reaction conditions described by Trost yielding 65 %<sup>§§§</sup> of (–)-methone after 5 d at 60°C in 5 mL THF and 5 mL water.<sup>69</sup> Subsequently the oxidation of *trans*-1,2-cyclohexanediol was investigated and the results of variation of reaction temperature, solvent systems and base concentration are listed in **Table 3.8**. The best result (**Entry 5**) was obtained with two equivalents of potassium carbonate and ten equivalents of hydrogen peroxide at room temperature giving a substrate conversion of 15 % to a mixture of α-hydroxy cyclohexanone and 1,2-cyclohexanedione after 24 h. Two factors could potentially account for the low conversions: (i) deactivation of the molybdenum centre by formation of a molybdenum diol chelate or (ii) a thermal deactivation of hydrogen peroxide, especially at elevated temperature of 60°C. However, the deactivation of hydrogen peroxide is probably not the cause of the low conversions observed as a dramatically increased stoichiometric amount of hydrogen peroxide improved the oxidation reaction only marginally (**Entries 4 to 6**, ). An increase in base yielded only marginally higher conversions as oxidation reaction is base dependent.<sup>69</sup>

<sup>§§§</sup> Literature value: 70 %.<sup>69</sup>

**Table 3.8** Oxidation of *trans*-1,2-cyclohexanediol with the  $(\text{NH}_4)_6\text{Mo}_7\text{O}_{24}/\text{H}_2\text{O}_2$  method.<sup>a</sup>

Entry	$\text{K}_2\text{CO}_3$ [mmol]	$\text{H}_2\text{O}_2$ [mmol]	Solvent	Temperature	Conversion (%) <sup>b</sup>
1	1.0	5.0	10 mL $\text{H}_2\text{O}$	60 °C	0 (24 h)
2	2.0	5.0	10 mL $\text{H}_2\text{O}$	60 °C	0 (24 h)
3	2.0	2 x 10	10 mL THF	RT	2 (24 h)
4	4.0	10 + 3 x 10 <sup>c</sup>	5 mL THF/ 5 mL $\text{H}_2\text{O}$	RT	4 (4 d)
5	2.0	10	10 mL $\text{H}_2\text{O}$	RT	15 (24 h)
6	4.0	10 + 5 x 10 <sup>c</sup>	10 mL $\text{H}_2\text{O}$	RT	1 (6 d)

<sup>a</sup> 1.0 mmol *trans*-1,2-cyclohexanediol, 0.5 mmol  $(\text{NH}_4)_7\text{Mo}_7\text{O}_{24}$ ,  $\text{H}_2\text{O}_2$  (as 30%wt in  $\text{H}_2\text{O}$ ), 1.0 mmol  $(n\text{-Bu})_4\text{NCl}$  and dimethyl sulfone (~50 mg) in 10 mL solvent.<sup>b</sup> Consumption of *trans*-1,2-cyclohexanediol determined by GC. <sup>c</sup>  $\text{H}_2\text{O}_2$  aliquots added every 24 h.

The nature and structure of the actual catalyst formed from the  $(\text{NH}_4)_6\text{Mo}_7\text{O}_{24}$  pro-catalyst is not known, but we hypothesized that the molybdate cluster,  $\text{Mo}_7\text{O}_{24}^{6-}$ , was broken up into  $\text{MoO}_4^{2-}$  fragments in aqueous solution, which then may constitute the actually catalytically active species. Consequently, we predicted that the use of  $\text{Na}_2\text{MoO}_4$  instead of the  $(\text{NH}_4)_6\text{Mo}_7\text{O}_{24}$  complex should increase the concentration of the active catalyst and enhance the oxidation reaction of *trans*-1,2-cyclohexanediol. However, under the investigated reaction conditions, 1.0 mmol *trans*-1,2-cyclohexanediol, 1.0 mmol  $\text{Na}_2\text{MoO}_4$ , 2.0 mmol  $\text{K}_2\text{CO}_3$ , and 10 mmol  $\text{H}_2\text{O}_2$  in 10 mL water, no conversion to the  $\alpha$ -hydroxy ketone was observed after 48 h at 60°C prompting us to dismiss the above hypothesis and abandon the  $(\text{NH}_4)_6\text{Mo}_7\text{O}_{24}/\text{H}_2\text{O}_2$  oxidation method due to its minimal success with the *trans*-1,2-cyclohexanediol model substrate.

### 3.3.1.2 $\text{MoO}_2(\text{acac})_2$ System

#### 3.3.1.2.1 Background of Oxidations with $\text{MoO}_2(\text{acac})_2$

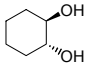
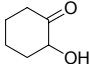
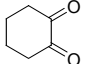
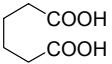
The molybdenum catalyst  $\text{MoO}_2(\text{acac})_2$  has been reported to catalyze the oxidation of alcohols in the presence of a phase transfer catalyst with sodium percarbonate as the stoichiometric oxidant.<sup>68</sup> Sodium percarbonate,  $\text{Na}_2\text{CO}_3 \times$

1.5 H<sub>2</sub>O<sub>2</sub> (SPC), is a readily available oxidant used in commercial detergents and can be used as a dry, solid form of hydrogen peroxide. The oxidation method gave high oxidation yields with various benzylic and aliphatic alcohols in acetonitrile or 1,2-dichloroethane at 80°C within 24 h. The oxidation reaction of one *vicinal* diol was reported as *meso*-hydrobenzoin was oxidized to benzoin in 45 % yield and benzoic acid in 35 % yield.<sup>68</sup> These results prompted us decided to investigate this catalyst in the context of our study as they suggest that adjustment of the reaction conditions and/or attenuation of the oxidation reactivity of the MoO<sub>2</sub>(acac)<sub>2</sub> catalyst might lead to an increase in the α-hydroxy ketone yield by lowering overoxidation to the diketone or dicarboxylic acid.

#### 3.3.1.2.2 Results and Discussion

In an initial control experiment, cyclohexanol was used to validate the literary procedure achieving a conversion of 95 % to cyclohexanone in less than 24 h.<sup>68</sup> The results of the oxidation of *trans*-1,2-cyclohexanediol as a function of the solvents and oxidants employed are listed in **Table 3.9**. With water as solvent no oxidation was observed and the dry carrier of hydrogen peroxide, sodium percarbonate gave superior results compared to hydrogen peroxide, which was added as 30 wt% solution in water. The catalyst, therefore, must have been deactivated in the presence of water probably through formation of molybdenum-hydroxo or -oxo complexes and/or cluster that may resemble the catalyst system discussed in the previous section.

**Table 3.9** Oxidation of *trans*-cyclohexanediol with the MoO<sub>2</sub>(acac)<sub>2</sub> / peroxide method.<sup>a</sup>

Entry	Oxidant	Amount oxidant [mmol]	Solvent	Content (%) after 24 h <sup>b</sup>			
							
1	SPC	4.0	10 mL H <sub>2</sub> O	0	0	0	0 <sup>c</sup>
2	SPC	4.0	10 mL CH <sub>3</sub> CN	11	36	12	41 <sup>c</sup>
3	SPC	4.0	8 mL CH <sub>3</sub> CN 2 mL H <sub>2</sub> O	0	0	0	0 <sup>c</sup>
4	H <sub>2</sub> O <sub>2</sub>	2.2	10 mL CH <sub>3</sub> CN	66	7	4	22 <sup>c</sup>
5	H <sub>2</sub> O <sub>2</sub>	1.1	10 mL H <sub>2</sub> O	0	0	0	0 <sup>c</sup>
6	H <sub>2</sub> O <sub>2</sub>	1.1	10 mL CH <sub>3</sub> CN	50	3	<1	47 <sup>c</sup>

<sup>a</sup> 1.0 mmol *trans*-1,2-cyclohexanediol, 0.10 mmol MoO<sub>2</sub>(acac)<sub>2</sub>, peroxide and dimethyl sulfone (~50 mg) in 10 mL solvent at 60 °C. <sup>b</sup> Determined by GC ± 3 %. <sup>c</sup> Calculated, i.e. adipic acid = 1.0 mmol – (unreacted diol + α-OH ketone + dione), ± 9 %. No other oxidation products were observed.

The limitation of the method is over-oxidation, i.e. formation of the dicarboxylic acid as the dominant product (**Entry 2, Table 3.9**). As mentioned in **3.1.3.3**, kinetic calculations accompanied by experimental conversion results provide the information needed to determine the relative rate constants, which in turn determine the product distribution. The conversion results in **Entry 2 Table 3.9** are inherent to a reaction having approximate relative rate constants  $k_1 = 0.06$ ,  $k_2 = 0.04$ , and  $k_3 = 0.14$  (**Figure 3.32**) where  $k_1$  is the rate constant for the reaction diol → α-hydroxy-ketone,  $k_2$  for the reaction α-hydroxy-ketone → dione and  $k_3$  for the reaction dione → dicarboxylic acid, respectively. The rate constants were determined by modeling theoretical distribution curves with the relative distributions of the experimentally (i.e. quantitative GC measurements) obtained concentrations of diol, α-hydroxy ketone, dione and dicarboxylic acid at different times.

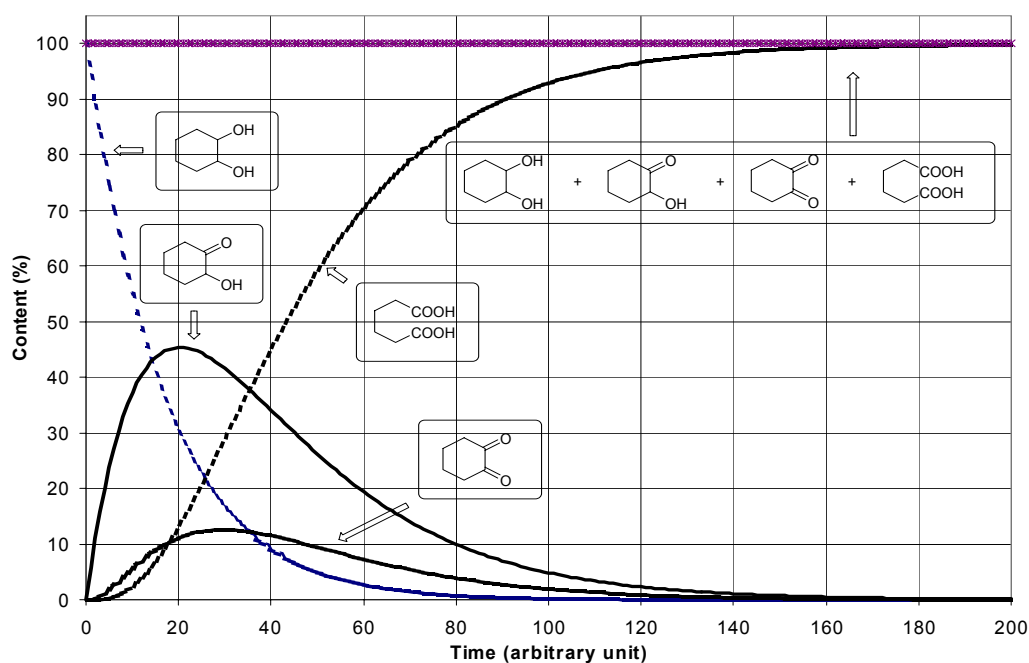


**Figure 3.32** Plot of conversion of *trans*-1,2-cyclohexanediol to oxidation products against an arbitrary time unit indicating the maximum possible conversion amounts for each oxidation product, with rate constants  $k_1 = 0.06$ ,  $k_2 = 0.04$ ,  $k_3 = 0.14$ .

By examining **Figure 3.32**, it is apparent that with this  $\text{MoO}_2(\text{acac})_2$ /SPC method the maximum  $\alpha$ -hydroxy ketone content for oxidation of *trans*-1,2-cyclohexanediol is 45%. The relative ratio of the rate constants  $k_1$  (diol  $\rightarrow$   $\alpha$ -hydroxy ketone), 0.06, and  $k_2$  ( $\alpha$ -hydroxy ketone  $\rightarrow$  dione), 0.04, is 1.5, indicating that the second reaction step is ~33 % slower than the first oxidation step.

Although, this result is a promising step towards a selective oxidation procedure of *vicinal* diols, the lower reactivity of second reaction step ( $k_2$ ) it is still far from the synthetically practicable  $0.1 k_1$ .

### 3.3.1.3 Modification of the Molybdenum Catalyst

#### 3.3.1.3.1 Attenuation of the Molybdenum Catalyst

We hypothesized that the over-oxidation problem can be addressed by attenuating the reactivity of the catalyst by modifying its structure as illustrated in **Figure 3.33**. The fine tuning of the oxidation reactivity should be possible by changing the electronic structure of the catalyst through variation of the ligands attached to the metal centre, as it is the activated metal complex and not the peroxide reagent itself that acts as the true oxidant.<sup>70</sup>

Molybdenum forms a seven coordinated diperoxomolybdate complex (**83**) with a pentagonal bipyramidal geometry with two nitrogen containing ligands such as pyridine.<sup>71</sup> Bipyridine and bipyrimidine derivatives of **83** have been used as catalytic species in epoxidation of C=C double bonds and alcohol oxidation.<sup>72</sup>

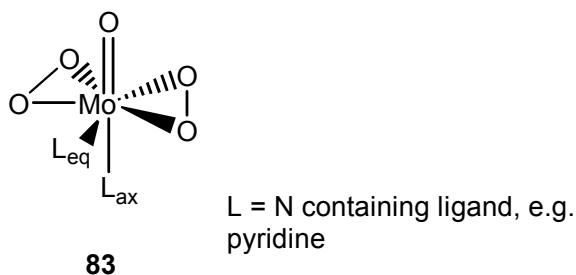
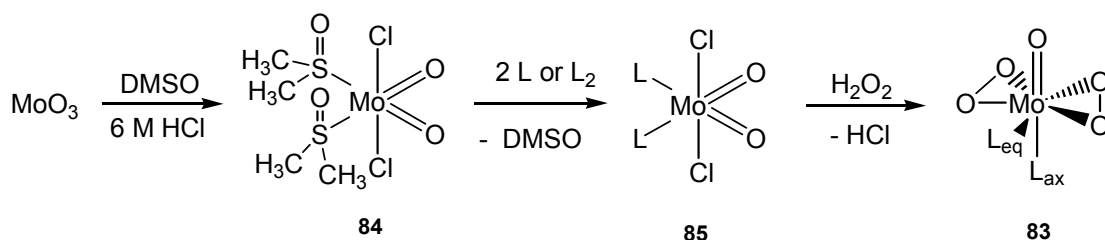


**Figure 3.33** Pentagonal bipyramidal geometry of  $\text{MoO}(\text{O}_2)_2\text{L}_2$ .

The diperoxo complex, **83**, can be synthesized from molybdenum trioxide in a three step process as illustrated in **Scheme 3.27**. The dichloro-dioxo-bis(dimethylsulfoxo)-molybdenum complex (**84**) is readily obtained from the reaction of molybdenum trioxide with dimethyl sulfoxide in hydrochloric acid solution.<sup>73</sup>  $\text{MoO}_2\text{Cl}_2(\text{DMSO})_2$  can then be transformed to  $\text{MoO}_2\text{Cl}_2\text{L}_2$ , **85**, through

a ligand exchange reaction with pyridine or bipyridine ligands.<sup>72</sup> The diperoxomolybdenum complex **83** is obtained by reaction of hydrogen peroxide and  $\text{MoO}_2\text{Cl}_2\text{L}_2$  **85**.<sup>74</sup>



**Scheme 3.27** Synthesis of  $\text{MoO}(\text{O}_2)_2\text{L}_2$  (**83**) from  $\text{MoO}_3$ .

### 3.3.1.3.2 Results and Discussion

Seven molybdenum dioxo-dichloro compounds (**86** to **92**) were prepared by this method in low to high yields (**Figure 3.34**). With terpyridine, a tridentate ligand, a trigonal bipyramidal structure is proposed for the formed complex **90** but structural determination by IR and a reaction of  $\text{AgNO}_3$  resulting in a quantitative, i.e. two equivalence, precipitation of silver chloride was inconclusive.

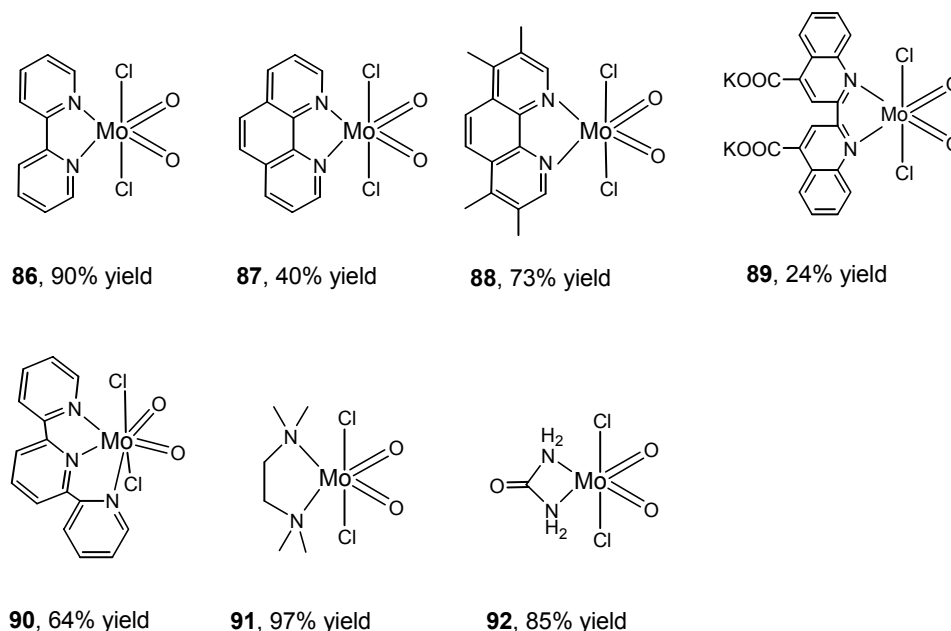


**Figure 3.34** Proposed structures of compounds **86** to **92** obtained through displacement of DMSO by the corresponding chelating ligand.

The characterization of the produced complexes **86** to **92** was very difficult due to the extremely low solubility of the complexes in various solvents. The solubilities of each complex in acetonitrile, dichloromethane and toluene are listed in **Table 3.10**. The solubilities were determined experimentally by stirring 20 mg of molybdenum complex in 5.0 mL solvent at room temperature. After 24 h the mass of a filtered aliquot of the solution was measured in a tared flask. The solvent was removed under reduced pressure and the remaining solid dried in high vacuum and weighed. The solubility of a complex was determined by division of the residual molybdenum complex mass with the mass difference of the solution containing the complex.<sup>\*\*\*\*</sup> As can be seen from **Table 3.10** the complexes **86** to **92** possess a very low solubility in the three solvents investigated, which probably arises from the high symmetry of the complexes resulting in high lattice energies. Remarkably, even complex **89**, which bears two carboxylate substituents on the ligand backbone is insoluble in aqueous media, even at high pH values. Consequently the complexes could only be analyzed by IR and characterized by the asymmetric MoO<sub>2</sub> deformation frequency in the range of 895 – 915 cm<sup>-1</sup>.<sup>72</sup> The proposed structures of the complexes shown in **Figure 3.34** and are therefore conjectural and postulated by analogy with the more soluble non-chelated complexes **84**.<sup>72</sup>

Due to the limited solubility of the complexes, only four complexes (**87**, **88**, **90** and **92**) with limited solubility in acetonitrile were screened in the oxidation experiment with cyclohexanol at various temperatures and different oxidants (**Table 3.11**).

---

<sup>\*\*\*\*</sup> Solubility = mass of Mo complex / (mass of aliquot – mass of Mo complex)

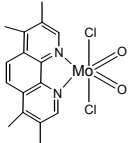
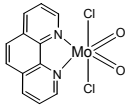
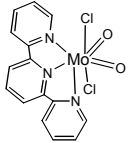
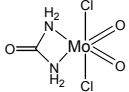


**Table 3.10** Solubilities of Mo<sub>2</sub>O<sub>2</sub>Cl<sub>2</sub>L<sub>2</sub> complexes in acetonitrile, dichloromethane and toluene.

Entry	Compound	Acetonitrile [g/kg]	Dichloromethane [g/kg]	Toluene [g/kg]
1	MoO <sub>2</sub> Cl <sub>2</sub> (DMSO) <sub>2</sub>	35	3.6	Insoluble <sup>a</sup>
2		Insoluble <sup>a</sup>	Insoluble <sup>a</sup>	1.6
3		<0.002	Insoluble <sup>a</sup>	Insoluble <sup>a</sup>
4		<0.002	Insoluble <sup>a</sup>	0.12
5		Insoluble <sup>a</sup>	0.082	Insoluble <sup>a</sup>
6		<0.002	Insoluble <sup>a</sup>	Insoluble <sup>a</sup>
7		Insoluble <sup>a</sup>	Insoluble <sup>a</sup>	Insoluble <sup>a</sup>
8		16	5.1	Insoluble <sup>a</sup>

<sup>a</sup> The solubility is smaller than 0.0001 g/kg.

**Table 3.11** Screening of oxidation methods of cyclohexanol with selected MoO<sub>2</sub>Cl<sub>2</sub>L<sub>2</sub> derivatives.<sup>a</sup>

Entry	Complex [0.20 mmol]	Oxidant [2.0 mmol]	Temperature	Produced Cyclohexanone (%)
1		H <sub>2</sub> O <sub>2</sub>	75 °C	0
2		H <sub>2</sub> O <sub>2</sub>	45 °C	0
3		TBHP <sup>b</sup>	60 °C	36
4		TBHP <sup>b</sup>	60 °C	25

<sup>a</sup> 1.0 mmol cyclohexanol, 0.20 mmol Mo complex, 2.0 mmol oxidant and dimethyl sulfone (~50 mg) in 10 mL CH<sub>3</sub>CN after 24h at various temperatures. <sup>b</sup> *Tert.*-butyl hydrogen peroxide.

At best, only 36 % conversion to cyclohexanone was achieved with the terpyridine containing complex **90** and *tert.*-butyl hydrogen peroxide as oxidant. Hydrogen peroxide as the oxidant gave no conversion in the oxidation of cyclohexanol to cyclohexanone.

The limited success of these MoO<sub>2</sub>Cl<sub>2</sub>L<sub>2</sub> complexes as catalysts in peroxide oxidations of secondary alcohols, which probably rooted in their extremely low solubility, lead us abandon this oxidation method and focus our investigations on other Mo-complexes.

### 3.3.1.4 Mo and W Oxo-Diperoxo-Pyridine-2-Carboxylate Complexes

#### 3.3.1.4.1 Mo and W Oxo-Diperoxo-Pyridine-2-Carboxylate Complexes as Catalysts in Oxidation Reactions

The stoichiometric oxidizing agents cetyl trimethyl ammonium [MoO(O<sub>2</sub>)<sub>2</sub>(pyridine-2-carboxylate)] (**93**) tetra *n*-butylammonium [MoO(O<sub>2</sub>)<sub>2</sub>(*N*-oxide-

pyridine-2-carboxylate) (**94**), and tetra *n*-butylammonium [WO(O<sub>2</sub>)<sub>2</sub>(*N*-oxide-pyridine-2-carboxylate)] (**95**) (**Figure 3.35**) oxidized primary and secondary alcohols under mild conditions in high yield.<sup>64,66,75,76</sup> Complex **93** was also used in the catalytic oxidation of secondary alcohols with hydrogen peroxide.<sup>77</sup> Furthermore it was reported that the *N*-oxide derivative (**94**) is about 50-fold more reactive than **93** in the oxidation of cyclohexanol in 1,2-dichloroethane.<sup>66</sup>

The use of *vicinal* diols as substrates with these complexes has however to date not been reported. The molybdenum and tungsten complexes, **94** and **95**, can be prepared in the reaction of sodium molybdate or tungstate, *N*-oxide-pyridine-2-carboxylic acid, tetra *n*-butylammonium hydroxide in basic, aqueous hydrogen peroxide solution and recrystallization of the complexes from ethanol.<sup>77</sup>

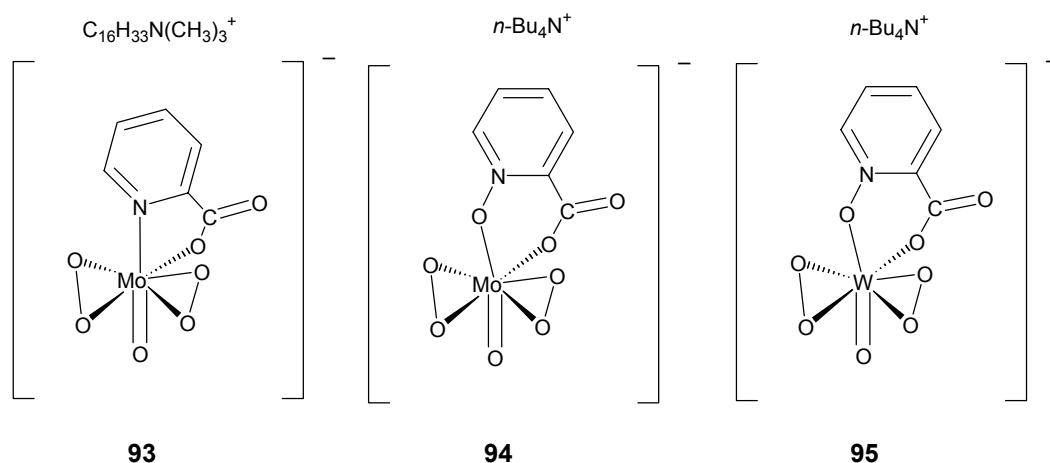


**Figure 3.35** Molybdenum and tungsten diperoxo complexes (**93** – **95**).

#### 3.3.1.4.2 Results and Discussion

A control experiment validated that 67 % of cyclohexanol was oxidized to cyclohexanone with one equivalent of **94** in 1,2-dichloroethane at 60°C in 24 h. Comparing this stoichiometric diperoxo picolinic *N*-oxide-molybdenum-oxide reagent to the previously described oxidation method using MoO<sub>2</sub>(acac)<sub>2</sub>/sodium

percarbonate, which oxidized >95 % of the cyclohexanol in 24 h, suggests that oxidative capability of picolinic *N*-oxide-molybdenum complex is somewhat lower possibly resulting in less over-oxidation with *vicinal* diol substrates.

The *N*-oxide derivative **94** has only been used as stoichiometric oxidant in the oxidation of alcohols and not as catalyst. However, the analog **93** showed catalytic activities with hydrogen peroxide.<sup>66</sup> It thus appeared logical to also test the supposedly more reactive *N*-oxide complex **94** as a catalyst and its activity in the catalytic oxidation of cyclohexanol to cyclohexanone was investigated with four different peroxide species with **94**. The results of this series of experiments are summarized in **Table 3.12** and establish that complex **94** can in fact be employed as a catalyst. Sodium percarbonate as the peroxide source showed the highest conversion to cyclohexanone with 47 % after 24 h in acetonitrile at 60°C.

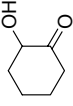
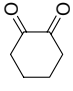
**Table 3.12** Oxidation of cyclohexanol with **94** and various peroxide oxidants.<sup>a</sup>

Entry	Oxidant [2.0 mmol]	Conversion to Cyclohexanone (%) <sup>b</sup>
1	Sodium Percarbonate <sup>c</sup>	47
2	<i>Tert.</i> -butyl Hydrogen Peroxide	14
3	Benzoyl Peroxide	36
4	Hydrogen Peroxide <sup>c</sup>	14

<sup>a</sup> 1.0 mmol cyclohexanol, 0.1 mmol **94**, 2.0 mmol oxidant and dimethyl sulfone (~50 mg) in 10 mL CH<sub>3</sub>CN at 60°C after 24h. <sup>b</sup> Determined by GC. <sup>c</sup> Peroxide in water.

The influence of oxidant and catalyst on the oxidation reaction of *cis*- and *trans*-1,2-cyclohexanediol was also investigated and the results are shown in **Table 3.13**. The oxidation reactions were monitored by GC with dimethyl sulfone as internal standard. The amount of adipic acid generated could not be measured directly by GC and was therefore calculated from the mass balance, i.e., the differences of the remaining diol and α-hydroxy ketone and dione produced. No other oxidation side-products were detected by GC and GC-MS.

**Table 3.13** Oxidation of *cis*- and *trans*-cyclohexanediol with **94** and **95** with various oxidants.<sup>a</sup>

Entry	MO(O <sub>2</sub> ) <sub>2</sub> (picN) <sup>+</sup> Catalyst [M = Mo; W]	Oxidant	Substrate [1.0 mmol]	GC Yields (%) <sup>b</sup>		
				Unreacted substrate		
<b>1</b>	Mo	SPC [2 mmol]	<i>trans</i> -1,2-cyclohexandiol	35	19	8
<b>2</b>	Mo	SPC [10 mmol]	<i>trans</i> -1,2-cyclohexandiol	27	19	4
<b>3</b>	Mo	H <sub>2</sub> O <sub>2</sub> [2 mmol]	<i>trans</i> -1,2-cyclohexandiol	69	15	6
<b>4</b>	Mo	H <sub>2</sub> O <sub>2</sub> [10 mmol]	<i>trans</i> -1,2-cyclohexandiol	70	9	4
<b>5</b>	W	SPC [2 mmol]	<i>trans</i> -1,2-cyclohexandiol	59	3	4
<b>6</b>	W	SPC [10 mmol]	<i>trans</i> -1,2-cyclohexandiol	51	7	3
<b>7</b>	W	H <sub>2</sub> O <sub>2</sub> [2 mmol]	<i>trans</i> -1,2-cyclohexandiol	64	18	6
<b>8</b>	W	H <sub>2</sub> O <sub>2</sub> [10 mmol]	<i>trans</i> -1,2-cyclohexandiol	52	24	9
<b>9</b>	Mo	H <sub>2</sub> O <sub>2</sub> [2 mmol]	<i>cis</i> -1,2-cyclohexandiol	17	28	10
<b>10</b>	W	H <sub>2</sub> O <sub>2</sub> [2 mmol]	<i>cis</i> -1,2-cyclohexandiol	24	18	6

<sup>a</sup> 0.05 mmol Catalyst *n*-Bu<sub>4</sub>N[Mo(O<sub>2</sub>)<sub>2</sub>(picN)]<sup>+</sup> M = Mo (**94**) or W (**95**), 1.0 mmol diol substrate, oxidant and dimethyl sulfone (~50mg) in 10 mL CH<sub>3</sub>CN after 24 h at 60°C. <sup>b</sup> Based on dimethyl sulfone as internal standard. +/- 0.03 mmol error. <sup>c</sup> Calculated from mass balance, i.e. adipic acid = 1.0 mmol – (unreacted diol + α-OH ketone + dione). +/- 0.09 mmol error. No other oxidation products were observed.

A general trend observed with both molybdenum and tungsten catalysts, **94** and **95**, was that sodium percarbonate was a more reactive peroxide source than hydrogen peroxide, which was added as 30 wt% aqueous solution. As found with the previously discussed systems, water might deactivate both Mo and W catalysts by formation of hydroxo- and oxo-complexes and thus inhibiting the formation of the molybdenum alkoxide complex postulated to be a key intermediate in the catalytic cycle.<sup>71,75</sup> Since water is produced as a necessary by-product during the oxidation process the activity of the catalyst falls off with time anyway, which has been found in all cases when the reactions were let to react for more than 24 h. After this period the oxidation reaction effectively stopped indicating deactivation of the catalytic system. The molybdenum catalyst **94** was found to be more reactive than the tungsten analog **95**. No concentration versus time data was collected for this catalysts system, but the low diol concentration found after 24 hours suggests the relative magnitude of the rate constants  $k_2$  and  $k_3$  is such that  $k_3 \geq k_2$ , while the yield of the desired  $\alpha$ -hydroxy-ketone, as in the previously analyzed case discussed above, suggest  $k_2 > 0.1 k_1$ .

The *cis*-diol substrate was more reactive than the *trans*-diol substrate as only 17 % and 24 % starting material remained after 24 and the  $\alpha$ -hydroxy ketone content was only marginally higher than with the *trans*-diol substrate (**Entry 9** and **10**, **Table 3.13**).

Nevertheless, the highest content of  $\alpha$ -hydroxy cyclohexanone was detected in the oxidation of *trans*-1,2-cyclohexanediol using **95** and two equivalents of hydrogen peroxide. These reaction conditions were then applied to the selective oxidation of sugar substrates as shown in **Figure 3.36**. Methyl 4,6-O-benzylidene- $\alpha$ -D-glucopyranoside (**96**), phenyl 4,6-O-benzylidene- $\alpha$ -D-glucopyranoside (**97**) and methyl 4,6-O-isopropylidene- $\alpha$ -D-mannopyranoside (**98**) were investigated with the catalytic oxidation using 5 mol% of complex **95** and two equivalents of hydrogen peroxide in acetonitrile at 60°C. The oxidation reaction were monitored by TLC. No change in starting material and no oxidation was detected after 5 days.

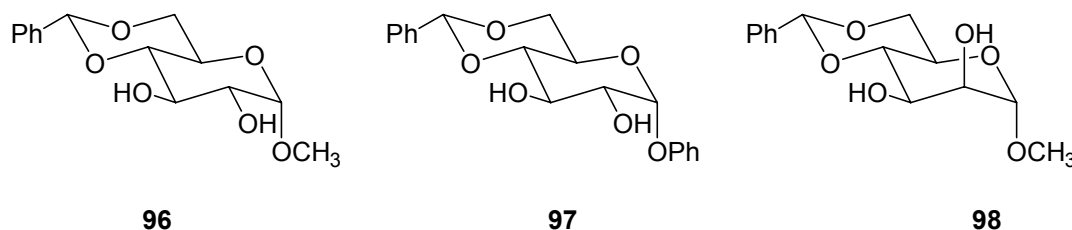


**Figure 3.36** Selected protected sugar substrates for the oxidation with tungsten complex **95**.

### 3.3.1.5 Concluding Remarks

The ammonium molybdate cluster,  $(\text{NH}_4)_6\text{Mo}_7\text{O}_{24}$ , and sodium molybdate  $\text{Na}_2\text{MoO}_4$  oxidation method proved to be ineffective for the selective oxidation of *trans*-1,2-cyclohexanediol. Difficulties with over-oxidation while employing the  $\text{MoO}_2(\text{acac})_2$  and SPC catalyst lead to the synthesis of seven molybdenum dioxo-dichloro-complexes (**86** to **92**) bearing chelating nitrogen ligands. For these complexes it was hypothesized that the ligands would attenuate the oxidative power of the active oxidant catalyst species thus limiting the amount of overoxidation of the desired  $\alpha$ -hydroxy-ketone to the undesired diones and dicarboxylic acids. Unfortunately due to their marginal solubility in organic solvents, these complexes demonstrated only very limited oxidation activity. In contrast the molybdenum and tungsten diperoxo-picolinic *N*-oxide complexes, **94** and **95**, demonstrated good oxidizing capabilities towards diol substrates. However again over-oxidation occurred with *cis*- and *trans*-cyclohexane-1,2-diol substrates. A general trend of deactivation of molybdenum and tungsten catalysts with water was found and it is proposed that the formation of hydroxo- and oxo- species inhibits the formation of a metal-alkoxide complex the postulated key intermediate in the catalytic oxidation cycle. Applying the tungsten diperoxo-picolinic-*N*-oxide complex, **95**, to the oxidation of three partially protected sugar derivatives in acetonitrile at 60°C showed no reactivity of the sugar substrates.

### 3.3.1.6 Experimental Section

Reactions were monitored using a Varian CP-3800 gas chromatograph using dimethyl sulfone as the internal standard. GC-MS analyses were conducted with a Saturn 2000. IR characterization of solid compounds was conducted by way of KBr pellets using a Bomem FT-IR spectrometer. All starting materials were purchased from commercial sources and used without further purification unless otherwise stated.

CAUTION: Reactions with peroxide compounds are potentially dangerous and a protective shield should be used. Excess of peroxide should be carefully quenched with saturated  $\text{Na}_2\text{S}_2\text{O}_3$  solution and properly discarded.

**General procedure for reactions involving  $(\text{NH}_4)_6\text{Mo}_7\text{O}_{24}$ .** In a 20 mL vial, *trans*-1,2-cyclohexanediol (1.0 mmol, 116 mg),  $(\text{NH}_4)_6\text{Mo}_7\text{O}_{24} \times 4 \text{ H}_2\text{O}$  (0.5 mmol, 618 mg) *n*-Bu<sub>4</sub>NBr (1.0 mmol, 322 mg), K<sub>2</sub>CO<sub>3</sub> (1.0 mmol, 138 mg) and dimethyl sulfon (~50 mg) were dissolved in THF (5.0 mL) and deionized H<sub>2</sub>O (5.0 mL). After addition of H<sub>2</sub>O<sub>2</sub> (5.0 mmol, 30 wt.% in water, 0.5 mL) with a syringe, the reaction mixture was stirred at 60 °C. The reaction was monitored periodically with GC by injection of the crude reaction mixture.

**General procedure for reactions involving Na<sub>2</sub>MoO<sub>4</sub>.** In a 20 mL vial, *trans*-1,2-cyclohexanediol (1.0 mmol, 116 mg), Na<sub>2</sub>MoO<sub>4</sub>  $\times$  2 H<sub>2</sub>O (1.0 mmol, 242 mg), K<sub>2</sub>CO<sub>3</sub> (2.0 mmol, 276 mg) and dimethyl sulfon (~50 mg) were dissolved in 10 mL water. The peroxide was added and the reaction mixture was stirred at 60 °C. The reaction was monitored periodically by GC injecting samples of the crude reaction mixture.

**General procedure of reactions involving MoO<sub>2</sub>(acac)<sub>2</sub>.** In a 20 mL vial, *trans*-1,2-cyclohexanediol (1.0 mmol, 116 mg), Adogen 464® (phase transfer catalyst) (0.2 mmol, 90 mg), dimethyl sulfon (~50 mg), acetonitrile (10 mL), sodium percarbonate, SPC, (4.0 mmol, 419 mg) were combined and stirred at 80 °C. The



reaction was monitored periodically by GC injecting samples of the crude reaction mixture.

**Preparation of  $\text{MoO}_2\text{Cl}_2(\text{DMSO})_2$  (84).**  $\text{MoO}_3$  (69 mmol, 10.0 g), HCl (12 M, 50 mL), and 50 mL of deionized  $\text{H}_2\text{O}$  were combined in a 250 mL round bottom flask equipped with a reflux condensor. The reaction mixture was heated to  $90^\circ\text{C}$  for 2 h until all  $\text{MoO}_3$  starting material was dissolved. Then, the solution was cooled to room temperature and dimethyl sulfoxide (37.5 mmol, 50 mL) was added. The mixture was stirred for 15 minutes and a white precipitate formed. The precipitate was filtered and washed with 3 x 30 mL acetone and dried *in vacuo* for 24 h. Yield 75 % (16.7 g, 51.8 mmol). IR (KBr,  $\text{cm}^{-1}$ )  $\nu$  3433, 3018, 3001, 2919, 2360, 2344, 1686, 1655, 1560, 1542, 1509, 1427, 1413, 1320, 1296, 1035, 995, 964, 952, 919, 890.

**General preparation of  $\text{MoO}_2\text{Cl}_2\text{L}_2$ :**  $\text{MoO}_2\text{Cl}_2(\text{DMSO})_2$  (1.41 mmol, 500 mg) was dissolved in 10 mL  $\text{CH}_3\text{CN}$  at room temperature. Then the ligand (1.41 mmol) was added in 5 mL of  $\text{CH}_3\text{CN}$  and a precipitation formed. After stirring for 1 h, the solids were filtered off and dried *in vacuo* and analyzed by IR. All synthesized  $\text{MoO}_2\text{Cl}_2\text{L}_2$  complexes did not melt  $< 250^\circ\text{C}$ .

**(86).** Yield 90 % (0.45 g, 1.27 mmol).  $\text{C}_{10}\text{H}_8\text{Cl}_2\text{MoN}_2\text{O}_2$ , MM =  $355 \text{ g mol}^{-1}$ . IR (KBr,  $\text{cm}^{-1}$ )  $\nu$  3112, 1605, 1599, 1573, 1496, 1475, 1442, 1318, 1269, 1244, 1226, 1173, 1154, 1101, 1079, 1062, 1044, 934, 903, 775.

**(87).** Yield 40 % (0.20 g, 0.56 mmol).  $\text{C}_{12}\text{H}_{10}\text{Cl}_2\text{MoN}_2\text{O}_2$ , MM =  $357 \text{ g mol}^{-1}$ . IR (KBr,  $\text{cm}^{-1}$ )  $\nu$  1604, 1623, 1579, 1517, 1493, 1426, 1343, 1306, 1223, 1196, 1143, 1106, 996, 938, 915, 897, 869, 850.

**(88).** Yield 73 % (0.45 g, 1.02 mmol).  $\text{C}_{16}\text{H}_{18}\text{Cl}_2\text{MoN}_2\text{O}_2$ , MM =  $437 \text{ g mol}^{-1}$ . IR (KBr,  $\text{cm}^{-1}$ )  $\nu$  1654, 1618, 1598, 1560, 1529, 1386, 1197, 1178, 933, 903, 831.

**(89).** Yield 24 % (0.21 g, 0.34 mmol).  $C_{20}H_{10}Cl_2K_2MoN_2O_6$ , MM = 619 g mol<sup>-1</sup>. IR (KBr, cm<sup>-1</sup>)  $\nu$  1697, 1585, 1547, 1505, 1452, 1428, 1392, 1327, 1283, 1246, 1202, 1157, 1082, 920, 796, 774, 743, 662.

**(90).** Yield 64 % (0.39 g, 0.90 mmol).  $C_{15}H_{11}Cl_2MoN_3O_2$ , MM = 432 g mol<sup>-1</sup>. IR (KBr, cm<sup>-1</sup>)  $\nu$  3088, 2738, 1607, 1585, 1464, 1443, 1408, 1634, 1289, 1256, 1238, 1187, 1162, 1093, 1065, 1035, 1004, 993, 941, 911, 841.

**(91).** Yield 97 % (0.44 g, 1.39 mmol).  $C_6H_{16}Cl_2MoN_2O_2$ , MM = 315 g mol<sup>-1</sup>. IR (KBr, cm<sup>-1</sup>)  $\nu$  3854, 3822, 3815, 3802, 3745, 3676, 3671, 3730, 3448, 3021, 2909, 2624, 2457, 1734, 1718, 1700, 1696, 1684, 1653, 1559, 1507, 1487, 1472, 1417, 1398, 1283, 1154, 1124, 999, 977, 925, 888, 840, 792.

**(92).** Yield 85 % (0.31 g, 1.19 mmol).  $CH_4Cl_2MoN_2O_3$ , MM = 259 g mol<sup>-1</sup>. IR (KBr, cm<sup>-1</sup>)  $\nu$  3870, 3854, 3821, 3816, 3802, 3745, 3349, 2917, 1734, 1700, 1696, 1684, 1635, 1559, 1507, 1458, 1319, 1298, 1148, 1031, 997, 927, 897, 759, 668, 594.

**Preparation of  $[MO(O_2)_2(C_5H_4NOCO_2)]^+nBu_4N^+$ , M = Mo (94), W (95)**<sup>66</sup> The synthesis involved the preparation to two separate solutions, A and B.

Solution A:  $Na_2MoO_4 \times 4 H_2O$  (3.5 mmol, 0.84 g) was dissolved in 2.5 mL of de-ionized water and adjusted to pH ~ 2 using 50%  $H_2SO_4$ . This was followed by the addition of  $H_2O_2$  (30%wt in water, 1.75 mL). The total volume of the solution was adjusted to 5 mL by addition of de-ionized water.

Solution B: Picolinic acid *N*-oxide,  $C_6H_5O_3N$ , (3.75 mmol, 0.535 g) was dissolved in 2.5 mL  $nBu_4NOH$  (1.5 M) and NaOH (~120 mg). The total volume of the solution was adjusted to 5 mL by addition of de-ionized water.

In an ice-bath, solution A was care fully added to solution B with a Pasteur pipette. The pH of the reaction solution was adjusted to pH 2 with 6 M H<sub>2</sub>SO<sub>4</sub> and allowed stir for an additional 30 minutes. A precipitate formed and was filtered, dried *in vacuo* and was recrystallized from hot ethanol. Yield for **94**: 52 % (1.01 g, 1.82 mmol). C<sub>22</sub>H<sub>40</sub>MoN<sub>2</sub>O<sub>8</sub>, MM = 556 g mol<sup>-1</sup>. Yield for **95**: 72 % (1.63 g, 2.53 mmol). C<sub>22</sub>H<sub>40</sub>N<sub>2</sub>O<sub>8</sub>W, MM = 644 g mol<sup>-1</sup>. <sup>1</sup>H and <sup>13</sup>C NMR as well IR spectroscopy data was in accordance with the literature.<sup>66</sup>

**General reaction of [MO(O<sub>2</sub>)<sub>2</sub>(C<sub>5</sub>H<sub>4</sub>NOCO<sub>2</sub>)]<sup>-</sup>nBu<sub>4</sub>N<sup>+</sup>, M = Mo, W, (Mo(picN), W(picN)).** In a 20 mL vial, 1.0 mmol of substrate, 2.0 mmol of oxidant, 0.05 mmol of complex (**94** or **95**) and dimethyl sulfon (~50 mg) were dissolved in 10 mL of CH<sub>3</sub>CN. The solution was stirred at 60°C. With simple alcohols as substrate the reaction was monitored by samples of the of crude reaction mixture into the GC. The analysis of sugar substrate reactions required TLC on silica plates in EtOAc. The TLC was analyzed by UV fluorescence and stained in 5% H<sub>2</sub>SO<sub>4</sub> solution.

### 3.3.2 NiCl<sub>2</sub> Mediated Benzoylperoxide System

#### 3.3.2.1 Known Applications of NiBr<sub>2</sub>/Bz<sub>2</sub>O<sub>2</sub> in Alcohol Oxidations

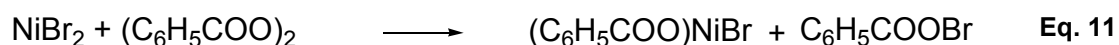
The NiBr<sub>2</sub> mediated benzoylperoxide method produced high yields in the oxidation of secondary alcohols to ketones and selective oxidation of  $\alpha,\omega$ -diols to the corresponding lactones.<sup>78-82</sup> The oxidation of primary alcohols to aldehydes and carboxylic acids showed a strong dependence of the amount of NiBr<sub>2</sub> equivalents added to the oxidation reaction and only produced high yields with activated alcohols such as benzyl alcohol.<sup>78</sup>

In a typical oxidation procedure, a secondary alcohol (10 mmol), NiBr<sub>2</sub> (2.6 mmol) and benzoylperoxide (12.7 mmol) were dissolved in 20 mL anhydrous acetonitrile and heated at 60°C for 24 h.<sup>78</sup> Upon cooling to room temperature and quenching of excess benzoylperoxide with potassium iodide solution, the organic compound was extracted with ether. After removal of the solvent the ketone product was obtained in 81 to 98% isolated yield as the sole product.<sup>78</sup> A list of investigated secondary alcohols is shown in **Table 3.14**.<sup>78</sup>

**Table 3.14** Oxidation of secondary alcohols with the NiBr<sub>2</sub>/ benzoylperoxide method.<sup>78</sup>

Entry	Alcohol	Ketone	Isolated Yield (%)
1	2-adamantanol	2-adamantanone	85
2	Benzhydrol	Benzophenone	85
3	Cyclobutanol	Cyclobutanone	93
4	Cyclopropylphenylmethanol	Cyclopropyl phenyl ketone	81
5	Cyclooctanol	Cyclooctanone	90
6	2,4-dimethyl-3-pentanol	2,4-dimethyl-3-pentanone	84
7	1,2-diphenyl-ethanol	2-phenylacetophenone	94
8	1-phenylethanol	Acetophenone	90

The proposed oxidation reaction mechanism is illustrated in **Scheme 3.28** and involves the formation of benzoylhypobromite by the reaction of nickel(II)bromide and benzoylperoxide (**Eq. 11**).<sup>78</sup> Benzoylhypobromite (**Figure 3.37**) is the active oxidant and oxidizes a secondary alcohol to the corresponding ketone generating benzoic acid and hydrobromic acid as by-products (**Eq. 12**). The strong acid, HBr, reacts with the mixed nickel benzoate bromide salt to form NiBr<sub>2</sub> and benzoic acid (**Eq. 13**). Although the stoichiometry of the reaction is known (**Eq. 14**), the actual oxidation mechanism of the reaction of benzoylhypobromite with a secondary alcohol is not well understood.<sup>78</sup>



**Scheme 3.28** Proposed reaction mechanism with benzoylhypobromite as intermediate.<sup>78</sup>

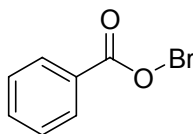
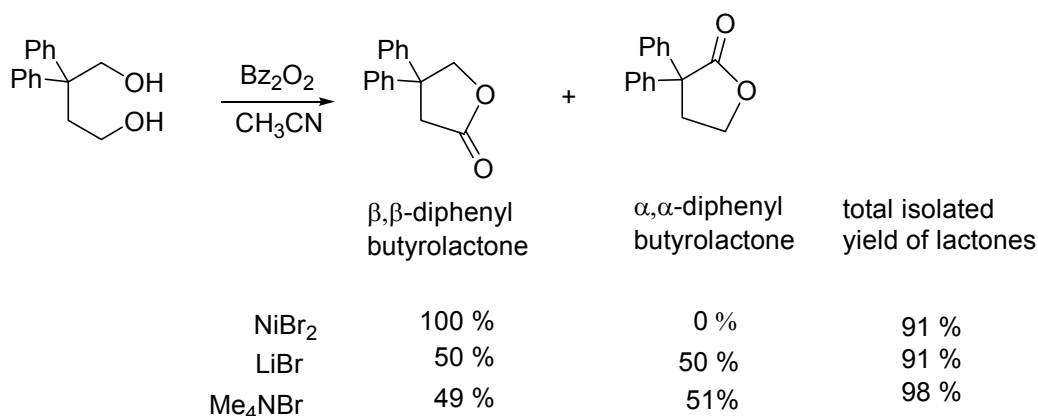


**Figure 3.37** Benzoylhypobromite.

As shown in **Scheme 3.29**, the NiBr<sub>2</sub> mediated benzoylperoxide method demonstrated high regioselectivity in the oxidation of 2,2-disubstitued-1,4-butanediols to the respective α,α- and β,β-disubstituted lactones, which were

obtained in high yields.<sup>79</sup> The regioselectivity only occurred when nickel(II)bromide was used as bromide source. Although the yields of the isolated lactones were high, lithium and tetramethylammonium bromide gave no regioselectivity. The regioselectivity was explained by the formation of a seven membered nickel diol complex, which allows better access for the benzoylhypobromite to the C4 hydroxyl group than the hydroxyl group at C1 as shown in **Figure 3.38**.<sup>82</sup> The two neighbouring phenyl groups at C2 shield the hydroxyl group at C1 from the benzoylhypobromite oxidant attack.



**Scheme 3.29** Regioselectivity of different bromides in the benzoylperoxide oxidation of 2,2-diphenyl-1,4-butanediol to  $\alpha,\alpha$ - and  $\beta,\beta$ -diphenyl-butyrolactones.<sup>79</sup>

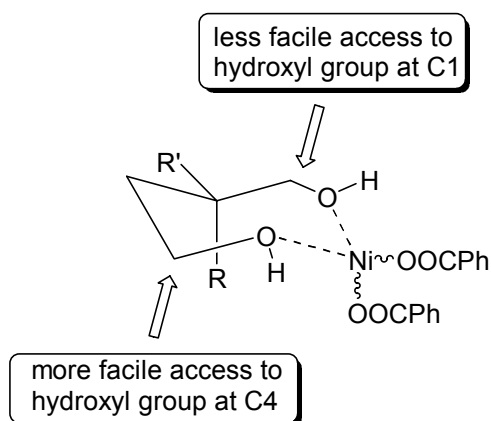


**Figure 3.38** Induction of regioselectivity in the Ni(II)-diol complex.<sup>79</sup>

The high yield and regioselectivity of the  $\text{NiBr}_2$  mediated benzoylperoxide oxidation method consequently prompted us to investigation of this method with regards to the selective oxidation of secondary alcohol functions in sugar substrates.

### 3.3.2.2 Results and Discussion

#### 3.3.2.2.1 Substrate, Oxidant Stoichiometry and Solvent

The reaction conditions and results of the published  $\text{NiBr}_2$  mediated benzoylperoxide method were verified using 1-phenylethanol. After 24 h stirring at  $60^\circ\text{C}$ , 1-phenylethanol oxidized in 92 % conversion to acetophenone. The oxidation reaction was monitored by quantitative GC analysis with naphthalene as internal standard. The obtained conversion is comparable to the isolated yield of 90 % of the published results (**Table 3.14, Entry 8**).

The results of the oxidation of cyclohexanol and cyclopentanol, which have not been previously reported, are shown in **Figure 3.39**. The oxidation of cyclohexanol and cyclopentanol leveled off after 12 h at 74 % and 62 %, respectively. Cyclopentanol and cyclohexanol have a lower oxidation conversion than 1-phenyl ethanol, which is activated as its hydroxyl group is in a benzylic position. At  $60^\circ\text{C}$  the oxidation of the alcohol substrates competes with a thermal decomposition of benzoylperoxide resulting in a lower conversion of the secondary alcohol substrate.

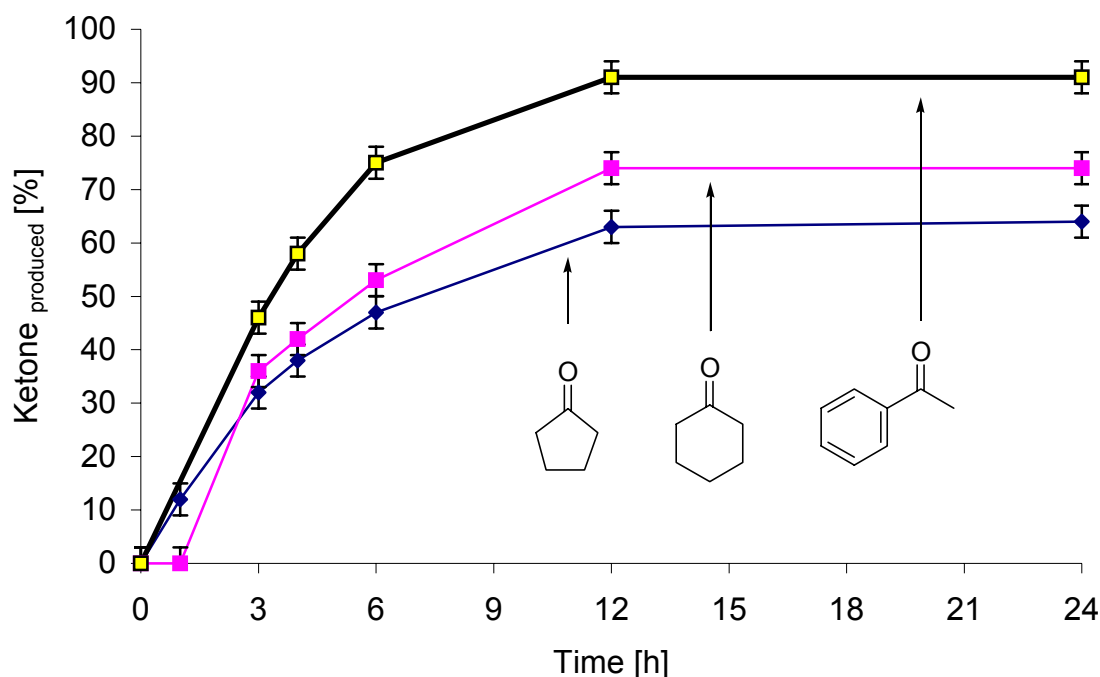


**Figure 3.39** GC analysis results from the oxidation of the three alcohols: 1-phenylethanol, cyclohexanol, and cyclopentanol. Reaction condition: 0.65 mmol alcohol, 0.163 mmol  $\text{NiBr}_2$ , *cis*-decalin (~50 mg) as internal GC standard and 0.81 mmol dry  $\text{Bz}_2\text{O}_2$  in anhydrous acetonitrile (6.0 mL) at 60°C.

Thus, the benzoylperoxide content was doubled to 2.5 equivalents resulting in an oxidation of cyclohexanol in 80 % yield after 24 h compared to 74 % with 1.25 equivalents of benzoylperoxide as illustrated in **Figure 3.40**. The hypothesis of decomposition of the benzoylperoxide oxidant is further supported by an increase in oxidation yield upon further addition of benzoylperoxide to the reaction mixture. E.g. in an oxidation reaction of cyclohexanol with 1.0 equivalent of benzoylperoxide at 60°C the cyclohexanone content leveled off at 65 %. After addition of an extra 1.5 equivalents of benzoylperoxide to the reaction mixture cyclohexanol completely oxidized to cyclohexanone.



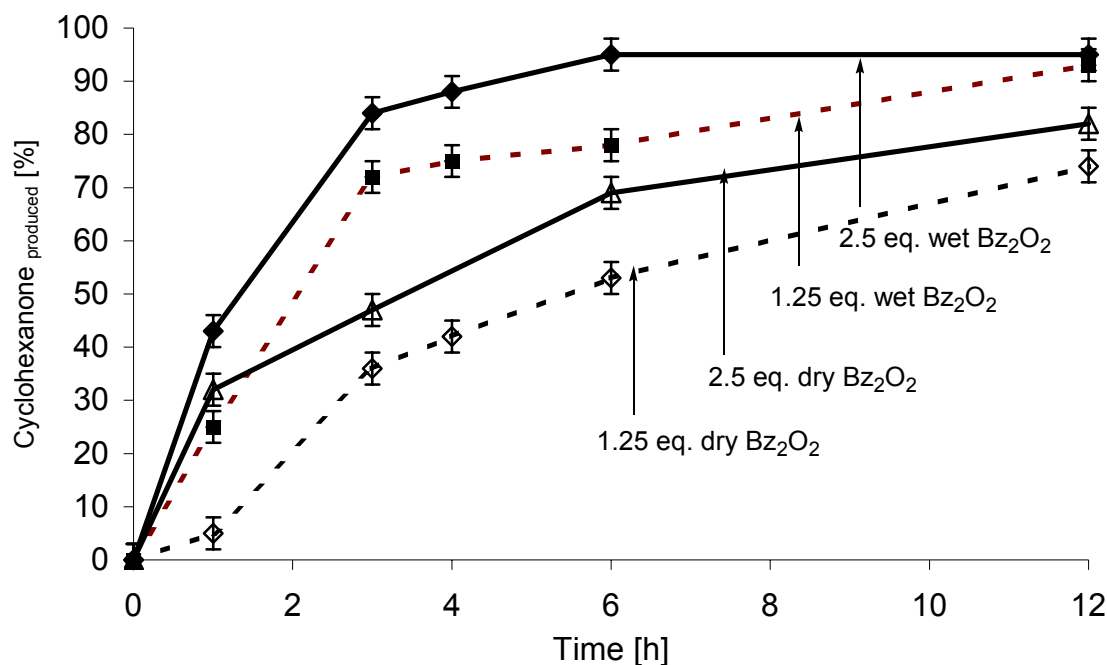


**Figure 3.40** GC analysis results from the oxidation of cyclohexanol. Reaction condition: 0.65 mmol alcohol, 0.163 mmol NiBr<sub>2</sub>, *cis*-decalin (~50 mg) as internal GC standard and Bz<sub>2</sub>O<sub>2</sub> in anhydrous acetonitrile (6.0 mL) at 60°C.. Anhydrous Bz<sub>2</sub>O<sub>2</sub> (open symbols), wet Bz<sub>2</sub>O<sub>2</sub> (filled symbols) 1.25 eq. oxidant (dotted line), 2.5 eq. (solid line).

The method published by Doyle stated anhydrous conditions.<sup>78-82</sup> However benzoylperoxide is generally only available as a 30 % solution in water. Dry benzoylperoxide was therefore generated by dissolving “wet” benzoylperoxide in diethyl ether, adding anhydrous MgSO<sub>4</sub> and filtering. Removal of the ether solvent at room temperature under reduced pressure gave pure dry benzoylperoxide as a pale yellow solid (CAUTION – EXPLOSIVE).<sup>†††</sup>

<sup>†††</sup> The removal of ether to obtain anhydrous benzoylperoxide must be conducted with **extreme caution** as benzoylperoxide is an explosive. Taped, shatter-proofed glassware and an explosion shield must be used and only small amounts of benzoylperoxide (i.e. less than 1 to 2 g) should be dried in one batch.

Subsequently it was however discovered that employing “wet” benzoylperoxide actually increased the reaction rates and conversion of secondary alcohols rendering the above procedure obsolete and greatly enhancing the utility of method from a safety standpoint. For example the oxidation reaction of cyclohexanol was 90 % complete after 6 h (**Figure 3.40**).

Since the actual research motivation was the selective oxidation of unprotected sugar substrates to keto-sugars, DMA was investigated as solvent the with the  $\text{NiBr}_2/\text{Bz}_2\text{O}_2$  system (**Figure 3.41**). In DMA the reaction does not proceed as well as in acetonitrile even with the use of “wet” benzoylperoxide. However, in spite of the lower yield of ~ 50 % all further oxidation reactions were carried out in DMA solvent, as it is a better solvent than acetonitrile for the unprotected sugar.

Under the reaction conditions listed in the captions of the preceeding figures, the water content from the wet benzoylperoxide (30 wt%) employed generates approximately 1 to 2 Vol% water content in the acetonitrile solvent reaction mixture. Based on the observed increase in reaction rate and alcohol conversion in presence of water, more water was added to the DMA system (**Table 3.15**) and it was found that the conversion of cyclohexanol to cyclohexanone increases when the water content was raised from 1 Vol% to 20 Vol% and 30 Vol%. The conversion to cyclohexanone reached a maximum of 98 % yield at 30 % water content, but fell off again to 83 % when a 1:1 water to DMA solvent mixture (i.e. 50 Vol%) was employed. This drop in conversion is however not a kinetic effect but rather rooted in the decreased solubility of the non-polar benzoylperoxide in a 1:1 water to DMA mixture compared to that in a 1:2 mixture. In fact in the 50 Vol% water reaction a small amount of undissolved benzoylperoxide was observed and its effectively available concentration is lower.

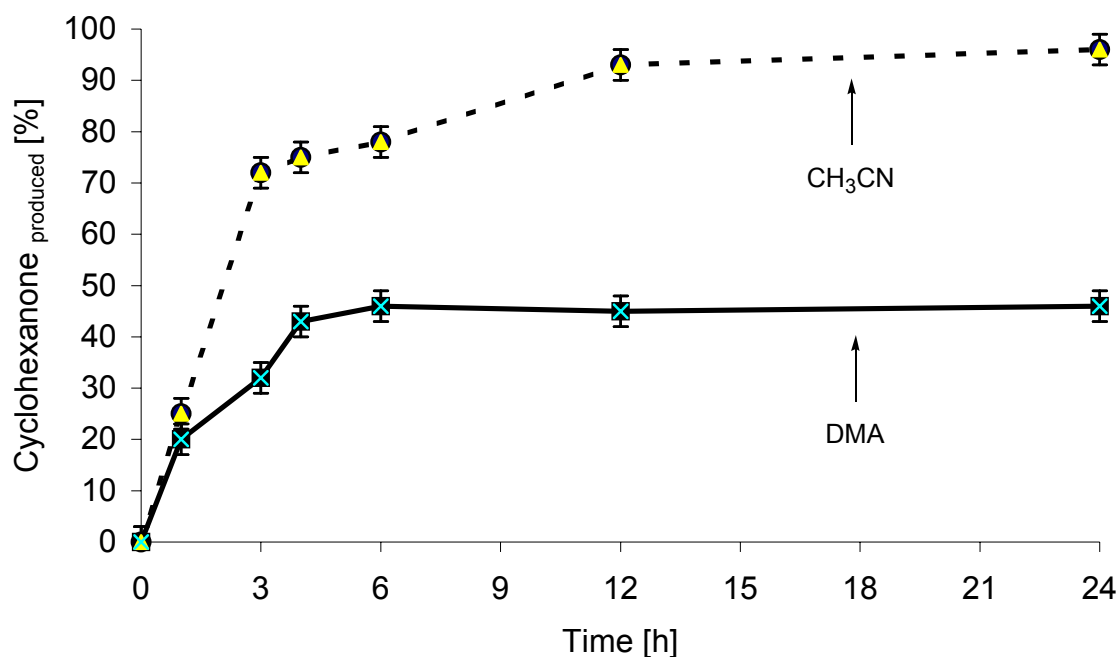


**Figure 3.41** GC analysis results from the oxidation of cyclohexanol. Reaction condition: 0.65 mmol alcohol, 0.163 mmol  $\text{NiBr}_2$ , *cis*-decalin (~50 mg) as internal GC standard and 0.81 mmol wet  $\text{Bz}_2\text{O}_2$  in 6.0 mL solvent at 60°C.

**Table 3.15** Influence of water content on the conversion of cyclohexanol.<sup>a</sup>

Entry	Vol % water in DMA solvent <sup>b</sup>	Conversion (%) of cyclohexanol after 1 h
1	1 Vol%	38 %
2	20 Vol%	95 %
3	30 Vol%	98 %
4	50 Vol%	83 %

<sup>a</sup> Cyclohexanol (0.65 mmol) with benzoyl peroxide (1.3 mmol) and  $\text{NiBr}_2$  (0.16 mmol) with in DMA at 60°C after 1 h. <sup>b</sup> Total solvent volume was 20 mL.

### 3.3.2.2.2 Investigation of the Reaction Mechanism

In order to investigate the role of the water in the increase in reaction rate an IR and UV/VIS experiment was devised. The effect of the order of addition of nickel(II) bromide, cyclohexanol and benzoylperoxide was investigated under

“wet” (i.e. using “wet” benzoylperoxide) and anhydrous conditions. After each addition, the IR and UV/VIS spectrum of the reaction mixture was recorded using  $\text{CaF}_2$  cells. Subtraction of the obtained IR and UV/VIS spectra with the same compounds from different addition sequences resulted in a flat line indicating that there is no dependence of the overall composition of the reaction mixture on the addition sequence of the reactants.

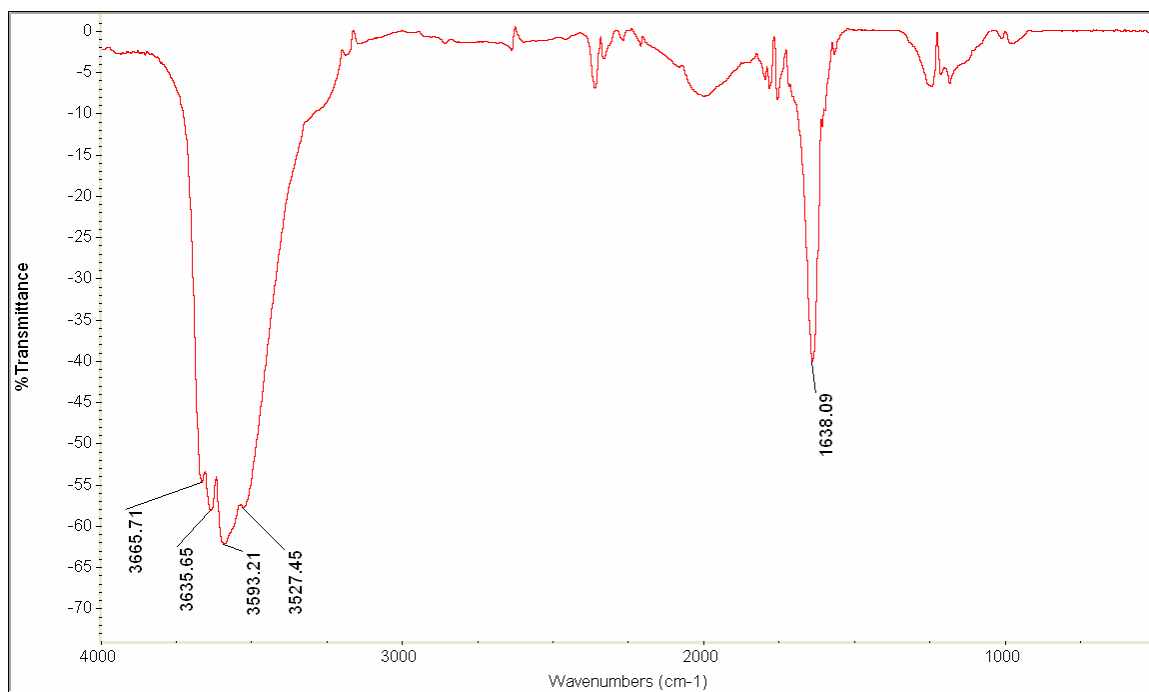
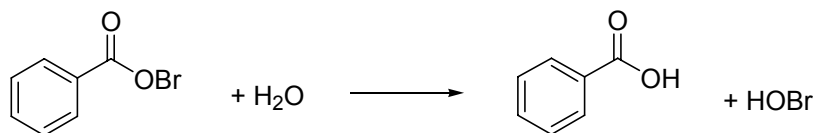


**Figure 3.42** Difference IR spectrum of  $\text{NiBr}_2$ , cyclohexanol and benzoylperoxide in acetonitrile in “wet” conditions subtracted from anhydrous condition.

However, upon comparison of the IR spectra of anhydrous and “wet” conditions<sup>+++</sup> broad hydroxyl bands in the range of  $3500\text{--}3660\text{ cm}^{-1}$  and a strong band at  $1638\text{ cm}^{-1}$  were observed in the difference IR spectrum as shown in **Figure 3.42**. Most likely these peaks originate from benzoic acid and perbenzoic acid formed from by hydrolysis of  $\text{Bz}_2\text{O}_2$  in the presence of water. The observed enhanced reactivity in the presence of water must then be the consequence of a

<sup>+++</sup> IR spectrum of ( $\text{NiBr}_2$ , cyclohexanol and “wet” benzoylperoxide in dry  $\text{CH}_3\text{CN}$ ) subtracted from IR spectrum ( $\text{NiBr}_2$ , cyclohexanol and benzoylperoxide in dry  $\text{CH}_3\text{CN}$ )

higher reactivity of perbenzoic acid with  $\text{Br}^-$  compared to that of the anhydride  $\text{Bz}_2\text{O}_2$  leading in either case to the formation of benzoylhypobromite, which then in turn is hydrolyzed to benzoic acid and hypobromous acid,  $\text{HOBr}$  (**Scheme 3.30**). The actual oxidation mechanism probably involves the formation of a  $\text{Br}^+$ -cation. The  $\text{Br}^+$ -species can be generated from either benzoylhypobromite or hypobromous acid and the reactivity increase with the water system is then ultimately due to the faster generation of  $\text{Br}^+$  with  $\text{HOBr}$  than with benzoylhypobromite.



**Scheme 3.30** Hydrolysis of benzoylhypobromite to benzoic acid and hypobromous acid.

The results for different nickel sources in the oxidation reaction of cyclohexanol with 2.5 equivalents of benzoylperoxide in 1:4 mixtures of water : DMA solvent are listed in **Table 3.16**. In absence of halides no oxidation reaction was observed. After 2 h, the highest conversion was observed with bromide.  $\text{NiBr}_2$  and  $\text{NiBr}_2(\text{PPh}_3)_2$  resulted in 47 % and 37 % conversion of cyclohexanol to cyclohexanone. (**Entries 1 and 2, Table 3.16**). The lower yield with  $\text{NiBr}_2(\text{PPh}_3)_2$  can be explained by the oxidation reaction of the phosphine ligand to the phosphine oxides and dissociation processes thus slowing the oxidation reaction. The cyclohexanone contents in the  $\text{NiCl}_2$  and  $\text{NiI}_2$  mediated oxidation reactions were 23 % and 20 % after 2 h, which probably reflects the different reactivities of the benzoylhypohalides and hypohalide acids. In addition the solubility of  $\text{NiCl}_2$  and  $\text{NiI}_2$  was also small in DMA so that not all catalyst was dissolved.

**Table 3.16** Oxidation of cyclohexanol with different Ni(II) catalysts.<sup>a</sup>

Entry	Nickel Substrate	Conversion <sup>b</sup> / Time
1	NiBr <sub>2</sub> (PPh <sub>3</sub> ) <sub>2</sub>	37 % / 2 h
2	NiBr <sub>2</sub>	47 % / 2 h
3	NiI <sub>2</sub> <sup>c</sup>	20 % / 2 h
4	NiCl <sub>2</sub> <sup>c</sup>	23 % / 2 h
5	Ni(OAc) <sub>2</sub>	No Rxn
6	NiSO <sub>4</sub> ·7H <sub>2</sub> O	No Rxn
7	Ni(ClO <sub>4</sub> ) <sub>2</sub> ·6H <sub>2</sub> O	No Rxn
8	NiO <sub>2</sub> (30% H <sub>2</sub> O)	No Rxn
9	Ni(NO <sub>3</sub> ) <sub>2</sub> ·6H <sub>2</sub> O	No Rxn

<sup>a</sup> Reaction condition: 1.0 mmol alcohol, 0.25 mmol Ni substrate, 1.25 mmol wet Bz<sub>2</sub>O<sub>2</sub> and dimethylsulfone as internal GC standard in DMA at 60°C <sup>b</sup> Determined by GC analysis. <sup>c</sup> Low solubility in DMA.

The results of variation of oxidant sources are listed in **Table 3.17**. *Tert*.-butyl hydroperoxide and *meta*-chloroperbenzoic acid (*m*CPBA) did not oxidize cyclohexanol after 2 days. There was a conversion of approximately 10 % with hydrogen peroxide after 24 h, which is presumably due to unselective oxidation of the H<sub>2</sub>O<sub>2</sub> with the alcohol substrate and does not necessarily originate from the NiBr<sub>2</sub> mediated reaction. Other oxidants containing peroxides such as percarbonate, i.e. Na<sub>2</sub>CO<sub>3</sub> x 1.5 H<sub>2</sub>O<sub>2</sub>, and Oxone®, i.e. salts of persulfuric acid, did not dissolve under the reaction conditions and no reaction was observed. When bromine was employed a complex reaction mixture was observed with the GC-MS analysis of the crude reaction mixture indicating that bromination of α-C had taken place. Common to all those alternative oxidants described is that the generation of benzoylhydropobromite is not possible from these systems.

**Table 3.17** Different oxidizing agents with  $\text{NiBr}_2^{\text{a}}$  and cyclohexanol in DMA at  $60^\circ\text{C}$ .

Entry	Oxidant	Observation/ Result <sup>b</sup>
1	Anhydrous benzoylperoxide	Reaction takes place
2	“wet” benzoylperoxide	Reaction rate is higher than dry $\text{Bz}_2\text{O}_2$
3	1.1 eq. <sup>c</sup> <i>tert.</i> -butylhydroperoxide	No reaction (24 h)
4	2.2 eq. <sup>c</sup> <i>tert.</i> -butylhydroperoxide	No reaction (48 h)
5	1.1 eq. <sup>c</sup> <i>meta</i> -chloroperbenzoic acid	No reaction (48 h)
6	1.1 eq. <sup>c</sup> hydrogen peroxide	10.5 % conversion (24 h)
7	1.1 eq. <sup>c</sup> $\text{Na}_2\text{CO}_3$ : 1.5 $\text{H}_2\text{O}_2$	Not dissolved, no reaction
8	1.1 eq. <sup>c</sup> Oxone® (monopersulfate)	Not dissolved, no reaction
9	1.1 eq. <sup>c</sup> $\text{Br}_2$	Complex reaction mixture

<sup>a</sup> 0.25 eq. with respect to cyclohexanol <sup>b</sup> Determined by GC analysis. <sup>c</sup> Based on 1 eq. cyclohexanol.

All oxidation reactions were monitored by GC and GC-MS. When acetonitrile was used as solvent there was a significant amount of bromobenzene generated. This was unambiguously determined by GC-MS and with an authentic sample. However, if the solvent system was water and DMA the bromobenzene signal was very small. We speculate that bromobenzene was formed via a radical side reaction. It is known that benzoylperoxide is cleaved homolytically under thermal conditions.<sup>12</sup> Upon loss of carbon dioxide the resulting phenyl radical can scavenge a bromine atom generating bromobenzene. As well, benzene was detected in the oxidation reaction. However, as there are small amounts of benzene present in the commercially available benzoylperoxide it is not possible to unambiguously link the benzene to the benzoylperoxide side reaction although the generated phenyl radical generated in the thermal decomposition of benzoylperoxide can in principle lead to the abstraction of a hydrogen from the solvent or substrate and form benzene.

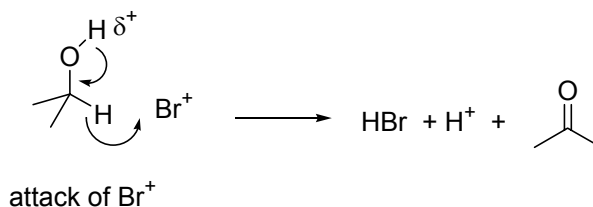
Once the optimized reaction conditions were established, i.e. 0.25 eq.  $\text{NiBr}_2$  and 2.5 eq. benzoylperoxide in 20 Vol% water : DMA solvent at  $60^\circ\text{C}$ , the investigations focussed on the different oxidation rates of various secondary alcohols (**Table 3.18**).

**Table 3.18** Oxidation of different secondary alcohols by the  $\text{NiBr}_2/\text{Bz}_2\text{O}_2$ .<sup>a</sup>

Entry	Alcohol	Conversion to Cyclohexanone <sup>b</sup>	
		1 h	3 h
1	Cyclohexanol	100	—
2	Cyclopentanol	23	100
3	1-Phenylethanol	94	100
4	Menthol	65	86
5	Neomenthol	100	—
6	Isomenthol	36	46

<sup>a</sup> 1.0 mmol alcohol, 0.25 mmol  $\text{NiBr}_2$ , 2.5 mmol “wet”  $\text{Bz}_2\text{O}_2$  and dimethyl sulfoxide as internal standard in 6.0 mL DMA at 60°C. Determined by GC.

Cyclohexanol is completely oxidized to cyclohexanone within 1 h and cyclopentanol requires 3 h for quantitative oxidation. The investigation of steric influences in the “menthol-series” showed that the oxidation of neomenthol was completed after 1 h while after the same period menthol was only 65 % converted and isomenthol 36 %. There is a preference for the oxidation of axial vs. equatorial OH functions studied in the menthol derivatives series, as the reactivity decreases from neomenthol > menthol > isomenthol. With  $\text{Br}^+$  postulated as the actual oxidant abstraction of a hydrogen atom from an equatorial position is preferred over abstraction from an axial position as the latter is more shielded due to 1,3-diaxial interactions (**Scheme 3.31**).

**Scheme 3.31** Proposed oxidation step.

In order to demonstrate the versatility of this reaction not only by GC results, the “menthol-series” products were isolated from an upscaled reaction batch. The work-up procedure involved controlled destruction of unreacted oxidant by slow



addition of saturated sodium thiosulfate solution, alkalization of the aqueous solution with sodium bicarbonate and extraction of the organic compounds with diethyl ether. The ether solvent was removed under reduced pressure and the products were recovered in 75 to 85 %. Loss of mass was due to the volatility of the oxidized methone products in the organic solvent removal step.

#### 3.3.2.2.3 Oxidation of Diols

The established oxidation conditions were then adapted to the oxidation of *cis*- and *trans*-1,2-cyclohexanediol using 0.5 mmol diol, 0.25 mmol NiBr<sub>2</sub> and 1.25 mmol benzoylperoxide in 4.9 mL DMA and 1.6 mL water at 60°C as the reaction conditions. As the internal standard an accurately weighed amount of naphthalene (~ 50 mg) was added to each reaction and the oxidation reaction monitored by quantitative GC.

In both diol oxidations consumption of the diol starting material was observed after 6 h, however a multitude of signals appeared in the GC traces, indicating that side reactions occurred. An analysis of the reaction mixtures by GC-MS revealed that brominated organic species were present in the reaction mixture as characteristic M and M+2 signals in almost 1:1 ratios representing the two abundant bromine isotopes were observed, however a full characterization of the brominated species was beyond our research objective and was therefore not further pursued. A lowering of the reaction temperature from 60°C to room temperature slowed the oxidation reaction but brominated compounds were still detected by GC and GC-MS analysis.

#### 3.3.2.3 Conclusion

The reactivity of the nickel(II)bromide mediated benzoylperoxide method for the oxidation of secondary alcohols to ketones was greatly improved by the development of an aqueous reaction protocol. The aqueous protocol allows the

direct use of commercially available  $\text{Bz}_2\text{O}_2$  solutions and gives higher yields with shorter reaction times. The oxidation reaction tolerates DMA solvent, however a slower oxidation rate is observed than in acetonitrile. A thermal decomposition of  $\text{Bz}_2\text{O}_2$  resulting in the formation of bromobenzene as a ubiquitous reaction side product competes with the oxidation of secondary alcohols. Exhaustive oxidation of the alcohol substrates therefore requires more than the stoichiometric amount of peroxide. The oxidation of diol compounds such as *cis*- and *trans*-1,2-cyclohexanediol failed with this method as  $\alpha$ -hydroxy cyclohexanone and 1,2-cyclohexanedione undergo side-reactions with the bromine oxidant yielding brominated species as the dominant reaction products.

### 3.3.2.4 Experimental Section

**CAUTION:** THE HANDLING OF SOLID PEROXIDE IS DANGEROUS AND CAN YIELD TO EXPLOSIONS ! EXTREME CAUTION IS ADVISED. EXCESS PEROXIDE IS TO BE DESTROYED WITH AQUEOUS SATURATED SODIUM THIOSULFATE SOLUTION. HANDLE ONLY SMALL QUANTITIES AT ANY TIME. THE GLASSWARE SHOULD BE TAPED FOR SHATTERPROOFNESS AND AN EXPLOSION-SHIELD SHOULD BE USED !!

**General procedure for small scale oxidations:** In an 8 mL screw top vial, alcohol (0.50 mmol), bromide salt (0.25 mmol = 0.5 eq. with respect to available bromide and alcohol) and naphthalene (~50 mg) are dissolved in 4.9 mL DMA and 1.6 mL water at 60°C. A GC sample is withdrawn defining the reaction mixture at  $T=T_0$ . After addition of benzoyl peroxide (1.25 mmol) the reaction mixture is stirred at 60°C and GC samples withdrawn at defined time intervals (typically every h). After the completion of the experiment the reaction mixture is safely destroyed by addition of a saturated, aqueous sodium thiosulfate solution.

**General procedure for large-scale oxidations:** In a 100 mL round-bottom flask, alcohol (2.0 mmol) and bromide salt (1.0 mmol = 0.5 eq. with respect to available bromide and alcohol) in 20 mL DMA and 7 mL water are stirred at 60°C. The reaction is stopped by quenching with sodium thiosulfate (1.0 g) and NaHCO<sub>3</sub> (0.8 g) in 15 mL water and stirring for 10 min. After cooling to RT, the reaction mixture is extracted with 4 x 25 mL diethyl ether. The combined organic solvents are washed with 4 x 20 mL water, dried over MgSO<sub>4</sub> and the solvent is removed under reduced pressure at RT. Without further purification, the ketone product was characterized by GC-MS and NMR spectroscopy and congruent to literature values.

### 3.4 Investigated Stoichiometric Oxidation Reaction

#### 3.4.1 Introduction to the NaBrO<sub>3</sub>/ NaHSO<sub>3</sub> System

A stoichiometric mixture of sodium bromate and sodium bisulfate has been reported to selectively oxidize *vicinal* diols to  $\alpha$ -hydroxy ketones with little or no over oxidation.<sup>83,100</sup> For example,  $\alpha$ -hydroxy cyclohexanone was obtained in 95 % isolated yield from 1,2-cyclohexanediol after slow addition of NaHSO<sub>3</sub> to the diol and NaBrO<sub>3</sub> reagents and stirring for 2 h at room temperature.  $\alpha$ -hydroxy cyclooctanone was obtained in 69 % yield with only 3 % overoxidation to the dione compound. A fast addition of bisulfite to bromate resulted in increased overoxidation, e.g. trace amounts of  $\alpha$ -hydroxy cyclooctanone and 94 % 1,2-cyclooctanone.

The simple oxidation reaction conditions for the NaBrO<sub>3</sub>/ NaHSO<sub>3</sub> reagent are particularly useful for organic syntheses, as the chemicals are commercially available and inexpensive off-the-shelf compounds. Yet, the actual reaction mechanism is very intriguing and displays good chemoselectivity. In a remarkable methodology, a mild oxidizing agent is generated *in situ* by addition

of both, an oxidant, sodium bromate, and a reductant, sodium bisulfite. Ishii *et al.* postulated that the actual oxidant was hypobromous acid, HOBr, as bromohydrins are formed when the reagent reacts with C=C bonds.<sup>83,84</sup> The NaBrO<sub>3</sub>/ NaHSO<sub>3</sub> reagent has also been successfully employed in the  $\gamma$ -lactone formation of *o*-alkyl substituted benzoic acids.<sup>85</sup> Other reactions that make use of bromate together with reducing agents are the Belousov Zhabotinskii class of oscillating reactions.<sup>86,87</sup> Metsger *et al.* reported that the oxidation of alkyl ethers occurred in  $\alpha$ -position by Br<sub>2</sub>, which is generated through the comproportionation reaction of bromate and bromide to provide a low but steady concentration of bromine.<sup>88</sup>

Here we report additional insights into the selective oxidation of *vicinal* diols to the corresponding  $\alpha$ -hydroxy ketones using the NaBrO<sub>3</sub>/NaHSO<sub>3</sub> reagent, specifically its scope and limitations with respect to *pH*, diol substrates, its reaction mechanism and the origin of the chemoselectivity.

### 3.4.2 Results

Oxidation reaction experiments were conducted on a small scale (4.2 mL, 0.24 M diol substrate) and monitored by quantitative gas chromatography calibrated against dimethyl sulfone as the internal standard. Oxidation products were identified by GC-MS and by comparison with authentic commercial samples when available. The oxidation experiments of the monosaccharide substrates were conducted on an NMR scale in D<sub>2</sub>O (0.7 mL, 0.24 M substrate) and directly monitored by <sup>1</sup>H and <sup>13</sup>C NMR spectroscopy.

#### 3.4.2.1 *pH* dependence

The oxidation reaction of *trans*-1,2-cyclohexanediol exhibited a strong *pH* dependence (**Table 3.19**), an important observation that has previously not been

reported. The reaction stoichiometry of diol substrate, sodium bromate and sodium bisulfite was adopted from the established oxidation procedure published by Ishii *et al.*<sup>83</sup> **Entry 2** corresponds to the reaction condition reported by Ishii *et al.*, resulting in an initial *pH* of 1.7.<sup>83</sup> Changes of the *pH* of the reaction solution were accomplished by addition of sulfuric acid or Na<sub>2</sub>HPO<sub>4</sub>. The desired  $\alpha$ -hydroxy cyclohexanone product was generated almost quantitatively within 1 h to 24 h while the overoxidation product, 1,2-cyclohexanedione, was only present in 0-5%. It was found that the oxidation reaction proceeded only in acidic solution at *pH* values < 4 and that the oxidation reactions were faster at lower *pH*. When the oxidation was completed the final *pH* values of the reaction solutions were higher than the initial *pH* values by approximately 0.5 units. In a control experiment, Na<sub>2</sub>SO<sub>3</sub> – instead of NaHSO<sub>3</sub> – was reacted with sodium bromate and no reaction occurred within 48 h (**Entry 5**). With *trans*-1,2-cyclohexanediol as the substrate, a reaction solution containing Na<sub>2</sub>SO<sub>3</sub> and NaBrO<sub>3</sub> had an only slightly acidic *pH* of 5. When this reaction solution was subsequently acidified with 0.5 equivalents of conc. sulfuric acid (0.6 mmol, 1.2 equiv. of H<sup>+</sup>) resulting in *pH* of 1.7, the oxidation reaction immediately proceeded as with the original NaHSO<sub>3</sub>/ NaBrO<sub>3</sub> reaction condition (**Entry 2**).

**Table 3.19** *pH* dependence of the effectiveness of the NaBrO<sub>3</sub>/NaHSO<sub>3</sub> reagent in the oxidation of *trans*-1,2-cyclohexanediol<sup>a</sup>.

Entry	<i>pH</i> <sub>initial</sub>	<i>pH</i> <sub>final</sub>	$\alpha$ -hydroxy cyclohexanone % (t) <sup>b</sup>
1	0 <sup>c</sup>	0.5	95 % (1 h)
2	1.7	2.3	74 % (4 h) 97 % (24 h)
3	2.3 <sup>d</sup>	2.8	25 % (4 h) 70 % (24 h)
4	4.0 <sup>d</sup>	4.4	No Reaction (48h)
5 <sup>e</sup>	5	5	No Reaction (48h)
	1.7 <sup>f</sup>	2.3	74 % (4 h) 97 % (24 h)

<sup>a</sup> Reaction conditions: 1.0 mmol diol, 1.2 mmol NaBrO<sub>3</sub>, 1.2 mmol NaHSO<sub>3</sub> in 2.2 mL H<sub>2</sub>O and 2.0 mL CH<sub>3</sub>CN at 21°C  $\pm$  1°C <sup>b</sup> Determined by GC. Content of 1,2-cyclohexanedione was < 5 %. <sup>c</sup> H<sub>2</sub>SO<sub>4</sub> added until desired *pH*<sub>initial</sub> value reached. <sup>d</sup> Na<sub>2</sub>HPO<sub>4</sub> added until desired *pH*<sub>initial</sub> value reached. <sup>e</sup> 1.2 mmol Na<sub>2</sub>SO<sub>3</sub> <sup>f</sup> Addition of 0.6 mmol H<sub>2</sub>SO<sub>4</sub>.

### 3.4.2.2 NaBrO<sub>3</sub>/ NaHSO<sub>3</sub> Reagent Stoichiometry

Various bromate and bisulfite amounts were added to *trans*-1,2-cyclohexanediol substrate in order to investigate the optimum oxidation reaction condition for the NaBrO<sub>3</sub>/ NaHSO<sub>3</sub> reagent (**Table 3.20**). Ishii *et al.* reportedly applied equal molar sodium bromate and sodium bisulfite quantities in slight excess with respect to the diol substrate (**Entry 2**).<sup>83</sup> Throughout all reactions (**Entries 1-12**), the initial concentration of *trans*-1,2-cyclohexanediol (0.24 M, 1.0 mmol) was held constant and yields of  $\alpha$ -hydroxy cyclohexanone were determined by quantitative GC analysis. Generally, it was found that even with more equivalents of oxidant, the 1,2-cyclohexanedione yield was not significantly increased always remaining in the range of 0-5%. An equimolar ratio of NaBrO<sub>3</sub> and NaHSO<sub>3</sub> in half to three equivalences with respect to the diol substrate generated the  $\alpha$ -hydroxy ketone quantitatively within 2 h to 120 h (**Entries 1-4**). The 1,2-cyclohexanedione content was 15% at the extended reaction time of 120 h (**Entry 1**). No reaction – neither oxidation nor reduction – of *trans*-1,2-cyclohexanediol occurred when sodium bromate and sodium bisulfite were added individually (**Entries 5 and 6**). The oxidation reaction leveled off at 51% conversion after 48 h when the relative ratio of bromate and bisulfite was 0.6 mmol to 1.2 mmol (**Entry 7**). However, addition of 1.2 mmol bromate and 2.4 mmol bisulfite to the diol substrate completed the oxidation reaction within 24 h (**Entry 9**). An oxidation reaction was not observed when the NaBrO<sub>3</sub> : NaHSO<sub>3</sub> ratio was less than 1 : 3 (**Entries 10-12**). Quantitative oxidation was observed with 1.2 mmol of NaBrO<sub>3</sub> and 0.6 mmol of NaHSO<sub>3</sub> within 48 h (**Entry 8**).

The colour of the NaBrO<sub>3</sub>/ NaHSO<sub>3</sub> oxidation solution is an excellent indicator for oxidation activity. The oxidation reaction proceeded only when the solution was yellow-orange coloured. No reaction occurred when the solution was colourless. The initial yellow colour of the oxidation reaction of **entry 7** disappeared when the  $\alpha$ -hydroxy-cyclohexanone content leveled at 51%. In a control experiment, it was found that the colour change was very sensitive to the amount of bromate,

bisulfite, sulfite and sulfuric acid. Adjusting the *pH* of the reaction solution with sulfuric acid (1.2 N) or NaOH (1.2 N) through a burette or Pasteur pipette changed the colour of the solution with one extra drop. The yellow colour/colourless sequence occurred fully reversibly when base and acid were alternatively added. When neutral or basic sulfite solutions were acidified quickly by addition of conc. sulfuric acid brown vapours of bromine were generated. The addition order of NaBrO<sub>3</sub>, NaHSO<sub>3</sub> or Na<sub>2</sub>SO<sub>3</sub> and H<sub>2</sub>SO<sub>4</sub> is irrelevant. Each different order of addition produced the same yellow coloured oxidizing reagent solution with the same activity towards the *trans*-1,2-cyclohexanediol substrate.<sup>89</sup>

**Table 3.20** *Trans*-1,2-cyclohexanediol oxidation with varying amounts of NaBrO<sub>3</sub> and NaHSO<sub>3</sub> reagent.<sup>a</sup>

Entry	NaBrO <sub>3</sub> (mmol)	NaHSO <sub>3</sub> (mmol)	<i>pH</i> <sub>initial</sub>	$\alpha$ -OH ketone % (time) <sup>b</sup>	Colour
1	0.6	0.6	2.0	20 % (1 h) 55 % (24 h) 70 % (48 h) 85 % (120 h) <sup>c</sup>	Yellow
2	1.2	1.2	1.7	74 % (4 h) 97 % (24 h)	Yellow
3	2.4	2.4	1.5	60 % (1 h) 96 % (4 h)	Yellow
4	3.6	3.6	1.3	73% (0.5 h) 100 % (2 h)	Yellow
5	1.2	0	5.0	No reaction	Colour-less
6	0	1.2	5.0	No reaction	Colour-less
7	0.6	1.2	1.8	15 % (1 h) 48 % (24 h) 51 % (48 h)	Yellow, colourless (48 h)
8	1.2	0.6	2.0	30 % (1 h) 54 % (6 h) 87 % (24 h) 98 % (48 h)	Light yellow
9	1.2	2.4	1.6	34 % (1 h) 54 % (4 h) 96 % (24 h)	Orange
10	1.2	3.6	1.0	No reaction	Colour-less
11	1.2	4.8	1.4	No reaction	Colour-less
12	0.6	1.8	1.3	No reaction	Colour-less

<sup>a</sup> Reaction conditions: 1.0 mmol diol in 2.2 mL H<sub>2</sub>O and 2.0 mL CH<sub>3</sub>CN at 21°C  $\pm$  1°C.<sup>b</sup> Determined by GC based on  $\alpha$ -hydroxy ketone. Content of dione was < 5 %.<sup>c</sup> Final 1,2-cyclohexanedione content was 15%.

To explore the possibility of deactivation or formation of other species originating from the oxidizing agent, four reagent solutions containing sodium bromate (1.2 mmol) and sodium bisulfite (1.2 mmol) were prepared and stirred for 24 h and 7 d at room temperature and 60°C, respectively. These prepared reagent solutions were then added to *trans*-1,2-cyclohexanediol (1.0 mmol) solutions at room temperature.<sup>90</sup> In each of the four experiments, the oxidation reaction proceeded quantitatively to the  $\alpha$ -hydroxy cyclohexanone and was identical to the reaction condition when the diol substrate and the NaBrO<sub>3</sub>/ NaHSO<sub>3</sub> reagent solution were combined immediately upon preparation.

#### 3.4.2.3 Solvent and Temperature

The NaBrO<sub>3</sub>/ NaHSO<sub>3</sub> reagent was active in various solvents such as pure water, aqueous-acetonitrile and aqueous-*N,N*-dimethylacetamide. The *trans*-1,2-cyclohexanediol oxidation reactions proceeded in these three solvent systems with similar reaction times, conversions and selectivities comparable with Ishii's published conditions using aqueous-acetonitrile solutions.<sup>83</sup> An increase of reaction rates without the formation of side products or degradation of substrate or oxidant was found when the temperature was increased from ambient temperature to 45°C and 60°C. The conversions of *trans*-1,2-cyclohexanediol to  $\alpha$ -hydroxy cyclohexanone were quantitative after 24 h, 6 h and 2 h, respectively. The contents of the overoxidation product, 1,2-cyclohexane-dione, were not significantly different and again remained within  $\leq 5\%$ .

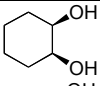
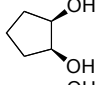
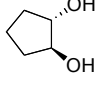
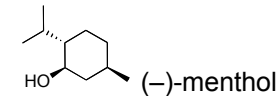
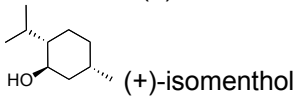
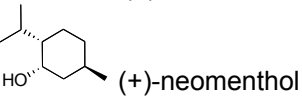
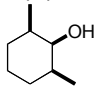
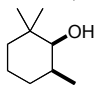
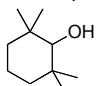
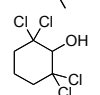
#### 3.4.2.4 Substrates

In order to investigate the reactivity and selectivity of the oxidation of sugar substrates, we focused on relative reactivity of *cis* and *trans vicinal* diols. Using Ishii's standard reaction conditions, the oxidation results for the diol substrates showed that the *cis* compounds were slightly more reactive than their corresponding *trans* isomers (**Table 3.19, Entries 1-3; Table 3.20, Entry 2**). The cyclopentanediol compounds were oxidized marginally slower than their cyclohexanediol homologues.



The influence of steric hindrance on the reactivity of secondary alcohols was explored by the oxidation of a series of monoalcohols (**Table 3.21**, **Entries 4-10**). The steric positioning of the hydroxyl function in cyclic systems with respect to an alkyl substituent in axial or equatorial position was investigated using menthol isomers and cyclohexanol derivatives. In solution, the hydroxyl functionality is predominantly equatorially oriented in (–)-neomenthol and axially in (+)-isomenthol. It has an intermediate axial-equatorial position in (–)-menthol. (–)-Menthol was oxidized in 2 h while its hydroxyl epimer, (+)-neomenthol, required less than 15 min to produce (–)-menthone. (+)-isomenthol was oxidized to (+)-isomethone in 8 h.

**Table 3.21** Oxidation of various diols and monoalcohols with NaBrO<sub>3</sub>/NaHSO<sub>3</sub> reagent.<sup>a</sup>

Entry	Diol/ monoalcohol substrate	Conversion % (t) <sup>b</sup>
1		64 % (1 h) 99 % (6 h)
2		64 % (1 h) 98 % (24 h)
3		50 % (1 h) 89 % (24 h)
4	 (–)-menthol	85 % (1 h) 100 % (2 h)
5	 (+)-isomenthol	34 % (1 h) 100 % (8 h)
6	 (+)-neomenthol	100 % (<15 min)
7		100% (1 h)
8		98 % (1.5 h)
9		100 % (2 h)
10		0 % (24 h)

<sup>a</sup>Reaction conditions: 1.0 mmol diol, 1.2 mmol NaBrO<sub>3</sub>, 1.2 mmol NaHSO<sub>3</sub> in 2.2 mL H<sub>2</sub>O and 2.0 mL CH<sub>3</sub>CN at RT and pH 1.7.

<sup>b</sup>Determined by GC based on α-hydroxy ketone or ketone. Content of dione was < 5 %. <sup>c</sup>21°C ± 1°C

Additional methyl groups alpha to the secondary alcohol functionality decreased the reactivity to the corresponding ketone compound only marginally (**Entries 7-9**). While the 2,2,6,6-tetramethylcyclohexanol was oxidized within 2 h, the oxidation of 2,2,6,6-tetrachlorocyclohexanol failed with the NaBrO<sub>3</sub>/ NaHSO<sub>3</sub> reagent (**Entries 9 and 10**).

The intrinsic challenges associated with the quantitative and qualitative detection of monosaccharide substrates and their reaction products by GC or GC-MS<sup>91</sup> lead us to conduct <sup>1</sup>H and <sup>13</sup>C NMR experiments in D<sub>2</sub>O instead. As demonstrated above, the reactivity of the NaBrO<sub>3</sub>/ NaHSO<sub>3</sub> reagent in aqueous-acetonitrile solutions was similar to water solvent systems. Methyl α-D-glucopyranoside (**99**), methyl α-D-galactopyranoside (**100**), methyl α-D-manno-pyranoside (**101**) and 1,6-anhydro-D-glucopyranoside (**102**) were examined under the NaBrO<sub>3</sub>/ NaHSO<sub>3</sub> oxidation conditions (**Figure 3.43**). No reaction occurred after 24 h at room temperature and thus the four samples were heated to 60°C. A slow oxidation process then occurred but after 5 d the sugar substrates had reacted unselectively to complex intractable product mixtures.

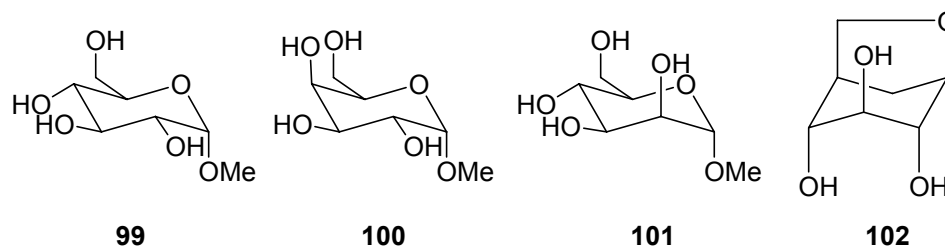
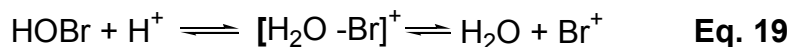
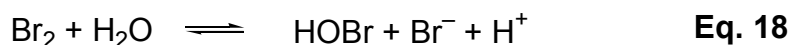
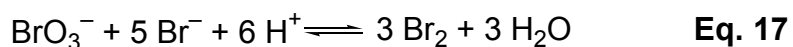
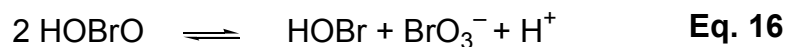
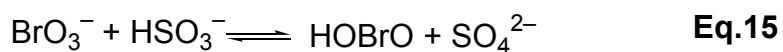


**Figure 3.43** Investigated monosaccharide substrates.

#### 3.4.2.5 Other Oxidizing Conditions

Control experiments were conducted in order to determine the oxidation mechanism and active oxidizing species. As elemental bromine could be a

possible oxidant, one equivalent of Br<sub>2</sub> was added to an aqueous-acetonitrile solution containing *trans*-1,2-cyclohexanediol. The reaction solution was yellow coloured and produced a complex product mixture, which was analyzed by GC-MS and contained α-hydroxy cyclohexanone, various brominated species and other undetermined compounds. To simulate a low but steady Br<sub>2</sub> concentration in the reaction solution, a diluted Br<sub>2</sub> solution (1 equiv.) was added with a syringe pump over a 6 h time period. Again, a complex product mixture was obtained containing α-hydroxy cyclohexanone along with a complex mixture of other products, albeit, less side products were formed. In the NaBrO<sub>3</sub>/ NaHSO<sub>3</sub> oxidation condition, no brominated side products were detected by GC-MS. Hypobromous acid, HOBr, was produced by mixing equal amounts of aqueous equimolar AgNO<sub>3</sub> and Br<sub>2</sub> solutions.<sup>92</sup> The *trans*-1,2-cyclohexanediol oxidation with *in situ* generated HOBr yielded a complex mixture of products after 6 h in stark contrast to chemoselective oxidation with the NaBrO<sub>3</sub>/ NaHSO<sub>3</sub> reagent.



### 3.4.3 Discussion

In consideration of above results, the nature of the active oxidant, the role of protons and the overall mechanism of the diol oxidation by the NaBrO<sub>3</sub>/ NaHSO<sub>3</sub> system remains elusive, however a few clear features of the apparently complex system emerge and certain conclusion can be made.

#### 3.4.3.1 Equilibria and HOBr

Ishii suggested that hypobromous acid, HOBr, is the actual oxidizing species as bromohydrins are synthesized when the NaBrO<sub>3</sub>/ NaHSO<sub>3</sub> reagent reacts with C=C double bonds.<sup>83,93</sup> It is however not immediately obvious that HOBr, is the actual oxidizing species, considering that a 1:1 NaBrO<sub>3</sub> : NaHSO<sub>3</sub> reagent would generate one equivalent of bromous acid, HOBrO, as bisulfite is oxidized to sulfate through a formal transfer of oxygen from bromate (**Eq. 15**). Disproportionation of HOBrO could then generate HOBr, but also reform bromate (**Eq. 16**), ultimately requiring an excess of bisulfite, but as our stoichiometry study showed the ratio of NaHSO<sub>3</sub> to NaBrO<sub>3</sub> does only influence the rate of reaction but not the selectivity of the oxidation. Therefore, the actual oxidant is probably not directly generated by NaHSO<sub>3</sub> and NaBrO<sub>3</sub> but through a cascade of intricate equilibria involving at least all of the steps listed in **Equation 15-20**. Thus the different bromo-species and potential oxidants HOBrO<sub>2</sub>, HOBrO, HOBr, Br<sup>•</sup>-radical, Br<sub>2</sub> and Br<sub>3</sub><sup>-</sup> can be produced in the reaction solution in various concentrations.<sup>86,87,94-97</sup> The NaBrO<sub>3</sub>/ NaHSO<sub>3</sub> reagent is not deactivated when kept at 60°C for 7 days. Thus the actual oxidant must be fairly stable and does not undergo side reactions once the equilibrium has been established.

#### 3.4.3.2 pH Dependence

Protons play a key role in the oxidation mechanism. The increased reaction rate at lower pH<sub>initial</sub> can be explained if Br<sup>+</sup> – or [Br-OH<sub>2</sub>]<sup>+</sup> – were the actual oxidizing

agent.  $\text{Br}^+$  formation is favoured at higher  $\text{H}^+$  concentration because the dehydration of  $\text{HOBr}$  is proton dependent (**Eq. 19**). Comproportionation and disproportionation reactions are known to proceed at  $\text{pH}$  1.5 to 2.5,<sup>97</sup> which asserts our experimental work as yellow colour and oxidation activity was only detected when the solution  $\text{pH}$  was  $< 4$ .

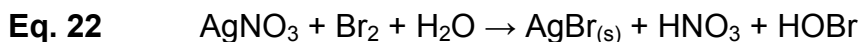
Furthermore, during the oxidation process the  $\text{pH}$  of the reaction solution increased, suggesting that protons were consumed. This is on first sight contradictory as the oxidation of a secondary alcohol with  $\text{HOBr}$  generates a proton along with bromide and carbonyl compound (**Eq. 21**). Another equilibrium must be responsible for the overall consumption of protons. As bromide ions are continuously produced, the comproportionation reaction of bromate and bromide to hypobromous acid will require a total of three protons (**Eq. 16** and **17**). The reaction is autocatalytic with respect of  $\text{Br}^-$  and a continuous low and steady regeneration of  $\text{HOBr}$  concentration is therefore established.



### 3.4.3.3 Control Experiments

The yellow colour – an indicator for oxidation activity – can be associated with  $\text{HOBr}$  and  $\text{Br}_2$  but not with bromide, bromate, sulfite and sulfate anions which are all colour-less.<sup>83</sup>  $\text{Br}_2$ , a potential active oxidant proposed by Metsger *et al*<sup>83</sup>, is probably not the active oxidant, as a very slow addition of diluted  $\text{Br}_2$  solution to the diol substrate to produce a low and steady  $\text{Br}_2$  concentration generated many side products of which some were bromo-species, while under our standard experimental  $\text{NaBrO}_3/\text{NaHSO}_3$  reaction conditions no carbon-bromine species have been detected. Ishii was able to isolate bromo-species only if a  $\text{C}=\text{C}$  double bond was present in the substrate.<sup>83</sup> This is an indicator that the mechanism is probably ionic rather than radical. In a control experiment when  $\text{HOBr}$  was

generated *in situ* from bromine and silver nitrate (**Eq. 22**),<sup>92</sup> the reaction products contained brominated species. However the HOBr concentration in the control experiment was presumably relative high so that HOBr can undergo bromination side reactions in contrast to a low and steady concentration generated by the NaBrO<sub>3</sub> / NaHSO<sub>3</sub> reagent.

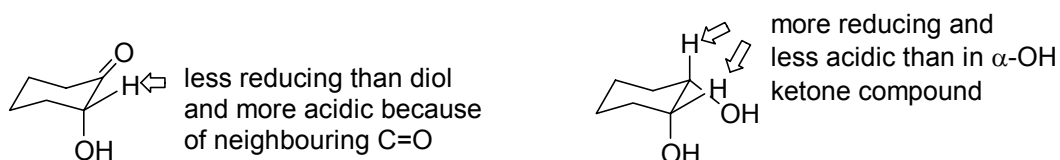


### 3.4.3.4 Oxidation Mechanism and Selectivity

The actual oxidation can in principle either occur directly at the hydroxyl function or at the alpha-position through an enol type intermediate. An oxidation mechanism that proceeds through an enol of the organic compound can however be excluded, as the complete oxidation of 2,2,6,6-tetramethylcyclohexanol, which contains no alpha-hydrogen, proceeded at similar reaction rates as the di- and trimethylated cyclohexanol derivatives.

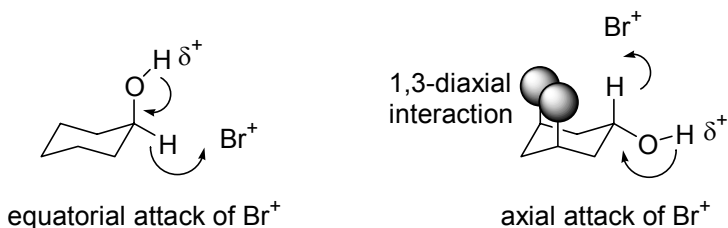
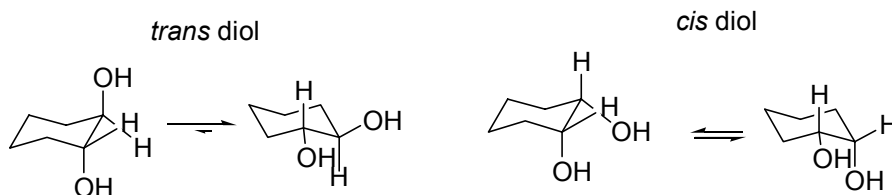
Based on the observed *pH* dependence, we now postulate that a small but persistent and continuously replenished concentration of Br<sup>+</sup> or possibly [H<sub>2</sub>O-Br]<sup>+</sup> rather than neutral HOBr as proposed by Ishii is the actual oxidizing agent. It is then logical to expect it to preferentially attack the least acidic hydrogens geminal to the OH functional group.

Once the first oxidation to the α-hydroxy ketone has occurred, the polarization of the remaining geminal H is slightly less negative than that in a vicinal diol as the carbonyl group withdraws electron density (**Scheme 3.32**) resulting in the observed chemoselectivity of diol oxidation.



**Scheme 3.32** Geminal hydrogen polarization in  $\alpha$ -hydroxy ketone and diol.

The preferential selectivity of axial vs. equatorial OH functions studied in the menthol derivatives series, can then also be rationalized by postulating  $\text{Br}^+$  as the actual oxidant which attacks the geminal hydrogen of the hydroxyl group (**Scheme 3.33**). An equatorial attack from the oxidant is more preferred than an axial attack, which is more shielded due to 1,3-diaxial interactions. This is also applicable for *cis*-diols which were oxidized faster than the *trans*-diol as there is always one geminal hydrogen in axial position while in the *trans*-diol isomer both OH functions occupy the equatorial position (**Scheme 3.34**). The oxidation of 2,2,6,6-tetrachlorocyclohexanol failed probably due to the high steric shielding and/ or the lowest negative polarization of the geminal hydrogen due to the four electron withdrawing chlorine atoms present.

**Scheme 3.33** Axial and equatorial attack of  $\text{Br}^+$  on cyclohexanol.**Scheme 3.34** Relative conformations of *trans*- and *cis*-1,2-cyclohexanediols.

The chemoselective oxidation of polyhydroxy substrates, e.g. monosaccharides failed or yielded only complex intractable reaction mixtures, probably because these substrates can undergo acid catalyzed condensation reactions.

### 3.4.4 Conclusion

The NaBrO<sub>3</sub>/ NaHSO<sub>3</sub> reagent establishes an intricate network of equilibria in which HOBr acts as the source of but probably is not the actual oxidizing agent. The low and constantly replenished concentration of the actual oxidant, possibly [H<sub>2</sub>O-Br]<sup>+</sup> or Br<sup>+</sup>, generates a constant redox potential of the reagent solution. We propose that the redox potential of the reaction solution reaches a specific value which is sufficient enough for the first oxidation step of the diol but does not allow – or only very little – of the second oxidation step of α-hydroxy ketone to the dione to occur, i.e. the NaBrO<sub>3</sub>/ NaHSO<sub>3</sub> reagent combination effectively acts as redox buffer.

In order to further elucidate the reaction mechanism a full quantitative analysis of each of the bromine containing species in the reaction solution in real time would be necessary, which constitutes a formidable challenge.

### 3.4.5 Experimental Section

*Trans*-1,2-cyclohexanediol, *cis*-1,2-cyclohexanediol, *trans*-1,2-cyclopentanediol, *cis*-1,2-cyclopentanediol, α-hydroxy cyclohexanone, cyclohexane-1,2-dione, cyclohexanone acetonitrile, 2,2,6,6-tetrachlorocyclohexanol, sodium bromate, sodium bisulfite and sodium sulfite are commercially available and were used as received. *Cis,cis*-2,6-dimethylcyclohexanol, *cis*-2,2,6-trimethylcyclohexanol and 2,2,6,6-tetramethylcyclohexanol were been obtained by methylation of cyclohexanone with MeI and subsequent reduction with LiAlH<sub>4</sub> according to literature procedure.<sup>98,99</sup> The pH values were measured with a Fisher Accumet® pH meter Model 620 and a calomel electrode. The NMR experiments were conducted on a Varian Avance 400 MHz spectrometer. GC and GC-MS experiments were conducted on a Varian CP-3800 and Varian CP-3800-Saturn



2000. Environmental note: Residual solutions of the oxidation reactions should be quenched with a saturated  $\text{Na}_2\text{S}_2\text{O}_3$  solution and properly discarded.

**General reaction conditions.** *Trans*-1,2-cyclohexanediol (116 mg, 1.0 mmol) and sodium bromate (181 mg, 1.2 mmol) were dissolved in 1 mL water and 2 mL acetonitrile. A solution of sodium bisulfite (124 mg, 1.2 mmol) in 1.2 mL water was then added via syringe. The *pH* was measured with *pH* meter, the reaction was then stirred at room temperature ( $21^\circ\text{C} \pm 1^\circ\text{C}$ ) and monitored by quantitative GC.

**NMR scale experiments.** Methyl  $\alpha$ -D-glucopyranoside (33 mg, 0.17 mmol) was reacted with  $\text{NaBrO}_3$  (30 mg, 0.20 mmol) and  $\text{NaHSO}_3$  (20 mg, 0.20 mmol) in 0.7 mL  $\text{D}_2\text{O}$  at room temperature for 24 h, then stirred at  $60^\circ\text{C}$  for 5 d and the reaction monitored by  $^1\text{H}$  and  $^{13}\text{C}$  NMR.

### 3.5 References

- 1) Lindberg, B.; Theander, O. *Acta Chem. Scand.* **1954**, *8*, 1870-1874.
- 2) Theander, O. *Acta Chem. Scand.* **1957**, *11*, 1557-1564.
- 3) Tsuda, Y.; Hanajima, M.; Mastuhira, N.; Okuno, Y.; Kanemitsu, K. *Chem. Pharm. Bull.* **1989**, *39*, 2344-2350.
- 4) Liu, H.-M.; Sato, Y.; Tsuda, Y. *Chem. Pharm. Bull.* **1993**, *41*, 491-501.
- 5) Freimund, S.; Huwig, A.; Giffhorn, F.; Koepper, S. *Chem. Eur. J.* **1998**, *4*, 2442-2455.
- 6) Giffhorn, F.; Koepper, S.; Huwig, A.; Freimund, S. *Enzy. and Micro. Tech.* **2000**, *27*, 734-742.
- 7) Stoppok, E.; Matalla, K.; Buchholz, K. *Appl. Microbiol. Biotechnol.* **1992**, *36*, 604-609.
- 8) Theander, O. *Acta Chem. Scand.* **1958**, *12*, 1887-1896.
- 9) Pietsch, M.; Water, M.; Buchholz, K. *Carbohydr. Res.* **1994**, *254*, 183-194.
- 10) Collins, P.; Ferrier, R. *Monosaccharides*; John Wiley & Sons, Ltd.: Chichester, UK, 1995.
- 11) Jencks, W. P. *Catalysis in Chemistry and Enzymology*; Dover Publications, Inc.: New York, 1986.
- 12) Smith, M. B.; March, J. *March's Advanced Organic Chemistry*; John Wiley & Sons, Inc.: New York, 2001.
- 13) Brückner, R. *Reactionsmechanismen*; Spectrum Akademischer Verlag: Heidelberg, 1996.
- 14) Andrews, M. A.; Voss, E. J.; Gould, G. L.; Klooster, W. T.; Kötzle, T. F. *J. Am. Chem. Soc.* **1994**, *116*, 5730-5740.
- 15) Kästle, X.; Klüfers, P.; Kunte, T. *Z. Anorg. Allg. Chem.* **2001**, *267*, 2042-2044.
- 16) Klüfers, P.; Kunte, T. *Angew. Chem. Intl. Ed.* **2001**, *40*, 4210-4212.
- 17) Herdin, S.; Klüfers, P.; Kunte, T.; Pootrowski, H. *Z. Anorg. Allg. Chem.* **2004**, *630*, 701-705.
- 18) Klüfers, P.; Labisch, O. *Z. Naturforsch.* **2004**, *57*, 1446-1453.

- 19) Klüfers, P.; Kunte, T. *Z. Anorg. Allg. Chem.* **2004**, 630, 553-557.
- 20) Benner, K.; Klüfers, P. *Carbohydrate Research* **2000**, 327, 287-292.
- 21) Iwahama, T.; Sakaguchi, S.; Nishiyama, Y.; Ishii, Y. *Tetrahedron Lett.* **1995**, 36, 6923-6926.
- 22) Iwahama, T.; Yoshino, Y.; Keitoku, T.; Sakaguchi, S.; Ishii, Y. *J. Org. Chem.* **2000**, 65, 6502-6507.
- 23) Amorati, R.; Luccarini, M.; Mugnaini, V.; Pedulli, G. F.; Minisci, F.; Recupero, F.; Fontana, F.; Astlofi, P.; Greci, L. *J. Org. Chem.* **2003**, 68, 1747-1754.
- 24) Inokuchi, T.; Mastumoto, S.; Torii, S. *J. Org. Chem.* **1991**, 56, 2416-2421.
- 25) Torii, S.; Inokuchi, T.; Sugiura, T. *J. Org. Chem.* **1986**, 51, 155-161.
- 26) Inokuchi, T.; Mastumoto, S.; Nisiyama, T.; Torii, S. *Synlett* **1990**, 57-58.
- 27) *The Merck Index*; 13th ed.; Merck & Co., Inc.: Whitehouse Station, NJ, 2001.
- 28) Atkins, P.; de Paula, J. *Elements of Physical Chemistry*; W. H. Freeman and Co.: New York, 2002.
- 29) Wilson, S. R.; Walters, M. E.; Orbaugh, B. *J. Org. Chem.* **1976**, 41, 378-380.
- 30) Bierenstiel, M.; Schlaf, M. *Eur. J. Org. Chem.* **2004**, 1474-1481.
- 31) Menashe, N.; Shvo, J. *Organometallics* **1991**, 10, 3885-3891.
- 32) Shvo, Y.; Czarkie, D.; Rahamim, Y. *J. Am. Chem. Soc.* **1986**, 108, 7400-7402.
- 33) Shvo, Y.; Goldberg, I.; Czerkie, D.; Reshef, D.; Stein, Z. *Organometallics* **1997**, 16, 133-138.
- 34) Shvo, Y.; Arisha, A. H. I. *J. Org. Chem.* **1998**, 63, 5640-5642.
- 35) Pamies, O.; Baeckwall, J.-E. *Chem. Eur. J.* **2001**, 7, 5052-5058.
- 36) Casey, C. P.; Singer, S. W.; Powell, D. R.; Hayashi, R. K.; Kavana, M. *J. Am. Chem. Soc.* **2001**, 123, 1090-1100.
- 37) Blum, Y.; Shvo, Y. *Isr. J. Chem.* **1984**, 24, 144-148.
- 38) Adkins, H.; Elofson, R. M.; Rossow, A. G.; Robinson, C. C. *J. Am. Chem. Soc.* **1949**, 71, 3622-3629.

- 39) Hashiguchi, S.; Fujii, A.; Takehara, J.; Ikariya, T.; Noyori, R. *J. Am. Chem. Soc.* **1995**, *117*, 7562-7563.
- 40) Takehara, J.; Hashoguchi, S.; Fujii, A.; Inoue, S.-I.; Ikariya, T.; Noyori, R. *Chem. Commun.* **1996**, 233-234.
- 41) Noyori, R.; Hashiguchi, S. *Acc. Chem. Res.* **1997**, *30*, 97-102.
- 42) Mikami, K.; Korenaga, T.; Ohkuma, T.; Noyori, R. *Angew. Chem. Int. Ed.* **2000**, *39*, 3707-3710.
- 43) Noyori, R. *Acta Chem. Scand.* **1996**, *50*, 380-390.
- 44) Noyori, R. *Angew. Chem. Int. Ed.* **2002**, *41*, 2008-2022.
- 45) Noyori, R. *Adv. Synth. Catal.* **2003**, *345*, 15-32.
- 46) Noyori, R.; Yamakawa, M.; Hashiguchi, S. *J. Org. Chem.* **2001**, *66*, 7931-7944.
- 47) Hayes, A.; Clarkson, G.; Wills, M. *Tetrahedron Asymm.* **2004**, *15*, 2079-2084.
- 48) Schwink, L.; Ireland, T.; Püntener, K.; Knochel, P. *Tetrahedron Asymm.* **1998**, *9*, 1143-1163.
- 49) Püntener, K.; Schwink, L.; Knochel, P. *Tetrahedron Lett.* **1996**, *37*, 8165-8168.
- 50) Bennett, M. A.; Huang, T.-N.; Matheson, T. W.; Smith, A. K. *Inorganic Synth.* 1982; Vol. 21, 75.
- 51) Noyori, R.; Ohkuma, T. *Angew. Chem. Int. Ed.* **2001**, *40*, 40-73.
- 52) Hashiguchi, S.; Fujii, A.; Haack, K.-J.; Matsumura, K.; Ikariya, T.; Noyori, R. *Angew. Chem. Int. Ed. Engl.* **1997**, *36*, 288-290.
- 53) Haack, K.-J.; Hashiguchi, S.; Fujii, A.; Ikariya, T.; Noyori, R. *Angew. Chem. Int. Ed. Engl.* **1997**, *36*, 285-288.
- 54) Wiberg, K. B.; Waldon, R. F. *J. Am. Chem. Soc.* **1991**, *113*, 7697-7705.
- 55) Saiyasombat, W.; Molloy, R.; Nicholson, T. M.; Johnson, A. F.; Ward, I. M.; Poshyachinda, S. *Polymer* **1998**, *39*, 5581-5585.
- 56) Cheng, H.-Y.; Cheng, P.-H.; Lee, C.-F.; Peng, S.-M. *Inorg. Chim. Acta* **1991**, *181*, 145-147.
- 57) Sayre, R. *J. Am. Chem. Soc.* **1955**, *77*, 6689-6690.

- 58) Proskurnina, M. V.; Lozinskaya, N. A.; Tkachenko, S. E.; S., Z. N. *Russ. J. Org. Chem.* **2002**, 38, 1149-1153.
- 59) Delbecq, F.; Sautet, P. *J. Am. Chem. Soc.* **1992**, 114, 2446-2455.
- 60) Huang, Y.-H.; Gladysz, J. A. *J. Chem. Education* **1988**, 65, 298-303.
- 61) *Gaussian 03*; B.03 Ed.; Gaussian Inc.: Pittsburgh, PA, 2003.
- 62) Barros, M. T.; Sineriz, F. *Tetrahedron* **2000**, 56.
- 63) Noyori, R.; Aoki, M.; Sato, K. *Chem. Commun.* **2003**, 1977-1986.
- 64) Campestrini, S.; Di Furia, F.; Modena, G. *J. Org. Chem.* **1990**, 55, 3658-3660.
- 65) Jacobson, S. E.; Muccigrosso, D. A.; Mares, F. *J. Org. Chem.* **1979**, 44, 921-924.
- 66) Bortolini, O.; Campestrini, S.; Di Furia, F.; Modena, G. *J. Org. Chem.* **1987**, 52, 5467-5469.
- 67) Kurusu, Y.; Masuyama, Y. *Tetrahedron* **1986**, 5, 289-296.
- 68) Maignien, S.; Ait-Mohand, S.; Muzart, J. *Synlett* **1996**, 439-440.
- 69) Trost, B. M.; Masuyama, Y. *Tetrahedron Lett.* **1984**, 25, 173-176.
- 70) Trost, B. M.; Merlic, C. *J. Am. Chem. Soc.* **1990**, 112, 9590-9600.
- 71) Dickman, M. H.; Pope, M. T. *Chem. Rev.* **1994**, 94, 569-584.
- 72) Kühn, F. E.; Groarke, M.; Bence, E.; Herdtweck, E.; Prazeres, A.; Santos, A. M.; Calhorda, M. J.; Romao, C. C.; Goncalves, I. S.; Lopes, A. D.; Pillinger, M. *Chem. Eur. J.* **2002**, 8, 2370-2383.
- 73) Cowley, A. H., *Inorganic Synth.*, 1997; Vol. 39, 246-247.
- 74) Chaumette, P.; Mimoun, H.; Saussine, L.; Fischer, J.; Mitschler, A. *J. Organomet. Chem.* **1983**, 250, 291-295.
- 75) Campestrini, S.; Di Furia, F. *Tetrahedron* **1994**, 50, 5119-5130.
- 76) Campestrini, S.; Conte, V.; Di Furia, F.; Modena, G. *J. Org. Chem.* **1988**, 53, 5721-5724.
- 77) Di Furia, F.; Fornasier, R.; Tonellato, U. *J. Mol. Catal.* **1983**, 19, 81-84.
- 78) Doyle, M. P.; Partie, W. J.; Williams, S. B. *J. Org. Chem.* **1979**, 44, 2955-2956.

- 79) Doyle, M. P.; Dow, R. L.; Bagheri, V.; Patrie, W. J. *Tetrahedron Lett.* **1980**, *21*, 2795-2798.
- 80) Doyle, M. P.; Dow, R. L. *Synth. Comm.* **1980**, *10*, 881-888.
- 81) Doyle, M. P.; Bagheri, V. *J. Org. Chem.* **1981**, *46*, 4806-4808.
- 82) Doyle, M. P.; Dow, R. L.; Bagheri, V.; Patrie, W. J. *J. Org. Chem.* **1983**, *48*, 476-480.
- 83) Sakaguchi, S.; Kikuchi, D.; Ishii, Y. *Bull. Chem. Soc. Jpn.* **1997**, *70*, 2561-2566.
- 84) Kikuchi, D.; Sakaguchi, S.; Ishii, Y. *J. Org. Chem.* **1998**, *63*, 6023-6026.
- 85) Hayat, S.; Atta-ur-Rahman; Choudhary, I. M.; Khan, K. M.; Bayer, E. *Tetrahedron Lett.* **2001**, *42*, 1647-1649.
- 86) Field, R. J.; Koros, E.; Noyes, R. M. *J. Am. Chem. Soc.* **1972**, *94*, 8649-8664.
- 87) Noyes, R. M. *J. Phys. Chem.* **1990**, *94*, 4404-4412.
- 88) Metsger, L.; Bittner, S. *Tetrahedron Lett.* **2000**, *56*, 1905-1910.
- 89) All possible reagent combinations of trans-1,2-cyclohexane-diol, NaBrO<sub>3</sub>, NaHSO<sub>3</sub>, Na<sub>2</sub>SO<sub>3</sub> and H<sub>2</sub>SO<sub>4</sub> were permuted yielding quantitative  $\alpha$ -hydroxy cyclohexanone within 24 h. The 1,2-cyclohexanedione content was less than 5%.
- 90) The solutions were allowed to cool to room temperature.
- 91) Derivation of these compounds, e.g. by exhaustive silylation would be required to make them analyzable by GC. Given that the reaction mixtures are aqueous and that the addition of silylation agents such as Me<sub>3</sub>Si-imidazolium chloride might influence the reaction equilibria, this is not practical.
- 92) Derbyshire, D. H.; Waters, W. A. *Nature* **1949**, *64*, 427-428.
- 93) Takase, K.; Masuda, H.; Kai, O.; Nishiyama, Y.; Sakaguchi, S.; Ishii, Y. *Chem. Lett.* **1995**, 871-872.
- 94) Toth, Z.; Fabian, I. *Inorg. Chem.* **2004**, *43*, 2717-2723.
- 95) Toth, Z.; Fabian, I. *Inorg. Chem.* **2000**, *39*, 4608-4614.

- 96) Beckwith, R. C.; Wang, T. X.; Margerum, D. W. *Inorg. Chem.* **1996**, 35, 995-1000.
- 97) Greenwood, N. N.; Earnshaw, A. *Chemistry of the Elements*; 2nd Ed.; Butterworth Heinemann: Oxford, 1997.
- 98) Lissel, M.; Neumann, B.; Schmidt, S. *Liebigs Ann. Chem.* **1986**, 263-264.
- 99) Becker, H. *Organicum*; Addison-Wesley Publishing Company: Reading, MA, 1973
- 100) Bierenstiel, M; D'Hondt, P. J.; Schlaf, M. *Tetrahedron*, **2005**, 61, 4911-4917.

## Appendix

Calculation spread-sheet

$^1\text{H}$  and  $^{13}\text{C}$  NMR spectra

Table of Figures

Table of Schemes

Table of Tables

Curriculum Vitae



Calculation spread-sheet for  $k_1 = k_2 = k_3$

$[A] = 100 e^{-k_1 t}$   
for  $k_1 = 0.1$

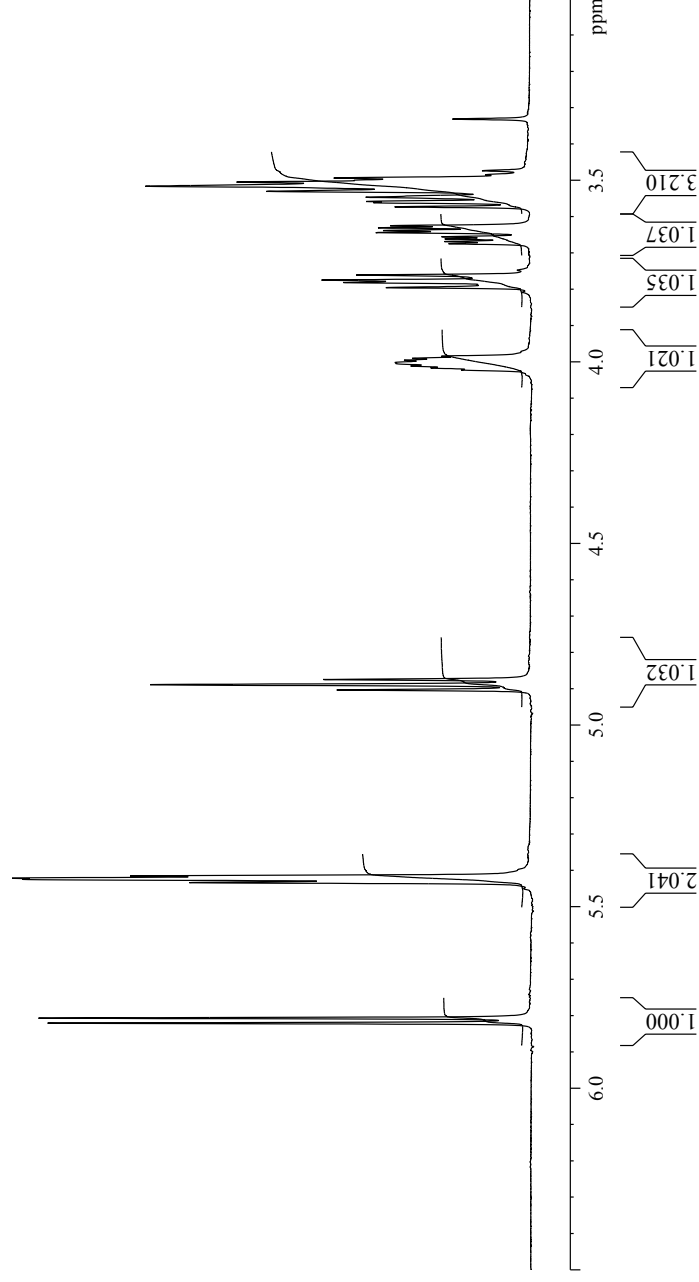
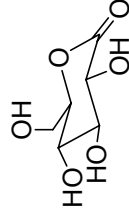
$[C_x] = [B_x]e^{-k_2}$   
for  $k_2 = 0.1$

$[D_x] = [C_x]e^{-k_3}$   
for  $k_3 = 0.1$

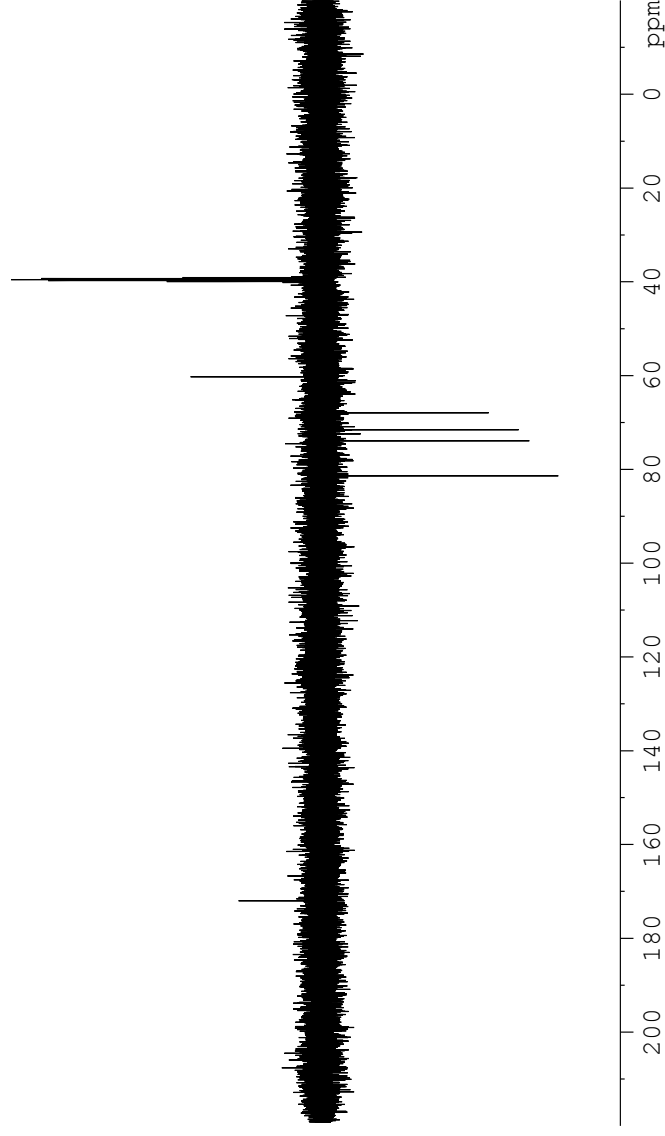
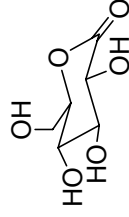
time (unit)	[A]	$[A_{n+1}] - [A_n]$	$[A_x]$	$[B] = \Sigma [A_x]$	$[B] = (\Sigma [A_x]) - [C_x]$	$[B]$ to $[C_x]$	available $[C_x]$ generated	$[C] = \Sigma [C_x] - [D_x]$	$[C]$ to $[D_x]$	available $[D_x]$ generated	$[D] = \Sigma [D_x]$	$[A] + [B] +$ $[C] + [D]$
0	100		0	0	0	0	0	0	0	0	0	100
1	90.4837418	9.516258196	9.516258196	9.516258196	9.516258196	0	0	0	0	0	0	100
2	81.87307531	8.610666496	18.12692469	18.12692469	17.22133299	8.610666496	0.905591701	0.905591701	0	0	0	100
3	74.08182207	7.79125324	25.91817793	25.91817793	23.37375972	15.58250648	2.458239769	2.458239769	0.819413256	0.086178444	0.086178444	100
4	67.0320046	7.049817465	32.9679954	32.9679954	28.19926986	21.14945239	2.224307325	4.44861465	2.224307325	0.233932443	0.320110888	100
5	60.65306597	6.378938632	39.34693403	39.34693403	31.89469316	25.51575453	2.683515329	6.708788323	4.025272994	0.423341656	0.743452544	100
6	54.88116361	5.771902362	45.11883639	45.11883639	34.63141417	28.85951181	3.035181352	9.105544057	6.070362704	0.638425619	1.381878163	100
7	49.65853038	5.22263323	50.34146962	50.34146962	36.55843261	31.33579938	3.29561479	11.53465176	8.239036974	0.866507083	2.248385245	100
8	44.93289641	4.725633967	55.06710359	55.06710359	37.80507174	33.07943777	3.47899484	13.91597936	10.43698452	1.097667244	3.346052489	100
9	40.65696597	4.275930438	59.34303403	59.34303403	38.48337394	34.2074435	3.597628238	16.18932707	12.59169883	1.324280526	4.670333016	100
10	36.78794412	3.869021857	63.21205588	63.21205588	38.69021857	34.82119671	3.662177227	18.31088613	14.64870891	1.540618164	6.21095118	100
11	33.28710837	3.500835747	66.71289163	66.71289163	38.50919322	35.00835747	3.681861096	20.25023603	16.56837493	1.742511203	7.953462383	100
12	30.11942119	3.167687179	69.88057881	69.88057881	38.01224614	34.84455896	3.664634256	21.98780554	18.32317128	1.927064746	9.880527128	100
13	27.2531793	2.866241888	72.7468207	72.7468207	37.26114454	34.39490265	3.617343489	23.51273268	19.89538919	2.092416347	11.97294347	100
14	24.65969639	2.593482909	75.34030361	75.34030361	36.30876073	33.71527782	3.545866722	24.82106705	21.27520033	2.237532351	14.21047583	100
15	22.31301601	2.346680379	77.68698399	77.68698399	35.20020569	32.8532531	3.455235419	25.91426564	22.45903022	2.362036828	16.57251265	100
16	20.1896518	2.123364215	79.8103482	79.8103482	33.97382745	31.85046323	3.349742459	26.79793967	23.44819721	2.466068428	19.03858108	100
17	18.26835241	1.921299394	81.73164759	81.73164759	32.6620897	30.74079031	3.233037139	27.48081568	24.24777854	2.550161131	21.58874221	100

18	16.52988882	1.738463583	83.47011118	31.2923445	29.55388091	3.108208788	27.97387909	24.86567031	2.615145375	24.20388759	100
19	14.95686192	1.5730269	85.04313808	29.8875111	28.3144842	2.977860298	28.28967283	25.31181253	2.662066562	26.86595415	100
20	13.53352832	1.423333599	86.46647168	28.46667197	27.04333837	2.844172725	28.44172725	25.59755452	2.692118309	29.55807246	100
21	12.24564283	1.287885498	87.75435717	27.04559547	25.75770997	2.708962005	28.44410105	25.73513905	2.7065882	32.26466066	100
22	11.08031584	1.165326989	88.91968416	25.63719376	24.47186677	2.573728695	28.31101565	25.73728695	2.706814098	34.97147476	100
23	10.02588437	1.0544431464	89.97411563	24.25192367	23.19749221	2.439701552	28.05656785	25.6168663	2.694149347	37.6656241	100
24	9.071795329	0.954089043	90.92820467	22.89813704	21.944048	2.307875674	27.69450809	25.38663242	2.669935438	40.33555954	100
25	8.208499862	0.863295467	91.79150014	21.58238666	20.7190912	2.179045843	27.23807304	25.05902719	2.635480896	42.97104044	100
26	7.427375821	0.781142041	92.57264218	20.30969306	19.52855102	2.05383564	26.69986332	24.64602768	2.592045358	45.5630858	100
27	6.720551274	0.706806547	93.27944873	19.08377678	18.37697023	1.932722831	26.09175822	24.15903539	2.540827931	48.10391373	100
28	6.081006263	0.639545011	93.91899374	17.90726032	17.26771531	1.816061472	25.42486061	23.60879914	2.48295908	50.58687281	100
29	5.502322006	0.578684257	94.49767799	16.78184345	16.20315919	1.704101128	24.70946636	23.00536523	2.419495382	53.00636819	100
30	4.978706837	0.523615169	95.02129316	15.70845507	15.1848399	1.597003553	23.95505329	22.35804974	2.351416617	55.35778481	100
31	4.504920239	0.473786597	95.49507976	14.68738452	14.21359792	1.494857143	23.17028571	21.67542857	2.279624722	57.63740953	100
32	4.076220398	0.428699842	95.9237796	13.71839493	13.28969509	1.397689433	22.36303093	20.9653415	2.204944213	59.84235374	100
33	3.68831674	0.387903658	96.31168326	12.8008207	12.41291705	1.305477882	21.54038505	20.23490717	2.128123764	61.97047751	100
34	3.337326996	0.350989744	96.662673	11.9336513	11.58266156	1.21815915	20.70870554	19.49054639	2.049838658	64.02031616	100
35	3.019738342	0.317588654	96.98026166	11.11560288	10.79801423	1.13563707	19.87364872	18.73801165	1.970693888	65.99101005	100
36	2.732372245	0.287366098	97.26762776	10.34517951	10.05781341	1.05778947	19.04021047	17.982421	1.891227726	67.88223778	100
37	2.472352647	0.260019598	97.52764735	9.620725115	9.360705517	0.984473993	18.21276887	17.22829488	1.811915589	69.69415337	100
38	2.237077186	0.235275461	97.76292281	8.940467534	8.705192072	0.915533042	17.3951278	16.47959476	1.733174111	71.42732748	100
39	2.024191145	0.212886041	97.97580886	8.3025556	8.089669559	0.850797974	16.5905605	15.73976253	1.655365275	73.08269275	100
40	1.831563889	0.192627256	98.16843611	7.705090228	7.512462973	0.790092628	15.80185256	15.01175993	1.578800574	74.66149333	100
41	1.65726754	0.174296349	98.34273246	7.146150297	6.971853948	0.73323628	15.03134375	14.29810747	1.503745089	76.16523842	100
42	1.499557682	0.157709858	98.50044232	6.623814041	6.466104183	0.680046113	14.28096838	13.60092227	1.430421481	77.5956599	100
43	1.356855901	0.142701781	98.6431441	6.136176576	5.993474795	0.630339247	13.5522938	12.92195456	1.359013824	78.95467372	100
44	1.22773399	0.129121911	98.77226601	5.68136408	5.552242169	0.583934406	12.84655694	12.26262253	1.28967127	80.24434499	100
45	1.110899654	0.116834336	98.88910035	5.257545142	5.140710805	0.540653275	12.16469869	11.62404541	1.222511528	81.46685652	100
46	1.005183574	0.105716079	98.99481643	4.862939651	4.757223571	0.50032157	11.50739612	11.00707455	1.157624136	82.62448065	100
47	0.90952771	0.095655864	99.09047229	4.495825622	4.400169758	0.462769893	10.87509249	10.41232259	1.095073527	83.71955418	100

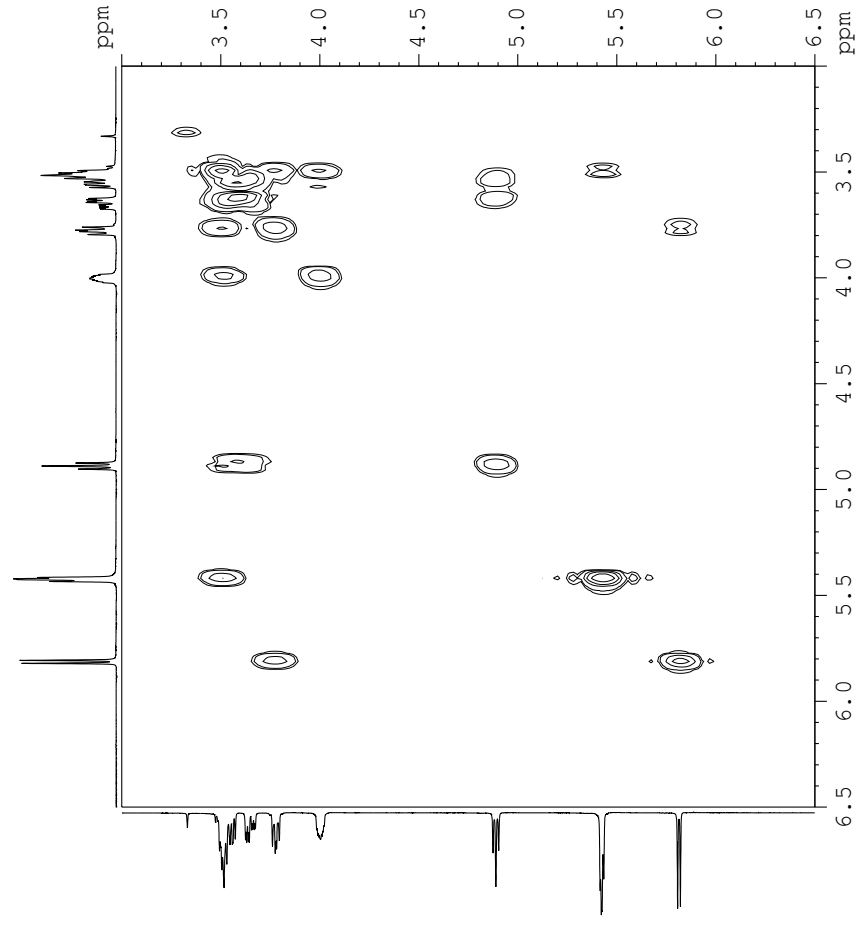
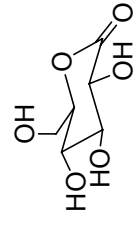
**$\delta$ -D-gluconolactone ( $^1\text{H}$ , 400 MHz,  $\text{DMSO-d}_6$ )**



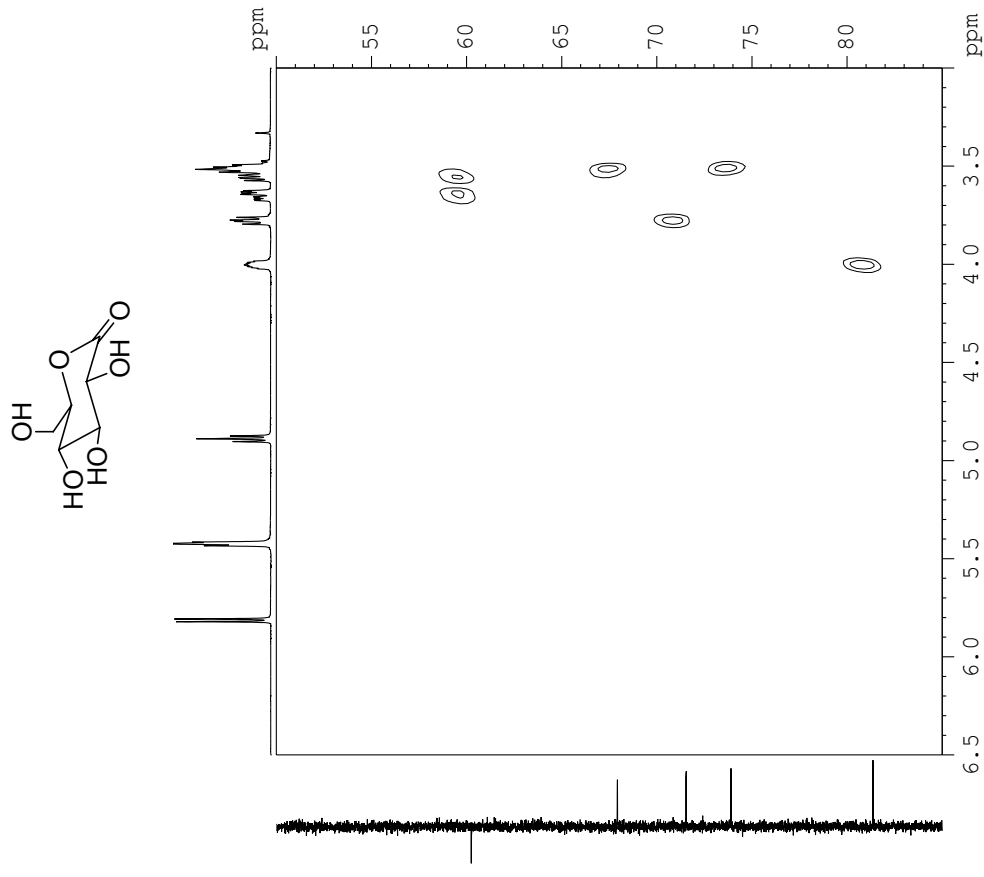
**$\delta$ -D-gluconolactone (jmod, 100 MHz, DMSO- $d_6$ )**



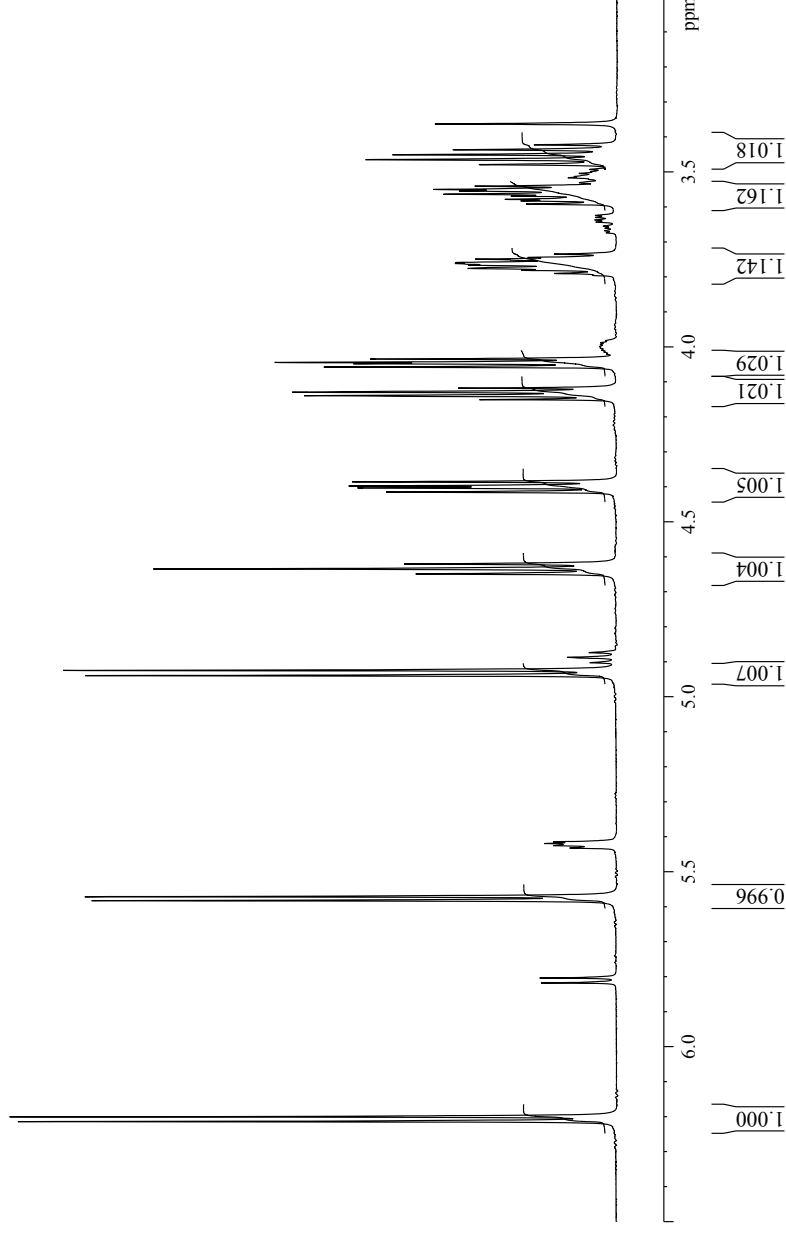
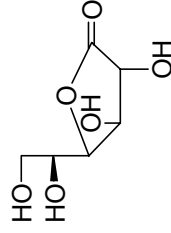
**$\delta$ -D-gluconolactone (COSY, 400 MHz, DMSO- $d_6$ )**



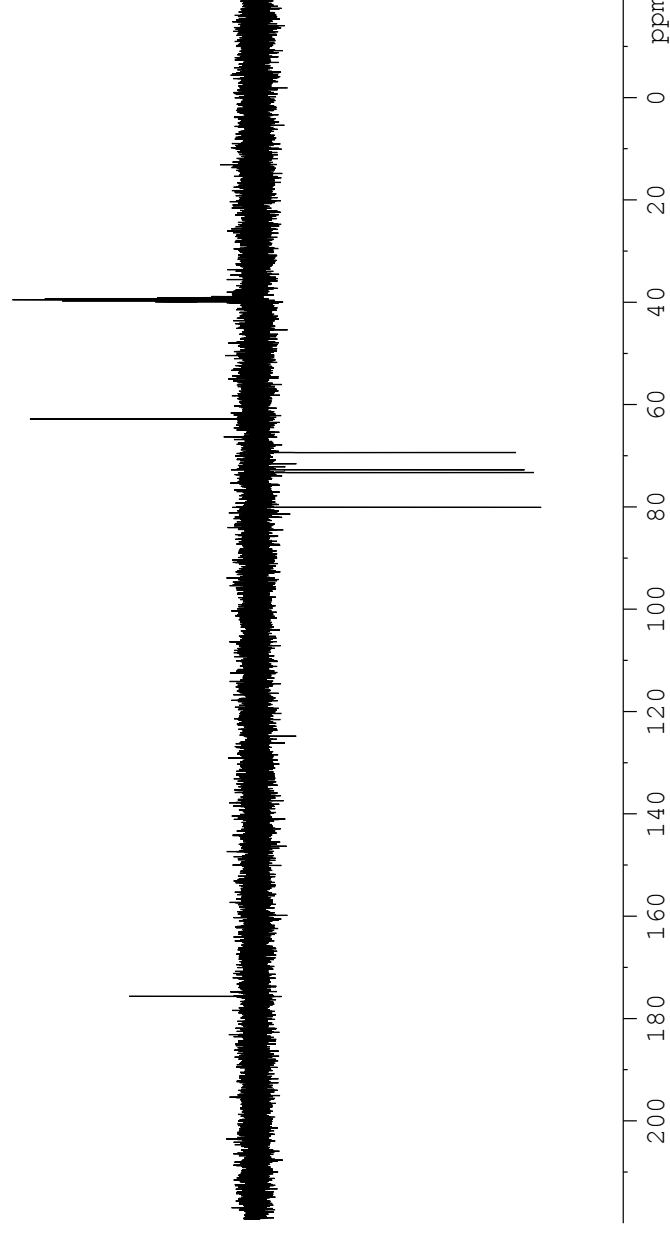
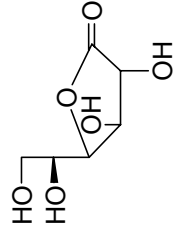
**$\delta$ -D-gluconolactone** (HSQC, 400 MHz/ 100 MHz, DMSO- $d_6$ )



**$\gamma$ -D-gluconolactone** ( $^1\text{H}$ , 400 MHz,  $\text{DMSO-d}^6$ ) (with small amount of  $\delta$ -D-gluconolactone)

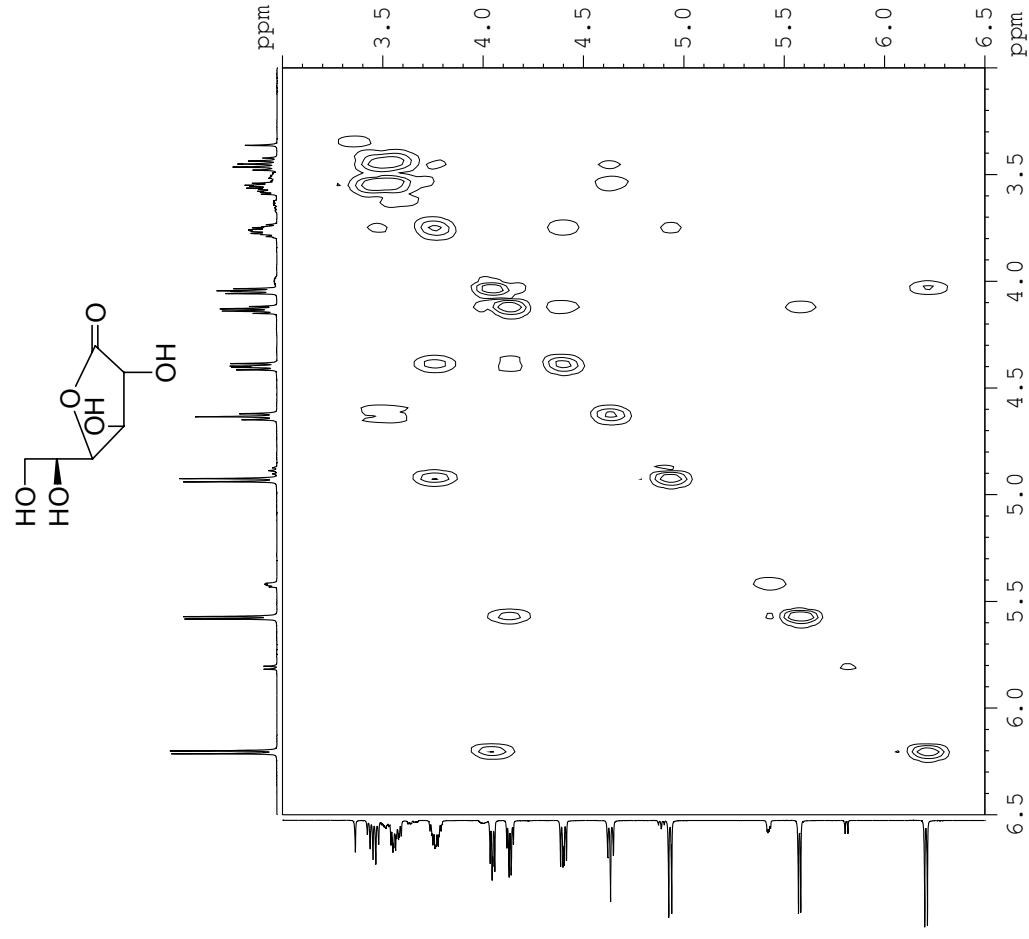


**$\gamma$ -D-gluconolactone** (jmod, 100 MHz, DMSO- $d^6$ ) (with small amount of  $\delta$ -D-gluconolactone)

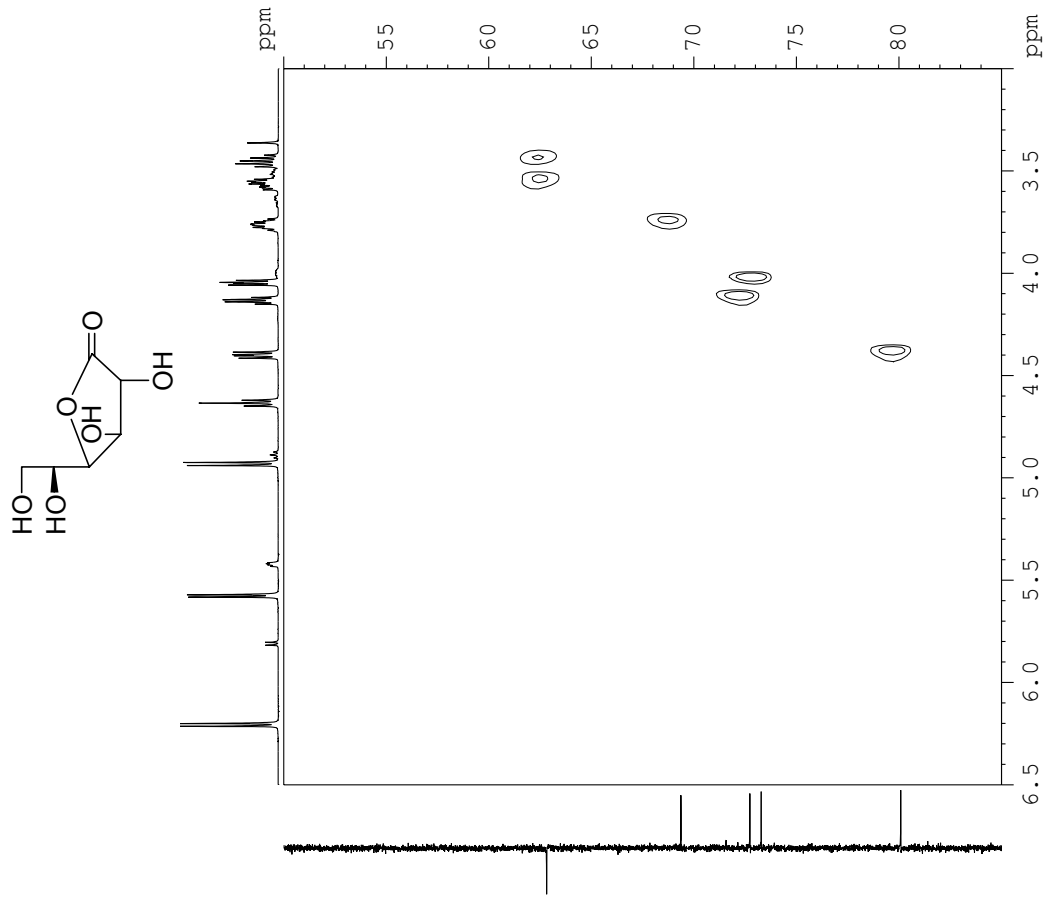




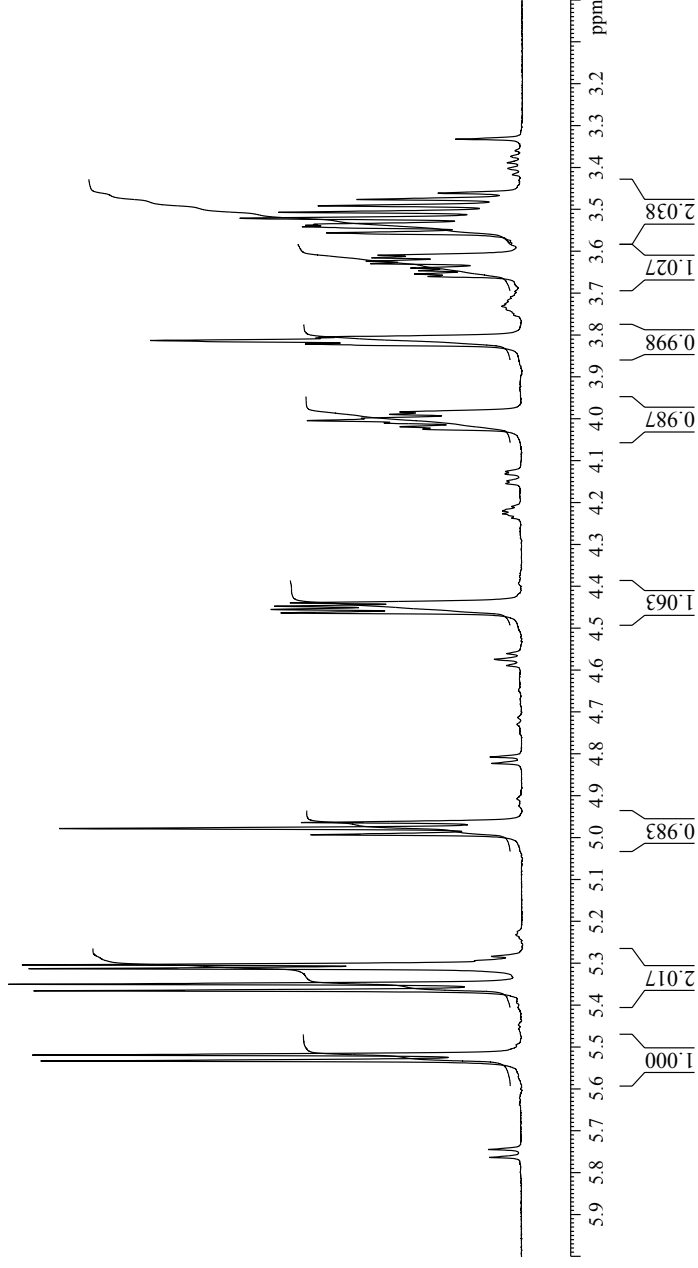
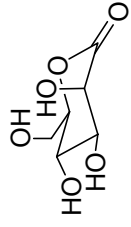
**$\gamma$ -D-gluconolactone (COSY, 400 MHz, DMSO- $d_6$ )(with small amount of  $\delta$ -D-gluconolactone)**



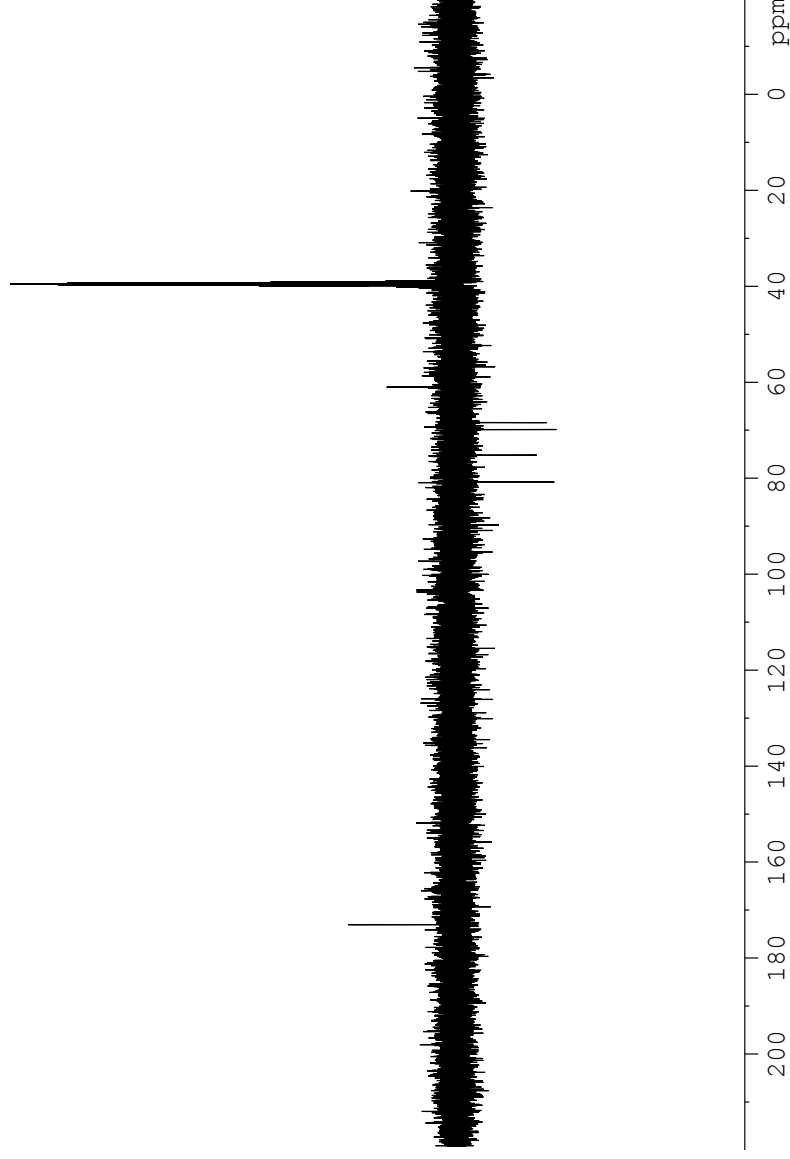
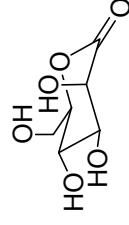
**$\gamma$ -D-gluconolactone** (HSQC, 400 MHz/ 100 MHz, DMSO- $d^6$ )(with small amount of  $\delta$ -D-gluconolactone)



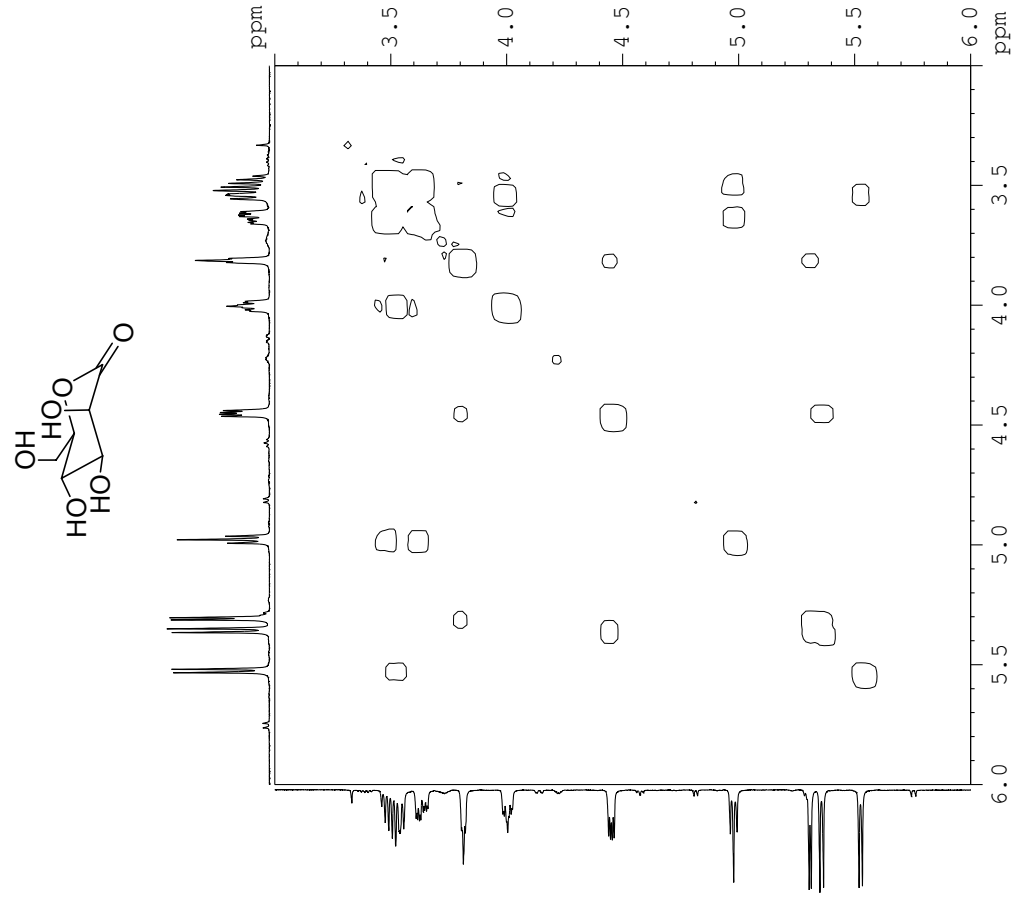
**$\delta$ -D-mannononolactone** ( $^1\text{H}$ , 400 MHz,  $\text{DMSO-d}^6$ ) (with small amount of  $\gamma$ -D-mannonolactone)



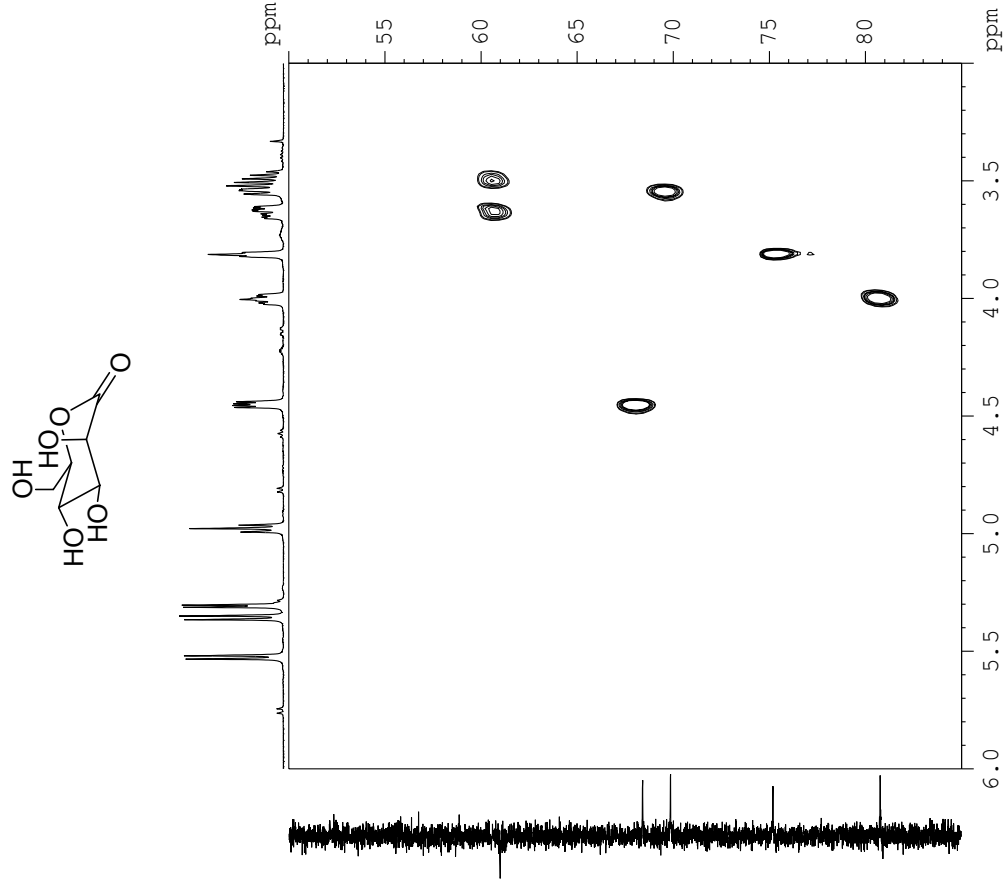
**$\delta$ -D-mannonolactone** (jmod, 400 MHz, DMSO- $d^6$ ) (with small amount of  $\gamma$ -D-mannonolactone)



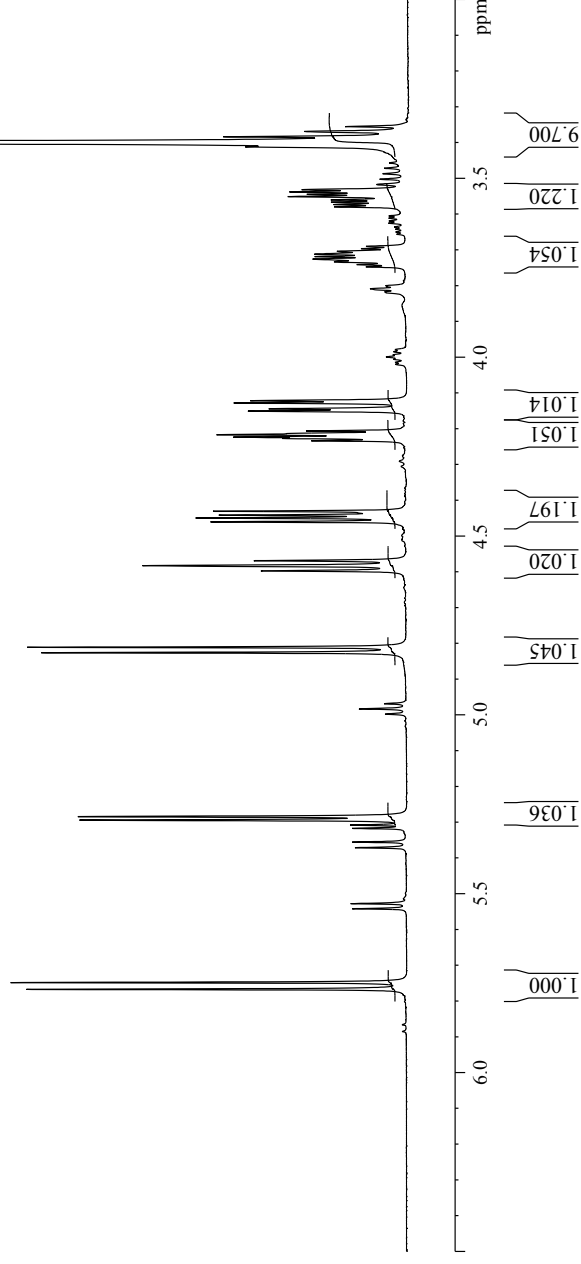
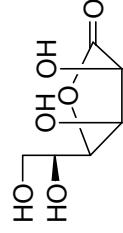
**$\delta$ -D-mannononolactone** (COSY, 400 MHz, DMSO- $d^6$ )(with small amount of  $\gamma$ -D-mannononolactone)



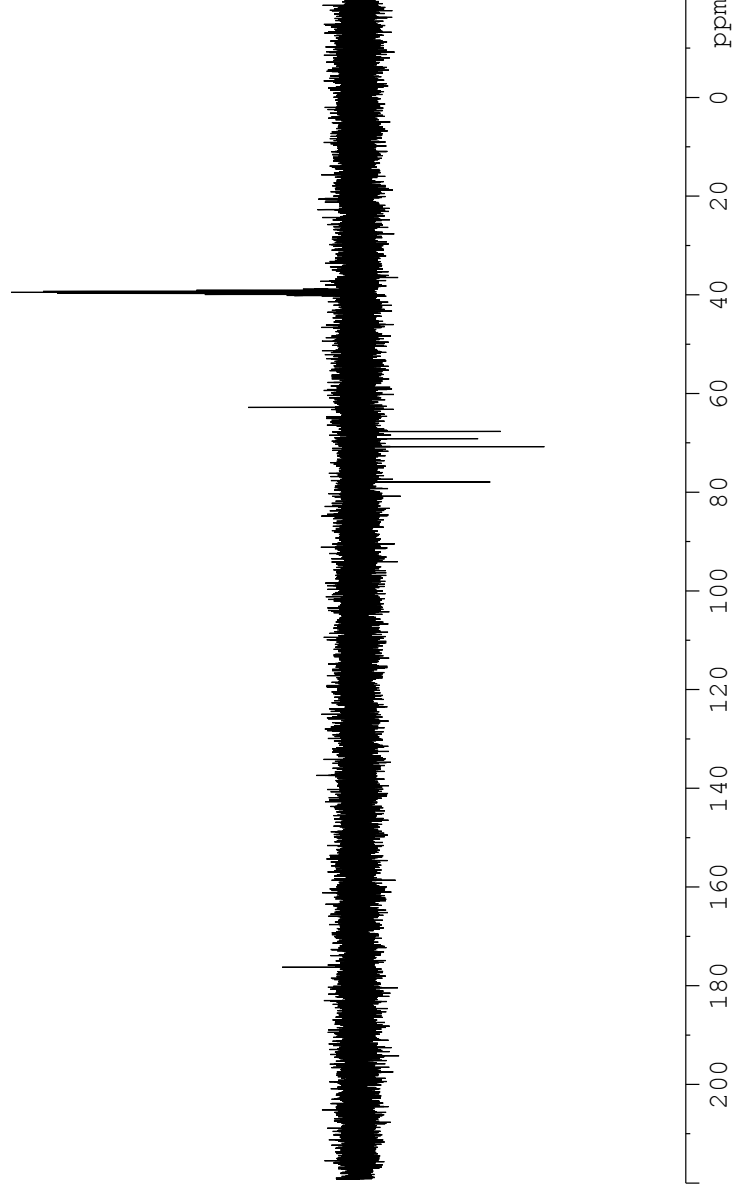
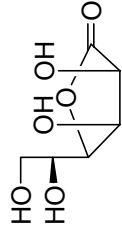
**$\delta$ -D-mannonolactone** (HSQC, 400 MHz/ 100 MHz, DMSO- $d^6$ )(with small amount of  $\gamma$ -D-mannonolactone)



**$\gamma$ -D-mannononolactone** ( $^1\text{H}$ , 400 MHz, DMSO- $d^6$ )(with small amount of  $\delta$ -D-mannonolactone and water)

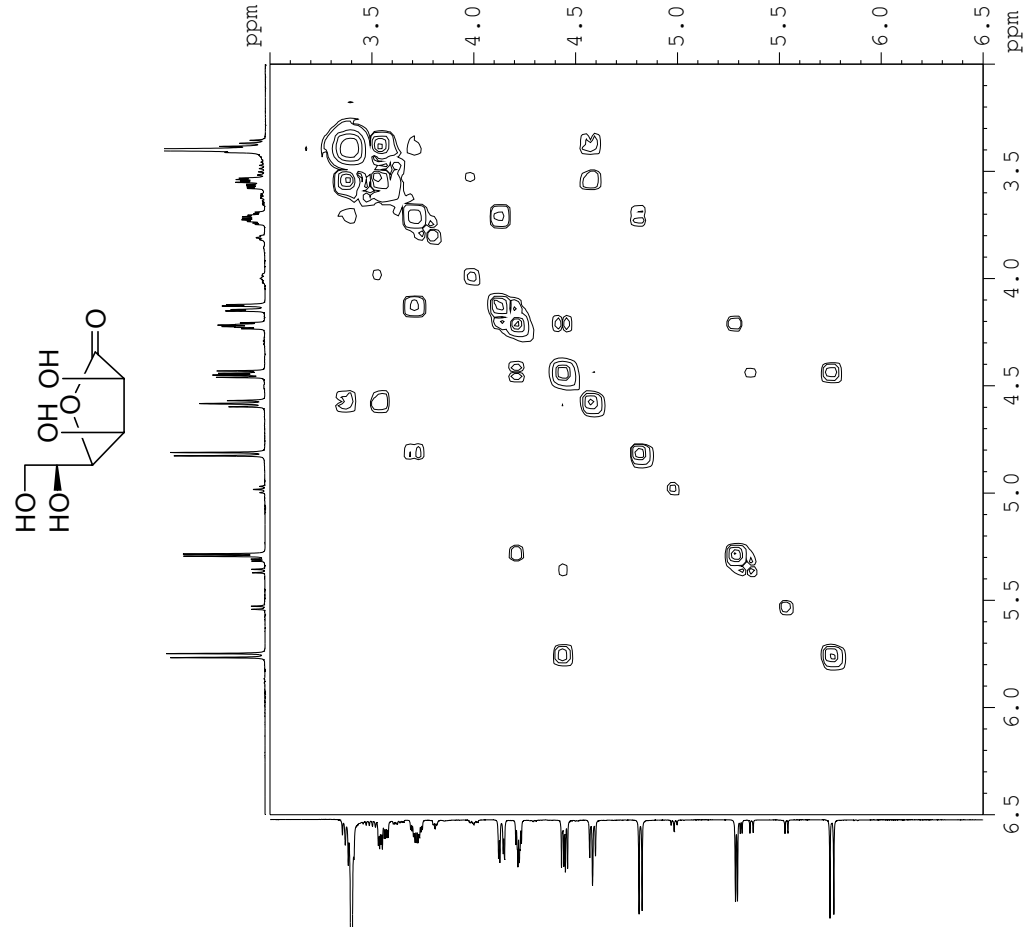


**$\gamma$ -D-mannononolactone** (jmod, 100 MHz, DMSO- $d^6$ ) (with small amount of  $\delta$ -D-mannonolactone)

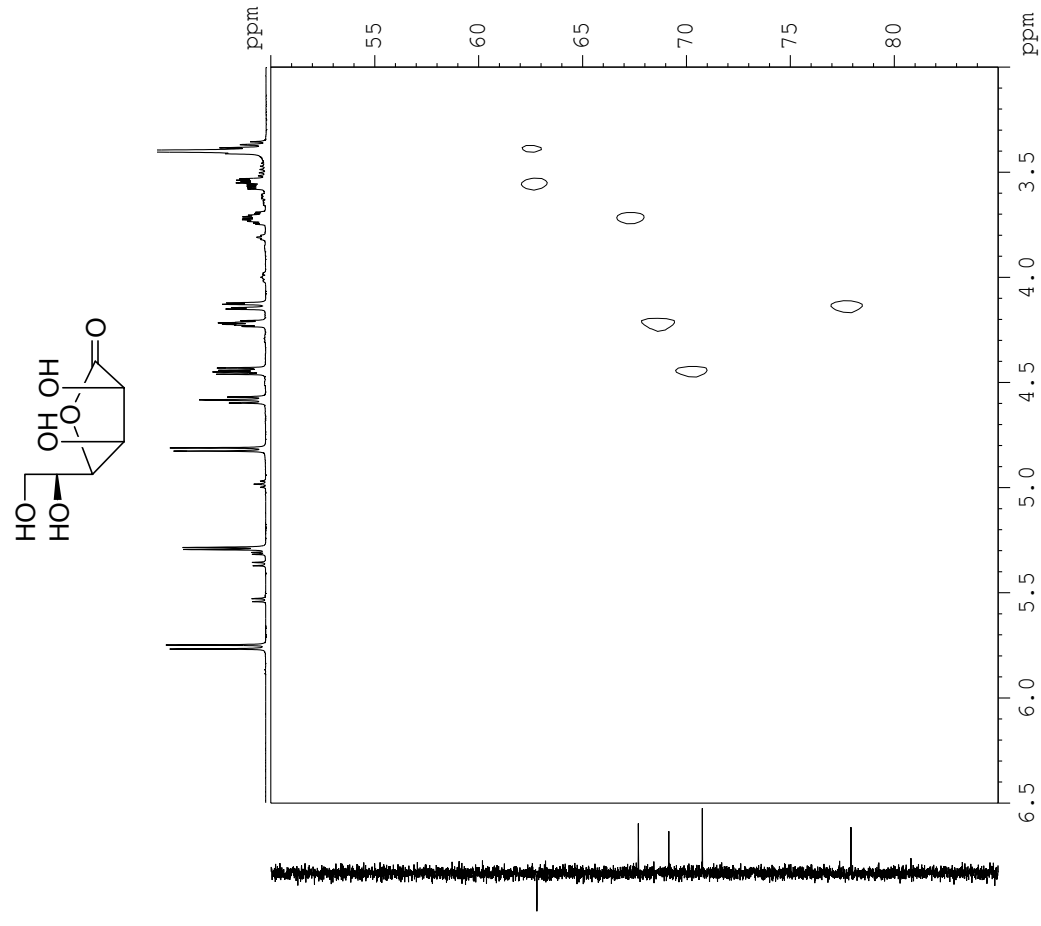




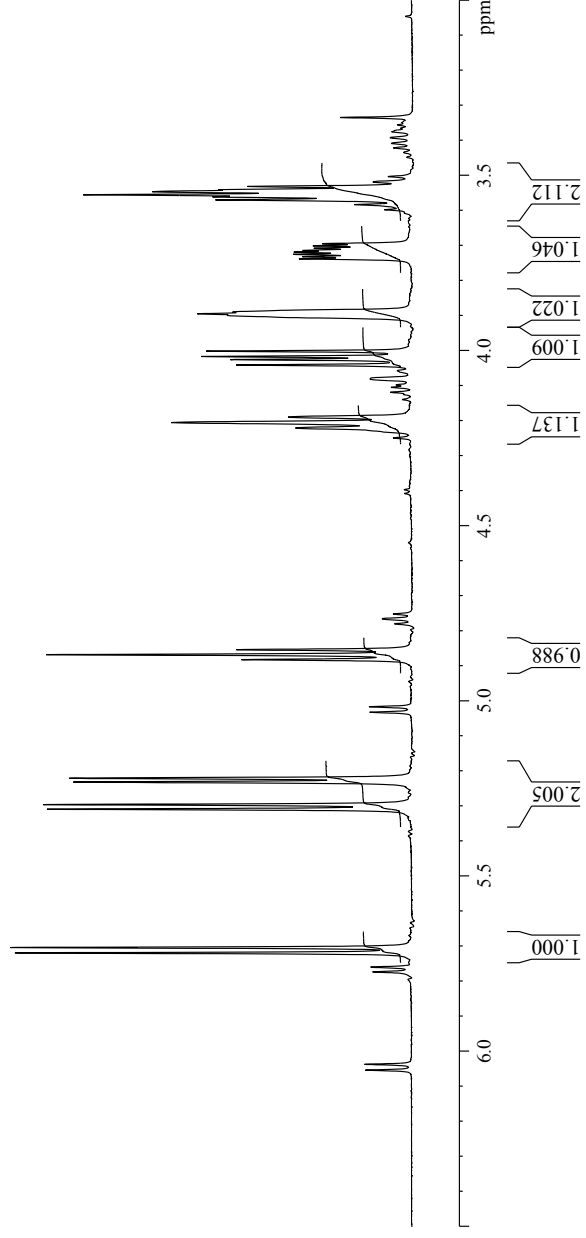
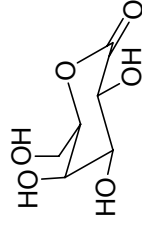
**$\gamma$ -D-mannonolactone (COSY, 400 MHz, DMSO- $d_6$ ) (with small amount of  $\delta$ -D-mannonolactone and water)**



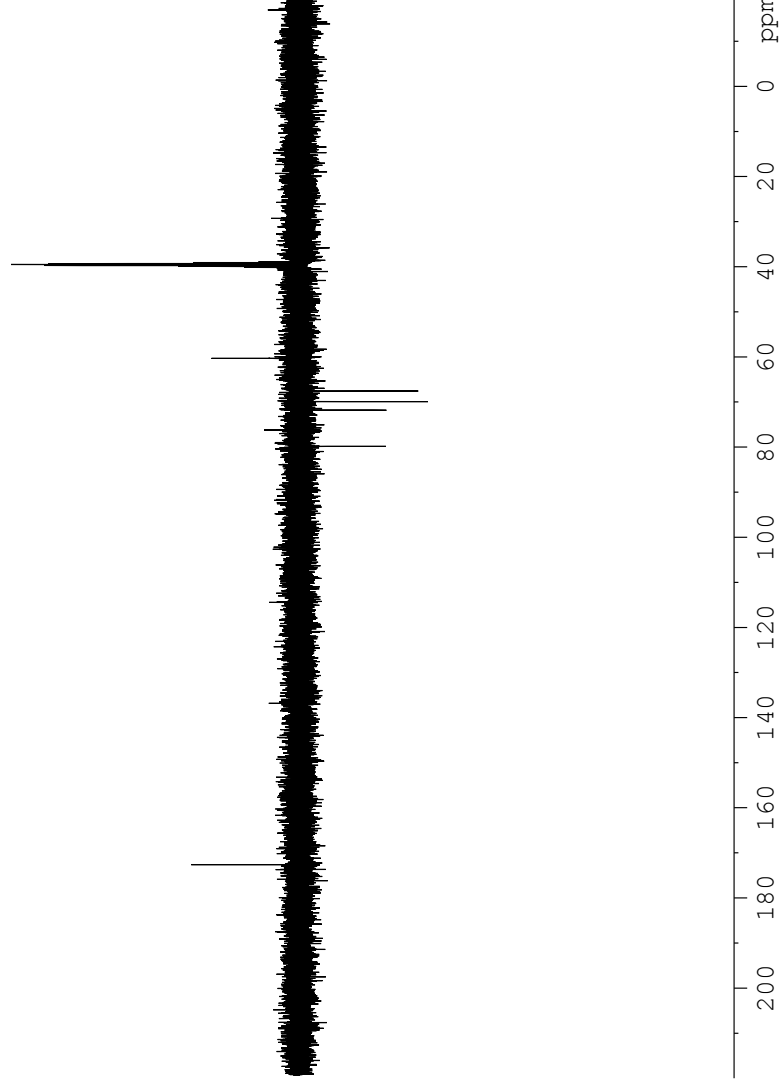
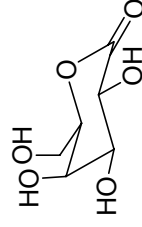
**$\gamma$ -D-mannonolactone** (HSQC, 400 MHz/ 100 MHz, DMSO- $d_6$ )(with small amount of  $\delta$ -D-mannonolactone and water)



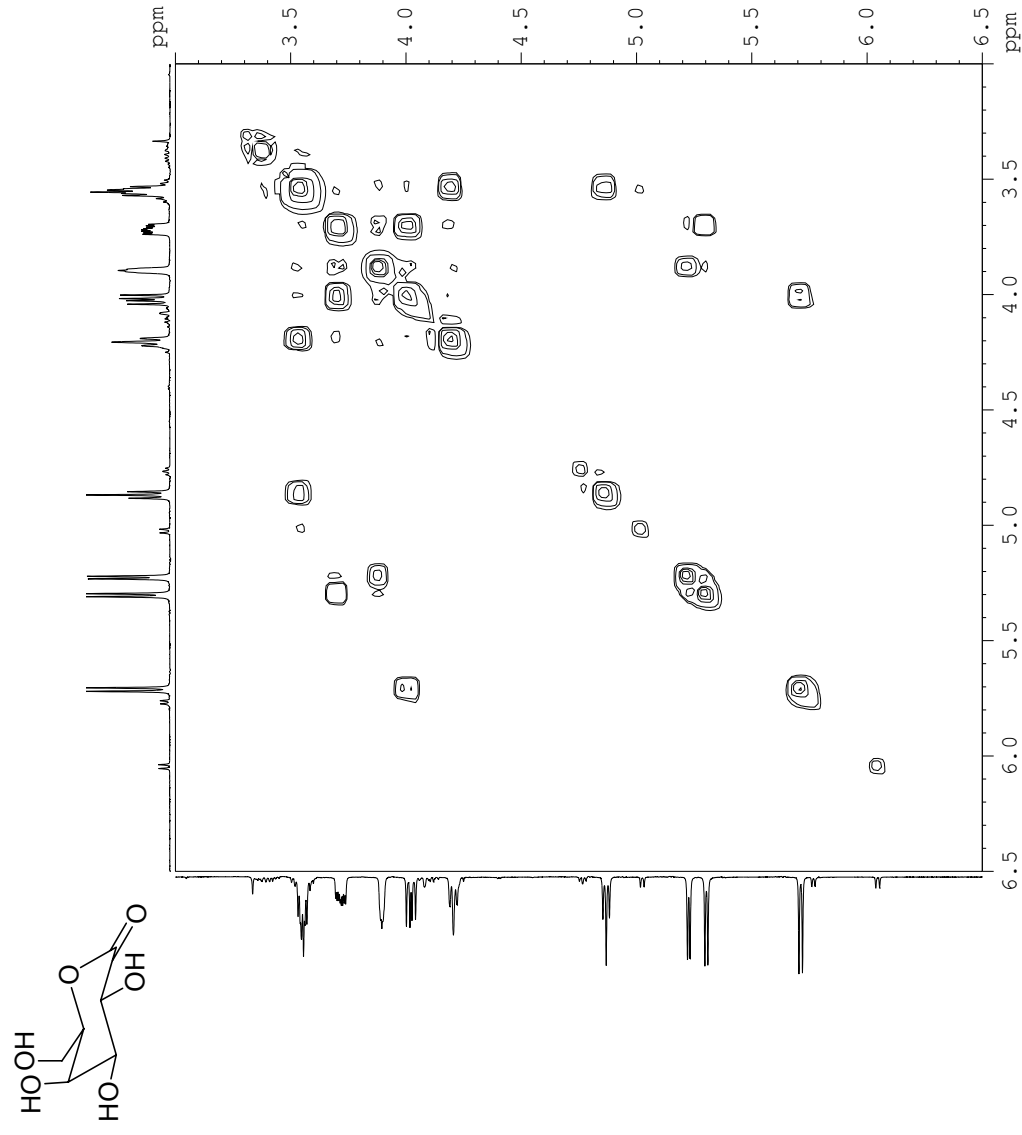
**$\delta$ -D-galactonolactone** ( $^1\text{H}$ , 400 MHz, DMSO- $d^6$ )(with small amount of  $\gamma$ -D-galactonolactone)



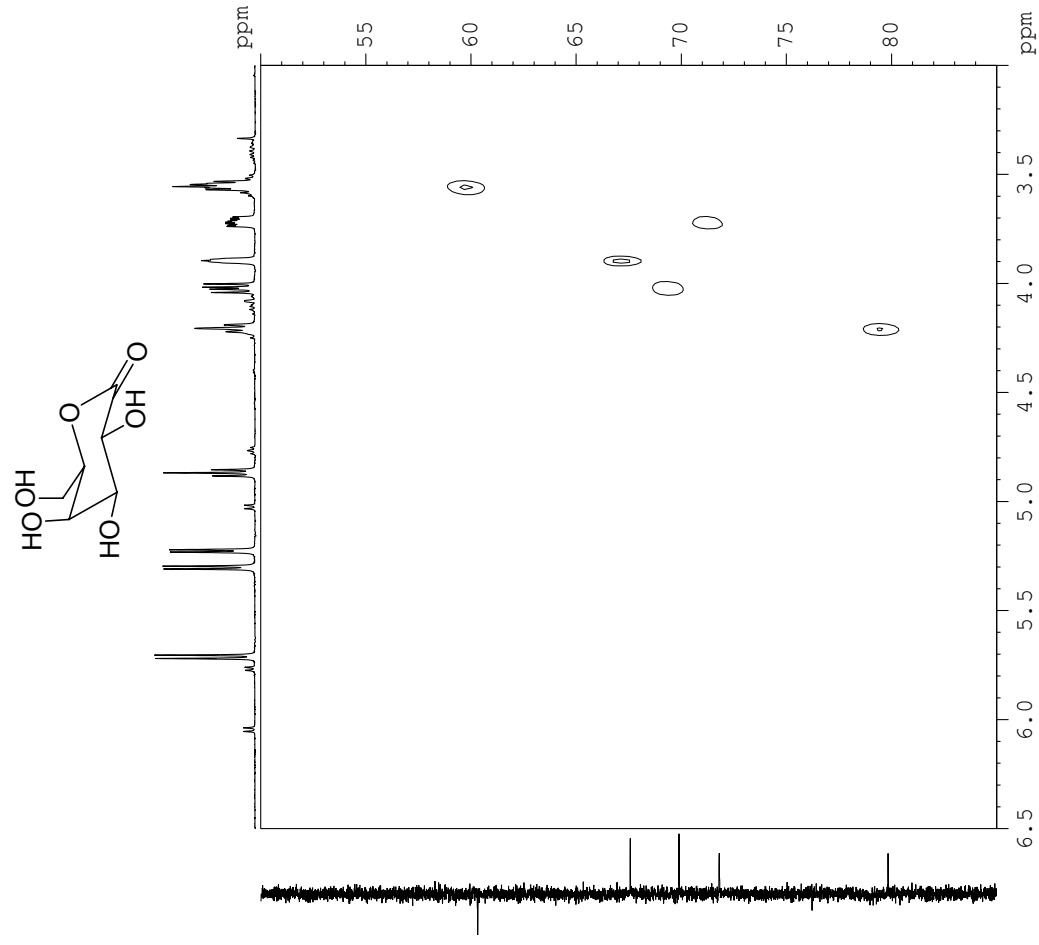
**$\delta$ -D-galactonolactone** (jmod, 100 MHz, DMSO- $d^6$ ) (with small amount of  $\gamma$ -D-galactonolactone)



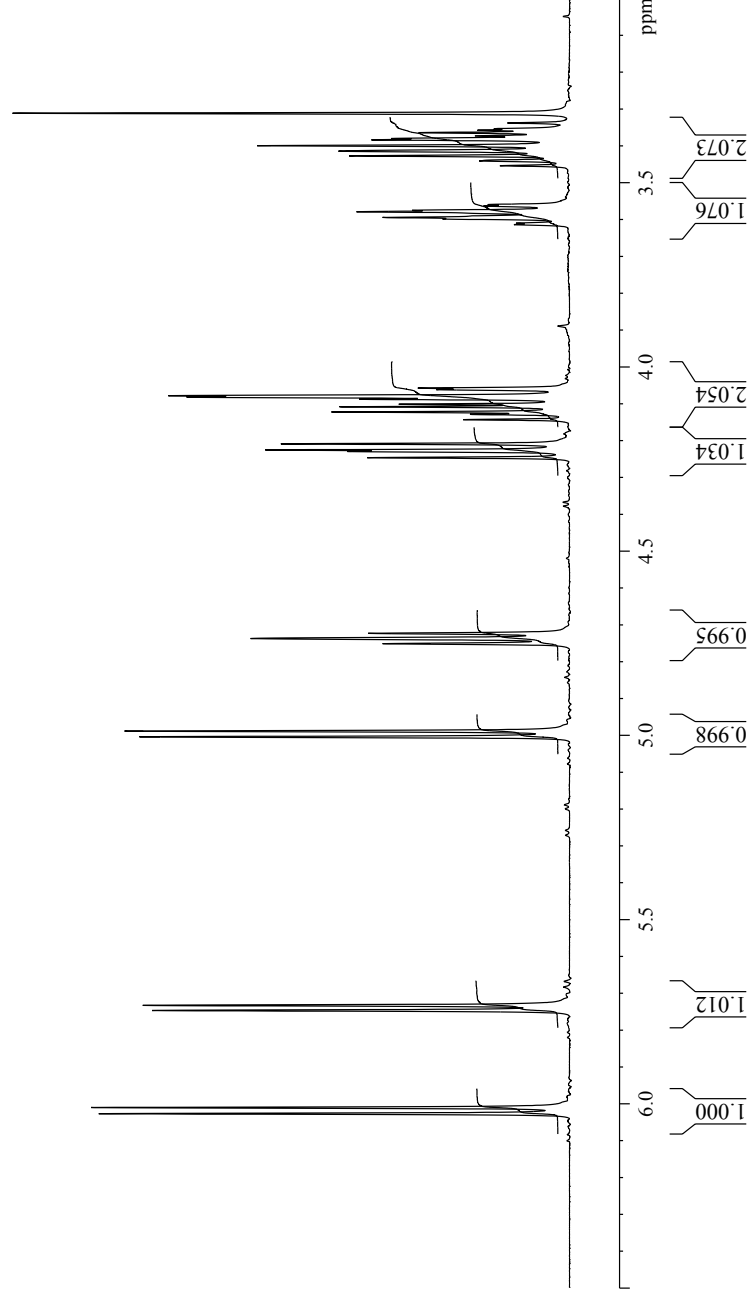
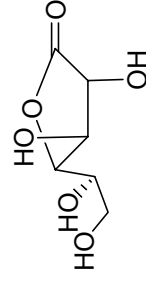
**$\delta$ -D-galactonolactone** (COSY, 400 MHz, DMSO- $d^6$ )(with small amount of  $\gamma$ -D-galactonolactone)



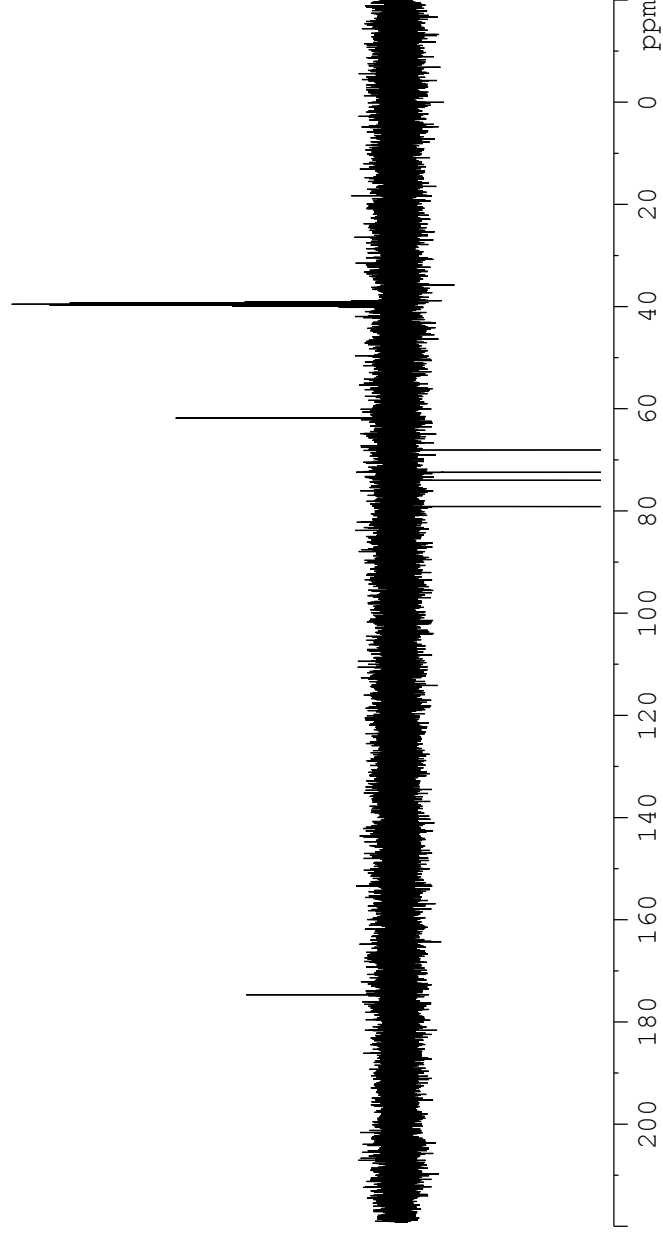
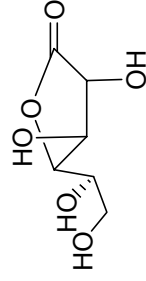
**$\delta$ -D-galactonolactone (HSQC, 400 MHz/ 100 MHz, DMSO- $d^6$ )(with small amount of  $\gamma$ -D-galactonolactone)**



**$\gamma$ -D-galactonolactone ( $^1\text{H}$ , 400 MHz, DMSO- $d_6$ )**



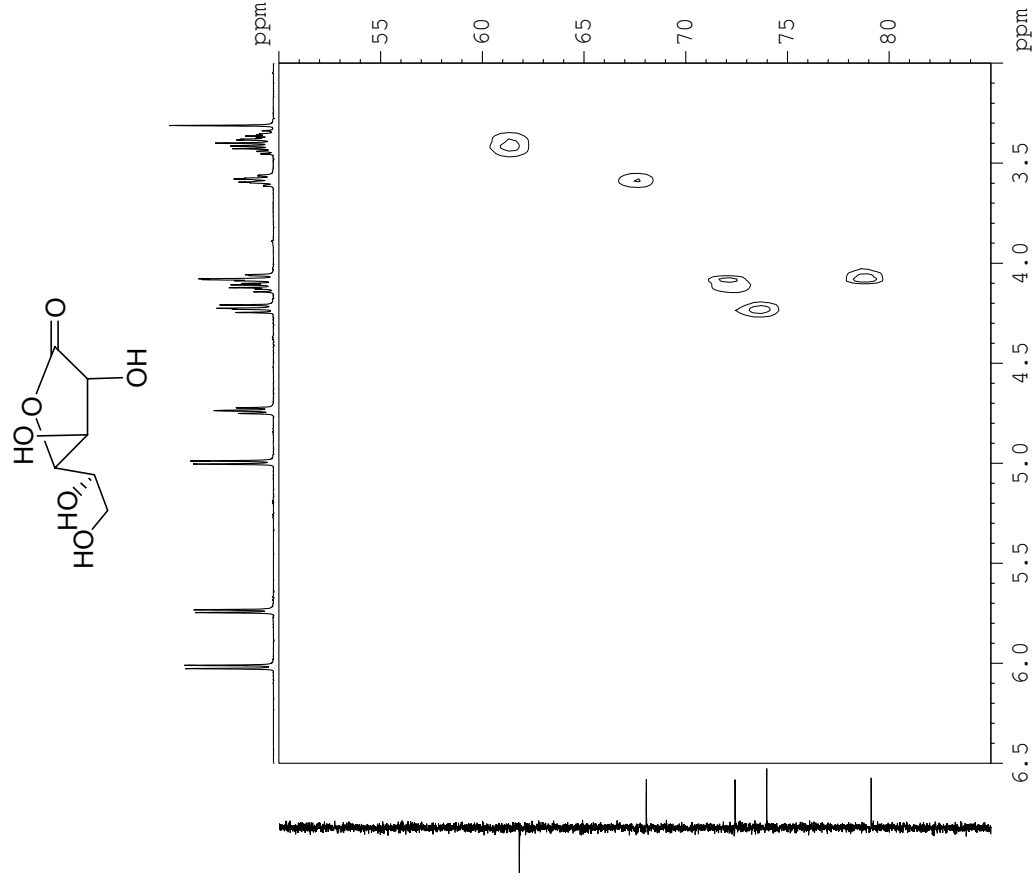
**$\gamma$ -D-galactonolactone (jmod, 100 MHz, DMSO-d<sup>6</sup>)**





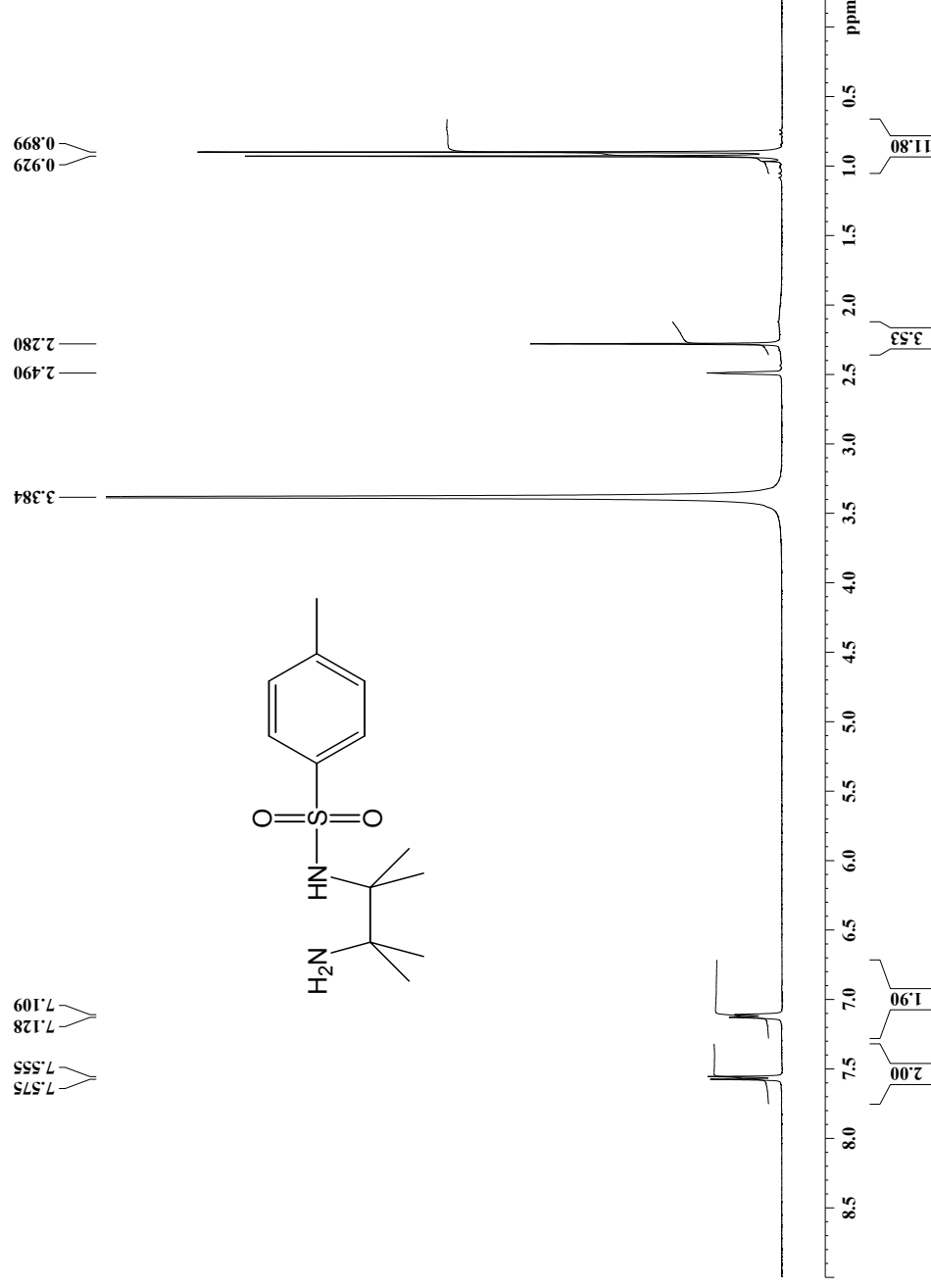


**$\gamma$ -D-galactonolactone (HSQC, 400 MHz/ 100 MHz, DMSO- $d_6$ )**



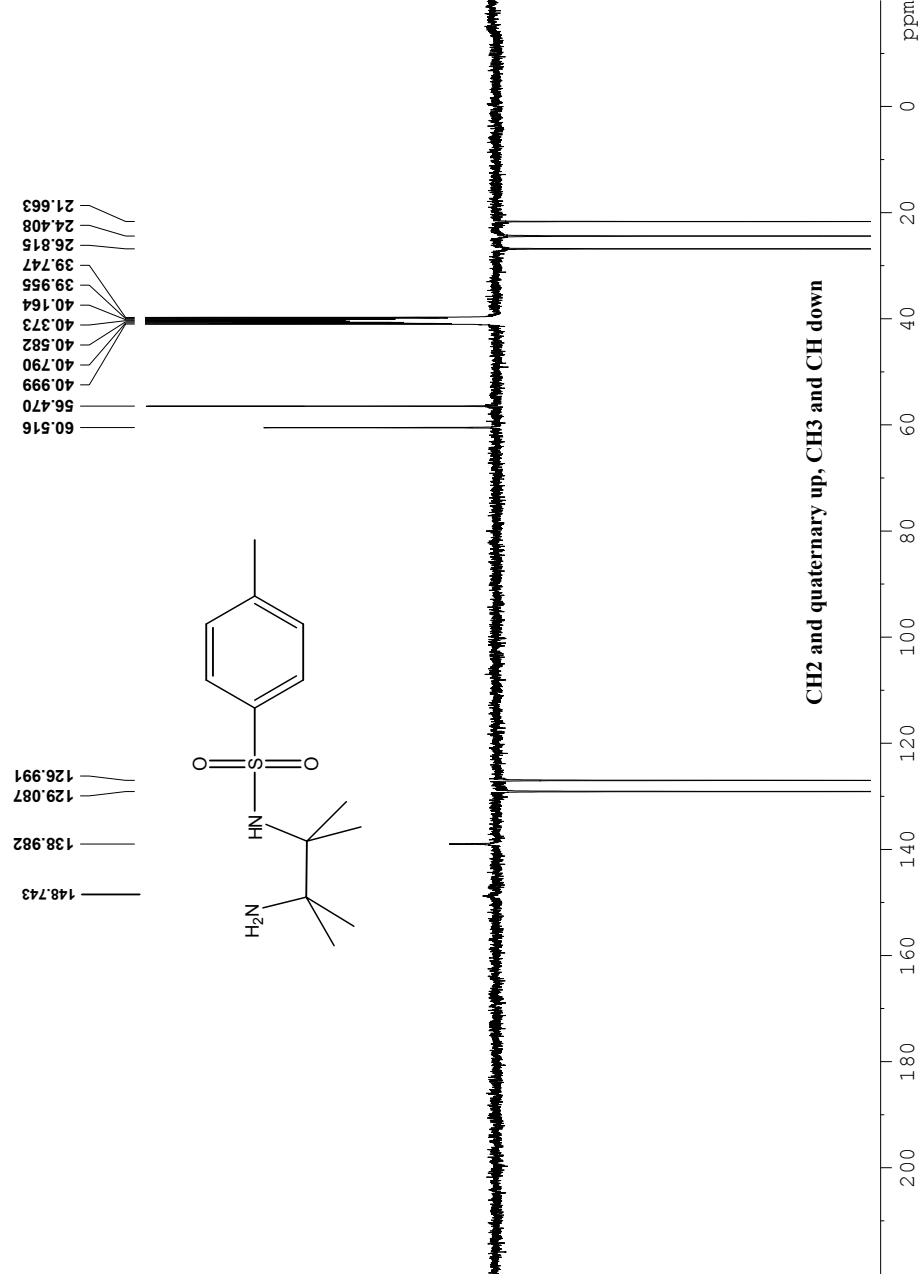
***N*-(*p*-toluyl-sulfonyl)-1,2-diamino-1,1,2,2-tetramethylethane (72)**

(<sup>1</sup>H NMR, 400 MHz, DMSO-d<sup>6</sup>)



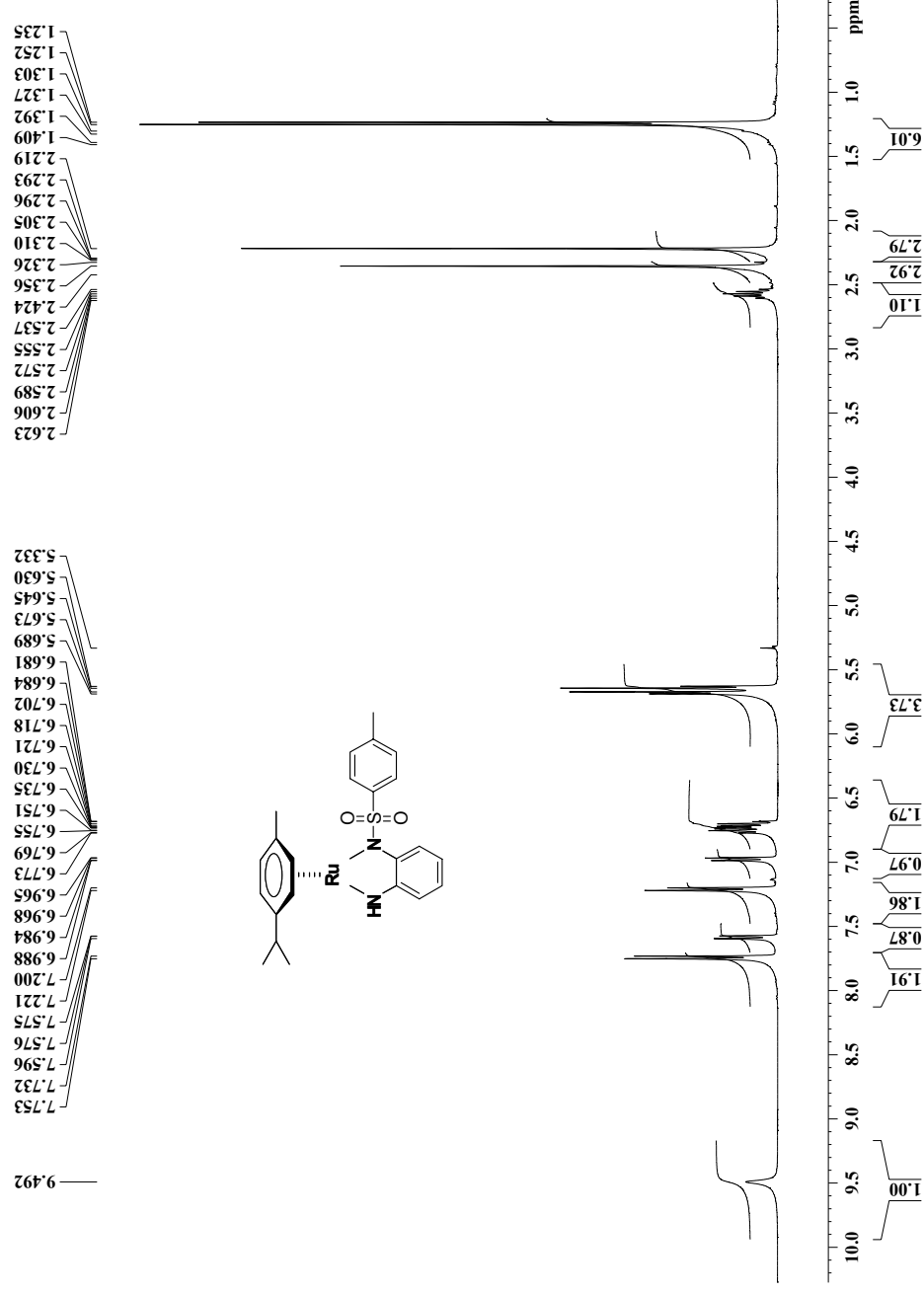
***N*-(*p*-toluyl-sulfonyl)-1,2-diamino-1,1,2,2-tetramethylethane (72)**

$^{13}\text{C}$  NMR (jmod, 100 MHz, DMSO- $\text{d}_6$ )



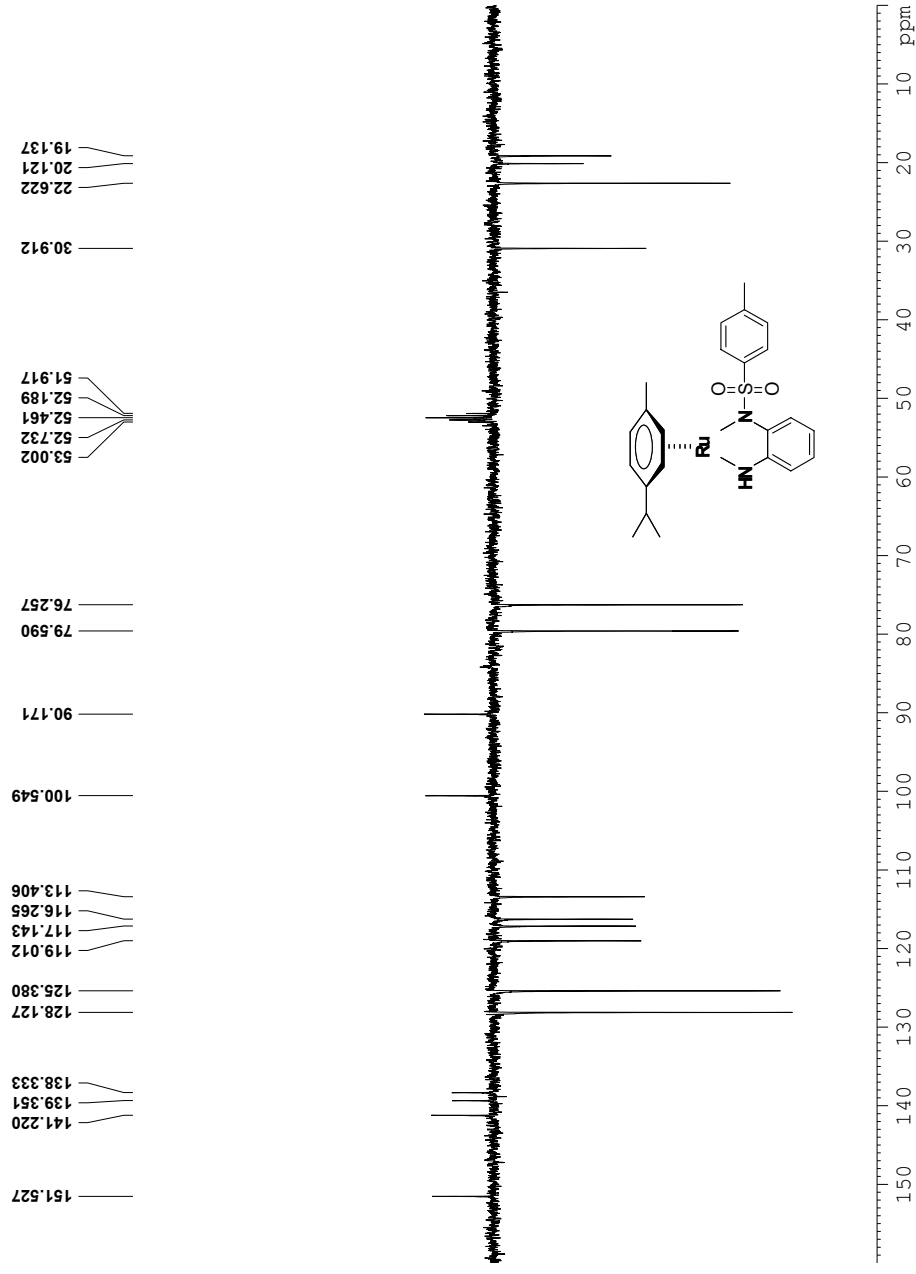
( $\eta^6$ -1-isopropyl-4-methyl-benzene)*N*-*p*-tosyl-*ortho*-diaminobenzene ruthenium(II) (77).

$^1\text{H}$  NMR, 400 MHz,  $\text{C}_6\text{D}_6$ )



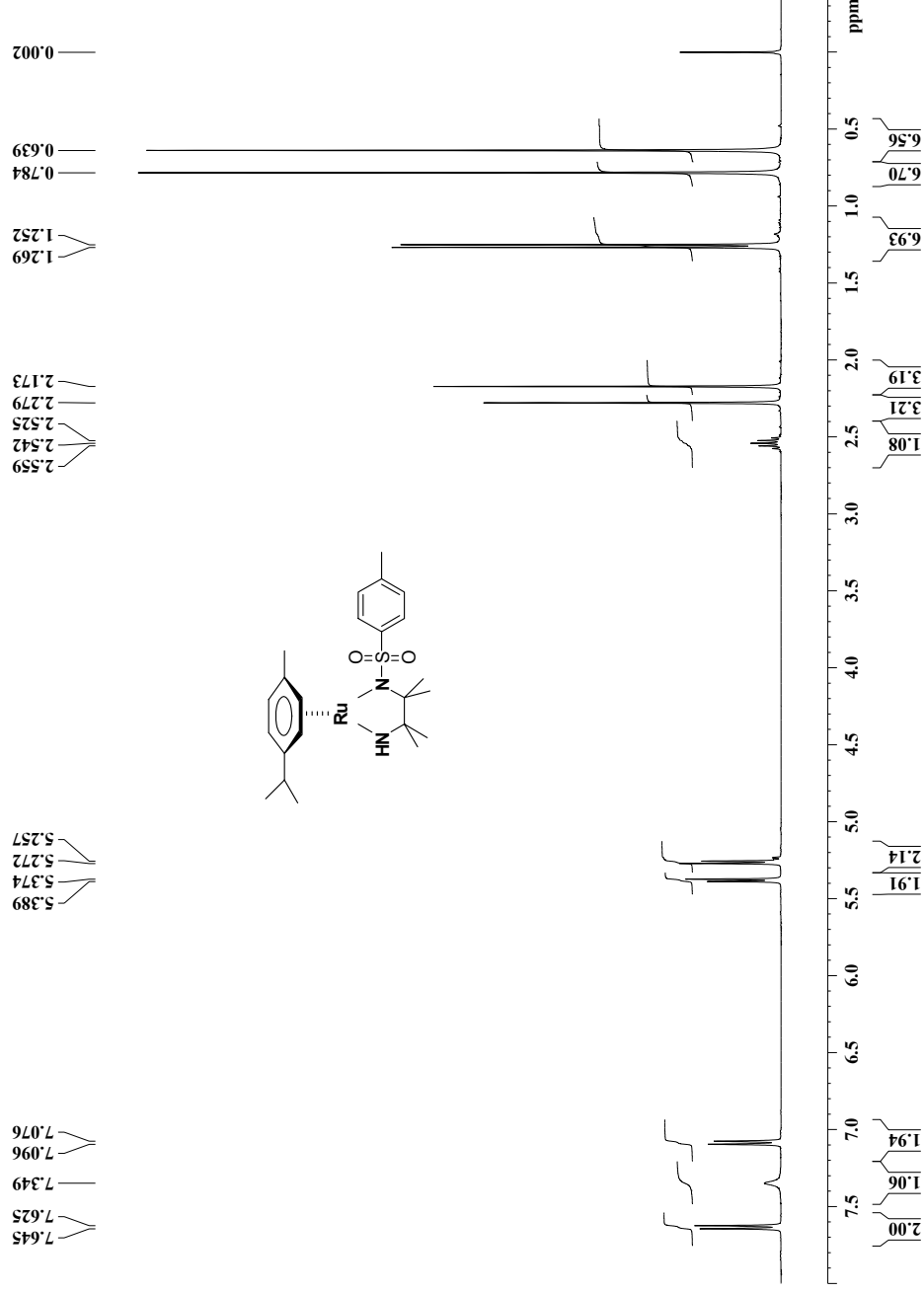
( $\eta^6$ -1-isopropyl-4-methyl-benzene)*N*-*p*-tosyl-*ortho*-diaminobenzene ruthenium(II) (77)

$^{13}\text{C}$  NMR (jmod, 100 MHz,  $\text{C}_6\text{D}_6$ )



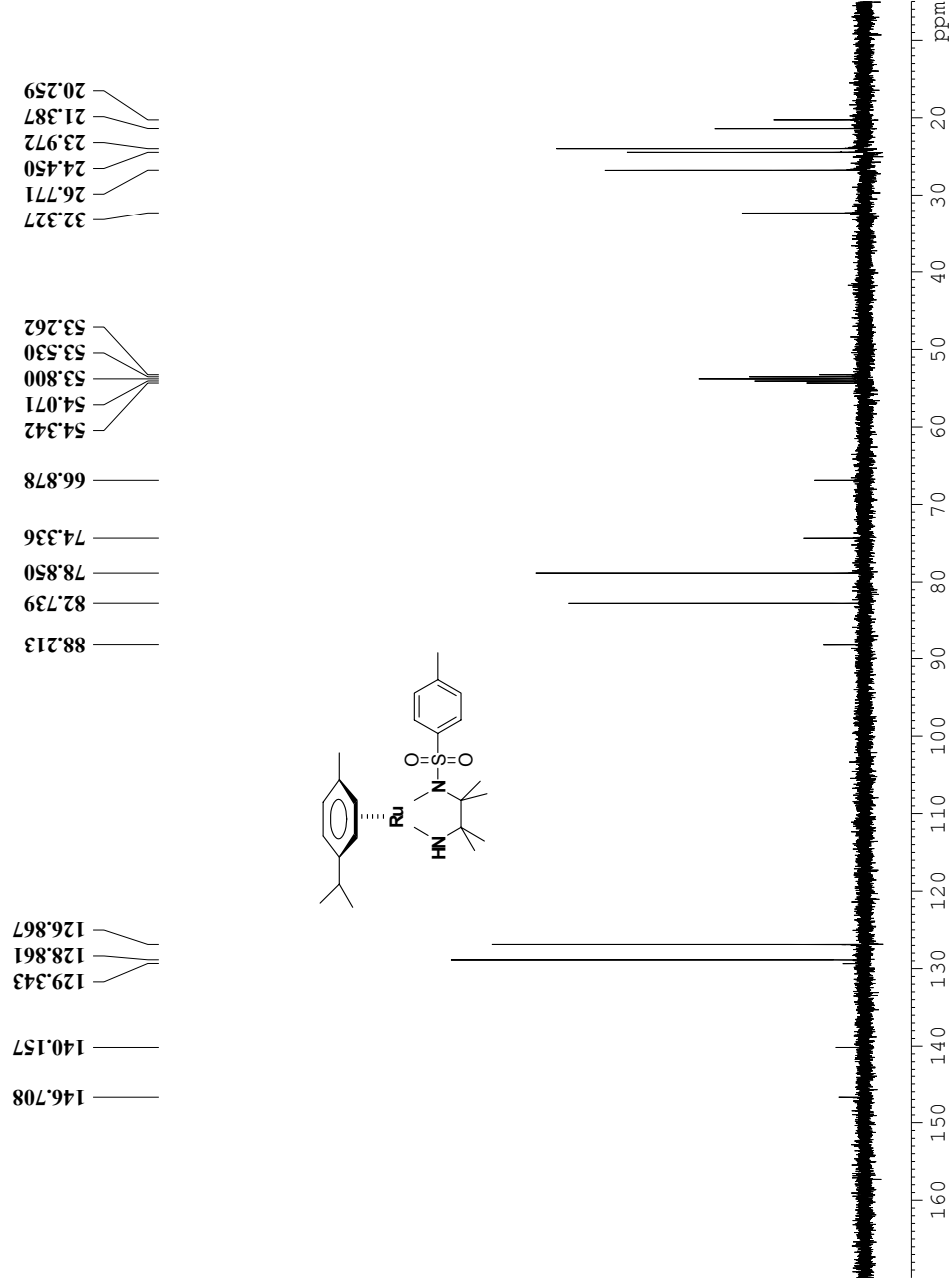
( $\eta^6$ -1-isopropyl-4-methyl-benzene)-*N*-(*p*-tolyl-sulfonyl)-1,2-diamino-1,1,2,2-tetramethyl-ethane ruthenium(II) (78)

( $^1\text{H}$  NMR, 400 MHz,  $\text{CD}_2\text{Cl}_2$ )



( $\eta^6$ -1-isopropyl-4-methyl-benzene)-*N*-(*p*-tolyl-sulfonyl)-1,2-diamino-1,1,2,2-tetramethyl-ethane ruthenium(II) (78)

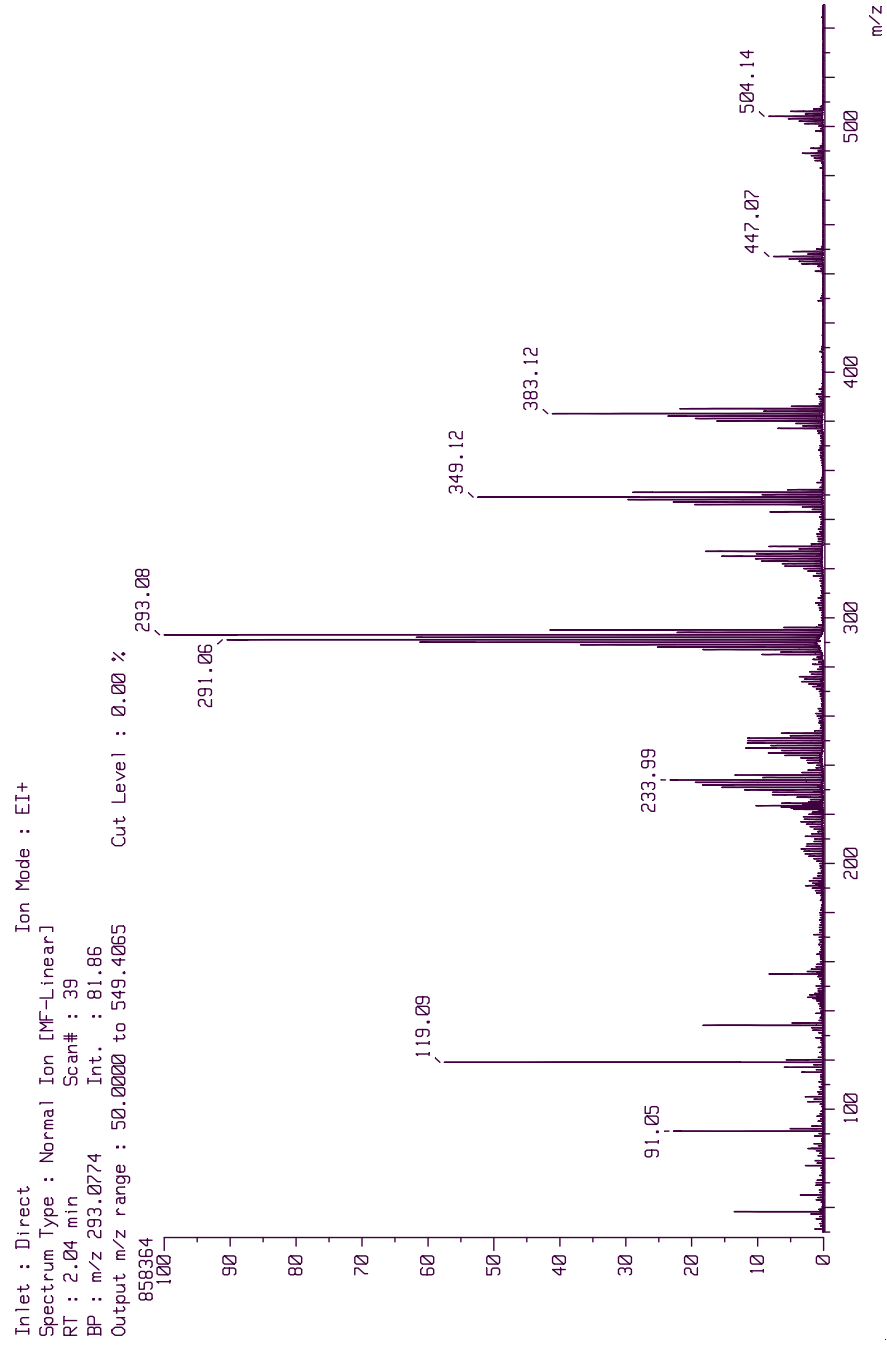
$^{13}\text{C}$  NMR (100 MHz,  $\text{CD}_2\text{Cl}_2$ )





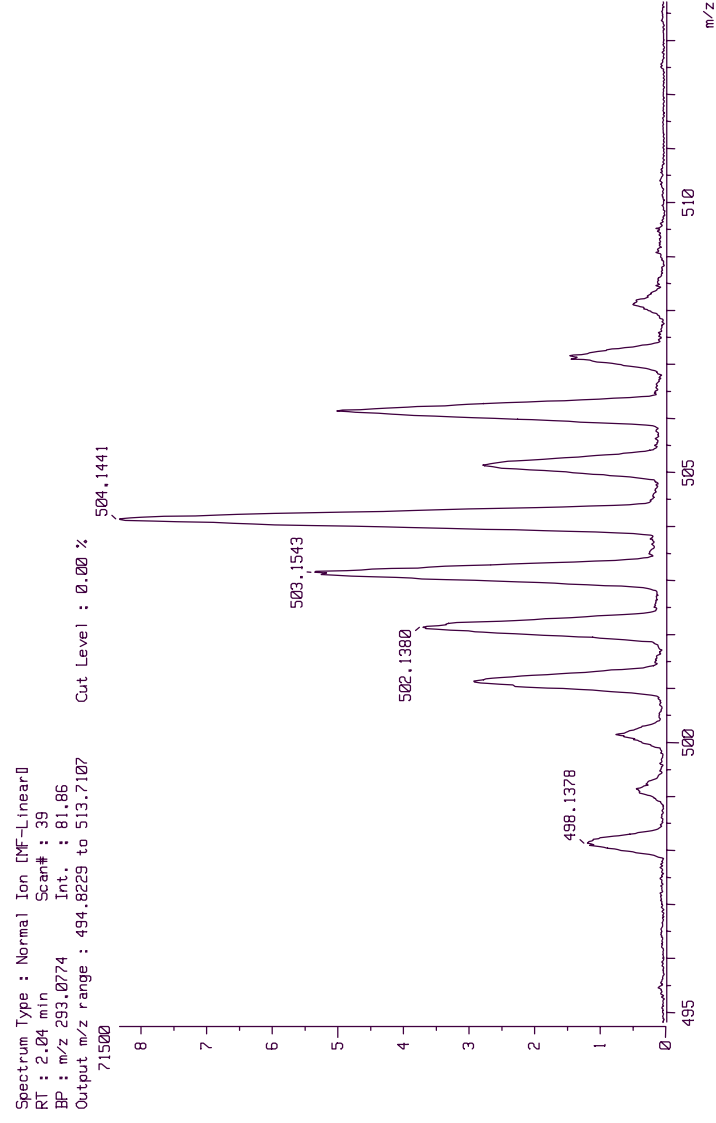
( $\eta^6$ -1-isopropyl-4-methyl-benzene)-N-(*p*-tolyl-sulfonyl)-1,2-diamino-1,1,2,2-tetramethyl-ethane ruthenium(II) (78)

MS (EI, 70 eV) Full Spectrum

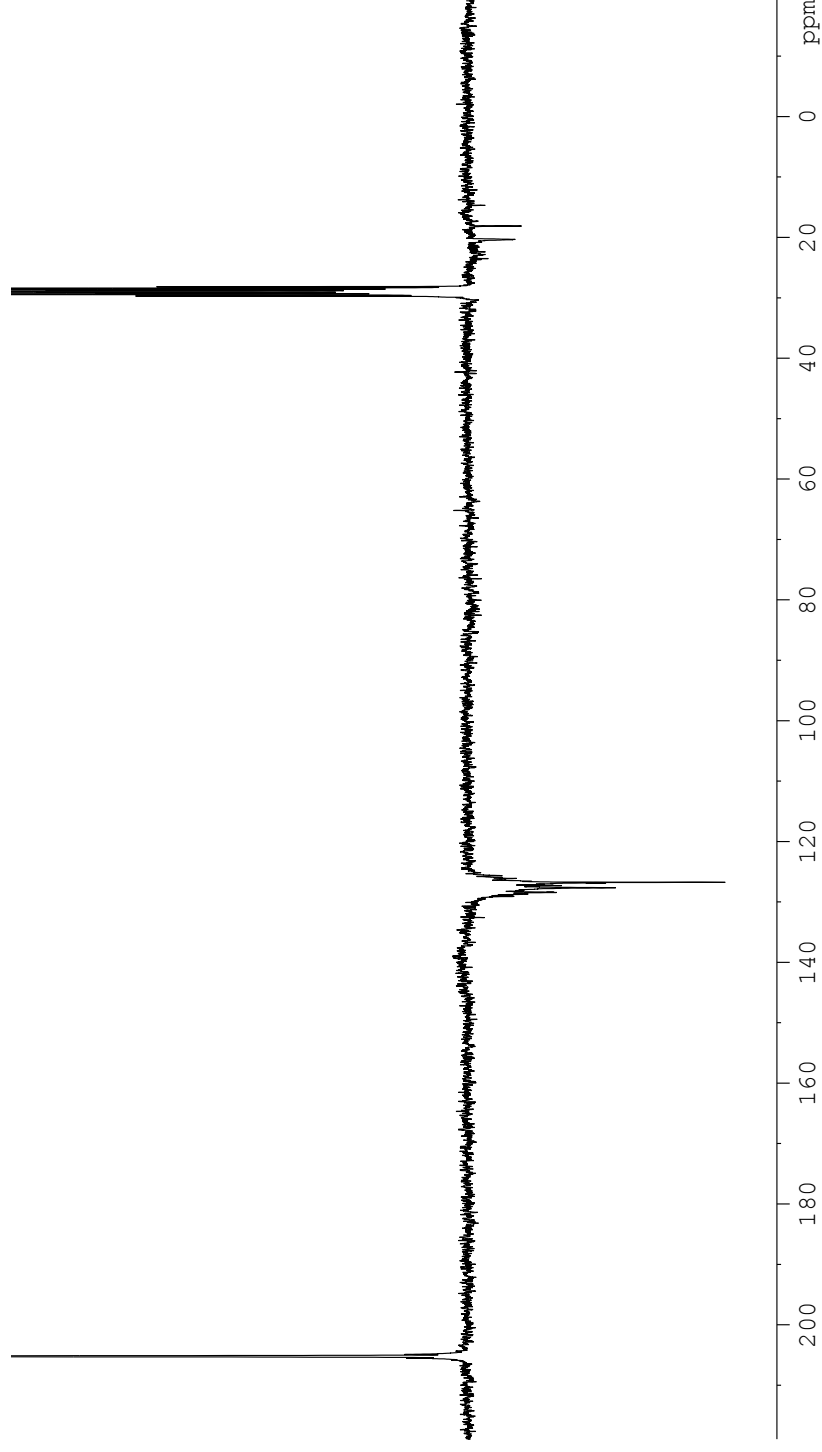


( $\eta^6$ -1-isopropyl-4-methyl-benzene)-*N*-(*p*-tolyl-sulfonyl)-1,2-diamino-1,1,2,2-tetramethyl-ethane ruthenium(II) (78)

MS (EI, 70 eV) Parent Ion



( $\eta^6$ -1-isopropyl-4-methyl-benzene)-*N*-(*p*-tolyl-sulfonyl)-1,2-diamino-*meso*-1,2-diphenyl-ethane ruthenium(II) (79).  
 $^{13}\text{C}$  NMR (jmod, 400 MHz, acetone- $d_6$ )



( $\eta^6$ -1-isopropyl-4-methyl-benzene)-*N*-(*p*-tolyl-sulfonyl)-1,2-diamino-*meso*-1,2-diphenyl-ethane ruthenium(II) (79).

MS (ESI, CH<sub>3</sub>CN, 3.5 kV spray voltage)

Top: experimental

Bottom: simulated

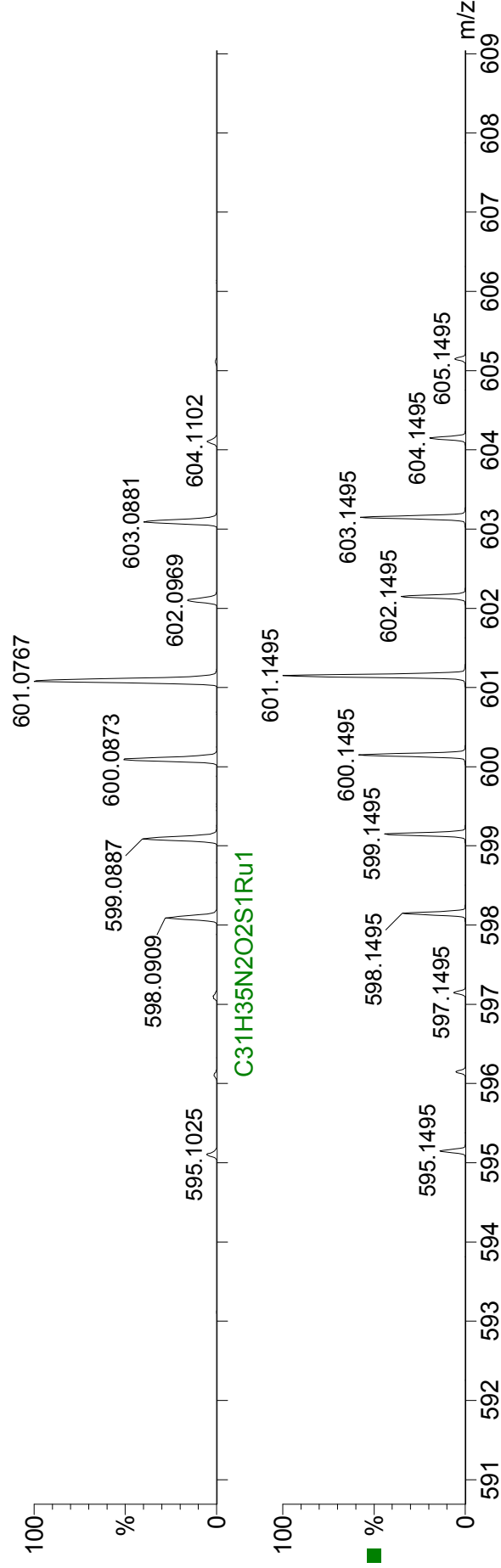


## Table of Figures

<b>Figure 1.1</b>	Epimeric relations of $\alpha$ - and $\beta$ -D-glucopyranose and $\alpha$ - and $\beta$ -D-idopyranose. ....	3
<b>Figure 1.2</b>	Examples of simple sugar derivatives. ....	5
<b>Figure 1.3</b>	Few highlights for sugar derived chiral ligands used in various chemical reactions. ....	6
<b>Figure 1.4</b>	Different hydroxyl groups of $\alpha$ -D-glucopyranose. ....	7
<b>Figure 1.5</b>	Six-membered and five-membered sugar lactones. ....	8
<b>Figure 1.6</b>	Hydrate of $\alpha$ -2-oxo-D-glucopyranose. ....	14
<b>Figure 1.7</b>	Examples of a 3-usolidulose and a 3-usoliduloside. ....	15
<b>Figure 1.8</b>	Overview of synthesized keto-sugars by the tris- <i>n</i> -butyltin-oxide/ bromine method. ....	16
<b>Figure 1.9</b>	Chiral stoichiometric oxidant based of fructose. ....	19
<b>Figure 1.10</b>	Noyori's Ruthenium $\eta^6$ arene based systems. ....	22
<b>Figure 1.11</b>	Mannitol / xylitol structures and observed equilibrium complexation regio-selectivities for (dppp)Pt(alditolate) complexes. ....	25
<b>Figure 1.12</b>	[(en) <sub>2</sub> Pd <sub>2</sub> ( $\alpha$ -D-glucopyranose1,2,3,4H <sub>4</sub> )] ..... 25	25
<b>Figure 2.1</b>	List of investigated hydrogen-acceptor molecules. ....	46
<b>Figure 2.2</b>	Shvo's catalyst <b>41</b> (20 mg, 2.5 mol% per Ru), $\alpha$ -D-glucose (1.47 mmol) and benzalacetone (2.94 mmol) at 45 °C in 10 mL of solvent monitored by GC of produced cyclohexanol. ....	49
<b>Figure 2.3</b>	Oxidation of sugars with Shvo's catalyst. ....	51
<b>Figure 2.4</b>	Oxidation of $\alpha$ -D-glucose to $\delta$ -D-gluconolactone with Shvo's catalyst in cyclohexanone solvent without DMF co-solvent. ....	52
<b>Figure 2.5</b>	Simulated and Experimental <sup>1</sup> H NMR Spectrum of <b>30</b> . ....	58
<b>Figure 2.6</b>	"Side" and "top" view of the minimum energy conformations $\delta$ -gluco ( <b>40</b> ), $\delta$ -manno ( <b>47</b> ) and $\delta$ -galactono ( <b>30</b> ) lactones determined by DFT ( <i>m</i> PW1PW91/6-31(d,p)) calculations. ....	61
<b>Figure 2.7</b>	Structures of the proposed bicyclic intermediates in the $\delta \rightarrow \gamma$ isomerization reactions. ....	66
<b>Figure 3.1</b>	Hydrated form of 2-keto-D-allopyranose. ....	73
<b>Figure 3.2</b>	<i>Cis</i> - and <i>trans</i> -annulated dimerized $\alpha$ -hydroxy-cyclohexanone. ....	78
<b>Figure 3.3</b>	Energy diagram of case 1 in oxidation of diol to $\alpha$ -OH ketone. ....	84
<b>Figure 3.4</b>	Energy diagram of case 1 in the oxidation of diols to $\alpha$ -OH ketone (uncatalyzed reaction is dotted, catalyzed reaction is solid). ....	84
<b>Figure 3.5</b>	Case 2 of the postulated energy diagram for the oxidation of <i>cis</i> / <i>trans</i> 1,2-cyclohexane-diol. ....	85
<b>Figure 3.6</b>	Theoretical product distribution when $k_1 = k_2 = k_3$ . ....	89
<b>Figure 3.7</b>	Theoretical product distribution when $k_1 = 10 k_2 = k_3$ . ....	91
<b>Figure 3.8</b>	Theoretical product distribution when $0.1 k_1 = k_2 = k_3$ . ....	91
<b>Figure 3.9</b>	Theoretical product distribution when $0.01 k_1 = k_2 = k_3$ . ....	92
<b>Figure 3.10</b>	Stereoisomers (–)-menthol, (+)-isomenthol and (+)-neomenthol. ....	94
<b>Figure 3.11</b>	Overview of diol model systems ( <i>cis</i> and <i>trans</i> configurations). ....	95
<b>Figure 3.12</b>	"NH-effect" ..... 102	102

<b>Figure 3.13</b>	$\beta$ -Aminoethanol and 1,2-diamino-ethane ligands used in the enantioselective reduction of prochiral ketones. ....	102
<b>Figure 3.14</b>	Model systems for oxidation of secondary alcohols in sugar substrates. ....	106
<b>Figure 3.15</b>	<i>N</i> -tosyl-1,2-diaminoethane and $\beta$ -amino-ethanol <i>p</i> -cymene-ruthenium(II). ....	110
<b>Figure 3.16</b>	Degradation resistant ligands. ....	111
<b>Figure 3.17</b>	<i>Exo</i> - and <i>endo</i> -conformation of <i>syn</i> -disubstituted 1,2-diaminoethane 16-electron ruthenium(II) complexes. ....	112
<b>Figure 3.18</b>	Synthesized 16-electron ruthenium (II) complexes. ....	114
<b>Figure 3.19</b>	$^1\text{H}$ -NMR of <b>78</b> in $\text{D}_2\text{O}$ solvent. ....	117
<b>Figure 3.20</b>	IR (KBr) of yellow solids of tetramethyl Ru complex ( <b>80</b> or <b>80</b> ). ...	118
<b>Figure 3.21</b>	<i>Ortho</i> -diaminobenzene as a non-innocent ligand. ....	119
<b>Figure 3.22</b>	Time dependence of alcohol content ....	120
<b>Figure 3.23</b>	Time dependence of ketone content. ....	121
<b>Figure 3.24</b>	Possible inhibition of the catalyst through acetone- $\text{d}^6$ ....	125
<b>Figure 3.25</b>	Mathematical calculation of $\Delta G_{\text{reaction}}$ in systems investigated. ...	131
<b>Figure 3.26</b>	$\Delta G_{\text{reaction}}$ calculated from DFT calculations as a function of produced ketone in acetone solvent from the corresponding alcohols. ....	131
<b>Figure 3.27</b>	$\Delta G_{\text{reaction}}$ calculated from DFT calculations as a function of produced alcohol in <i>iso</i> -propanol solvent from the corresponding ketone. ....	132
<b>Figure 3.28</b>	Mathematical derivation of $\Delta G_{\text{reaction}}$ under equal concentration experiment. ....	134
<b>Figure 3.29</b>	Determination of initial rates and equilibrium concentrations of alcohol and substrate from concentration vs. time graphs. ....	135
<b>Figure 3.30</b>	Calculation of $\Delta G^\circ_{\text{exp}}$ with error margin based on cumulative 5 % error in GC. ....	138
<b>Figure 3.31</b>	Graph of initial rate versus $\Delta G^\circ_{\text{exp}}$ of equal concentration experiment with ruthenium catalysts <b>78</b> and <b>79</b> . ....	140
<b>Figure 3.32</b>	Plot of conversion of <i>trans</i> -1,2-cyclohexanediol to oxidation products with rate constants $k_1 = 0.06$ , $k_2 = 0.04$ , $k_3 = 0.14$ . ....	158
<b>Figure 3.33</b>	Pentagonal bipyramidal geometry of $\text{MoO}(\text{O}_2)_2\text{L}_2$ . ....	159
<b>Figure 3.34</b>	Proposed structures of compounds <b>86</b> to <b>92</b> obtained through displacement of DMSO by the corresponding chelating ligand. ....	160
<b>Figure 3.35</b>	Molybdenum and tungsten diperoxo complexes ( <b>93</b> – <b>95</b> ). ....	164
<b>Figure 3.36</b>	Selected protected sugar substrates for the oxidation with tungsten complex <b>95</b> . ....	168
<b>Figure 3.37</b>	Benzoylhypobromite. ....	174
<b>Figure 3.38</b>	Induction of regioselectivity in the Ni(II)-diol complex. ....	175
<b>Figure 3.39</b>	GC analysis results from the oxidation of the three alcohols. ....	177
<b>Figure 3.40</b>	GC analysis results from the oxidation of cyclohexanol. ....	178
<b>Figure 3.41</b>	GC analysis results from the oxidation of cyclohexanol. ....	180
<b>Figure 3.42</b>	Difference IR spectrum of $\text{NiBr}_2$ , cyclohexanol and $\text{Bz}_2\text{O}_2$ . ....	181
<b>Figure 3.43</b>	Investigated monosaccharide substrates. ....	195

## Table of Schemes

<b>Scheme 1.1</b>	D-glucose transformation into $\alpha$ - and $\beta$ -D-glucopyranose and D-glucofuranose.....	1
<b>Scheme 1.2</b>	Equilibria of glucose in aqueous solution.....	4
<b>Scheme 1.3</b>	D-Mannitol as source for enantiopure glyceraldehyde and glyceric acid derivatives.....	5
<b>Scheme 1.4</b>	First oxidation products of glucopyranose. ....	7
<b>Scheme 1.5</b>	Oxidation of $\alpha$ -D-glucopyranose and $\beta$ -D-glucopyranose to $\delta$ -D-gluconolactone.....	10
<b>Scheme 1.6</b>	Possible products in the oxidation at C1 and C6 terminus of glucose.....	10
<b>Scheme 1.7</b>	Synthesis of $\gamma$ -L-gulonolactone from D-glucuronate by reduction with NaBH <sub>4</sub> and lactonization. ....	11
<b>Scheme 1.8</b>	Reaction pathways of D-glucitol to $\gamma$ -D-gluconolactone and $\gamma$ -L-gulonolactone. ....	12
<b>Scheme 1.9</b>	Synthesis of 2-oxo- $\alpha$ -D-glucose from $\alpha$ -D-glucose with an enzymatic process.....	14
<b>Scheme 1.10</b>	Schematic pathway of the tris- <i>n</i> -butyltin-oxide/ bromine method	16
<b>Scheme 1.11</b>	Oxidation of methyl $\beta$ -D-glucopyranoside with sodium dichromate.....	17
<b>Scheme 1.12</b>	Synthesis of 3 <sup>g</sup> -keto-sucrose from sucrose by an enzymatic process.....	18
<b>Scheme 1.13</b>	Reaction pathways of 3 <sup>g</sup> -ketosucrose. ....	19
<b>Scheme 1.14</b>	Generic equations of transfer hydrogen catalysis.....	21
<b>Scheme 1.15</b>	Reduction of acetophenone to 1-phenyl-ethanol with the Noyori system.....	23
<b>Scheme 1.16</b>	Formation of 1,2-xylitolato-platinum(II)-dppp in CD <sub>2</sub> Cl <sub>2</sub> .....	24
<b>Scheme 1.17</b>	Hydrocracking of fructose with H <sub>2</sub> Ru(PPh <sub>3</sub> ) <sub>4</sub> .....	26
<b>Scheme 1.18</b>	Motivation of this research project.....	28
<b>Scheme 1.19</b>	Objectives of this research project. ....	29
<b>Scheme 2.1</b>	Possible pathways of the oxidation of galactose ( <b>29</b> ) to the lactones ( <b>30</b> and <b>31</b> ).....	36
<b>Scheme 2.2</b>	Equilibrium of $\delta$ -D-galactonolactone ( <b>30</b> ) and $\gamma$ -D-galactonolactone ( <b>31</b> ) in aqueous buffered solution.....	37
<b>Scheme 2.3</b>	Conversion of protected arabinose <b>33</b> with NaBH <sub>4</sub> and subsequent <i>cis</i> -RuH <sub>2</sub> (PPh <sub>3</sub> ) <sub>4</sub> catalyzed oxidation of the arabinol intermediate <b>34</b> to the corresponding lactones ( <b>35</b> and <b>36</b> ).....	39
<b>Scheme 2.4</b>	Reaction pathway from $\alpha,\omega$ -diol ( <b>37</b> ) to lactone ( <b>39</b> ). ....	39
<b>Scheme 2.5</b>	Oxidation and isomerization of D-glucose ( <b>2</b> ) to the $\delta$ - and $\gamma$ -lactone ( <b>40</b> and <b>10</b> ).....	40
<b>Scheme 2.6</b>	Synthesis of [( $\eta^4$ -C <sub>4</sub> Ph <sub>4</sub> CO)(CO) <sub>2</sub> Ru] <sub>2</sub> from Ru <sub>3</sub> (CO) <sub>12</sub> and tetralone. ....	41
<b>Scheme 2.7</b>	Hydrogen-transfer reaction of Shvo's catalyst ( <b>42</b> ).....	42

<b>Scheme 2.8</b>	Dehydrogenation reaction mechanism of Shvo's catalyst. ....	43
<b>Scheme 2.9</b>	Reaction pathway of primary alcohols to corresponding ester. ..	43
<b>Scheme 2.10</b>	Transformation of primary alcohols to esters by Shvo's catalyst with diphenyl-acetylene as hydrogen acceptor. ....	44
<b>Scheme 2.11</b>	Synthesis of "Methyl"-Shvo catalyst ( <b>45</b> ). ....	53
<b>Scheme 2.12</b>	Equilibrium between 4-hydroxy- $\delta$ -valero-lactone ( <b>48</b> ) and 4-hydroxymethyl- $\gamma$ -butyrolactone ( <b>49</b> ). ....	63
<b>Scheme 3.1</b>	Preparation of the O-methyl oxime derivatives of 2-keto-D-allopyranose. ....	74
<b>Scheme 3.2</b>	Preparation of isopropylidene derivatives of 2-keto-D-allopyranose. ....	74
<b>Scheme 3.3</b>	Isomerization of methyl 3-keto- $\alpha$ -glucopyranoside to its 2-keto and 4 keto isomers in basic environment. ....	75
<b>Scheme 3.4</b>	Degradation of methyl $\alpha$ -D-3-oxo-glucopyranoside to saccharinic acids in basic medium ....	76
<b>Scheme 3.5</b>	Dehydration reaction of a 2-keto-sugar. ....	77
<b>Scheme 3.6</b>	Dimerization of $\alpha$ -hydroxy-cyclohexanone. ....	77
<b>Scheme 3.7</b>	Deduction of complex sugar substrates to model systems. ....	82
<b>Scheme 3.8</b>	<i>Vicinal</i> diol oxidation at the example of cyclohexane 1,2-diol. ....	83
<b>Scheme 3.9</b>	Trapping of $\alpha$ -hydroxy-cyclohexanone by complexing with transition metal of the tautomeric enediol form. ....	86
<b>Scheme 3.10</b>	Possible regioisomers after decomplexation of metal-enediol complex. ....	86
<b>Scheme 3.11</b>	Oxidation of <i>vicinal</i> diol. ....	87
<b>Scheme 3.12</b>	Variety of mono-alcohols as test system for oxidation reaction condition. ....	94
<b>Scheme 3.13</b>	Oxidation of 1,2;5,6-O-diisopropylidene $\alpha$ -D-gluco-furanoside with Shvo's catalyst and cyclohexanone as hydrogen-acceptor. ....	99
<b>Scheme 3.14</b>	Hydrogen transfer reaction of acetophenone in <i>iso</i> -propanol catalyzed by chiral ruthenium complex. ....	101
<b>Scheme 3.15</b>	Synthesis of ruthenium catalysts. ....	103
<b>Scheme 3.16</b>	Proposed mechanism of a hydrogen transfer reaction in metal-ligand bifunctional catalysis. ....	104
<b>Scheme 3.17</b>	Different resting states of catalyst under reducing and oxidizing condition. ....	109
<b>Scheme 3.18</b>	Possible decomposition products of complexes <b>25</b> and <b>26</b> through $\beta$ -hydride elimination. ....	110
<b>Scheme 3.19</b>	Synthesis <i>N</i> -tosyl- <i>ortho</i> -diaminobenzene ( <b>71</b> ). ....	113
<b>Scheme 3.20</b>	Synthesis <i>N</i> -tosyl-1,2-diamino-1,1,2,2-tetramethylethane ( <b>72</b> ). ....	113
<b>Scheme 3.21</b>	Synthesis <i>N</i> -tosyl- <i>meso</i> -1,2-diphenyl-1,2-diaminoethane( <b>73</b> ). ..	114
<b>Scheme 3.22</b>	Two possible aquo complexes <b>80</b> and <b>81</b> . ....	116
<b>Scheme 3.23</b>	Generic hydrogen-transfer reaction for calculation of $\Delta G^\circ$ . ....	128
<b>Scheme 3.24</b>	Hydrogen transfer reactions and peroxide oxidation reactions. ....	152
<b>Scheme 3.25</b>	Selective oxidations with $H_2O_2$ catalyzed by $(NH_4)_7Mo_7O_{24}$ . ....	153
<b>Scheme 3.26</b>	Base dependent oxidation step of secondary alcohol ....	154
<b>Scheme 3.27</b>	Synthesis of $MoO(O_2)_2L_2$ ( <b>83</b> ) from $MoO_3$ . ....	160



<b>Scheme 3.28</b>	Proposed reaction mechanism with benzoylhypobromite.....	174
<b>Scheme 3.29</b>	Regioselectivity of different bromides with Bz <sub>2</sub> O <sub>2</sub> .....	175
<b>Scheme 3.30</b>	Hydrolysis of benzoylhypobromite.....	182
<b>Scheme 3.31</b>	Proposed oxidation step.....	185
<b>Scheme 3.32</b>	Geminal hydrogen polarization in $\alpha$ -hydroxy ketone and diol...	200
<b>Scheme 3.33</b>	Axial and equatorial attach of Br <sup>+</sup> on cyclohexanol.....	200
<b>Scheme 3.34</b>	Relative conformations of <i>trans</i> - and <i>cis</i> -1,2-cyclohexanediols.	200

### Table of Tables

<b>Table 2.1</b>	Oxidation of glucose with Shvo's catalyst ( <b>42</b> ) with various hydrogen-acceptors .....	47
<b>Table 2.2</b>	Effectiveness of excess hydrogen acceptors for the catalytic dehydrogenation of D-glucose in DMF by <b>41</b> .....	48
<b>Table 2.3</b>	Oxidation of sugars with the Shvo's catalyst system and cyclohexanone as the hydrogen acceptor at 45 °C.....	54
<b>Table 2.4</b>	Comparison of the NMR Data for $\delta$ -D-galactonolactone ( <b>30</b> ) with $\delta$ -D-gluconolactone ( <b>40</b> ) and $\delta$ -D-mannonolactone ( <b>47</b> ).....	56
<b>Table 2.5</b>	Calculated dihedral angles and coupling constants for $\delta$ -lactones ..	60
<b>Table 2.6</b>	Experimental and DFT calculated $\gamma$ : $\delta$ ratios of the lactones .....	64
<b>Table 3.1</b>	Maximum $\alpha$ -hydroxy ketone content based on the ratio of $k_1$ (diol $\rightarrow$ $\alpha$ -hydroxy ketone) and $k_2$ ( $\alpha$ -hydroxy ketone $\rightarrow$ dione).....	93
<b>Table 3.2</b>	Oxidation of secondary alcohols with <i>p</i> -cymene-Ru- $\beta$ -aminoethanol hydride ( <b>23</b> ) as catalyst.....	108
<b>Table 3.3</b>	Ruthenium catalyst <b>78</b> under oxidizing and reducing conditions at different temperatures.....	122
<b>Table 3.4</b>	Rate constants assuming a 1 <sup>st</sup> order rate law in alcohol or ketone substrate, respectively with ruthenium catalyst <b>78</b> .....	123
<b>Table 3.5</b>	Results of DFT calculations of alcohol and ketone substrates with B3LYP/6-31g(d) level in gas phase at 298 K. ....	129
<b>Table 3.6</b>	Results of equal concentration experiments with ruthenium catalysts <b>78</b> and <b>79</b> . <sup>a</sup> .....	137
<b>Table 3.7</b>	Initial rates and $\Delta G^\circ_{\text{exp}}$ of equal concentration reactions with ruthenium catalysts <b>78</b> and <b>79</b> .....	139
<b>Table 3.8</b>	Oxidation of <i>trans</i> -1,2-cyclohexanediol with the (NH <sub>4</sub> ) <sub>6</sub> Mo <sub>7</sub> O <sub>24</sub> /H <sub>2</sub> O <sub>2</sub> method.....	155
<b>Table 3.9</b>	Oxidation of <i>trans</i> -cyclohexanediol with the MoO <sub>2</sub> (acac) <sub>2</sub> / peroxide method.....	157
<b>Table 3.10</b>	Solubilities of Mo <sub>2</sub> O <sub>2</sub> Cl <sub>2</sub> L <sub>2</sub> complexes in acetonitrile, dichloromethane and toluene.....	162
<b>Table 3.11</b>	Screening of oxidation methods of cyclohexanol with selected MoO <sub>2</sub> Cl <sub>2</sub> L <sub>2</sub> derivatives .....	163
<b>Table 3.12</b>	Oxidation of cyclohexanol with <b>94</b> and various peroxide oxidants .	165

<b>Table 3.13</b>	Oxidation of <i>cis</i> -and <i>trans</i> -cyclohexanediol with <b>94</b> and <b>95</b> with various oxidants .....	166
<b>Table 3.14</b>	Oxidation of secondary alcohols with the NiBr <sub>2</sub> /benzoylperoxide method.....	173
<b>Table 3.15</b>	Influence of water content on the conversion of cyclohexanol .....	180
<b>Table 3.16</b>	Oxidation of cyclohexanol with different Ni(II) catalysts .....	183
<b>Table 3.17</b>	Different oxidizing agents with NiBr <sub>2</sub> and cyclohexanol .....	184
<b>Table 3.18</b>	Oxidation of different secondary alcohols by the NiBr <sub>2</sub> /Bz <sub>2</sub> O <sub>2</sub> .....	185
<b>Table 3.19</b>	pH dependence of the effectiveness of the NaBrO <sub>3</sub> /NaHSO <sub>3</sub> reagent in the oxidation of <i>trans</i> -1,2-cyclohexanediol.....	190
<b>Table 3.20</b>	<i>Trans</i> -1,2-cyclohexanediol oxidation with varying amounts of NaBrO <sub>3</sub> and NaHSO <sub>3</sub> reagent.....	192
<b>Table 3.21</b>	Oxidation of various diols and monoalcohols with NaBrO <sub>3</sub> /NaHSO <sub>3</sub> reagent .....	194

---

Matthias BIERENSTIEL

---

## EDUCATION

- 2001 – 2005** **PhD in Inorganic Chemistry**, Ludwig-Maximilians-Universität, München, Germany (PhD defense April, 29<sup>th</sup> 2005)  
Supervisor: Dr. Marcel Schlaf at the University of Guelph, Guelph, ON, Canada and advisory representative Dr. Peter Klüfers  
PhD thesis: "Transition Metal Catalyzed Selective Oxidations of Sugars and Polyols."
- 1999 – 2001** Ludwig-Maximilians-Universität, Fakultät für Chemie und Pharmazie, München, Germany, **Diplom-Chemiker**, grade "1.2" (A+)  
Supervisor: Dr. Klaus Meerholz and Dr. Thomas J. J. Müller  
Thesis: "Synthesis and Investigations of Oxetane Based Polymerizable Layers in Organic Light Emitting Diodes, OLED's"
- 1998 – 1999** University of Guelph, Department of Chemistry, Guelph, Ontario  
Participant in the Ontario Baden-Württemberg **Student Exchange Program**, Undergraduate research project in organic chemistry with supervisor Dr. Adrian Schwan
- 1996 – 1998** Universität Konstanz, Konstanz, Germany, Fakultät für Chemie  
**Vordiplom**, grade "sehr gut (1.5)" (A)
- 1987 – 1996** Vöhl-Gymnasium, Memmingen, Germany  
**Allg. Hochschulreife**, grade "1.4" (A)

## ACADEMIC AWARDS AND SCHOLARSHIPS

- Doctoral Fellowship Stipend** from the Ernst-Schering-Research Foundation (ESRF), Berlin, Germany (2001 – 2003); [www.schering-fg.de](http://www.schering-fg.de)
- Ontario Baden-Württemberg Student Exchange Program** (1998 – 1999);  
[www.yorku.ca/ontbw/index.html](http://www.yorku.ca/ontbw/index.html)
- Book award** from Department of Chemistry at Ludwig-Maximilians-Universität München for excellent grade in chemistry Diplom examination
- Book award** from FCI (Foundation of the Chemical Industry) for best high-school graduate in chemistry

## TEACHING RELATED ACTIVITIES

2004 *Lecturer* "General Chemistry I" at University of Guelph, Guelph, Ontario with Course Coordinator Dr. Bryan Henry

2001 – 2004 *Teaching Assistant* at University of Guelph, Guelph, Ontario  
First year level: Introduction to General Chemistry Labs  
General Chemistry Tutorial Seminar Sessions  
Third year level: Advanced Inorganic Preparative Labs

1997 – 1998 Tutorial Seminar Lectures for 1<sup>st</sup> year chemistry students at Universität Konstanz, Konstanz, Germany, supervisor Prof. Dr. H.-H. Brintzinger

## Laboratory Supervision of Undergraduate Student Research Projects

2004 "Selective Oxidation of *vic.* Diols with Mo and W Catalysts", De-ann Rollings  
2003 "Selective Oxidation of *vic.* Diols with NaBrO<sub>3</sub>/NaHSO<sub>3</sub>", Paul J. D'Hondt  
2002 "Bromide Mediated Benzoylperoxide Oxidations", Jennessa Youm

## EXTRACURRICULAR ACTIVITIES AND HOBBIES

Music 1987 – present Singing, currently Univ. of Guelph Symphonic Choir  
1988 – present Playing trombone

Sports Actively involved in intramural soccer, dragon boat racing  
Golf and curling

Hobbies Avid collector of board and card games  
Reading good books  
Carpentry

## LEGAL STATUS

born July, 3<sup>rd</sup> 1976 in Memmingen, Germany

German citizen

Married



Guelph, 17<sup>th</sup>, March 2005

Matthias Bierenstiel